Université Fédérale
Toulouse Midi-Pyrénées

THÈSE

En vue de l'obtention du

DOCTORAT DE L'UNIVERSITÉ DE TOULOUSE

Délivré par :

École Nationale Supérieure des Mines d'Albi-Carmaux

Cotutelle internationale avec "Institute for Thermal Power Engineering of Zhejiang University", Chine

---

Présentée et soutenue par :
Jun Dong
le mardi 29 novembre 2016

Titre :

MSWs gasification with emphasis on energy, environment and life cycle assessment

---

Ecole doctorale et discipline ou spécialité

ED MEGEP : Génie des Procédés et de l'Environnement

Unité de recherche :

Centre RAPSODEE, CNRS - UMR 5302, École des Mines d'Albi-Carmaux

Directeur/trice(s) de Thèse :

Ange NZIHOU
Yong CHI

Jury :

Gilles FLAMANT, Directeur de recherche, Université de Perpignan Via Domitia, Rapporteur
Jean-Michel LAVOIE, Professeur, Université de Sherbrooke, Rapporteur
Carlo VANDECASTEELE, Professeur, Université Catholique de Louvain, Président
Mingjiang NI, Professeur, Zhejiang University, Examinateur
Capucine DUPONT, Docteur, CEA, Examinateur
Ange NZIHOU, Professeur, Mines Albi-Carmaux, Directeur de thèse
Yong CHI, Professeur, Zhejiang University, Co-directeur de thèse
Elsa WEISS-HORTALA, Maître assistant, Mines Albi-Carmaux, Co-encadrant de thèse

Abstract

Due to the potential benefits in achieving lower environmental emissions and higher energy efficiency, municipal solid waste (MSW) pyro-gasification has gained increasing attentions in the last years. To develop such an integrated and sustainable MSW treatment system, this dissertation mainly focuses on developing MSW pyro-gasification technique, including both experimental-based technological investigation and assessment modeling. Four of the most typical MSW components (wood, paper, food waste and plastic) are pyro-gasified in a fluidized bed reactor under N_2, steam or CO_2 atmosphere. Single-component and multi-components mixture have been investigated to characterize interactions regarding the high-quality syngas production. The presence of plastic in MSW positively impacts the volume of gas produced as well as its H_2 content. Steam clearly increased the syngas quality rather than the CO_2 atmosphere. The data acquired have been further applied to establish an artificial neural network (ANN)-based pyro-gasification prediction model. Although MSW composition varies significantly due to geographic differences, the model is robust enough to predict MSW pyro-gasification performance with different waste sources. To further enhance syngas properties and reduce gasification temperature as optimization of pyro-gasification process, MSW steam catalytic gasification is studied using calcium oxide (CaO) as an in-situ catalyst. The influence of CaO addition, steam flowrate and reaction temperature on H_2-rich gas production is also investigated. The catalytic gasification using CaO allows a decrease of more than 100°C in the reaction operating temperature in order to reach the same syngas properties, as compared with non-catalyst high-temperature gasification. Besides, the catalyst activity (de-activation and re-generation mechanisms) is also evaluated in order to facilitate an industrial application. 650 ^{o}C and 800 ^{o}C are proven to be the most suitable temperature for carbonation and calcination respectively, while steam hydration is shown to be an effective CaO re-generation method. Afterwards, a systematic and comprehensive life cycle assessment (LCA) study is conducted. Environmental benefits have been achieved by MSW gasification compared with conventional incineration technology. Besides, pyrolysis and gasification processes coupled with various energy utilization cycles are also modeled, with a gasification-gas turbine cycle

system exhibits the highest energy conversion efficiency and lowest environmental burden. The results are applied to optimize the current waste-to-energy route, and to develop better pyro-gasification techniques.

Keywords: Municipal solid waste; Pyro-gasification; High-quality syngas production; Artificial neural network; In-situ catalyst; Life cycle assessment

Résumé

Récemment, la pyro-gazéification de déchets ménagers solides (DMS) a suscité une plus grande attention, en raison de ses bénéfices potentiels en matière d'émissions polluantes et d'efficacité énergique. Afin de développer un système de traitement de ces déchets, durable et intégré, ce manuscrit s'intéresse plus spécifiquement au développement de la technique de pyro-gazéification des DMS, à la fois sur l'aspect technologique (expérimentations) et sur son évaluation globale (modélisation). Pour cette étude, quatre composants principaux représentatifs des DMS (déchet alimentaire, papier, bois et plastique) ont été pyro-gazéifiés dans un lit fluidisé sous atmosphère N_2, CO_2 ou vapeur d'eau. Les expériences ont été menées avec les composés seuls ou en mélanges afin de comprendre les interactions mises en jeu et leurs impacts sur la qualité du syngas produit. La présence de plastique améliore significativement la quantité et la qualité du syngas (concentration de H_2). La qualité du syngas est améliorée plus particulièrement en présence de vapeur d'eau, ou, dans une moindre mesure, en présence de CO_2. Les résultats obtenus ont été ensuite intégrés dans un modèle prédictif de pyro-gazéification basé sur un réseau de neurones artificiels (ANN). Ce modèle prédictif s'avère efficace pour prédire les performances de pyro-gazéification des DMS, quelle que soit leur composition (provenance géographique). Pour améliorer la qualité du syngas et abaisser la température du traitement, la gazéification catalytique in-situ, en présence de CaO, a été menée. L'impact du débit de vapeur d'eau, du ratio massique d'oxyde de calcium, ainsi que de la température de réaction a été étudié en regard de la production (quantité et pourcentage molaire dans le gaz) d'hydrogène.la présence de CaO a permis d'abaisser de 100°C la température de gazéification, à qualité de syngas équivalente. Pour envisager une application industrielle, l'activité du catalyseur a aussi été évaluée du point de vue de sa désactivation et régénération. Ainsi, les températures de carbonatation et de calcination de 650°C et 800°C permettent de prévenir la désactivation du catalyseur, tandis que l'hydratation sous vapeur d'eau permet la régénération. Ensuite, une étude a été dédiée à l'évaluation et à l'optimisation de la technologie de pyro-gazéification par la méthode d'analyse de cycle de vie (ACV). Le système de gazéification permet d'améliorer les indicateurs de performances environnementales comparativement à l'incinération

conventionnelle. De plus, des systèmes combinant à la fois la transformation des déchets en vecteur énergétique et la mise en œuvre de ce vecteur ont été modélisés. La pyro-gazéification combinée à une turbine à gaz permettrait de maximiser l'efficacité énergétique et de diminuer l'impact environnemental du traitement. Ainsi, les résultats permettent d'optimiser les voies actuelles de valorisation énergétique, et de d'optimiser les techniques de pyro-gazéification.

Mots clés: Déchets ménagers solides; Pyro-gazéification; Syngas de haute qualité; Réseau de neurones artificiels; Catalyseur in-situ; Analyse de cycle de vie

Résumé Long en Français

➢ Introduction Générale

En raison d'une rapide industrialisation et urbanisation des sociétés, la quantité de déchets ménagers solides (DMS) générés ces dernières décennies a augmenté de manière très importante. Ceci s'est accompagné d'une variation significative de leur composition en fonction des régions. Dans ce contexte, le développement de systèmes de gestion des déchets intégrés et adaptés, c'est-à-dire respectant les aspects de développement durable, fait face à différents challenges, que ce soit pour les pays développés ou en voie de développement. Ils peuvent se résumer à partir des points suivants :

- Le développement de technologies adaptées au lieu, et permettant une adéquation avec les problématiques énergétiques et environnementales
- La nécessité de développer un système holistique et un processus complet optimisé.

En raison de ses bénéfices potentiels comparativement à l'incinération conventionnelle, la pyro-gazéification des déchets ménagers a émergé ces dernières années. Cependant, le développement de la technologie de pyro-gazéification n'en est qu'à ses prémices, en raison des verrous suivants :

- Assurer le taux conversion de déchets en produits valorisables le plus élevé possible. Ces produits pouvant être des vecteurs énergétiques (gaz énergétique) ou des produits à valeur ajoutée (char),
- Développer un outil prédictif permettant d'ajuster les paramètres opératoires en fonction de la variabilité de composition des déchets entrants,
- Augmenter significativement la qualité du gaz synthétique (syngas) produit en utilisant potentiellement des catalyseurs in situ.

Une évaluation adaptée est d'autant plus essentielle qu'elle permettra de garantir le bon fonctionnement du système à la fois de manière durable et sur le long terme. Ceci inclue l'analyse des systèmes utilisés actuellement pour la gestion des déchets, ainsi que leur modernisation/amélioration nécessaire pour une meilleure efficacité énergétique et adéquation avec l'environnement. Dans ce contexte, l'analyse de cycle de vie (ACV) est reconnue comme un outil très utile précisant la méthodologie d'évaluation. Cependant, une comparaison quantitative entre les technologies de pyro-gazéification et d'incinération est nécessaire pour garantir la compréhension de leurs impacts sur les aspects énergétiques et environnementaux.

Dans ce contexte global, le principal objectif de la thèse est donc d'étudier « la gazéification des déchets ménagers solides, avec un accent particulier porté à l'analyse combinée énergie-environnement-cycle de vie ». La structure générale du manuscrit est décrite à la **Figure 0.4**.

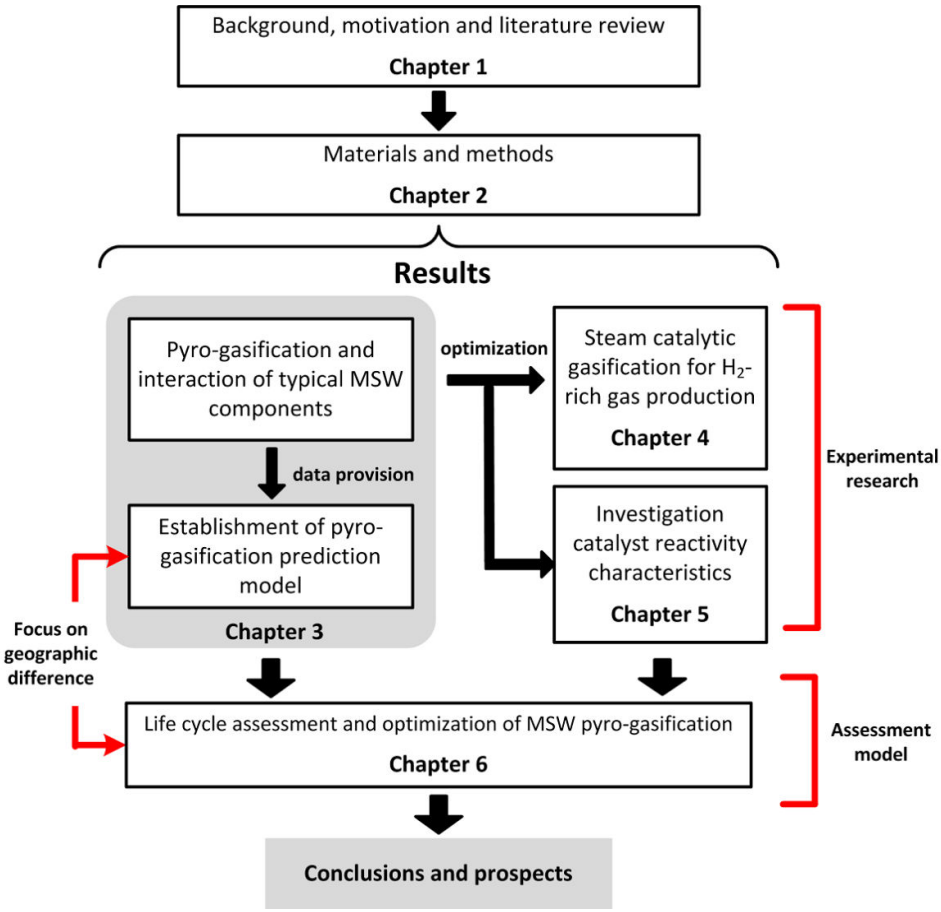

Figure 0.4 Structure de la thèse

➢ Chapitre 1: Revue Bibliographique

Ce chapitre a pour objectif de poser le contexte et d'indiquer l'état actuel des recherches développées dans le domaine de la pyro-gazéification des déchets ménagers. Une attention particulière est adressée aux aspects efficacité énergétique et intégration environnementale. Ces éléments vont ainsi permettre de mettre en lumière les verrous encore existants et de détailler les pistes de développement.

La **Section 1.1** détaille les éléments de compréhension de la pyro-gazéification de déchets ménagers solides : le procédé de pyro-gazéification en lui-même et les réactions chimiques, ses bénéfices potentiels en regard des aspects énergie et environnement, et enfin les verrous technologiques existants qui limitent son développement. Bien que la littérature indique les avantages potentiels de cette technique, notamment en regard de l'incinération conventionnelle, elle est toujours en cours de développement. La **Figure 1.2** résume les challenges techniques relatifs à une complète industrialisation du procédé à travers le monde. Plus spécifiquement, les challenges actuels sont directement liés aux applications, c'est-à-dire le type de vecteur énergétique produit et la technologie mise en œuvre en aval du réacteur. Ceci nécessite donc une amélioration plus ou moins poussée de la qualité du syngas (syngas upgrading), implique un choix sélectif de technologies pour la pyro-gazéification, et un éventuel prétraitement du flux entrant. Tous ces aspects doivent ensuite s'intégrer pour une optimisation du système.

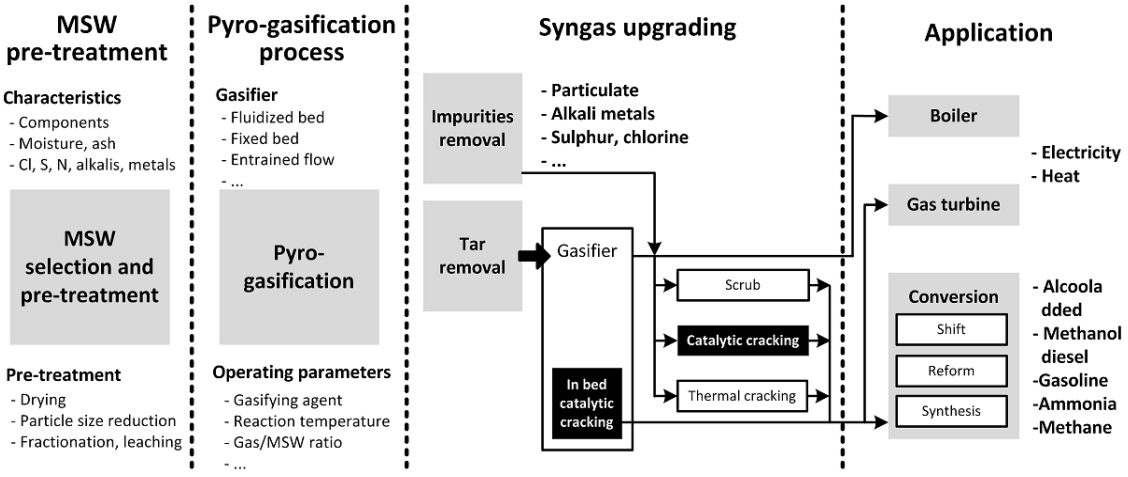

Figure 1.2 Système de traitement des déchets ménagers par pyro-gazéification : applications énergétiques et verrous techniques du processus

Les verrous relatifs à la production d'un gaz de synthèse de haute qualité sont détaillés dans la **Section 1.2**. Les effets des propriétés des déchets ménagers, leur prétraitement et les conditions opératoires utilisées (agent gazéifiant, température de réaction, rapport massique agent gazéifiant et quantité de déchet) sont discutés en détail. Les caractéristiques du syngas, incluant la pyro-gazéification de composés seuls ou en mélange, ainsi que les méthodes impactant la qualité du syngas sont ensuite exposées. Comme la qualité du syngas peut être améliorée en utilisant des catalyseurs, une partie présente l'état de l'art dans ce domaine.

La **Section 1.3** est plus spécifiquement dédiée aux procédés de mise en œuvre du syngas. Différentes alternatives existent : génération d'énergie, production d'hydrogène, synthèse Fisher-Tropsch, et synthèse d'intermédiaires chimiques (méthanol, alcools, diméthyl ether, méthane). Parmi toutes ces options, les procédés de production les plus usités sont décrits en détail. De plus, la configuration de procédés commerciaux de pyro-gazéification de déchets ménagers est aussi exposée.

Le développement technologique de cette solution passe automatiquement par une évaluation globale du système. Pour cela, une approche par analyse de cycle de vie (ACV) combinée à une évaluation des impacts énergétiques et environnementaux est présentée à la **Section 1.4**. Les principes et le cadre de l'ACV sont présentés, suivis de la possibilité de l'introduire comme outil d'évaluation d'un système de gestion. Ainsi, l'application actuelle de l'ACV dans les technologies de valorisation énergétique des déchets est présentée.

A partir de tous les éléments développés dans les sections précédentes, la **Section 1.5** présente plus spécifiquement les challenges et verrous actuels de développement de la pyro-gazéification de déchets ménagers solides. Les objectifs et motivations de la présente étude sont détaillés et résumés au travers des 4 aspects suivants :

- Pyro-gazéification de composés représentant typiquement les déchets ménagers solides et établissement d'un modèle prédictif ;
- Optimisation du procédé de pyro-gazéification : amélioration de la qualité du syngas en présence de catalyseur ;
- Etude de la réactivité et de la régénération du catalyseur ;
- Analyse de cycle de vie et optimisation de la technologie de pyro-gazéification.

➢ Chapitre 2: Matériels et Méthodes

Ce chapitre présente les matériaux, les méthodes expérimentales et analytiques, ainsi que les modèles mathématiques utilisés au cours de cette étude.

Les caractéristiques des composés modèles sélectionnés et du catalyseur sont présentées à la **Section 2.1**. Les déchets ménagers sont constitués de plusieurs familles de composés, et 4 composés modèles ont été choisis pour représenter les 4 familles majoritaires : bois de peuplier (bois), carton (papier et carton), pain (résidus alimentaires) et polyéthylène (plastiques). Les matériaux ont été caractérisés par analyses immédiates et ultimes avant introduction dans le procédé de pyro-gazéification. Le catalyseur in situ, CaO, a été introduit en lit fixe dans le réacteur pour réaliser la gazéification catalytique du bois en présence de vapeur d'eau, et caractérisé avant et après les expériences (porosité, surface spécifique, structure chimique).

La **Section 2.2** décrit les procédés expérimentaux, ainsi que les procédures. Un réacteur à lit fluidisé de laboratoire a été utilisé pour réaliser les expériences de pyro-gazéification des composés modèles, la gazéification catalytique sous vapeur d'eau, ainsi que l'étude du cycle de carbonatation/calcination du catalyseur CaO. Les conditions opératoires pour chaque série d'expériences sont détaillées. Le montage d'ATG (analyse thermogravimétrique) est aussi décrit car utilisé spécifiquement pour étudier la variation de masse de CaO au cours de cycles de sorption/désorption de CO_2.

Les méthodes analytiques et l'échantillonnage des produits sont décrits à la **Section 2.3**, incluant la caractérisation des goudrons et du char. L'analyse des solides (char et catalyseur) vise à étudier les propriétés thermiques et physico-chimiques en utilisant les méthodes suivantes : l'ATG, la microscopie électronique à balayage, la diffraction de rayons X et l'adsorption de gaz (théorie Brunauer-Emmett-Teller, BET).

Enfin, les méthodes de modélisation mathématique sont présentées en **Section 2.4.** La méthode du réseau de neurones artificiels (ANN) est utilisée pour développer un modèle prédictif de la pyro-gazéification. Ses concepts, principes et le processus d'implémentation sont présentés en détail. Cette partie détaille aussi les procédures d'utilisation de l'analyse de cycle de vie (ACV) dans la gestion des déchets et plus particulièrement pour l'analyse du système de pyro-gazéification.

➢ Chapitre 3: Pyro-gazéification des Déchets

La pyro-gazéification des déchets est un procédé thermochimique complexe, en raison de la complexité de composition des déchets et des agents réactifs. Pour atteindre l'objectif de production d'un syngas de haute qualité, deux parties ont été étudiées et consignées dans ce chapitre. Tout d'abord, le procédé a été caractérisé en utilisant des composés modèles et en mélange. Les 4 déchets modèles, tels que le bois de peuplier, le carton, le pain et le polyéthylène (PE), ont été étudiés en atmosphère inerte (azote) ou réactive (CO_2, vapeur d'eau). Ensuite, un modèle prédictif de la qualité du syngas obtenu par pyro-gazéification de composés modèles sous différentes atmosphères a été développé. Celui-ci s'est basé sur les résultats expérimentaux obtenus au cours de la première partie (composition entrante et composition du syngas produit). Ce modèle a ensuite permis de comparer l'application du procédé de pyro-gazéification à des compositions variables de déchets, comme celles rencontrées en France et en Chine. Les principaux résultats de ce chapitre sont résumés dans les paragraphes suivants.

La **Section 3.2** présente la pyro-gazéification des 4 composés seuls sous différentes atmosphères (N_2, vapeur d'eau et CO_2), afin d'évaluer l'impact de la composition de la ressource et de l'atmosphère. Les résultats indiquent que la composition du syngas est dépendante de la ressource. Bien que le bois et le carton produisent le même type de composés majeurs dans le syngas, la réactivité du carton est supérieure en raison d'une structure plus aérée que celle du bois. Le pain, représentatif des déchets alimentaires, produit la plus grande quantité de gaz et le char récupéré est plus poreux. La modification de la phase solide au cours de la réaction améliore, en particulier en termes de surface spécifique, améliore significativement les réactions de craquage qui conduisent à la production de gaz. La pyro-gazéification du PE conduit à une concentration importante de H_2 et CH_4, mais le char résultant a une réactivité limitée.

Concernant l'impact de l'atmosphère, la vapeur d'eau améliore significativement la quantité de gaz par rapport au CO_2, ce qui est lié à une augmentation de la cinétique des réactions. La présence de vapeur d'eau favorise considérablement la production de H_2, permettant de produire un syngas de ratio H_2/CO compatible avec un procédé Fischer-Tropsch. La présence de CO2 comme atmosphère réactive impacte positivement la quantité de CO produit.

Après une étude de la pyro-gazéification des composés seuls, la **Section 3.3** relate les résultats obtenus avec les mélanges de 2, 3 puis 4 composés. Les résultats expérimentaux

sont systématiquement comparés à une valeur théorique, provenant des résultats obtenus à la section précédente, afin d'identifier les possibles interactions entre les composés. Une interaction est systématiquement observée et généralement, elle est de type synergie positive. Ces interactions peuvent être expliquées par de nombreux facteurs, tels que les liaisons chimiques présentes dans les ressources, la structure du char, l'effet catalytique des minéraux alcalins, la réactivité liée à l'atmosphère, etc.

En raison de la complexité du système et des facteurs influençant l'efficacité du procédé, un modèle prédictif a été développé (**Section 3.4**), sur la base d'un réseau de neurones artificiels (ANN). Ce modèle utilise une structure en 3 couches (données d'entrée, données de sortie et données cachées), et est résolu à l'aide de MATLAB Neural Network Toolbox. Un total de 45 expériences issues des sections précédentes a été utilisé pour établir le modèle. Les données ont été intégrées aux 3 étapes d'établissement du modèle : essai, validation et test. Les résultats confirment que ce modèle est adéquat pour représenter de manière prédictive la composition du syngas en fonction de la composition initiale de l'atmosphère choisie.

Enfin, ce modèle est ensuite appliqué pour comparer les caractéristiques de la pyro-gazéification de déchets solides ménagers en France et en Chine (**Section 3.5**). Les résultats indiquent que la quantité de syngas produit est supérieure en France, mais que les concentrations de H_2 et CH_4 sont supérieures en Chine, en raison de la composition des déchets. Les ratios H_2/CO obtenus dans le syngas se trouvent dans la gamme 1,2-3,2 ; ce qui rend son utilisation compatible avec les procédés de synthèse Fischer-Tropsch ou de récupération d'énergie. En conclusion, le modèle ANN est approprié pour prédire les caractéristiques du procédé de pyro-gazéification des déchets, basé sur la composition entrante.

➢ Chapitre 4: Gazéification Catalytique du Bois

L'optimisation du procédé de pyro-gazéification des déchets ménagers solides est étudiée en vue de produire un syngas de haute qualité. Pour cela, la gazéification sous vapeur d'eau du bois de peuplier a été menée expérimentalement en lit fluidisé, en présence de CaO, un catalyseur in situ. L'impact des paramètres suivant a été étudié : le ratio massique catalyseur/bois, le débit de vapeur d'eau et la température de réaction. Les performances du procédé ont été comparées au procédé non catalytique. L'objectif du travail est double : (1)

identifier les conditions opératoires optimales pour la production d'un syngas riche en H_2 ; (2) abaisser la température de la réaction en présence de catalyseur pour minimiser l'apport énergétique, tout en conservant un syngas de haute qualité. Les principaux résultats sont résumés à la **Figure 4.17**.

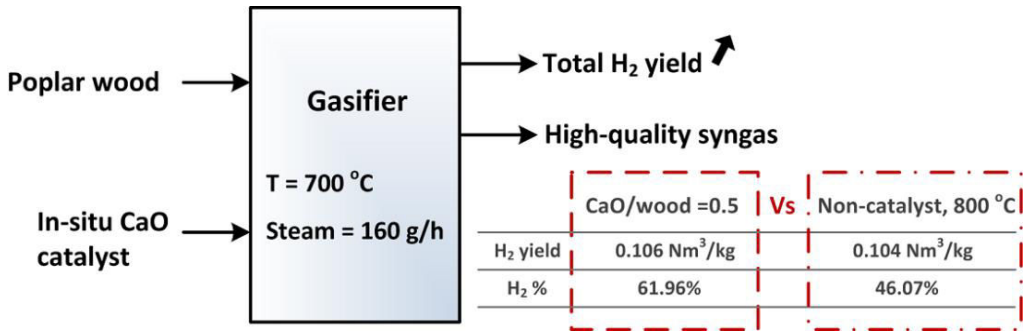

Figure 4.17 Structure et principales conclusions du Chapitre 4

Tout d'abord, la recherche des conditions opératoires optimales à la réalisation de la gazéification catalytique du bois en présence de vapeur d'eau est résumée comme suit :

- L'ajout de CaO démontre un effet catalytique evident permettant l'augmentation de la quantité de H2 dans le syngas. Simultanément, l'augmentation du ratio massique catalyseur/bois de 0 à 1 abaisse de manière conséquente la production de goudrons, en favorisant les réactions de reformage.

- L'augmentation du débit de vapeur d'eau impacte positivement les réactions du gaz à l'eau, augmentant ainsi la quantité de H_2 produite. Cependant la qualité du syngas se détériore aux débits les plus élevés. Ainsi, la quantité et qualité de syngas les plus élevées sont ainsi obtenues à un débit de 160g/h.

- L'élévation de température favorise la réaction du gaz à l'eau et le reformage, améliorant ainsi la production de H_2 et réduisant de la quantité de goudrons. Cependant, la concentration de H_2 diminue lorsque la température excède 700°C. en conclusion, la température de réaction optimale doit donc être déterminée en tenant compte de l'effet de la température sur l'efficacité de la gazéification elle-même et la capacité de carbonatation de CaO.

A la suite de cette première partie, les résultats obtenus par le procédé catalytique ont été comparés à ceux issus de la pyro-gazéification sous vapeur d'eau en l'absence de catalyseur. Les résultats indiquent que la même quantité de gaz est obtenue à 700°C en gazéification catalytique (addition de 50% en masse de CaO) et à 800°C sans catalyseur. De

plus, la concentration en H_2 et le ratio H_2/CO sont améliorés en condition catalytique. De ce fait, l'addition de catalyseur CaO (50% en masse) permet de réduire de 14% la température de réaction (de 800°C à 700°C) de la gazéification du bois sous vapeur d'eau.

L'ensemble de ce travail montre que la gazéification catalytique, menée avec un catalyseur abondant et à bas coût tel que le CaO, est une approche potentielle favorable au développement du procédé en terme d'efficacité de la gazéification, de qualité du syngas et de consommation énergétique.

➢ Chapitre 5: Désactivation et Régénération du Catalyseur

Les résultats présentés au chapitre précédent ont démontré l'intérêt d'utiliser CaO comme catalyseur in situ pour améliorer l'efficacité de la gazéification et la qualité du syngas. L'objet de ce travail est maintenant d'étudier la régénération du catalyseur pour faciliter son introduction industrielle. L'étude de la régénération est basée sur des cycles successifs de carbonatation/calcination de CaO, où le CO_2 est piégé pendant le cycle de carbonatation puis éliminé lors de la calcination.

Cependant, la réactivité de CaO diminue signification après de multiples cycles. Dès lors, le travail met plus spécifiquement l'accent sur les mécanismes impliqués dans la désactivation du catalyseur, et le meilleur moyen de le régénérer. Les résultats principaux sont résumés au travers de la **Figure 5.12**.

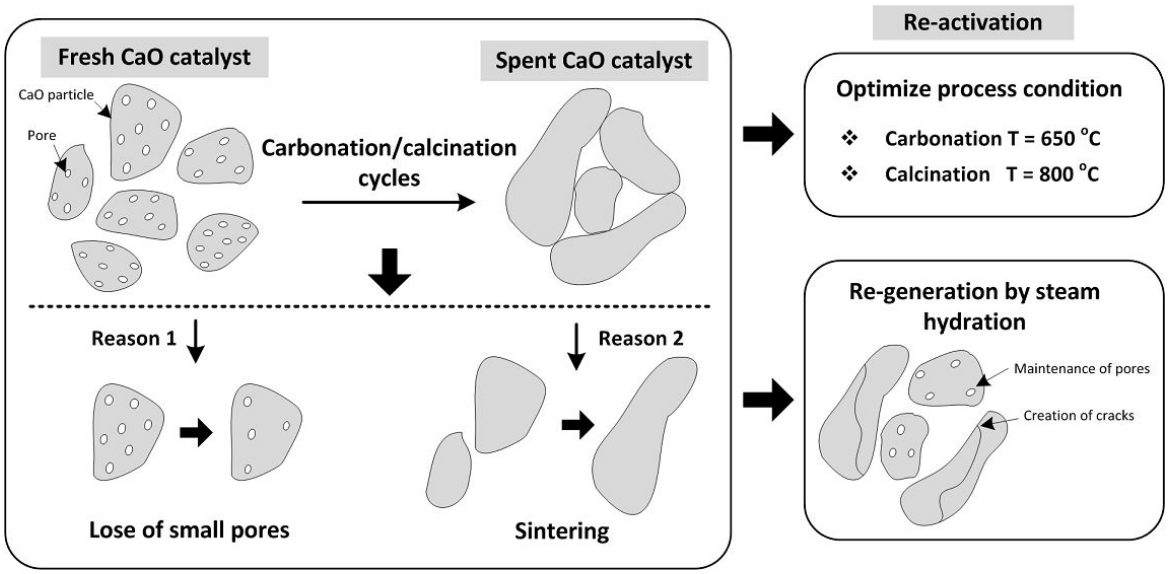

Figure 5.12 Mécanismes de désactivation et de réactivation du catalyseur CaO proposés au cours du développement du Chapitre 5

Tout d'abord, la capacité d'adsorption de CO_2 par le CaO et la morphologie du catalyseur ont été étudiés après plusieurs cycles. Ainsi, le mécanisme et la cinétique de désactivation du catalyseur CaO ont été discutés. Deux phénomènes peuvent expliquer la désactivation (comme indiqué à la **Figure 5.0.1**). Une première raison concerne l'obstruction des petits pores au cours de la carbonatation, ceux-ci n'étant pas réouverts durant la calcination (phénomène irréversible). Une seconde raison concerne aussi la perte de porosité et de surface spécifique par frittage. La « coalescence » des particules au cours du cycle de calcination réduit ainsi la porosité, et donc la surface active pour la captation du CO_2.

A partir de ces premiers résultats, l'étude de la réactivité de CaO et de sa régénération conduit aux conclusions suivantes :

- L'étude des températures des réactions de carbonatation et de calcination pour différents cycles indique que la température de carbonatation de 650°C est idéale pour combiner une cinétique de réaction et une réactivité élevées. Une température de calcination au-delà de 800°C est défavorable à la réactivité de CaO en raison d'une accélération du phénomène de frittage et une faible capacité de stockage du CO2.
- L'hydratation de CaO par la vapeur d'eau est la voie de régénération étudiée. Après un cycle de carbonatation/calcination, l'hydratation réalisée sous vapeur d'eau est efficace pour maintenir la réactivité de CaO, en termes de surface spécifique et de morphologie. En d'autres termes, la gazéification sous vapeur d'eau, déjà plébiscitée pour améliorer l'efficacité de la gazéification (voir chapitres précédents), est bénéfique pour maintenir l'activité du catalyseur CaO, en assurant sa régénération.

➢ Chapitre 6: Analyse de Cycle de Vie

Ce chapitre est dédié à l'évaluation et à l'optimisation de la technologie de pyro-gazéification des déchets par la méthode d'analyse de cycle de vie (ACV). L'objectif est d'orienter le développement de la technologie de manière appropriée, mais aussi de déterminer les améliorations potentielles en regard des plans locaux de gestion des déchets. Dans ce cadre, deux études ACV ont été réalisées au cours de ce travail.

Une première étude (**Section 6.2**) repose sur la comparaison quantitative de trois sites industriels de valorisation énergétique : un en Finlande, basé sur la gazéification des déchets,

et deux systèmes conventionnels d'incinération basés en France et en Chine (voir **Figure 6.7**). Le système démontrant la meilleure performance environnementale est basé sur la gazéification. Ceci s'explique par : (1) l'efficacité de la récupération énergétique (la réduction de l'émission des polluants dans le syngas produit améliore la quantité d'électricité récupérée) ; (2) les émissions directes du procédé sont réduites significativement grâce aux réactions homogènes en phase gazeuse qui limitent la production de NOx.

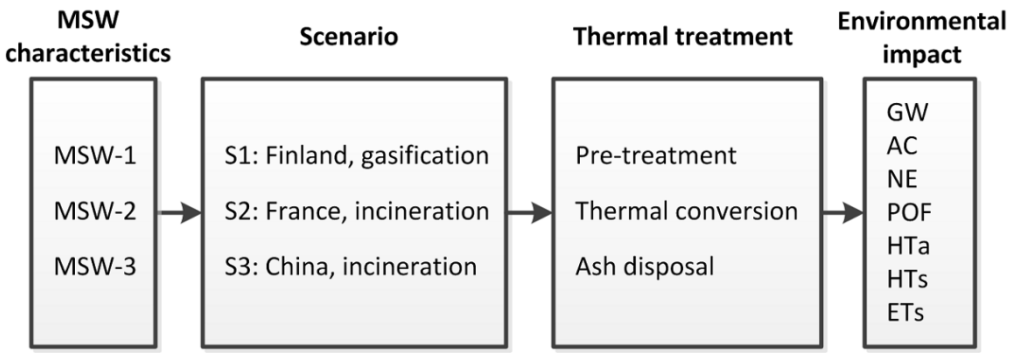

Figure 6.7 Structure et méthodologies de l'ACV utilisées pour comparer les procédés de gazéification et d'incinération des déchets ménagers.

Une comparaison des deux procédés d'incinération est aussi menée, de manière à identifier les pistes d'amélioration en regard de la situation géographique. L'incinération (en France) est particulièrement affectée par l'émission de NOx (près de 5 fois plus que le scénario chinois), ce qui nécessite un contrôle strict des émissions. En Chine, la faible capacité calorifique de la ressource implique une consommation énergétique élevée pour une faible quantité d'énergie récupérée. Cette capacité calorifique pourrait être améliorée au travers de la collecte et du tri de la ressource. Les émissions de dioxines restent plus élevées en Chine mais les normes devenant plus restrictives, l'impact est supposé diminuer.

La **Section 6.3** traite la modélisation du couplage des procédés thermochimiques (pyrolyse et gazéification) à l'utilisation du vecteur énergétique (chaudière à gaz-turbine à vapeur, turbine à gaz et moteur à combustion interne). Comme le montre la **Figure 6.12**, les différents scénarios sont évalués en regard de leur impact énergétique et environnemental. Les indicateurs environnementaux plébiscitent le scénario gazéification/turbine à gaz en raison d'une génération importante d'électricité et une réduction des émissions polluantes. Dans l'ensemble, la pyrolyse présente des performances moindres comparée à la gazéification en raison de sa consommation énergétique élevée. Du point de vue de la conversion énergétique, la tendance est similaire. Ceci indique que la purification du syngas

avant son introduction dans une turbine à gaz est la voie principale d'amélioration suggérée pour les technologies de gazéification actuelles. Cependant, une attention particulière doit être portée à l'étape de refroidissement du syngas pour garantir une récupération efficace de la chaleur et éviter la lixiviation des métaux lourds dans les cendres.

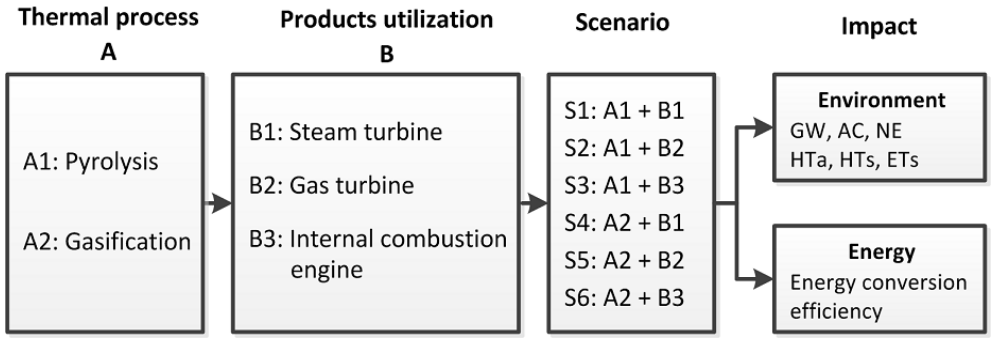

Figure 6.12 Principale structure de l'ACV utilisées pour comparer des approches d'utilisation des produits de pyro-gazéification

Ces résultats sont ensuite concaténés pour analyser l'importance des paramètres clés sur les impacts environnementaux (**Section 6.4**). Trois cas sont discutés, incluant l'utilisation de la cogénération chaleur-électricité, l'effet de la substitution d'énergie et la source des facteurs d'émissions. La maximisation de l'efficacité énergétique et la minimisation des impacts environnementaux sont obtenues en combinant la cogénération aux procédés de gazéification ou d'incinération. De ce fait, le mix énergétique est un paramètre crucial influençant l'évaluation globale. A partir des données des sites en opération, on peut conclure que la valorisation énergétique des déchets basée sur la technique de pyro-gazéification est faisable pour satisfaire les normes de contrôle de pollution et peuvent servir de pistes d'amélioration potentielle des technologies actuelles d'incinération.

➢ Chapitre 7: Conclusions et Perspectives

Ce travail s'est attaché à étudier la pyro-gazéification des déchets ménagers solides du point de vue du procédé, mais aussi du système dans son ensemble, afin de proposer des pistes d'optimisation. Les résultats principaux sont résumés dans les 3 points suivants :

- **Caractéristiques de la pyro-gazéification de composés modèles et développement d'un modèle prédictif.** Quatre composés modèles (bois, carton, pain et polyéthylène) ont été pyro-gazéifiés sous 3 atmosphères différentes (N_2, CO_2, vapeur d'eau), seuls ou en mélanges.

Les expériences menées avec les mélanges ont démontré des interactions positives conduisant à une amélioration de la quantité et de la quantité du syngas. L'ensemble des données expérimentales ont ensuite servi à l'établissement d'un modèle de type réseau de neurones, capable de prédire la quantité et la composition du syngas en fonction de la composition de la ressource et de l'atmosphère utilisée.

- **Amélioration de la qualité du syngas par gazéification catalytique sous vapeur d'eau et étude de la réactivité du catalyseur CaO.** La gazéification catalytique du bois de peuplier a été réalisée en présence de CaO comme catalyseur in situ, en vue d'optimiser la production d'hydrogène. L'influence du ratio massique catalyseur/biomasse, du débit de vapeur d'eau et de la température de réaction a été étudiée. La présence de CaO augmente la quantité de gaz et la concentration de H_2 jusqu'à un certain seuil. A quantités de gaz produit égales, la gazéification catalytique (50% CaO) permet d'abaisser de 100°C la température de réaction (de 800 à 700°C). Donc, le catalyseur in situ permet d'augmenter la quantité et la qualité du gaz (température constante), ou d'abaisser la température de réaction (quantité de gaz constante) et donc la consommation énergétique.

L'utilisation d'un catalyseur à l'échelle industrielle est viable si sa durée d'opération est suffisante. La réactivité de CaO repose sur sa capacité à capter le CO_2 et à améliorer les réactions de craquage des goudrons. Des mécanismes responsables de la désactivation ont été identifiés après plusieurs cycles de carbonatation/calcination. L'occlusion des micropores au cours de la carbonatation et le frittage lors de la calcination sont les 2 principaux mécanismes responsables de la désactivation. Ainsi, la carbonatation doit idéalement se dérouler à 650°C tandis que la température de calcination ne doit pas dépasser 800°C. Une étape d'hydratation a montré un effet bénéfique sur la régénération du catalyseur.

- **Utilisation de l'analyse de cycle de vie (ACV) pour évaluer et optimiser la technologie de pyro-gazéification.** Deux études d'ACV ont été réalisées dans le but de développer une technologie de valorisation énergétique efficace énergétiquement et respectueuse de l'environnement tout en mettant en évidence les voies d'amélioration. Trois scénarios de systèmes commerciaux ont été considérés puis comparés : une technologie de gazéification (Finlande) et l'incinération conventionnelle (France et Chine). Les indicateurs des performances environnementales du système de gazéification sont meilleurs que ceux de l'incinération. Ces bénéfices sont dus à : (1) une réduction des émissions polluantes, et (2) une meilleure génération d'énergie. Pour atteindre une vision plus intégrée du gestion des déchets ménagers, une seconde analyse a été réalisée en combinant à la fois la

transformation des déchets en vecteur énergétique et la mise en œuvre de ce vecteur (chaudière à gaz-turbine à vapeur, turbine à gaz et moteur à combustion interne). L'impact environnemental le plus faible revient à la turbine à gaz, suivi de la turbine à vapeur puis du moteur à combustion. En conclusion, le scénario optimisé serait l'association de la gazéification avec une turbine gaz, à condition de mettre en place une étape intermédiaire de purification du syngas efficace.

L'ensemble de ces résultats peuvent servir de base à des recherches futures, dont les perspectives peuvent être énoncées autour de trois grands axes :

1) Approfondir la connaissance et la compréhension des émissions polluantes (fines particules, chlore…) au cours de la pyro-gazéification des déchets ;
2) Optimiser le procédé en améliorant les qualités et les propriétés du catalyseur
3) Evaluer systématiquement et comparer les différents procédés de pyro-gazéification.

Acknowledgment

I would like to express the deepest appreciation to my supervisors, Professor Ange Nzihou and Professor Yong Chi, for introducing me to the subjects of this thesis and for providing me the opportunities and mentorship throughout my Ph.D studies. Both professors provided me with every bit of guidance, assistance, and expertise that I needed during my research; at the same time they took time to discuss any problems I encountered. Without their guidance and persistent help this dissertation would not have been possible.

I am deeply indebted to my advisor Elsa Weiss-Hortala, for her fundamental role in my doctoral work. When branching out into new research areas, Elsa continued to contribute valuable feedback, advice, and encouragement. In addition to our academic collaboration, I greatly value the close personal rapport that Elsa and I have forged over the years. I quite simply cannot imagine a better advisor.

I owe a great debt of gratitude to the 'Program of Introducing Talents of Discipline to University (111-project)' of Zhejiang University in China, for their financial support granted through this research work. It has provided me the opportunity to study in both Ecole des Mines d'Albi (France) and Zhejiang University (China), to have the chance getting accustomed with waste management in both countries and finally formed the context of this dissertation. I would like to thank Professor Mingjiang Ni, who is the leader of this collaborative project and also my supervisor in Zhejiang University, for all his help, advice, support and encouragement. He has long been an inspiring figure for me, and I feel extremely privileged to be his student. In addition, I gratefully acknowledge the members of my Ph.D. committee for their time and valuable feedback on a preliminary version of this thesis. Their spirit of adventure in regard to research and scholarship will always guide a bright path forward my academic career.

I am very thankful to the faculty at RAPSODEE, Ecole des Mines d'Albi. Thanks to the technicians for their kind support in helping me running experiments and sharing with me their knowledge of analytical techniques. Thanks to Nathalie Lyczko for her help with the XRD experiments and analysis; to Céline Boachon with the TG tests; to Christine Rolland with

the SEM experiments and imaging; to Sylive Delconfetto with the BET tests; and to Jean Marie Sabathier with the elemental analysis. I am grateful to Mickael Ribeiro, for his expertise and commitment to helping me setting up and running the reactor. I also would like to thank for the help of secretaries, Chrystel Auriol Alvarez, Anne-Marie Fontes and Valérie Veres, their works are always extremely valuable.

I could not have completed the PhD program without the inspiration, friendship and support of my colleagues and friends. I am thankful to Marion Ducousso, who has guided me to use the reactor and worked with me in the same lab for more than 2 years. Also many thanks to Bruna Vero de Vasconcelos, who taught me to use different analyzing equipements. Their capabilities as well as the enthusiasm and motivation are a great help in completing my work. I am very grateful to the research group I worked with, Doan Pham Minh, Elias Daouk, Pierre-Marie Nigay, Marwa Said, Augustina Ephraim, Maxime Hervy, Maxime Deniel, Chaima Chaabani, Ludovic Moulin, Lina Maria Romero Millan, Abdoul Razac Sane and Rabbe Sani, for their kind help to me whenever I needed, for providing me with the resources during each of my visits to France, for their infinite patience teaching me French, for all the great times that we have shared. I am particularly thankful to Yuanjun Tang, who has worked together with me for more than 5 years in both France and China; we are not only partners in research work but also intimate friends in the life. I would like to express my deeply grateful to Zheng Jiang, I really do not know how can I thank you enough for your kind and warm help whenever and wherever.

Finally, this last word of acknowledgment I have saved for my family. Thank you for the love, support, and patience. Without you, I would not have reached this point.

Jun DONG

December 2016

Content

Abbreviation List

AC	Acidification
ANN	Artificial neural networks
BET	Brunauer-Emmett-Teller
BP	Backpropagation
$CaCO_3$	Calcium carbonate, or limestone
CaO	Calcium oxide
$Ca(OH)_2$	Calcium hydroxide
CCE	Carbonation conversion efficiency
CCS	Carbon capture and storage
CFD	Computational fluid dynamics
CH_4	Methane
CHP	Combined heat and electricity
CO_2	Carbon dioxide
CO_2/M	Carbon dioxide to MSW ratio
CO	Carbon monoxide
EDIP	Environmental Development of Industrial Products
EDX	Energy-dispersive X-ray spectroscopy
ER	Equivalence ratio
ESEM	Environmental Scanning Electron Microscope
ETs	Ecotoxicity via solid
ETwc	Ecotoxicity via water chronic
GW	Global warming
GHG	Greenhouse gas
H_2	Hydrogen
HTa	Human toxicity via air
HTs	Human toxicity via solid
HTw	Human toxicity via water
IGCC	Gas turbine combined cycle

IPCC	Intergovernmental Panel on Climate Change
ISO	International Organization for Standardization
LCA	Life cycle assessment
LCI	Life cycle inventory
LCIA	Life cycle impact assessment
LHV	Lower heating value
MSW	Municipal solid waste
NE	Nutrient enrichment
OD	Ozone depletion
PE	Polyethylene
Pe	Person equivalence
POF	Photochemical ozone formation
PP	Polypropylene
RDF	Refuse derived fuels
RE	Relative error
S/M	Steam to MSW ratio
SEM	Scanning Electron Microscopy
SETAC	Society of Environmental Toxicology and Chemistry
SETs	Stored ecotoxicity in soil
SETw	Stored ecotoxicity in water
SGWR	Spoiled groundwater resources
SRF	Solid recovered fuel
TG/DTG	Thermogravimetric and derivative thermogravimetric
TGA	Thermogravimetric analyzer
WtE	Waste-to-Energy
XRD	X-ray diffraction

General Introduction

Worldwide MSW production

As the world hurtles towards rapid industrialization and urbanization, the amount of municipal solid waste (MSW), one of the most important and abundant by-products of an urban lifestyle, has increased dramatically during the last decades. Currently, about 1.3 billion tons of MSW are generated annually worldwides; and this volume is expected to reach 2.2 billion tons by 2025 according to the estimation of the World Bank [1]. However the local waste characteristics vary with cultural, climatic, socioeconomic variables, and institutional capacity [2]. Globally, MSW composition varies significantly with regions. A comparison of average MSW compositions relative to the countries' income level is illustrated in **Figure 0. 1**.

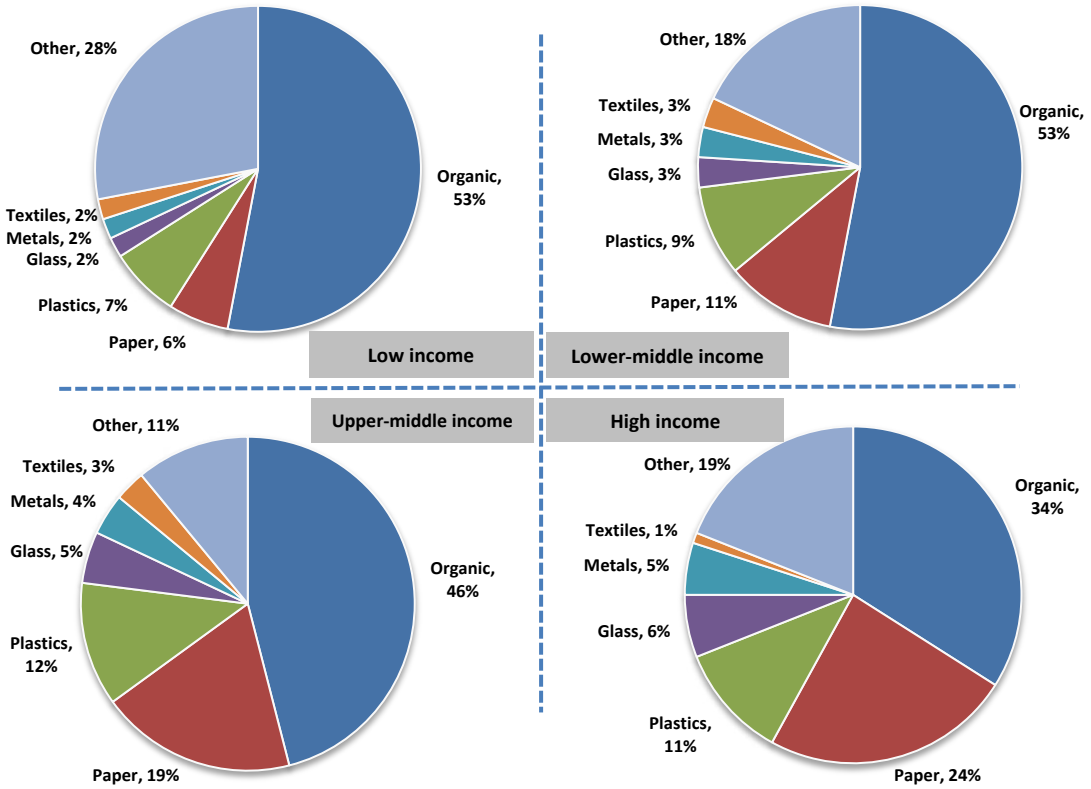

Figure 0. 1 MSW compositions grouped by the country income levels

Data source: Data derived from the report by United Nations Environment Programme

(UNEP) [3]**.**

Note: **(1) "Other" represents inorganic waste;**

(2) The data are based on 97 countries between 1990-2009, including 22 in Africa, 14 Asia-Pacific, 35 Europe, 19 Latin America/Caribbean, 2 North America and 5 West Asia.

(3) Countries are classifed into four income levels according to World Bank estimates of 2005 GNI per capita. Low income: USD 875 or less; lower-middle income: USD 876 - 3,465; upper-middle income: USD 3,466 - 10,725; high income: USD 10,726 or above.

One major difference is found for the proportion of organic, which represents a relatively high concentration of the MSW stream for lower-income countries (average 46-53%) when compared with high-income countries (average 34%). Conversely, the ratio of paper appears to raise in accordance to the income levels, which has steadily climbed from 6% in low-income to 24% in high-income countries. This is in line with the data representing of the European situation, which reveal that almost half of the MSW generated originates from packaging material [4]. Besides, energy sources are also found to impact the percentage of inorganic. This is especially true in low-income countries where energy for cooking, heating, and lighting might not come from district heating/electricity system, so that the ash content due to energy use will probably be higher.

There has long been speculated that MSW composition affects the physical characteristics of waste. High fraction of organic will lead to a dense and humid MSW that impacts not only on the collection and transport system but also its subsequent energy recovery potential. In many developing countries, MSW generally has a low caloric value because of its high moisture content combined to the prior removal of paper and plastic by waste pickers [5]. This in a large extent, hinders efficient thermal process, and additional fuel (usually oil or coal), are required in order to maintain the wastes burning [6]. The variation in regional MSW composition thus requires development in local waste management system.

Efficient MSW management system

From the perspective of economy, the cost of MSW management will keep increasing from today's annual USD 205.4 billion to about USD 375.5 billion in 2025 [1]. This holds particularly severe impacts in low income countries, where the average cost is estimated to

experience more than 5-fold increases and will certainly impose heavy burdens to local authorities. Meanwhile, improperly treated MSW can also lead to a major impact on the environment and human health. Poorly treated MSW may contaminate nearby water bodies with organic and inorganic pollutants [2]; thus threatens public health by attracting disease vectors leading to human and ecological toxicity. MSW treatment, especially landfill, may also emit a variety of greenhouse gas (GHG) as a result of organics decomposition and incomplete gas collection. Such quantity is non-negligible and according to the estimation of IPCC (Intergovernmental Panel on Climate Change) [7], waste management accounts for 5% of the global GHG emissions and 9% of the methane released in the atmosphere. Realizing these facts, proper waste management is hence an urgent and important requirement for the sustainable development of the urban world [8].

With continuously growing concerns from cities and municipalities, the concept of 'integrated waste management' has been developed and widely accepted to inspire the waste management policy. The waste hierarchy, as defined by European Directive 2006/12/EC [9] and updated by Directive 2008/98/EC [10] in 2008, is regulating which waste technologies should be applied preferentially. As illustrated in **Figure 0. 2**, the hierarchy starts from the '3R principle': reduce, reuse, and recycle. The waste diversion is then followed by a series of MSW treatment options. From most to least environmentally friendly, the hierarchy lists the following: recovery (e.g. high-efficient incineration, digestion and composting), disposal (low-efficient incineration and landfill), with controlled dump ranking last. As could be realized, the core principal of integrated MSW management highlights the importance of sustainable resource and environmental management [11, 12]. MSW system should be designed holistically to minimize resource input, to maximize energy utilization efficiency, and to reduce the associated environmental impacts as well.

Figure 0. 2 Diagram of waste hierarchy as regulated by European Directive 2008/98/EC

Globally, attempts are made through policies and technological development toward building optimal MSW management systems. **Figure 0. 3** shows the most recent waste management situation in different countries. As indicated in the figure, recycling is well implemented in most European countries. This is mainly achieved via MSW source-separated collection and bio-waste utilization. There is a clear evidence of a shift up the waste hierarchy, thanks to the legislation guidance by the European environmental policy. Actually, the EU's Waste Framework Directive [10] and Landfill Directive [13] have set binding targets for recycling MSW and diverting biodegradable waste from landfill, for which a 50% recycling target is expected to be fulfilled by 2020. In a report assessing the effective implementation of these policies, it is shown that 12 EU countries have substantially increased the percentage of recycled materials by more than 10% between 2001 and 2010 [14] and recycling has resulted in a turnover of more than EUR 60 billion in 2008 [15]. It was also reported that recycling practices a positive effect in some countries like Korea and Singapore. However, developed countries have a higher MSW recycling ratio than developing countries.

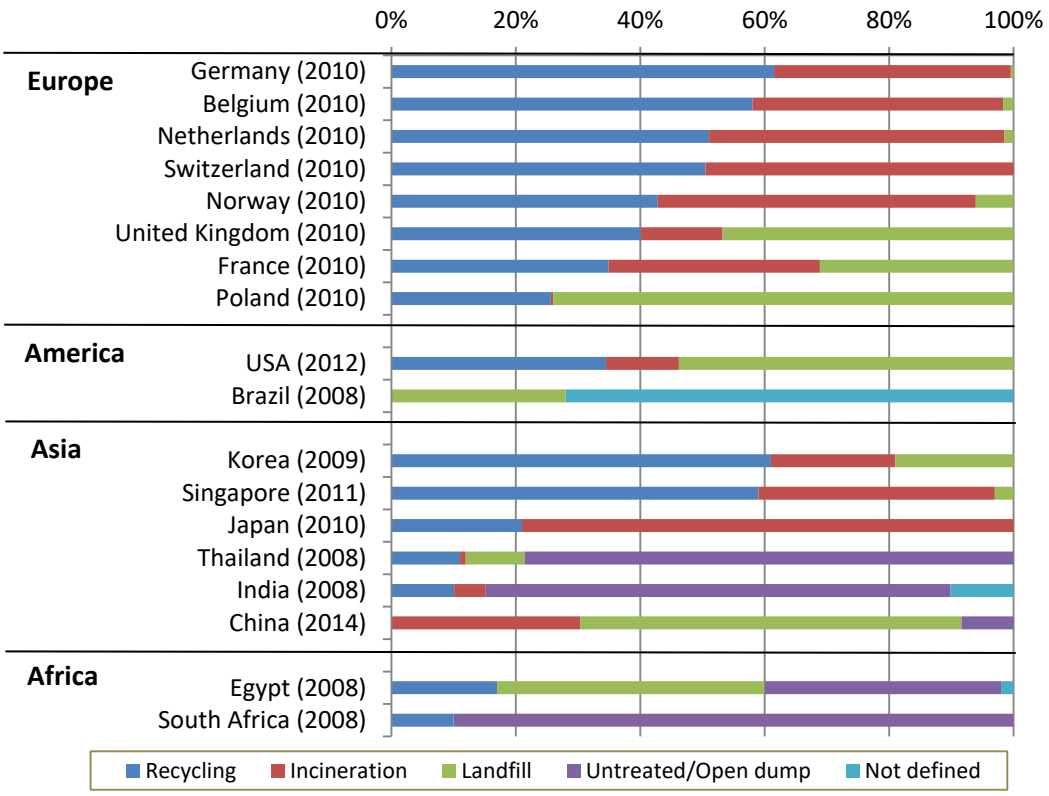

Figure 0. 3 MSW management in selected countries

Data source: Data on European countries are derived from European Environment Agency [14]; data related to other countries are derived from [4, 16].

Note: (1) The category of "recycling" consists of material recycling and food waste

recycling including composting;

(2) The recycling proportion of China is not identified because of the existence of informal waste recycling and the limited information.

However, technological development also paves the way toward more integrated waste management. Great efforts are made to reduce open and uncontrolled dumping. Open-burning and incineration alone without energy recovery are also discouraged because of pollution and/or process costs [5]. Instead, growing attentions have been paid to extract more energy from wastes. Such technologies include efficient gas capture from landfills, anaerobic digestion and composting of organic waste, as well as waste incineration for electricity/heat production (referred to as Waste-to-Energy, WtE). As shown in **Figure 0. 3**, Japan leads in incineration percentage, reaching 79% because of its advanced incineration technology and equipment being regarded as environmentally friendly. In addition, the proportion of landfill is negligible in Germany, Belgium and Netherlands. Currently, WtE in Europe has already supplied considerable amounts of renewable energy (some 38 billion kWh in 2006). This amount might reach as much as 98 billion kWh by 2020, enough to supply 22.9 million inhabitants with electricity and 12.1 million inhabitants with heat [5]. In USA, 88 WtE plants are in operation by 2009, serving a population of 30 million [17]; whereas in China, the number of WtE plants has increased by a 3.5-folds from 2004 to 2014 [16]. As could be speculated, WtE will keep and play a more prior role in the future waste management system.

Nevertheless and despite the aforementioned progress, developing a well-functioned waste management system is a complex task. For a system to be sustainable in the long term, it has to face the critical bottlenecks that still exist, such technological gaps occur both for developed and developing countries. **The key challenges of an efficient MSW management system could be summarized into the following aspects:**

- Technological development with emphasis on location, energy and environment;

- The need for holistic evaluation and optimization the entire system.

A detailed analysis of those challenges is discussed in the following part.

- **Challenge I: Technological development with emphasis on location, energy and environment**

Over the past decades, WtE has become a most commonly used MSW treatment method as a result of the advantages of significant waste volume reduction (by up to 90%), combined with complete disinfection and energy recovery [1, 18]. However, its broader spread is still not fully accepted in some countries. The reluctance comes both from environmental and energy aspects. The environmental pressure is mainly owing to the toxic emissions, particularly with respect to dioxin, heavy metals and particulate matters, which severely threaten the health of citizens. From the perspective of energy, the European Commission has introduced one criterion called 'R1 formula' [10, 19], stating that if the energy recovery efficiency of an incineration plant is below the designated threshold value (0.65 for plants permitted from 2009 up while 0.60 for older plants), the plant could just be classified as a 'disposal' plant rather than a 'recovery' one. However, almost 40% (119 out of 279) of the European incinerators could not comply with this requirement and are still considered as 'disposal'. As a result, technical development to a more energy-efficient and environmentally-sound MSW treatment method is a very pressing necessity.

In recent years, advanced MSW thermal process, pyro-gasification, has received increasing attention. It is defined as the thermochemical decomposition of MSW in absence of oxygen (pyrolysis) or in partial combustion conditions (gasification). The main product, syngas, mainly consists of a mixture of carbon monoxide (CO), hydrogen (H_2), carbon dioxide (CO_2) and methane (CH_4) [18]. This energetic carrier is further introduced into gas turbine, internal combustion engine, fuel cell, etc. For the development of advanced MSW treatment technologies especially pyro-gasification, in-depth understanding for the pyro-gasification characteristics under different MSW composition becomes essential, in order for parameters optimization towards a more energy-efficient process appropriate to particular local situations. **The following advantages and drawbacks are currently addressed to MSW pyro-gasification.**

Advantages:

- Cleaner combustion stage providing purer H_2 for which further use in an engine produces almost no pollution [18].
- Lower formation of specific pollutants (such as NO_x, dioxin) in an oxygen-deficient atmosphere [20].

- Higher energy recovery efficiency by HCl removal prior to syngas combustion.
- Enlarged syngas utilization routes, e.g., to be used as a fuel to generate electricity or as a basic chemical feedstock in the petrochemical and refining industries [5].

Bottlenecks:

- Pyro-gasification is currently limited by the global efficiency of the process since by-products such as tar and char are produced. In order to produce high-quality syngas, the optimization of multiple parameters, including the selection of MSW composition, gasifying agent (N_2, air, steam, CO_2, etc.), temperature and pressure require in-depth investigation. Besides, researches also focus on the utilization of char for its utilization in many applications including sorbent, catalyst and soil amendment. **Therefore the objectives are to improve the conversion efficiency of MSW into useful products including syngas and char**.
- Pyro-gasification process is not already based on predictive models. This affects the development of the process since operating conditions should always be obtained experimentally. **Therefore a crucial issue is to provide a predictive tool of MSW pyro-gasification based on their various compositions**.
- Energetic aspects, as well as environmental pollutions, should be taken into account in developing pyro-gasification technology. Pyro-gasification process is endothermic that it needs an energy load or input to operate. An important issue is related to the use of catalysts allowing reduction of the reaction temperature as well as by-products generation. **Therefore the use of an in-situ catalyst and its lifetime should be studied**.

However, the development of MSW pyro-gasification technology is still in its early stage. The availability of operation data is still limited, while a number of technical aspects remain a barrier with regards to its commercial exploitation. Moreover, some impurities, especially tar, often remain above acceptable ranges for some specific downstream applications such as gas turbine, internal combustion engine, fuel cell etc. Such reality hence requires a mandatory cleaning of the syngas, which could be achieved by tar separation or catalytic tar reduction. However, an efficient method is yet to be developed for commercial purpose [21].

- **Challenge II: The need for holistic evaluation and optimization of the entire system**

Experience suggests that, developing an integrated and sustainable waste management system is not merely a technological-oriented problem, proper evaluation is also essential to guarantee a well-functioning system that works sustainably for long term. This includes analysis of the current MSW system as well as attempting to modernize the waste treatment through potential improvements toward more efficient energy use and friendly balance with the surrounding environment.

In light of the integrated MSW management concept, the traditional 'end-of-pipe' thinking, focusing only on the last stage of waste treatment, is no longer appropriate. This is because end-of-pipe solutions may not completely solve the problems, but merely move the environmental loadings in space (from upstream to downstream) and time (leaching from landfills in the future) [22]. In this context, integrating the entire system in a holistic way becomes a priority, with the main target to take into account the wider issues of energy and environment across the whole waste management system. From this point of view, life cycle thinking is useful to be severed as the evaluation methodology; and life cycle assessment (LCA) thus emerges to evaluate all the environmental and energy impacts that could possibly occur through the whole lifecycle from cradle to grave.

Guided by the ISO (International Organization for Standardization) 14040 standards [23], LCA has developed for a wide range of applications. LCA applied to integrated MSW management systems shows a great development potential. Particularly, the results of LCA can be used to arrange the available treatment options for a specific type of waste into a priority order [3]. It allows the comparison of different MSW technological options such as landfill, incineration and composting; while providing as well the assessment of different MSW management scenarios as decision making support tool and regional waste strategy planning [24].

A detailed LCA is required to provide options in any specific context, since the option considered 'better' can vary depending on the precise questions asked and the particular local circumstances [3]. In this sense, a quantitative comparison of the newly-developed advancing MSW treatment technologies with traditional ones is needed to guarantee good sense of the impacts on energy and environmental aspects. The assessment should also include a regional-level waste system guiding for the future waste technologies development and strategies.

Given a comprehensive review of the aforementioned challenges, the aim of this thesis is hence aimed at '**MSWs gasification with emphasis on energy, environment and life cycle assessment**'. Thanks to a collaborative research between France (Ecole des Mines d'Albi) and China (Institute for Thermal Power Engineering of Zhejiang University), the author had the chance to get accustomed with waste management in both countries. As a result, this research mainly focuses on MSW gasification for syngas production, involving both experimental-based technological investigation and assessment modeling. Besides, the geographical difference in MSW characteristics is also considered, reflecting both in the pyro-gasification prediction model establishment as well as the LCA comparison of WtE technologies in different regions. The structure of this thesis is presented in **Figure 0. 4**, with a brief introduction of each chapter as follows.

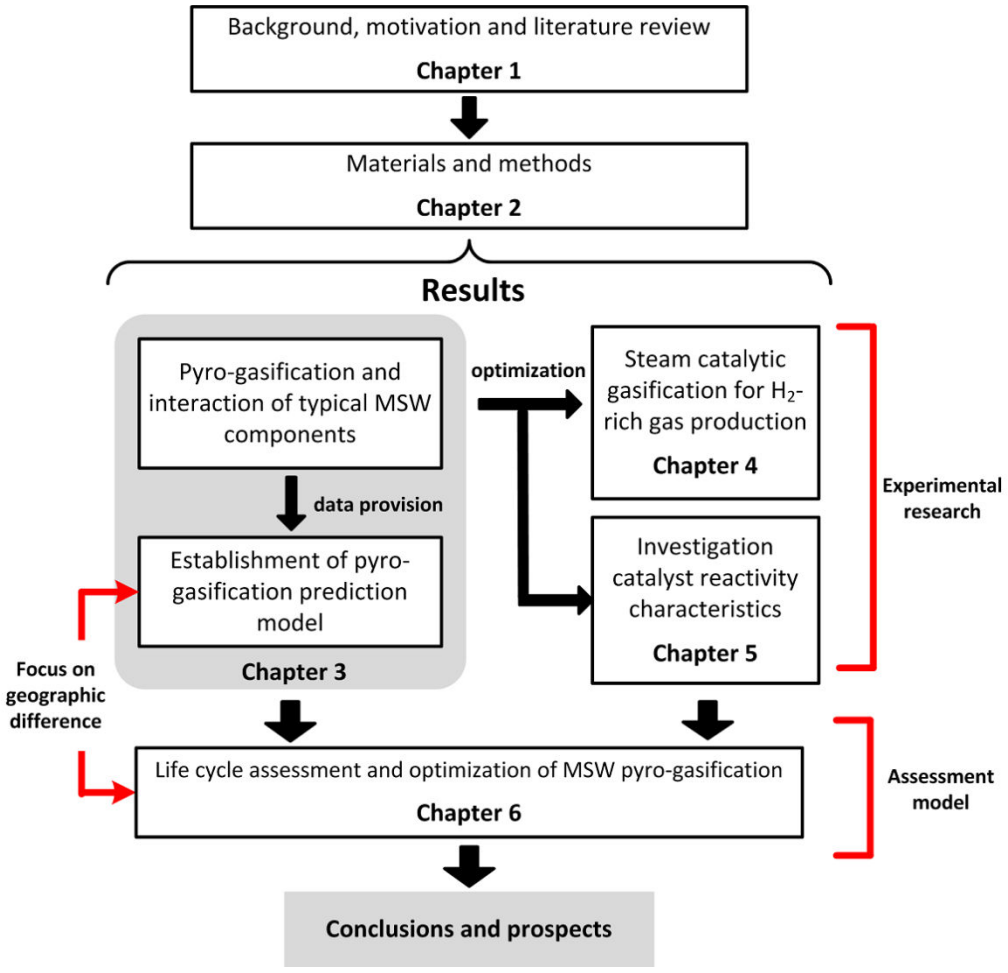

Figure 0. 4 Structure of the thesis

- **Chapter 1** is dedicated to the literature review showing the basics of MSW pyro-gasification, its potential advantages, the main technologies being considered and the state-to-art bottlenecks. Then, attention will be given to the operating parameters that affect MSW pyro-gasification characteristics, and their prediction methods followed by the process optimization and syngas utilization approaches. LCA is applied as evaluation model; and its definition, implementation procedures and current development are thus extensively reviewed.

- **Chapter 2** presents the materials and methods that have been employed to carry out the experimental research and modeling work. Four typical MSW components including wood, paper, food waste and plastic, are used as feedstock; while calcium oxide (CaO) is used as the catalyst. Experiments are mainly conducted in a lab-scale fluidized bed reactor. As well a thermogravimetric analyzer is also used to analyze the CaO reactivity related to **Chapter 5**. Different sampling analysis methods, which are used to qualify both the obtained gas and solid characteristics, then introduced and described. With regard to the modeling aspect, artificial neural network is applied to establish the MSW pyro-gasification prediction model. In addition, LCA is used for the quantitative assessment of the energy and environmental impacts. The modeling framework of both methods is described in detail in this chapter.

- **Chapter 3** focuses on pyro-gasification experiment applied to MSW, in order to "tackle" the following bottlenecks of the technology: MSW composition, hig-quality syngas production, and predictive model development. Firstly, four typical MSW components as aforementioned are pyro-gasified using three reaction agents (N_2, steam and CO_2). Both the pyro-gasification characteristics of single-component and the mixture of multi-components are investigated, aiming at gaining a better understanding of the syngas properties and the interaction mechanisms. Secondly, the obtained data are used as basis for the establishment of a pyro-gasification prediction model. The model is then applied to compare MSW pyro-gasification characteristics between France and China considering their geographical difference in MSW composition.

- **Chapter 4** is dedicated to optimize the gasification process, in which steam gasification is experimentally investigated uusing CaO as an in-situ catalyst. The objectives are to improve the production of H_2-rich syngas as well as to study a reduction of reaction temperature to improve the energy balance. The influence of several operating

parameters such as steam flowrate, CaO addition ratio and reaction temperature are examined. The results are then compared with non-catalyst high-temperature gasification situations in order to investigate the potential of reducing the operating temperature through the use of a catalyst.

- **Chapter 5** analyzes the CaO de-activation and re-generation characteristics, in order to facilitate its recycling as catalyst during long series of carbonation-calcination cycles at industrial scale. First, the CO_2 adsorption capacity of CaO is experimentally examined, and, the de-activation mechanism is discussed. Afterwards, operating variables including the effects of carbonation/calcination temperature and steam hydration are investigated, in order to optimize the process as well as for catalyst re-generation.

- **Chapter 6** conducts LCA modeling work related to pyro-gasification technology. First, three commercially operated WtE plants, including one MSW gasification-based power plant in Finland and two conventional incineration plants both in France and China, are quantitatively compared to verify their environmental performance. Then, pyrolysis and gasification coupled with three types of energy utilization cycles, i.e., gas boiler-steam turbine, gas turbine and internal combustion engine, are further modeled, and potential improvement pathways with emphasis on energy and environment are proposed.

Finally, the general conclusions related to the present work are summarized, and prospects are proposed for future research works to complete the current investigations.

Bibliography

[1] Hoornweg Daniel, Bhada-Tata Perinaz. What a waste: a global review of solid waste management. Washington DC: The World Bank; 2012.

[2] Vergara Sintana E, Tchobanoglous George. Municipal solid waste and the environment: a global perspective. Annual Review of Environment and Resources. 2012;37:277-309.

[3] Wilson David C. Global Waste Management Outlook: United Nations Environment Programme (UNEP); 2015.

[4] Eawag Sandec CWG. Global Waste Challenge, Situation in Developing Countries. Dubendorf, Switzerland: EAWAG - Institut de Recherche de l'Eau du Domaine des EPF; 2008.

[5] UNEP Global Environmental Alert Service. Municipal solid waste: Is it garbage or gold? UNEP Report (http://www.unep.org/geas), October 2013.

[6] UN-HABITAT. Collection of municipal solid waste in developing countries. United Nations Human Settlements Programme (UN-HABITAT), Nairobi; 2010.

[7] Parry Martin L. Climate change 2007-impacts, adaptation and vulnerability: Working group II contribution to the fourth assessment report of the IPCC: Cambridge University Press; 2007.

[8] Habitat UN. Solid waste management in the world's cities. United Nations Human Settlement Program. 2010.

[9] Directive Waste Framework. Directive 2006/12/EC of the European Parliament and of the Council of 5 April 2006 on waste. Official Journal of the European Union. 2006;144.

[10] Council of European Communities. Directive 2008/98/EC of the European Parliament and of the Council of 19 November 2008 on waste and repealing certain Directives. Official Journal of the European Union L. 2008;312.

[11] Clift R, Doig A, Finnveden Göran. The application of life cycle assessment to integrated solid waste management: Part 1—Methodology. Process Safety And Environmental Protection. 2000;78:279-287.

[12] Clift R. Pollution ad Waste Management 1: Cradle to Grave Analysis. Science in Parliament. 1993;50.

[13] Council of European Communities. Directive 1999/31/EC on the landfill of waste. Official Journal of the European Union L. 1999;182:1-19.

[14] Fischer C, Gentil E, Ryberg M, Reichel A. Managing municipal solid waste-a review of achievements in 32 European countries. European Environment Agency, Copenhagen,

Denmark. 2013.

[15] European Environment Agency. Earnings, jobs and innovation: the role of recycling in a green economy. European Environment Agency, Copenhagen 2011.

[16] Mian Md Manik, Zeng Xiaolan, Nasry Allama al Naim Bin, Al-Hamadani Sulala MZF. Municipal solid waste management in China: a comparative analysis. Journal of Material Cycles and Waste Management. 2016:1-9.

[17] Psomopoulos CS, Bourka A, Themelis Nickolas J. Waste-to-energy: A review of the status and benefits in USA. Waste Management. 2009;29:1718-1724.

[18] Arena Umberto. Process and technological aspects of municipal solid waste gasification. A review. Waste Management. 2012;32:625-639.

[19] Münster Marie, Lund Henrik. Comparing waste-to-energy technologies by applying energy system analysis. Waste Management. 2010;30:1251-1263.

[20] Weber Roland, Hagenmaier Hanspaul. Mechanism of the formation of polychlorinated dibenzo-p-dioxins and dibenzofurans from chlorophenols in gas phase reactions. Chemosphere. 1999;38:529-549.

[21] Asadullah Mohammad. Barriers of commercial power generation using biomass gasification gas: a review. Renewable and Sustainable Energy Reviews. 2014;29:201-215.

[22] Sonesson U., Björklund A., Carlsson M., Dalemo M. Environmental and economic analysis of management systems for biodegradable waste. Resources, Conservation and Recycling. 2000;28:29-53.

[23] ISO. ISO 14040: Environmental management-Life cycle assessment-Principles and Framework. Geneva: ISP copyright office; 1997.

[24] Morselli Luciano, De Robertis Claudia, Luzi Joseph, Passarini Fabrizio, Vassura Ivano. Environmental impacts of waste incineration in a regional system (Emilia Romagna, Italy) evaluated from a life cycle perspective. Journal Of Hazardous Materials. 2008;159(2-3):505-511.

Chapter 1

Background and Literature Review

The objective of this chapter is to provide insights into the background and current research progress on developing an energy-efficient and environmentally-sound MSW pyro-gasification process. This will set the stage in identifying the choices made in pursuing the research directions. With this overall aim, the structure of this chapter is set as follows:

- **Section 1.1** provides basic knowledge about MSW pyro-gasification features;

- **Section 1.2** focuses on the processes and operating parameters related to high-quality syngas production as well as on the state-of-the-art progress focusing on the use of catalyst for syngas upgrading;

- **Section 1.3** is dedicated to the utilization of syngas, including alternative cycles and process configuration of current applications;

- **Section 1.4** presents the principle and framework of LCA as evaluation tool for waste system, and its current status application in WtE technologies;

- Based on reviewing these different aspects in the field of MSW pyro-gasification, the current challenges and bottlenecks are put forward in **Section 1.5**; in addition to the objectives and motivations to perform this study.

1.1 MSW pyro-gasification basic features

1.1.1 Process steps and reaction chemistry

Pyro-gasification can be broadly defined as a thermochemical process where a carbon-based material, such as MSW, is converted into gaseous products using an oxidizing agent or gas vector (N_2 and/or non-stoichiometric oxidant) [1]. Unlike combustion, where the feedstock is completely oxidized into a hot flue gas, pyro-gasification is conducted in an oxidant medium which is usually lower than what is required for combustion, resulting in a high calorific hot fuel gas (syngas). The latter is also accompanied by a small fraction of liquid and solid products as tar and char.

Pyro-gasification of MSW includes a sequence of successive reactions, which can be divided into three steps: (1) heating and drying, (2) pyrolysis (or devolatilization) and (3) gasification [2]. Each of the latter provides a different range of products and features. A simplified scheme of the pyro-gasification process is depicted in **Figure 1. 1**. The main chemical reactions during the pyro-gasification process are summarized in **Table 1. 1**.

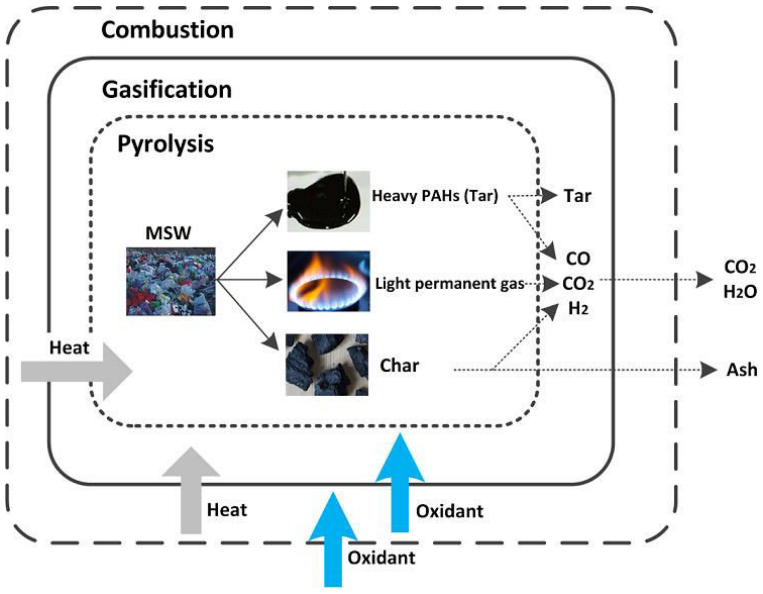

Figure 1. 1 Comparison of pyrolysis, gasification and combustion process. Redrawn from the research of Arena et al. [2]

Table 1. 1 Main reactions during MSW pyro-gasification process

No.	Reaction equation	Heat (ΔH) [b]	Description
Pyrolysis reaction [a, c]			
R1	$C_xH_yO_z \rightarrow H_2O + CO + H_2 + CO_2 + CH_4 + C_nH_m$ + tar + char	Endothermic	Pyrolysis reaction
Gasification reactions involving oxygen [c]			
R2	$C + 1/2\ O_2 \rightarrow CO$	-111 MJ/kmol	Carbon partial oxidation
R3	$CO + 1/2\ O_2 \rightarrow CO_2$	-283 MJ/kmol	Carbon monoxide oxidation
R4	$H_2 + 1/2\ O_2 \rightarrow H_2O$	-242 MJ/kmol	Hydrogen oxidation
R5	$C_nH_m + n/2\ O_2 \leftrightarrow nCO + m/2\ H_2$	Exothermic	C_nH_m partial oxidation
Gasification reactions involving steam [c]			
R6	$C + H_2O \leftrightarrow CO + H_2$	+131 MJ/kmol	Water-gas reaction
R7	$CO + H_2O \leftrightarrow CO_2 + H_2$	-41 MJ/kmol	Water-gas shift reaction
R8	$C_nH_m + nH_2O \leftrightarrow nCO + (n + m/2)\ H_2$	Endothermic	Steam reforming
Gasification reactions involving hydrogen			
R9	$C + 2H_2 \leftrightarrow CH_4$	-75 MJ/kmol	Hydrogasification
R10	$CO + 3H_2 \leftrightarrow CH_4 + H_2O$	-227 MJ/kmol	Methanation
Gasification reactions involving carbon dioxide [c]			
R11	$C + CO_2 \leftrightarrow 2CO$	+172 MJ/kmol	Boudouard reaction
R12	$C_nH_m + nCO_2 \leftrightarrow 2nCO + m/2\ H_2$	Endothermic	Dry reforming
Decomposition reactions of tar and hydrocarbons [c]			
R13	$Tar \rightarrow xC_nH_m + yH_2$	Endothermic	Dehydrogenation
R14	$C_nH_m \rightarrow nC + m/2\ H_2$	Endothermic	Carbonization

[a] Data source: Data derived from Tillman [3] and Arena et al. [2];

[b] Heat of reaction: "+" means the reaction is endothermic; "-" means exothermic reaction;

[c] $C_xH_yO_z$ represents MSW feedstock; while C_nH_m represents light hydrocarbons.

- **Heating and drying**: refers to the evaporation of the moisture that inherently composes the MSW. This endothermic reaction occurs at temperature up to ca. 160 ^oC.

- **Pyrolysis**: corresponds to the thermochemical decomposition of the organic material ($C_xH_yO_z$) in MSW at elevated temperatures, e.g., up to ca. 700 ^oC, in the absence of oxygen. The global MSW pyrolysis reaction could be represented by R1 in **Table 1. 1**. The products are gases (such as H_2, CO, CO_2, CH_4, H_2O, light hydrocarbons), tar (condensable hydrocarbons) and char (the remaining carbonaceous solid). Pyrolysis differs from other thermal processes

like combustion and gasification in that it refers to devolatilization of the feedstock, i.e., reactions with oxygen, water, or any other reagents usually do not involved. The proportion, composition and characteristics of products formed are strongly dependent on the feedstock and operating parameters, mainly MSW composition, the reaction temperature and time, pressure, and heating rate imposed by the type of reactor [4, 5]. Those factors will be discussed in detail in **Section 1.2**. Generally, high temperatures and long residence times promote the formation of syngas, while moderate temperatures and short vapor residence times enhance the proportion of tar [6]. Also, secondary reactions may occur in the vapor phase or between vapor and solid phase; thus reducing the tar yield to form mostly gas [7].

- **Gasification**: the following step is a partial oxidation reaction using an oxidant which could be air, steam, CO_2 or pure oxygen. Some of the pyrolysis products (including tars and the char) are converted into non-condensable gases; together with various gaseous-phase reactions. The temperature in case of MSW is typically between 600 and 1000 ^{o}C [8].

With regard to the various reactions involved in the gasification process (**Table 1. 1**), a number of reactions are endothermic, which require energy to keep the temperature of the process up [1]. The heat needed for gasification process may be supplied internally in the gasifier by a controlled partial oxidization (R2), which is categorized as 'direct gasification' [1, 8]. Particularly, if the quantity of heat produced from this reaction is enough to supply the endothermic reactions including the thermal cracking of tars and hydrocarbons, as well as the gasification of char using steam or CO_2. Such observation clearly indicates that the operating temperature inside the gasifier could be kept constant without an additional energy source [2]. However, if the process does not occur with an oxidizing agent, it is called 'indirect gasification'. An external energy source is therefore needed, which could be provided by superheated steam, heated bed materials or by separately burning some of the char or gases [9, 10].

Under air, steam and CO_2 gasification, the syngas is mainly produced via carbon partial oxidation reaction (R2), the water-gas reaction (R3) and the Boudouard reaction (R11), respectively. The selection of a gasification agent is found to significantly affect the gasification reaction rate. It is proven that, combustion has the highest reaction rate, which is 50 times faster than that of steam gasification. CO_2 gasification exhibits the lowest reaction rate, which is known to be 2-5 times slower than the steam gasification [11]. **The main challenge faced by pyro-gasification process is to obtain syngas that has higher calorific value than the energy used to produce the syngas.**

1.1.2 Potential benefits with emphasis on energy and environment

Continuously increasing concerns about energy and environment have pursued technological improvement towards more efficient and cleaner WtE process. A large body of literature has indicated that MSW pyro-gasification presents several potential advantages and benefits over conventional waste incineration technology. They can be summarized both from the energy and environmental aspects as follows.

- Rather than MSW direct incineration that converts all the energy into thermal energy via flue gas, the main product of pyro-gasification process is an intermediate substance, namely syngas. After proper treatment, it can be used, in a wide range of applications, such as energy recovery, high-quality fuels (diesel, gasoline or H_2) or chemicals; thus enlarging the range of utilization [12].

- Pyro-gasification process provides a potential to increase the energy conversion efficiency in case of pyro-gasification-based WtE plant. On one side, syngas could be burned in a more efficient energy conversion device, such as a gas turbine, an internal combustion engine, or better, an integrated gasifier combined cycle. On the other side, syngas could undergo clean-up prior to the subsequent combustion. For example, as it has been reported, the steam data of new Lahti gasification plant in Finland attain 120 bar and 540 ^{o}C, so the efficiency of the power cycle is quite high [13].

- As a result of the reducing atmosphere, the formation of dioxin, furans and NO_x can be strongly prohibited. This is accompanied by an improvement of the quality of solid residues especially metals could mainly remain in a non-oxidized form. Since their volatilization is limited, they could be retained and collected at the bottom of the reactor.

- The homogeneous gas generated by pyro-gasification is easier to handle, meter and control than raw MSW. When comparing with conventional WtE process, the gas-phase combustion of syngas can be carried out under more favorable conditions than a direct heterogeneous solid-gas oxidation of MSW, thus allowing the reduction of excess air, and the subsequent operating costs related to pollution control.

In light of the benefits brought by pyro-gasification, several technologies have been developed in the last two decades and are now commercially available for WtE plants [14-16]. Most of the applications have been designed for heat/power generation; while a few exist in Japan for the production of chemicals [17]. The environmental performance of several existing gasification-based WtE plants is recently reviewed by Arena et al [2]. The emission

data are presented in **Table 1. 2**. The data indicate that, the technology is able to meet the regulatory constraints of both the European Community and Japanese standards.

Table 1. 2 Emission data for several existing gasification-based WtE plants

Plant (location)	Nippon Steel (Japan)	JFE (Japan)	Energos (Norway)	Plasco (Canada)	EC/Japanese standard
Capacity	200 t/d	300 t/d	100 t/d	110 t/d	-
Emissions, mg/Nm^3 (at 11% O_2)					
SO_x	< 15.6	-	19.8	19	50/161
NO_x	22.3	-	42	107	200/229
HCl	< 8.9	8.3	3.61	2.2	10/90
Particulate	10.1	< 3.4	0.24	9.1	10/11
Hg	-	-	0.0026	0.0001	0.03/-
Dioxin/funans, n-TEQ/Nm^3	0.032	0.018	0.0008	0.006	0.1/0.1

Data source: Data derived from Arena et al. [2]

1.1.3 Pyro-gasification bottlenecks

Despite the potential advantages that pyro-gasification may bring, or, even if a number of practical applications do exist currently, MSW pyro-gasification is still being developed. A series of challenges have prevented it from fully industrilization and commercialization worldwide. Basically, a pyro-gasification-based WtE system could be divided into several steps: MSW pre-treatment, pyro-gasification process, syngas upgrading, and downstream applications. **Figure 1. 2** illustrates the different possible applicable routes of the whole system. As expected, the core objective of MSW pyro-gasification is to obtain high-quality syngas. This objective raises: (i) technical, which requires each of the steps involved in the process be optimized; (ii) assessment, to ensure that the innovative alternative could achieve better environmental, cost and operational performance than conventional MSW treatment technologies.

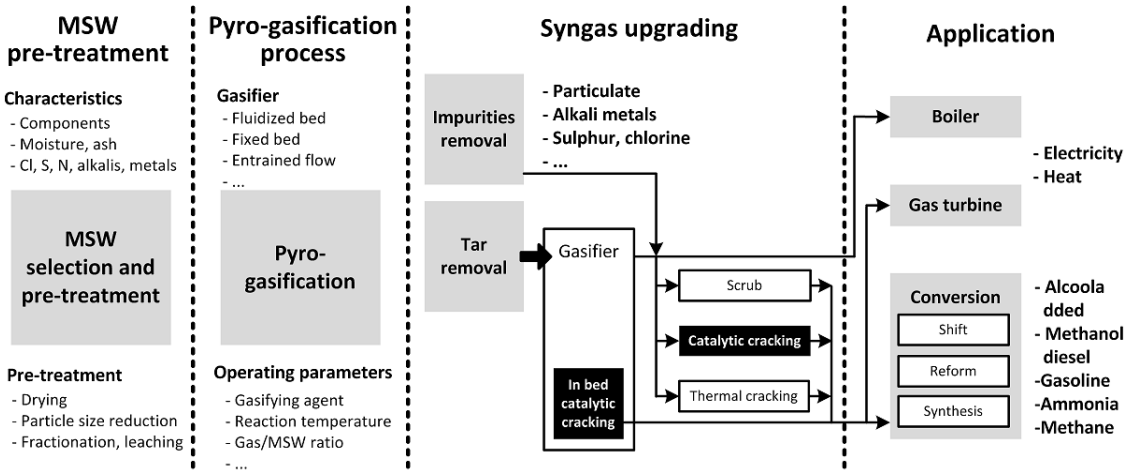

Figure 1. 2 Different possible applicable routes and technical issues of pyro-gasification system

The key issues are depending on fuel selected, the pyro-gasification technology, the gas upgrading, a suitable downstream application, as well as an integrated system optimization. This is because, the peculiar and most variable characteristics of MSW tend to make gasification much more challenging and troublesome [12]; the selection of operating parameters directly determine the syngas properties; syngas upgrading is sometimes needed to satisfy specified downstream applications; and, the whole system requires quantitative assessment to be compared with other technologies.

In fact, current researches have long focused on those topics, and some findings have already been revealed. As a result, the key issues related to high-quality syngas production will be reviewed in **Section 1.2**, with the potential utilizations of the gas discussed in **Section 1.3**. Then, apart from the technical aspect, current research status that will be bottlenecks with respect to LCA work will be presented in **Section 1.4**.

1.2 Focus on high-quality syngas production

Obtaining high-quality syngas is far beyond a matter of simplicity and is highly dependent on various factors. As a result, the effect of MSW properties, its pre-treatment and pyro-gasification operating parameters, syngas characteristics, as well as syngas upgrading by the use of catalyst, are discussed in detail in this section.

1.2.1 MSW properties and pre-treatment

1.2.1.1 MSW composition

MSW is a complex mixture of components that consists mainly of food waste, paper, plastics, wood, textiles, etc. The nature and composition of different fractions are highly variable, which in turn significantly affect the pyro-gasification plant of given design [18]. **Table 1. 3** illustrates the composition and properties of some typical MSW fractions. The main differences are found in the C/H/O elemental content, which directly determines the property of produced syngas. In addition, the lower heating value (LHV) is generally higher for fractions like plastics; while food waste, glass and metals contain relatively low amount of energy. And, it is also proven that the composition of MSW depends greatly on its origin, geographical location, weather and seasons, which will as well influence its performance as a fuel [19].

Table 1. 3 Composition and characteristics of typical MSW fractions

Component	Moisture	Ultimate analysis (wt. % dry basis)						LHV
	(wt. %)	C	H	O	N	S	Ash	(MJ/kg)
Food waste	70.0	48.0	6.4	37.6	2.6	0.4	5.0	3.90
Paper	10.2	43.4	5.8	44.3	0.3	0.2	6.0	13.43
Plastics	1.2	60.0	7.2	22.8	0.0	0.0	10.0	29.00
Wood	1.3	49.6	6.0	42.6	0.2	0.1	1.5	18.28
Textiles	10.0	48.0	6.4	40.0	2.2	0.2	3.2	17.08
Glass	2.0	0.5	0.1	0.4	0.1	0.0	98.9	-0.05
Metals	2.0	4.5	0.6	4.3	0.1	0.0	90.5	-0.05

Data source: Information on ultimate analysis and moisture are acquired from Zhao et al. [20]; while data related to LHV are acquired from Consonni et al. [21].

1.2.1.2 Moisture content

Moisture contained in MSW is removed through evaporation inside the gasifier before thermal-chemical reactions can occur, thus affecting the production and composition of syngas. With a high moisture content MSW might reduce the reaction temperature, resulting in the incomplete cracking of the hydrocarbons generated from the pyrolysis process. As reported by McKendry [22], fuel with moisture content above ca. 30% makes ignition difficult.

However Narvaez et al. [23] indicated that, some amount of moisture in the feed seems to improve the LHV of the syngas since it accelerates the steam tar reforming reaction and water-gas shift reaction hence producing more H_2. Nevertheless under higher moisture content, the gain in H_2 in the syngas could not compensate for the loss of energy as a result of the reduced CO, CH_4 and hydrocarbon generation, and the gasification performance will thus degrade [24].

1.2.1.3 Ash content

The ash content is another key factor affecting the performance of pyro-gasification process. As it has been reported, fuels with a high ash content may lead to clinkering/slagging problems in the hearth, if the oxidation temperature exceeds the melting point of the MSW ash [22]. The slagging behavior of several wood and biomass waste in relation to ash content has been reported by Reed et al. [25] (see **Table 1. 4**). Especially, the slagging, fouling and ash agglomeration phenomenon may become severe if the ash contains high content of alkali metals that produce eutectic mixtures with low melting points. Recent research also reported on the inhibition of the gasification reaction rate under higher ash content [26].

Table 1. 4 Slagging behavior of wood and biomass waste

Feedstock	Ash content, wt. %	Degree of slagging
Cotton gin trash	17.6	Severe
Pelleted rice hulls	14.9	Severe
Refuse derived fuels (RDF) pellets	10.4	Severe
Wheat straw and corn stalks	7.4	Severe
Corn stalks	6.4	Moderate
Safflower straw	6.0	Minor

Data source: Data excerpted from Reed et al. [25]

1.2.1.4 Role of mineral composition

The chemical composition shows that some endogenous inorganic species such as Cl, S, N, alkalis and heavy metals, are commonly found in MSW. There is well-documented evidence in the literature that the oxides and salts of alkaline and alkaline earth metals, act

as catalysts and improve the efficiency of pyro-gasification [27-29]. The species having the highest catalytic effect are potassium, sodium, calcium, and magnesium. It has been reported that incorporated as carbonate and sulphate minerals, these species allow increasing the reactivity of the feedstock and hence promoting the degradation of MSW at lower temperature [27]. The catalytic effect is related to the interparticle mobility of the metals. As it has been observed by Habibi et al. [26] and Parvez et al. [30], transfer of the catalyst has effectively resulted in enhanced interactions between different MSW components during co-gasification of MSW.

On the other hand, the presence of mineral content may cause several operational problems. As an example, alkali silicates formed by the reaction of alkali with silica may melt or soften at low temperatures (even can occur < 700 ^{o}C depending on the composition). Alkali may also react with sulphur to form alkali sulphates that causes fouling on heat transfer surfaces [31]. Special attentions on the elemental composition of the char/ash are thus required in the current application.

1.2.1.5 MSW pre-treatment

MSW pre-treatment is often necessary to facilitate the operation of the gasifier and for the production of a high-quality syngas. The degree of pre-treatment is often dependent on the pyro-gasification technology used. Generally, the main pre-treatment methods include:

- **Drying**: the aim of drying is to reduce the moisture content of the feedstock. Usually the MSW moisture content needs to be reduced below 10-15% before pyro-gasification [22], in order to increase the overall efficiency of the process. However, drying is energy intensive and this step may decrease the overall pyro-gasification process energy efficiency.

- **Particle size reduction**: particle size of MSW needs to be adapted to a suitable level to prevent pipe clogging and to improve heat exchange. Indeed, particle size influences the interfaces for mass and heat transfer, that impacts the syngas quality [32]. This was reported by Lv et al. [33], who observed that smaller particles result in higher gas yield, gas LHV and carbon conversion efficiency. Research by Luo et al. [34] also shows that H_2 and CO contents are effectively increased if the particle size is reduced from 1.2 mm to 0.075 mm.

- **Fractionation and leaching**: the aim of these two methods is to reduce the nitrogen and alkali contents of the MSW, as those substances may be released in gas phase and are critical to the quality of syngas.

1.2.2 Pyro-gasification operating parameters

Once the MSW has been selected and, if necessary, pre-treated, the next is directly linked to the pyro-gasification process itself. There are series of operating parameters altering the heat generation, heat transfer and reaction rates in a complicated manner, which in turn affect the syngas characteristics. Of special importance are the gasifying agent, reaction temperature and gasifying agent-MSW ratio. These factors are discussed in details below. Note that the reaction pressure and feedstock residence time also crucially impacts the syngas. However, regular pyro-gasification is largely performed at atmospheric pressure while the MSW residence time is essentially determined by the type of gasifier.

1.2.2.1 Gasifying agent

Gasifying agent is a key factor influencing the quality of syngas, as well as its suitability for different end-use applications [8]. Inert atmosphere is required for pyrolysis and normally N_2 is selected to such purpose. For gasification, the most commonly used gasifying agents include air, steam or their mixture, but CO_2 and pure oxygen can also used. Gasification using air produces a syngas of low LHV, mainly due to its rich N_2 content [35]. When pure oxygen is used, the N_2 content in the produced syngas is logically reduced while the gas heating value increases; however the cost of pure oxygen gasification is relatively high [35]. Steam as a gasifying agent produces a syngas with a moderate LHV and its cost is comprised between air and oxygen. CO_2 could also be served as gasifying agent; the starting point is more concerned on CO_2 recycling for the alleviation of GHG emissions. The main advantages and technical challenges using different gasifying agents are summarized in **Table 1.5** [36].

Table 1. 5 Advantages and technical challenges using different gasifying agents

Gasifying agent	Main advantages	Main technical challenges	Main researches
Air	1. Partial combustion for heat supply of gasification, process auto-thermal may achieved; 2. Moderate char and tar content	1. Low heating value (3-6 MJ/Nm^3); 2. Large amount of N_2 in syngas (e.g., > 50 vol. %); 3. Difficult determination of equivalence ratio (usually 0.2-0.4)	[23, 37, 38]
Steam	1. Syngas with high heating value (10-15 MJ/Nm^3); 2. H_2-rich syngas (e.g., > 50 vol. %)	1. Require indirect or external heat supply for gasification; 2. High tar content in syngas; 3. Require catalytic tar reforming	[39-41]
CO_2	1. Syngas with high heating value; 2. High H_2 and CO in syngas	1. Require indirect or external heat supply; 2. Required catalytic tar reforming	[42-44]

Data source: Data excerpted from Wang et al. [36]

When using air as gasifying agent, Kinoshita et al. [45] reported that the tar content was decreased sharply when the ratio of air increases, since the oxidation reaction of the tar is gradually enhanced. However, too high air supplied may decrease largely the concentration of H_2 and CO and simultaneously a high CO_2 content may be formed in the product gas, thus degrading the syngas quality. Hernández et al. [46] observed enhanced syngas properties under mixed steam/air gasification of biomass. And, gasification performance including syngas production, syngas composition, cold gas efficiency, etc., by the use of different agents, has been also compared by different studies [18, 42, 47].

According to its quality and composition, the syngas generated exhibits different utilization approaches. Low LHV gas is mainly suitable to be directly combusted in conventional boilers or as an engine fuel [22]. Syngas with medium/high LHV can be utilized as feedstock for other processes, such as H_2 production, fuel cell feed, chemical and fuel synthesis, which will be discussed later in **Section 1.3**.

1.2.2.2 Reaction temperature

Temperature also plays an important role in affecting syngas yield and composition since it impacts on all chemical reactions as well as their chemical equilibrium. According to Le Chatelier's principle, the endothermic reactions are favored at higher temperature. This has resulted in an increased gas yield due to high releases of gaseous products from further pyrolysis, steam reforming, gasification and cracking reactions [48]. For instance, Lahijani et al. [49] investigated the effect of temperature (650-1050 ^{o}C) on gasification performance of two wood waste in an air-blown fluidized bed, observing an increased syngas yield from 1.36 to 2.10 Nm^3/kg and from 1.28 to 1.95 Nm^3/kg for the two feedstocks, respectively, under the tested temperature range. Besides, gasification at high temperature can lead to lower tar content and a higher carbon conversion [36]. The Waterloo concept, widely accepted to account for this phenomenon [4], is illustrated in **Figure 1. 3**. During biomass and MSW decomposition, char, gas, and tar are first formed, followed by the secondary reactions that convert part of the tar into an additional amount of gas and char. Higher temperatures provide more favorable conditions for primary decomposition of char, which is converted into tar and gas vapors. Subsequently, the secondary cracking of tar (reaction R13 in **Table 1. 1**) becomes strengthened, leading to a decrease in tar production.

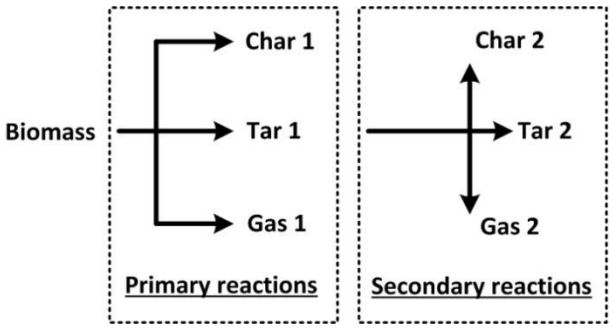

Figure 1. 3 Biomass pyrolysis concept proposed by the University of Waterloo [4]

With regard to syngas composition, the contents of H_2, CO, CO_2 and CH_4 in the product gas are also significantly affected by temperature. At temperature above 750-800 ^{o}C, steam reforming and water-gas reactions will be enhanced and result in an increased H_2 content and a decreased CH_4 content. At temperature above 850-900 ^{o}C, both steam reforming and Boudouard reactions dominate, resulting in increases of the CO content [32]. González et al. [50] observed that when using air gasification the concentration of H_2 and CO increases when temperature rises from 700 to 900 ^{o}C while the content of CH_4 and CO_2 decreases. This is also accompanied by a change in gas properties, i.e., the ratio of CO/CO_2 has experienced a

linearly increase from 0.85 to 2.7. The effect of temperature using different gasifying agents was also compared by Hernández et al. [46] in an entrained bed. They found that air gasification mainly increases the CO and H_2 content in the product syngas via the Boudouard and the steam reforming reactions; whereas for mixed steam/air gasification (56.4 vol.% steam) the boost in H_2 production is primary attributed to the char-steam reforming and water-gas shift reactions, as well as an increase in the CH_4 content.

Generally, raising the temperature has a positive impact on increasing the concentration of CO and H_2 in the syngas. This is considered effective for improving the gas quality, as H_2 and CO are the components with the greatest bearing on syngas LHV and potential applications. However, too high operating temperature might decrease the energy efficiency and also increase the risk of ash sintering and agglomeration as discussed in **Section 1.2.1** [36, 51].

1.2.2.3 Gasifying agent-MSW ratio

Gasifying agent-MSW ratio represents the mass ratio of the gasifying agent to the MSW feedstock fed into the reactor. If air or O_2 is used as gasifying agent, this parameter is defined as equivalence ratio (ER), i.e., the ratio of O_2 injected to that required for stoichiometric combustion of a given amount of feedstock. Under steam or CO_2 gasification, this parameter actually reflects the steam/CO_2 flow rate, which is often defined as steam to MSW ratio (S/M) or CO_2 to MSW ratio (CO_2/M), respectively.

For air/O_2 gasification, ER controls the extent of partial combustion. While ER value close to zero corresponds to pyrolysis condition, values equal or greater to one represents combustion. For pyro-gasification, ER is likely the most important operating parameter affecting the syngas properties. Higher ER results in higher temperature which leads to higher fuel conversion and a higher quality of gas. However, an excess degree of ER results in decreased energy content of the syngas produced because part of energy is spent in combustion [35]. Wang et al. [52] observed an increase of H_2 content from 8.5% to 13.9%, CO content from 12.3% to 14%, and cold gas efficiency from 57% to 74% when increasing the ER from 0.16 to 0.26. But Narváez et al. [23] found the decreasing trend of syngas LHV as well as the content of H_2, CO, CH_4 and C_2H_2 with an increase in ER from 0.20 to 0.45, although the syngas yield keeps steadily increasing. Accordingly, ER around 0.25-0.35 appears to be the optimal value suitable for large-scale commercial plants [2].

When supplying steam as gasifying agent, the increased partial pressure of H_2O inside the reactor will favor the steam-related reactions such as water gas, water gas shift and methane reforming reactions; thus leading to an enhanced H_2 production. Similarly, CO_2 gasification could increase CO production as a result of an enhanced Boudouard reaction. Increasing S/M or CO_2/M ratio is proven to be effective for H_2 or CO production, respectively [35]. Turn et al. [53] observed that when increasing S/M from 1.1 to 4.7, the H_2 yield and concentration increases, while the content of CO, CH_4 and C_2H_2 decreases. Raising the S/M ratio was also reported to be effective for the reduction of tar content in the gas generated [54]. However, steam might exhibit negative effects when the S/M ratio exceeds a threshold value. For example, Li et al. [55] and Acharya et al. [56] observed a decreased H_2 production at higher steam flowrates (S/M ratio in a range of 1.33-2.66 and 0.83-1.58 in each of the studies, respectively). This phenomenon could probably due to that at higher S/M ratio, a significant amount of heat is absorbed by the steam, which in turn, result in a decrease of the available heat which may even lead to lower temperature in the reactor [32].

1.2.3 Syngas characteristics

For high-quality syngas production with respect to the aforementioned various influence parameters, the current research hotspots are mainly focused on:

- How to select proper feedstock for specific application;

- What are the optimal working conditions;

- And, if the general pyro-gasification process could be modeled to predict the syngas properties.

With these overall aims, different research topics are proposed and developed, as illustrated in detail in the following.

1.2.3.1 Pyro-gasification of MSW single component

Heterogeneity of MSW composition and the difference in the thermal behavior of their components make design, operation and optimization of pyro-gasification systems a challenge [18, 57]. Indeed, the produced syngas characteristics, such as its total yield, content of H_2 and CO, molar ratio of H_2/CO, and so on, are highly dependent on the specified

MSW composition. To better determine process parameters for high-quality syngas production and to identify the potential application routes, pyro-gasification of MSW single component is essential.

With this standing point, a great number of researches appear focusing on different kinds of MSW components, including paper, plastics, rubber, wood waste, food residue, textiles, and some other biomass. For example, Umeki et al. [58] studied the steam gasification of wood waste to generate H_2-rich gas. Results reveal that both the steam temperature and the steam/carbon molar ratio affected strongly the gasification temperature and gas composition. The H_2 concentration is found to be as high as 35-55 vol.% while the cold-gas efficiency could attain 60.4%. Air gasification of waste tire powder (another MSW common component) was investigated at a temperature of 350-900 ^{o}C by Leung et al. [59]. Results show that the highest syngas yield rate (11 Nm^3/h at LHV about 6 MJ/Nm^3) can be generated by adjusting the ER value to the optimum. Pyrolysis and CO_2 gasification of six representative MSW components, namely, poplar, paper, polyethylene, rubber, dacron and rice, were conducted by Chen et al. [18]. Three generic thermal events, including pyrolysis characteristics (stage I), gasification incomplete carbonization char (stage II), and gasification of fixed carbon (stage III), were identified.

Comparison of pyro-gasification characteristics for a given feedstock under different gasifying agents is also investigated. Ahmed et al. [60] compared syngas properties during pyrolysis and steam gasification using paper as feedstock. Pyrolysis was conducted at 400-700 ^{o}C while the temperature for steam gasification was set at 600-1000 ^{o}C. Syngas generation rate, gas composition and energy yield were compared. Their results show that H_2 and energy were better with gasification as compared to pyrolysis, which was attributed mainly to the advantages brought by char gasification process. High-temperature pure-steam gasification of plastics, automobile tire rubber, mixed MSW and wood was investigated and compared with air gasification [61]. It was observed that the H_2 concentration from steam gasification is relatively high while the syngas LHV for all four types of feedstock reaches 8-10 MJ/Nm^3 which is approximately 2.5 times higher by weight and 1.6 times by volume as compared to those produced from the air gasification.

1.2.3.2 Co-pyro-gasification of MSW multi-components

Due to the complexity of MSW, pyro-gasification of mixtures has also aroused great interest, since some synergistic interactions may take place, leading to significant variations in the thermal reactivity of the samples or in the physical or chemical properties of the products [62]. It has been proven that co-pyro-gasification could be beneficial with respect to increasing the heating value of the syngas, char reactivity, reducing both the reaction time and emissions of CO_2, NO_x and SO_x [63, 64], and, to economic benefits for the operators.

Currently, co-pyro-gasification has been studied with respect to different MSW multi-components, in reactors of different types and scales. Jakab et al. [65] studied the co-pyrolysis behavior of polypropylene (PP) in the presence of wood flour, lignin, cellulose and charcoal using a thermogravimetric analyzer (TGA). Results showed that biomass materials decompose at temperatures lower than plastic while the char produced from biomass accelerates the decomposition of PP. In their study using a U-shaped tube reactor for co-pyrolysis the mixture of pine and polyethylene (PE) under different mass ratios at 800 ^{o}C, Dong et al. [66] observed strong interactions of volatiles, which subsequently affected syngas properties. CO formation decreases with an increase in PE addition ratio and the yield of hydrocarbons increases. This change is nonlinear with the proportion of PE.

The phenomenon of feedstock interactions also widely exists during co-gasification process, where the pyrolysis products and char can interact with each other as well as with the gasification agent. Pinto et al. [67] studied steam gasification of biomass (pine) and plastics (PE) using a fluidized bed. They found that an increased H_2 and C_xH_y when raising the proportion of PE in the mixture, as well decreased production of CO and CO_2. The change in syngas composition was also found to be nonlinear, and the greatest syngas yield reached at 60 wt.% of PE. The catalytic effect of alkali and alkali earth metals present in the biomass-derived components was investigated by Habibi et el. [26] during the gasification of biomass and non-biomass feedstock. CO_2 gasification of single and mixed materials including switchgrass, coal and fluid coke were conducted at temperatures of 750-950 ^{o}C by TGA. Results showed that both synergistic and inhibition effects exist during co-gasification of mixed samples. Furthermore, they showed that the tendency was highly influenced by the composition of feedstock ash.

1.2.3.3 Optimal syngas production from pyro-gasification of mixed MSW

Pyro-gasification characteristics of mixed MSW are also widely studied, with the aim to search for optimal operating conditions for syngas production. For example, Luo et al. [68] carried out pyrolysis and steam gasification of MSW in a lab-scale fixed bed reactor, in order to evaluate the effects of particle size at different bed temperatures on product yield and syngas composition. The MSW samples were collected from a transfer station in China and the results indicate that minimizing the MSW size was effective to improve the gas quality. Syngas production from pyrolysis of MSW was investigated over a temperature range of 750-900 ^{o}C by He et al. [69]. The influence of weight hourly space velocity and reactor temperature was studied. Higher operating temperature results in a higher syngas production with a significant increase of the H_2 and CO contents. The LHV attains ca. 13.87 MJ/Nm^3, which is particularly suitable for Fischer-Tropsch synthesis.

To support better designs and optimization of important industrial processes [70], several researchers have focused on the pyro-gasification reaction kinetics. It has been found that the kinetic parameters, such as the pre-exponential factor and activation energy, are among the key factors for determining the reaction mechanism of fuels [71]. Lai et al. [72] studied the thermal decomposition behavior of MSW in N_2, CO_2 and CO_2/N_2 atmospheres using a TGA. The nth order reaction model consisting of several independent fractions is proposed, which is proven to be useful to characterize the MSW conversion and fits the weight loss well. Besides, some current researches also tend to propose pyro-gasification mechanism in order to generalize pyro-gasification reaction processes [4, 73].

1.2.3.4 Prediction of syngas characteristics

Since experimental runs conducted on industrial gasification plants or even on pilot scale gasification plants can be extremely expensive, a large segment of studies uses mathematical models to characterize pyro-gasification process, with the aim of quantifying and predicting of syngas characteristics. In fact, these models, with the ability to theoretically simulate the physical and chemical condition of MSW, allow studying the pyro-gasification process without resorting to major investments and/or the need for long waiting periods [74]. The most widely developed approaches are: thermodynamic analysis, numerical model, and artificial neural networks (ANN).

Thermodynamic analysis is a steady state simulation model based on mass, energy and chemical balance, which could help determining the effect of parameters on the optimal system's operating point. Aspen Plus has been developed as a widely used thermodynamic modeling tool, which is based on the minimization of the total Gibbs free energy at equilibrium. Mitta et al. [75] modeled a fluidized-bed tire gasification process using air and steam as gasifying agent. This model was able to predict the syngas composition under various working conditions including flowrate, composition and temperature of the feed materials, as well as the reaction pressure and temperature. The modeling results showed only a small deviation with a pilot gasification plant. Niu et al. [76] simulated enriched air and steam gasification of MSW in a bubbling fluidized bed. Effects of operating gasification temperature, ER, oxygen percentage, MSW moisture content, and steam/MSW ratio on the syngas composition and gasifier efficiency are analyzed. The simulation results provide the optimization method in search of an efficient and clean utilization of MSW energy.

Numerical model, for example computational fluid dynamics (CFD), is also developed in order to solve the complexity of fluid flow, heat transfer and complex chemical reactions during MSW gasification. For instance, Gungor et al. [77] developed a two-dimensional model for an atmospheric circulating fluid bed biomass gasifier. The radial and axial profiles of the bed temperature, syngas composition (H_2, CO, CO_2 and CH_4) and tar concentration versus gasifier temperature were predicted; and results show that the maximum error is less than 25% when compared with experimental results gathered in laboratory setups.

ANN has an inherent ability to learn and recognize highly nonlinear relationships, thus it has been selected as an ideal tool to predict the pyro-gasification characteristics of MSW [78]. Particularly, one of the most outstanding advantages of this method is that, the prediction could on basis of MSW physical composition, so that the pyro-gasification characteristics regarding geographic differences could be reflected and compared easily. Lately researches found in the literature have attempted to apply ANN for gasification. For example, Xiao et al. [78] established an ANN model to predict the syngas LHV, gasification products and gas yield from five typical MSW organic components (wood, paper, kitchen garbage, plastic and textile), using air as gasifying agent in a fluidized bed at 400-800 ^{o}C with an ER ranging from 0.2 to 0.6. Mikulandric et al. [79] used ANN for the modeling of biomass gasification process in fixed bed, which showed good correlation with measured data and good capability to predict biomass gasification process parameters with reasonable accuracy and speed. Puig-Arnavat et al. [80] established two architectures for ANNs models: one for circulating fluidized bed gasifiers and the other for bubbling fluidized bed gasifiers, in order to

determine the syngas composition (CO, CO_2, H_2, CH_4) and gas yields. The obtained results showed good agreement with the experimental data.

With regards to the recent advances on the subpath in open literatures, this thesis will focus on the production of high-quality syngas and the establishment of a pyro-gasification prediction model. Syngas compositions such as H_2, CO, CH_4 and CO_2 are selected for the investigation; however emissions such as NO_x, SO_2 and PM are not included in this study.

1.2.4 Catalytic syngas upgrading

1.2.4.1 Syngas cleaning and catalytic tar cracking

The raw generated syngas contains various impurities, such as particulates, tar, and emissions but not limited to H_2S, CS_2, COS, AsH_3, PH_3, HCl, NH_3, HCN, and alkali salts. Those impurities have to be removed to satisfy the subsequent downstream use of syngas, depending on the application of interest [8]. For example, particulate which is essentially derived from ash, char, condensing compounds and bed material from fluidized bed reactor, may cause erosion of metallic components or interfere as pollutant if discharged to the atmosphere. The most commonly used removal technique is through a cyclone separator in a fluidized bed, or, it could also be captured by filtration or scrubbing [1]. Acid gases such as H_2S and HCl may cause corrosion of the pipe and equipment; and lime or sodium bicarbonate scrubbing could serve as an effective gas-cleaning device [1].

Among those impurities, tar formation is of particular concerned regarding MSW pyro-gasification, since it may decrease the system efficiency and even block or damage downstream equipments [81]. The latter has become a major challenge in inhibiting the commercialization of the technology [82].

In general, tar can be removed by mechanical/physical method, thermal cracking or catalytic tar cracking [83]. Generally, mechanical/physical method includes separation in a condensed form. However, the major disadvantage of this method is that the produced syngas needs to be cooled down, hence the energy contained in the syngas will be lost. Besides, a huge amount of wastewater with high organic content is produced. Thermal cracking is another tar removal method and two approaches are commonly used in fixed bed gasifier: use of higher temperatures in the core and/or increase of gas residence time [1]. However, since waste-derived tar is quite stable, the operation temperature for thermal

cracking has to be maintained at temperature higher than 1000 ^{o}C [84], hence reducing the efficiency of the process.

From a technical and economic point of view, catalytic tar cracking represents a promising alternative. One of the great advantage of this method is that the reaction temperature needs not to be maintained as high as that of thermal cracking, and simultaneously the gas yield and LHV could be improved [85]. Generally, catalytic tar cracking involves two methods [86]: in-bed tar cracking and secondary tar cracking. Both have been illustrated in **Figure 1.2**, and a brief introduction of these two methods is provided as follows.

- **In-bed catalytic tar cracking**: The catalyst is incorporated or mixed with the fed MSW. This solution uses the heat produced by the gasifier, and thus, in fact, achieves catalytic pyro-gasification (also called in-situ) [83]. The advantage is that the tar could be removed at the source inside the gasifier, thus making the process economically attractive. However the catalyst lifetime is not very long [1], which impacts the economy of such process.

- **Secondary catalytic tar cracking**: In this case, tar is removed downstream from the gasifier in a secondary reactor. The outstanding advantage of this method is that the catalyst is protected from de-activation; however extra energy is needed to increase the reaction temperature [1].

1.2.4.2 Catalyst for tar elimination

Due to the advantages of converting tar into useful gases and adjusting the compositions of product gases, catalyst cracking has been of interest [87]. Several kinds of catalysts have been developed and applied, which can be divided into two classes: minerals and synthetic catalysts.

The advantages and disadvantages of those catalysts have been reviewed by Abu El-Rub et al. [88]. Among all those catalysts, the most widely used catalysts are dolomite, olivine and Ni-based catalysts. Especially, great attentions have been dedicated to use the catalysts as an active in-bed additive during pyro-gasification, although only few have been tried so far [51]. The primary aim is that in-bed additives could avoid complex downstream tar removal processes. Besides, catalysts also provide a great potential to promote the char gasification, modify the product gas composition and increase the syngas LHV.

Among all the active catalysts, calcined minerals are the most popular and most commonly studied as in-bed catalysts [51]. The latter generally includes limestone (calcium carbonate, $CaCO_3$), magnesium carbonate ($MgCO_3$), dolomite ($CaCO_3 \cdot MgCO_3$), etc. These materials show catalytic activity for tar elimination when calcined, due to their content in alkaline earth metal oxides (CaO and/or MgO) [88]. **Table 1. 6** depicts some typical chemical compositions of such materials [89]. It has been proven that those materials could facilitate reactions including steam reforming (reaction R8 in **Table 1. 1**), dry reforming (reaction R12 in **Table 1. 1**), thermal cracking (reaction R13 in **Table 1. 1**), and hydrocracking or hydro-reforming of tars (see Eq. (1.1) below), thus effectively reducing the concentration of tar in the produced syngas.

$$C_nH_m + H_2 \leftrightarrow CO + CO_2 + H_2 + CH_4 + \ldots + \text{coke} \quad (1.1)$$

Table 1. 6 Typical chemical compositions of limestone, magnesium carbonate and dolomite

Composition	Calcite morata	Magnesite navarra	Dolomite norte
CaO	53.0	0.7	30.9
MgO	0.6	47.1	20.9
CO_2	41.9	52.0	45.4
SiO_2	2.7		1.7
Fe_2O_3	0.8		0.5
Al_2O_3	1.0		0.6

Data source: Data derived from Delgado et al. [89]

1.2.4.3 Issue of catalyst de-activation

Despite the above-mentioned advantages brought by the use of catalyst, de-activation as well as the loss over time of catalytic activity and/or selectivity is a thorny problem towards industrial processes [90]. As a result, special attentions should also be paid to this issue when using catalysts for syngas upgrading.

There are many paths leading to catalyst decay; however they can be grouped into six intrinsic mechanisms according to the review of Bartholomew [91], as shown in **Table 1. 7**.

Table 1. 7 Mechanisms of catalyst de-activation

Mechanism	Type	Description
Poisoning	Chemical	Strong chemisorption of species on catalytic sites, thereby blocking sites for catalytic reaction
Fouling	Mechanical	Physical deposition of species from fluid phase onto the catalytic surface and in catalyst pores
Thermal degradation	Thermal	Thermally induced loss of catalytic surface area, support area, and active phase-support reactions
Vapor formation	Chemical	Reaction of gas with catalyst phase to produce volatile compound
Vapor-solid and solid-solid reactions	Chemical	Reaction of fluid, support, or promoter with catalytic phase to produce inactive phase
Attrition/crushing	Mechanical	Loss of catalytic material due to abrasion; Loss of internal surface area due to mechanical-induced crushing of the catalyst particle

Data source: Data derived from Bartholomew [91]

The thermally-induced de-activation of catalysts is of particular concern to pyro-gasification process. It could result from: (i) loss of catalytic surface area due to crystallite growth of the catalytic phase; (ii) loss of support area due to support collapse and of catalytic surface area due to pore collapse on crystallites of the active phase; and/or (iii) chemical transformations of catalytic phases to non-catalytic phases [91]. Typically, the first two processes belong to 'sintering', which easily occur at high reaction temperatures (e.g. > 500 ^{o}C) and are generally accelerated by the presence of water vapor. For example, research by Sun et al. [92] observed a phenomenon of pore shrinkage and grain growth at elevated temperature when using CaO as catalyst. The rate of catalyst sintering will increase at temperature exceeding 900 ^{o}C, or, increasing the partial pressure of CO_2 and steam according to the study of Borgwardt et al. [93].

Besides, other types of catalyst de-activation are also widely observed. Successive decrease of the mechanical strength of the dolomite with time during catalytic runs was reported by Vassilatos et al. [94], which is found to be common in fluidized bed. When using potassium carbonate (K_2CO_3) as an in-bed catalyst for wood steam gasification, phenomena of particle agglomeration and carbon deposition were observed. The latter appears to be the main cause of catalyst de-activation [95]. As for Ni-based catalyst, de-activation due to

carbon fouling was also reported in various researches [96-98], resulting in short lifetimes of the catalyst.

While catalyst de-activation is inevitable for most processes, interest is dedicated to understand and treat catalyst decay, as well as to seek for catalyst re-generation methods. For example, Lammers et al. [99] proved that when dolomite is used as in-situ catalyst for tar removal, the addition of secondary air to the catalytic reactor is effective to reduce the de-activation rate of the catalyst. Steam used in gasification is also found to have an important effect on maintaining the activities of the catalysts, attributed to the steam reforming of any carbon deposited [100]. Overall, catalyst de-activation needs to be addressed highly when utilizing catalysts in pyro-gasification process. Great efforts should be paid to prevent or slow the catalyst de-activation for a better development, design, and operation of commercial processes.

1.3 Utilization of syngas

1.3.1 Alternative cycles

There are different available alternative cycles for the utilization of syngas: energy generation, H_2 production, Fischer-Tropsch synthesis, methanol and dimethyl ether synthesis, higher alcohol synthesis and methanation (synthetic natural gas). Key factors determining the process design are syngas LHV and H_2/CO ratio [8]. Some of the most typical production processes are discussed in detail as follows.

1.3.1.1 Energy generation

Syngas obtained from pyro-gasification can be burned in a combustor for energy generation, in a similar way as conventional MSW incineration [101]. Three energy recovery devices exist, which are the steam cycle, gas turbine, and gas engine. **Table 1. 8** lists the required gas properties for these devices, together with their energy efficiency.

Table 1. 8 Comparison between the main energy recovery devices

Device	Net electrical efficiency of gasification plant	Required gas properties
Steam turbine	15-24%	Tar: not limited; Dust: not limited; Alkalis: not limited; Heavy metals: not limited; H_2S: not limited
Gas turbine	20-30%	Tar: 10 mg/Nm^3; Dust: 5 mg/Nm^3; Alkalis: 0.1 ppm, wb; Heavy metals: 0.1 ppm, wb; H_2S: 20 ppm, vb
Gas engine	14-26%	Tar: 100 mg/Nm^3; Dust: 50 mg/Nm^3; Alkalis: 0.1 ppm, wb; Heavy metals: 0.1 ppm, wb; H_2S: 20 ppm, vb

Data source: Data excerpted from Arena et al. [2]

Steam turbine is the simplest cycle since no gas pre-treatment is needed. However, the maximum net electrical efficiency of a gasification-steam cycle plant is limited by the theoretical limit of a steam turbine, resulting in a quite comparable energy efficiency as conventional MSW incineration plant. The limitation is mainly derived from the maximum metal temperature of the superheater tubes, which should be lower than 450 ^{o}C to prevent HCl corrosion of the tubes [1]. As a result, the steam temperature and the subsequent overall plant efficiency are quite low. Nonetheless, this limitation could be overcome by gas pre-treatment for HCl removal before going into the boiler. As reported by Rensfelt et al. [102], this would allow a steam temperature of 520 ^{o}C, with a 6% improvement in energy recovery efficiency.

Clean and high-quality syngas could also be fed into highly efficient energy conversion devices such as gas turbine and gas engine. Principally extremely low levels of contaminants can be tolerated (as shown in **Table 1. 8**), since these devices are very sensitive to the quality of the inlet gas. Both gas turbine and gas engine can transform syngas to mechanical energy and thus increase the energy efficiency of conversion [8]. As reported, modern gas engines

which are correctly modified can reach over 25% of net electricity output [1]. Pyro-gasification process could also be integrated by a gas turbine combined cycle (IGCC), where the syngas from the gasifier is firstly fed into a gas turbine as the top cycle; after what the hot exhaust gas from the gas turbine is used to generate steam to serve a steam turbine in the bottom cycle, which would offer the generation of additional electricity or could be used as processing heat. Miccio et al. [103] reported that the overall efficiency of a biomass-based IGCC could reach 83% with an electricity efficiency of 33%. However, challenge for the use of such engines is that syngas normally has to be cooled down for purification, thus raises the pressure for effective syngas cleaning as well as energy recovery for the sensitive heat of the gas.

1.3.1.2 Hydrogen production

The use of H_2 as fuel is highly efficient and produces only water without causing direct CO_2 emission, thus the utilization of syngas for H_2 production has attracted increasing attention nowadays. Generally syngas produced from MSW pyro-gasification is a mixture of H_2, CO, CO_2 and CH_4. To convert syngas into the desired H_2-rich composition, reforming of CH_4 to H_2 and CO (reversed reaction R10 in **Table 1. 1**), water-gas shift reaction of CO to H_2 and CO_2 (reaction R7 in **Table 1. 1**) becomes necessary.

Steam gasification is effective for a high H_2 concentration in the produced syngas. The use of steam also provides the benefit that H_2 could be obtained from the steam. Besides, the use of adsorbent such as CaO given in Eq. (1.2) is also proven useful for the removal of CO_2 from the gas while simultaneously stimulating H_2 generation [56, 104].

$$CaO + CO_2 \rightarrow CaCO_3 + 178\,kJ/mol \quad (1.2)$$

1.3.1.3 Fischer-Tropsch synthesis

The aim of Fischer-Tropsch reaction is to produce hydrocarbons of variable chain length, which represents an alternative to conventional diesel, kerosene and gasoline [36]. The principle of the Fischer-Tropsch reaction is illustrated as Eq. (1.3).

$$CO + 2H_2 \rightarrow -CH_2- + H_2O - 165\ kJ/mol \quad (1.3)$$

Basically the product from Fischer-Tropsch reaction, $-CH_2-$, is a precursor of long-chain hydrocarbons. For an effective Fischer-Tropsch synthesis, a 2:1 H_2/CO ratio is required according to Eq. (1.3); or in a range of 1.5-3.0 [105]. This could be achieved by steam reforming reaction (reaction R8 in **Table 1. 1**) and water-gas shift reaction (reaction R7 in **Table 1. 1**) to adjust the H_2 and CO ratio. However, the use of catalyst is proven to be more efficient. Alkali-doped iron catalysts are mainly investigated; while cobalt is currently developed and widely used as a modern Fischer-Tropsch synthesis catalyst [8]. Currently, commercial scale Fischer-Tropsch processes have been developed to produce liquid fuels from coal-derived syngas in South Africa and natural gas-derived syngas in Malaysia [106].

1.3.1.4 Methanol and dimethyl ether synthesis

Both methanol and dimethyl ether are promising and clean liquid fuels as alternatives to gasoline and diesel fuels [36, 107]. Syngas synthesis for methanol can be based on CO or CO_2 hydrogenation, which is illustrated by Eq. (1.4) and Eq. (1.5), respectively.

$$CO + 2H_2 \rightarrow CH_3OH \quad (1.4)$$

$$CO_2 + 3H_2 \rightarrow CH_3OH + H_2O \quad (1.5)$$

Dimethyl ether could be synthesized by further dehydration of methanol, as Eq. (1.6):

$$2CH_3OH \rightarrow CH_3OCH_3 + H_2O \quad (1.6)$$

Also, the molar ratio of H_2/CO should be adjusted for the synthesis. Catalysts that are proven effective for the enhancement of the process include $Cu/ZnO/Al_2O_3$ and $Cu/ZnO/Cr_2O_3$, which show highly active performance.

1.3.2 Process configuration of current applications

Alternative syngas utilization cycles and the configurations of a pyro-gasification plant have been reviewed by Consonni et al. [12], as illustrated in **Figure 1. 4**. There are actually as many as 100 plants around the world that use pyro-gasification systems to process MSW [108]. Most of these plants have been developed and commercialized for energy generation; and only a few are operated to produce chemicals (in particular ammonia) [2].

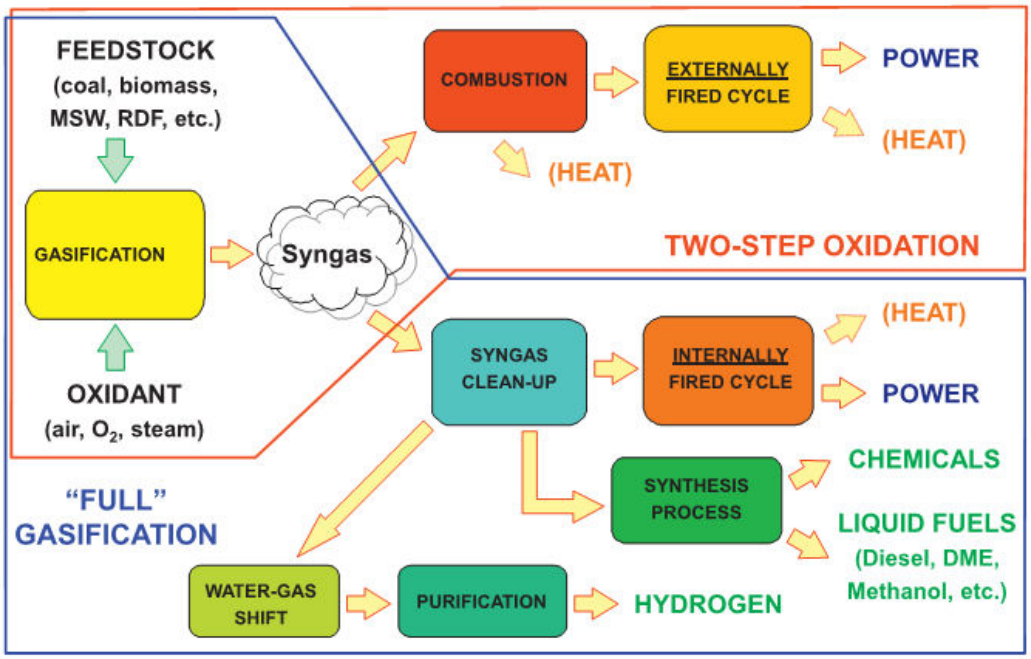

Figure 1. 4 Schematic representation of the alternative syngas utilization cycles and configurations of a pyro-gasification plant. Data source from Consonni et al. [12]

Among the energy generation applications, it is obvious that two configurations exist as potential syngas utilization routes. If raw syngas is combusted in a boiler for energy recovery then undergoes flue gas cleaning, the pyro-gasification plant is very similar to a conventional MSW incineration plant, with the difference that full oxidation is carried out in two steps. This type of WtE plant is defined as '*heat gasifier*', or, '*two-step oxidation*'. On the other hand, if the syngas is firstly cleaned then burned in an internally-fired cycle, then the system is defined as '*power gasifier*' [12]. Actually the most common configuration is currently related to two-step oxidation, since the simplest option is the steam cycle that does not require gas pre-treatment, and the generated tar can be burned directly without damaging the boiler [108]. Power gasifier is obviously more efficient; however syngas requires cleaning and cooling prior to be used in gas turbine or gas engine. In addition the syngas cleaning system is very complex and some practical problems still persist nowadays [108]. Today only one example exists for the utilization of syngas as IGCC, which is the gasification plant SVZ in Schwarze Pumpe in Germany, for which only little information is available for its operation.

In spite of the fact that world-wide implementation of MSW pyro-gasification has not been achieved yet, the innovative plants operated currently have demonstrated a good technological and environmental reliability. Some most typical pyro-gasification plants, together with their capacities and used technologies, have been reported by Panepinto et al. [108], as listed in **Table 1. 9**.

Table 1. 9 Typical pyro-gasification plants of MSW in the world

Plant	Capacity	Supplier	Start date	Technology
SVZ, Germany	250,000	Envirotherm	2001	Gasification + melting
Shin Moji, Japan	220,000	Nippon Steel	2007	Gasification + melting
Ibaraki, Japan	135,000	Nippon Steel	1980	Gasification + melting
Aomori, Japan	135,000	Ebara	2001	Gasification + combustion + melting
Kawaguchi, Japan	125,000	Ebara	2002	Gasification + combustion + melting
Toyohashi, Japan	108,000	Mitsui	2002	Pyrolysis + combustion + melting
Akita, Japan	120,000	Nippon Steel	2002	Gasification + melting
Oita, Japan	115,000	Nippon Steel	2003	Gasification + melting
Chiba, Japan	100,000	Thermoselect	2002	Gasification + melting
Hamm, Germany	100,000	Techtrade	2002	Pyrolysis + combustion

Data source: Date derived from Panepinto et al. [108]

1.4 Life cycle assessment of waste management system

As has been aforementioned, a holistic evaluation of the entire pyro-gasification system is very important apart from its technological development. LCA is a tool for the evaluation of the energy use and environmental impacts associated with a product or service through all stages of its life cycle from cradle to grave, i.e., from raw material acquisition throughout processing, manufacture, distribution, use, repair and maintenance, as well as final disposal or recycling. The advantage of LCA over other environmental analysis methods, such as environmental impact assessment or environmental audit, mainly lies in broadening the system boundaries to include all burdens and impacts in the life cycle of a product or a process. Hence it does not focus on the associated emissions and wastes generated by the plant or manufacturing site only [109]. It is thus proven to be a holistic and systematic methodology helping avoid to a narrow outlook on environmental concerns. As a result, LCA could be successful to quantify the relevant energy, material inputs and environmental releases of a specified system, as well as to evaluate the potential impacts associated with identified inputs and releases; hence leading to a more informed decision [110].

1.4.1 Principles and framework of LCA

After realizing the drawback from 'net energy analysis' methodology, the concept of LCA is first defined then developed by SETAC (Society of Environmental Toxicology and Chemistry) in 1990 [111]. Soon afterwards, ISO has carried out a set of principles and frameworks trying to standardize the definition and implementation of LCA [112-116]. A general consensus on the methodological framework between the two bodies has started to emerge [109], forming today's four-phase LCA framework as shown schematically in **Figure 1. 5**.

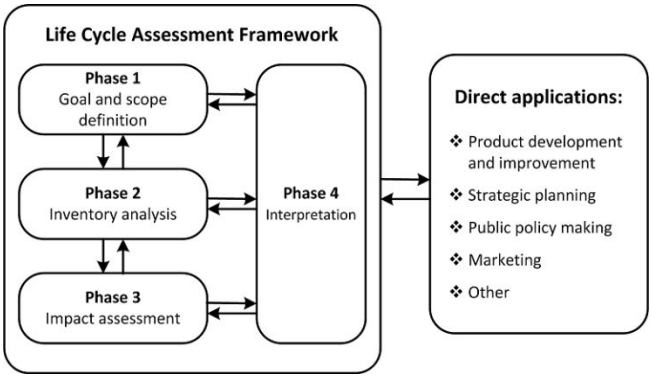

Figure 1. 5 Phases and applications of an LCA standardized by ISO [112]

The technical framework for the LCA methodology includes [112]:

- Goal and scope definition: the product(s) or service(s) to be assessed are defined, a functional basis for comparison is chosen and the required level of detail is defined;

- Life cycle inventory (LCI) analysis of extractions and emissions: the energy and raw materials used, and emissions to the atmosphere, water and land, are quantified for each process, then combined in the process flow chart and related to the functional basis;

- Life cycle impact assessment (LCIA): the effects of the resource use and emissions generated are grouped and quantified into a limited number of impact categories which may then be weighted for importance;

- Interpretation: the results are reported in the most informative way possible and the need and opportunities to reduce the impact of the product(s) or service(s) on the environment are systematically evaluated.

The broad system perspective makes LCA a powerful tool for environmental management. As such, LCA could be applied for two main objectives. First would be to quantitatively evaluate the environmental performance of a product or a process, or, to

choose a superior one among alternatives. Another objective of LCA is related to potential improvements of a system, especially towards environmental sustainability decision making.

Because of this, LCA has been increasingly used in the last decades in different fields like green product development, process design and optimization, pollution prevention, waste management planning, public policy making, etc [117-119]. These applications have mainly included, but are not limited to the following uses [109]:

- Strategic planning or environmental strategy development;
- Product and process optimization, design, and innovation;
- Identification of environmental improvements opportunities;
- Environmental reporting and marketing;
- Creating a framework for environmental audits.

1.4.2 LCA applied in waste management field

In the definition of LCA, the term 'product' includes not only product systems but can also include service systems such as waste management systems [120]. Currently, the onset of global issues has led to higher concerns about the environment. Therefore waste management system should move from end-of-pipe treatment towards an integrated approach [121]. Under such starting point, LCA therefore becomes an effective and useful evaluation tool in the waste management field. The National Waste Management Plan in Netherlands is an earlier application of LCA in waste management. By introducing LCA, this plan successfully compared alternative planning options and made decision on the configuration of end-treatment techniques for waste (landfill, incineration and separation/fermentation) [122]. The practical experience supports the feasibility and reliability of this innovative environmental management tool. Afterwards following its development in the latest decades, LCA has been widely applied to compare different treatment technologies, to support decision making, as well as for methodology and database development. These different aspects are discussed in detail as follows.

(i) LCA applied for the comparison of MSW treatment technologies

Using LCA, increasing studies have emerged aimed at evaluating different MSW treatment technologies [123, 124]. For example, Cherubini et al. [125] focused on four waste management strategies: landfill, landfill with biogas combustion to generate electricity, sorting plant combined with RDF to electricity and organic anaerobic digestion, and direct incineration. Results were based on the situation of Roma (Italy) but are reliable for most of the big European cities, and showed that landfill was always the worst option. Significant environmental savings could be achieved from undertaking energy recycling, which was able to substitute 15% of the total Roma electricity consumption. Finnveden et al. [126] tested the waste hierarchy based on the situation in Sweden. Included in the study were different options such as landfill, incineration, recycling, digestion and composting. In addition, factors such as energy system, time and space of the interventions and treatment of paper and plastic may impact the overall results. Hence the possible application of site-dependent impact assessment methods should be tried to better understand the implications of simplifications.

LCA has also been used to compare different scenarios for the implementation of a specific technology [127-129]. Kong et al. [130] modeled the GHG of organic waste landfill, composting and anaerobic digestion in the USA. Results indicated that the latter two methods could be served as effective alternatives to substitute organic landfill. Dahlbo et al. [131] conducted a comparison of treatment options for newspaper, including material recycling, energy recovery and landfill. Results showed that the life cycle phase causing the most environmental impacts was the paper mill. In any cases comparing the different waste management systems, the energy recovery options were in general superior to landfill.

(ii) LCA applied as decision making support tool

LCA has also gained applications as a tool for decision and policy-making, ranging from local planning to policy making at national and international levels. An example of this is the recent thematic strategy on waste management presented by the European Commission [132]. Chaya et al. [133] performed a LCA study to analyze the 'waste-to-energy schemes' in Thailand. Four environmental impacts as global warming, acidification, stratospheric ozone depletion and photo-oxidant formation were evaluated for the two energy schemes currently practiced: incineration and anaerobic digestion. The LCA results were useful for decision makers to pinpoint where improvements could be made for both schemes. Consonni et al.

[21] analyzed the optimal breakdown between material recovery and energy recovery from MSW, aiming at finding the most attractive waste management strategy applicable in Italy and Europe. In addition, LCA is also used for the prediction of resource consumption and environmental pollutions in the future. For example, Park et al. [134] conducted a comparative analysis for reducing GHG emissions in Korea by 2050. The use of final energy, primary energy and electricity generation are examined, which can be considered as a reference for developing strategies in reducing GHG emissions in the long term.

(iii) Methodology and database development of LCA

Studies are also focused on methodology and database development. On the one hand, researches are concentrated on quantitation of different environmental impacts; and some reasonable and acceptable life cycle impact assessment methods were thus developed, e.g. EDIP, Eco-indicator. On the other hand, researches also focused on inventory database and computer-based software development, with the aim to enhance the process feasibility and operability. Some of the most commonly applied impact assessment methods, database and software are summarized in **Table 1. 10**.

Table 1. 10 Some impact assessment methods, database and software implemented in LCA field

	Method	Developer	Characteristics
Impact assessment	EDIP 97	Technical University of Denmark, several Danish industry companies and Danish EPA	Impacts are grouped into three categories: environment, resources and working environment. The weighting is based on Danish policy targets.
	EPS 2000	Swedish Environmental Research Institute in cooperation with Volvo and the Swedish Federation of Industries	The method describes impacts to the environment as: biodiversity, production, human health, resources, and aesthetic values. The weighting uses Environmental Load Units according to willing-to-pay economic values.
	Eco-indicator 99	Pré Consultants, Netherlands	A damage oriented method that links different environmental effects into three categories: human health, ecosystem quality and resources. Three perspectives are available for normalization and weighting step: individualist, egalitarian and hierarchist.
	CML 2001	Centre of Environmental Science–Leiden University Netherlands	It groups the categories by midpoint approach. It uses primarily European data to derive its impact factors.
	Impact 2002+	Swiss Federal Institute of Technology - Lausanne (EPFL)	It provides a feasible approach of combined midpoint/damage method, takes advantage of both CML and Eco-indicator 99 via 14 midpoint categories to four damage categories.
Database	Ecoinvent	Ecoinvent Centre, the Swiss Centre for Life Cycle Inventories	It is the most famous LCA database worldwide. The database contains international industrial life cycle inventory data on energy supply, resource extraction, material supply, chemicals, metals, agriculture, waste management

			services and transport services that can be imported easily in open LCA.
	ELCD	European Platform on Life Cycle Assessment, JRC	It provides inventory data from front-running EU-level business associations and other sources, including more than 440 processes for key materials, energy carriers, transport, and waste management.
Software	Gabi	IPTS, Germany	It includes 4700 inventory datasets including situations in EU, China, US and worldwide. It could help enhance sustainability decision-making and LCA projects
	SimaPro	Pré Consultants, Netherlands	It supports LCA and always includes a variety of LCI databases; is developed to help effectively apply LCA expertise to drive change.
	EASEWASTE	Technical University of Denmark (DTU)	It is designed for waste management. The model consists of 48 waste fractions and chemical composition, and 8 waste treatment processes
	ORWARE	Royal Institute of Technology (KTH), Swedish	A simulation model for waste management. It includes all kinds of MSW as well as submodels for calculation of economic aspects.

1.4.3 LCA of WtE technologies: Current status

Up to date, LCA has been successfully applied to evaluate different MSW treatment technologies like landfill, incineration, composting and anaerobic digestion. However, LCA studies of novel MSW thermal technologies, particularly for pyrolysis and gasification, are rarely performed. For example, Khoo et al. [135] evaluated eight advanced thermal technologies including pyrolysis, gasification as well as a combined approach. Results showed that thermal cracking gasification of granulated MSW and the gasification of RDF exhibited

the highest environmental impacts, and steam gasification of wood and pyrolysis-gasification of MSW were the most environmental friendly approaches. However, their assessment did not include the downstream utilization of the products, and a parallel comparison with conventional incineration was lacking. Consonni et al. [12] compared two gasification technologies with conventional incineration plants. A process simulation model has been set up for plant modeling. However, their comparison was mainly focused on parametric analysis, and a quantitative comparison for the energy consumption and environmental impacts from life cycle perspective has not been performed. Pa et al. [136] investigated the potential replacement of natural gas combustion for district heating by wood waste and wood pellets gasification; Ning et al. [137] clarified the feasibility and potential effects of a pyrolysis-based bioenergy system by evaluating its cost, energy and environmental efficiency. However, the feedstock used in these studies was mainly relying on biomass materials, studies analyzing MSW characteristics are still lacking.

1.5 Motivation and objective of the study

The literature review has demonstrated the current research progress and hotspots in the field of MSW pyro-gasification. Nevertheless, even if previous studies have provided good insights into different topics, further investigations are still required to fulfill the research as well as to facilitate the industrial application of MSW pyro-gasification technology. Therefore, the objective of this study will be to focus on four aspects, together with the detailed motivation of each aspect presented as follows.

- **Pyro-gasification of typical MSW components and the establishment of prediction model**

Establishing a practical MSW pyro-gasification prediction model is very important since MSW composition and characteristics vary significantly with geographies. If a general model could help quantify and predict pyro-gasification and especially syngas properties, then a large segment of test and verification works could be saved, which could effectively reduce the project cost and make system optimization more efficient. Particularly, since the data related to MSW composition in different countries and periods are usually easy to obtain, prediction models based on MSW physical composition would be greatly beneficial.

As highlighted in **Section 1.2.3**, the thermal behavior of MSW is highly variable owing to the complexity of MSW components and reaction agent. Better understanding of the pyro-gasification characteristics of a given MSW component is hence essential for process design, operation and optimization. Nevertheless, such systematic analysis is still quite lacking, and the effect of MSW components and gasifying agent on high-quality syngas production still requires in-depth investigation and comparison. It is anticipated that the outcomes of such study could provide insights into the pyro-gasification processes of different MSW components, and as well permit to identify proper application routes for the syngas obtained.

Open literature has provided obvious evidence of the nonlinear effects that may occur during pyro-gasification of MSW multi-components. It has been proven that, pyro-gasification of multiple components would pose synergetic or inhibition effect for the products. However, current researches are mainly conducted on TGA, where the mass of inlet feedstock is limited to several milligrams with the aim to study the thermolysis characteristics. Hence studies focusing on syngas properties are quite limited. As a consequence, it is important to investigate feedstock mixtures to better obtain interaction mechanisms, with the final aim to facilitate high-quality syngas production.

The broadly acquired pyro-gasification characteristics based on MSW physical composition could serve as database for the development of a MSW pyro-gasification prediction model. Among different models as reported in **Section 1.2.3**, ANN is here considered as an ideal means, since less system information is demanded compared to equilibrium and kinetic based modeling, and this model exhibits the ability to address highly nonlinear relationships. Hence, its possibility and feasibility to be applied in MSW pyro-gasification field needs further study. These aspects of research will be presented in **Chapter 3**.

- **Pyro-gasification optimization: Syngas upgrading by the use of a catalyst**

The H_2-rich and tar-free gas is attractive as high-quality syngas production, in light of the energy content of H_2 (relatively high) and its use does not cause any emission. In addition, tar reduction is also important, since it may decrease the system efficiency and even block and damage downstream gasifier. Because of these facts, in-depth investigation for pyro-gasification optimization with emphasis on these aims is significant meaningful.

CaO has gained growing interest as an in-situ catalyst during pyro-gasification. The catalyst could react via different pathways. First, CaO exhibits the impact on tar reduction. Therefore as reported in **Section 1.2.4**, CaO could catalytically contribute to tar cracking and accelerate the reaction between tar and H_2O, which would significantly reduce the tar content and upgrade the syngas quality. Another advantage of CaO is its potential to act as a sorbent for CO_2 adsorption via carbonation reaction, as already pointed out in **Section 1.3.1** by Eq. (1.2). Following a decrease in CO_2 partial pressure, the water-gas shift reaction (Reaction R7 in **Table 1.1**) is enhanced and the H_2 production can be improved.

CaO can be derived from a wide range of naturally occurring precursors as limestone and dolomite. Owing to its low cost (e.g., about 200-500 CNY/t) and abundant availability [56, 138], CaO has exhibited great potential to be served as catalyst for industrial large-scale application. As a result, the use of CaO as an in-situ catalyst for pyro-gasification optimization requires in-depth investigation. This aspect of research will be presented in **Chapter 4**.

- **Investigation of catalyst reactivity and re-generation**

This part of the work is an in-depth extension of **Chapter 4**, aiming at further investigating the recycling potential of CaO catalyst during its long cycles of carbonation/calcination process. **Section 1.2.4** investigates on catalyst de-activation. It is found that CaO is far from reversible recycling in practice; its reactivity will be significantly reduced during the long series recycling between carbonation/calcination reactions. For a better use of CaO as catalyst in industrial application, the catalytic performance should be guaranteed for long operation periods with niminal loses. As a consequence, investigation for the reactivity of CaO, especially its de-activation mechanism, influence factors, as well as potential re-generation methods, is of greatly importance. This aspect of research will be presented in **Chapter 5**.

- **Life cycle assessment and optimization of MSW pyro-gasification technology**

Review on the current literature has revealed that, a comprehensive comparison between MSW thermal technologies including pyrolysis, gasification and incineration is still lacking. Although MSW pyro-gasification has exhibited several benefits over conventional incineration, using this novel technology does not imply necessarily environmental

sustainability. A systematic evaluation is therefore required to quantify the overall energy and environmental performance, including all waste processing stages from MSW pre-treatment, conversion, energy recovery, pollution control, to final ash disposal. As a result, a LCA study is urgently required to help quantify the overall energy and environmental effects. Besides, thermal treatment systems under different reagions, for example France and China, also need to be analyzed to guide for the appropriate development of WtE technology worldwide.

Nevertheless, one outstanding advantage of pyro-gasification is the possibility to obtain a syngas suited for different applications. Literature review has proved that, LCA is feasible for the prediction and selection of a future system. Regarding the fact, a quantitative assessment of different pyrolysis and gasification utilization approaches is essential, to help guide and optimize an energy-efficient and environmental-sound syngas application route. This aspect of research will be presented in **Chapter 6**.

1.6 Bibliography

[1] Belgiorno V, De Feo G, Della Rocca C, Napoli RMA. Energy from gasification of solid wastes. Waste Management. 2003;23:1-15.

[2] Arena Umberto. Process and technological aspects of municipal solid waste gasification. A review. Waste Management. 2012;32:625-639.

[3] Tillman David. The combustion of solid fuels and wastes. San Diego, CA: Academic Press; 1991.

[4] Van de Velden Manon, Baeyens Jan, Brems Anke, Janssens Bart, Dewil Raf. Fundamentals, kinetics and endothermicity of the biomass pyrolysis reaction. Renewable Energy. 2010;35:232-242.

[5] Kawaguchi Kuniyasu, Miyakoshi Kazutada, Momonoi Kiyoshi. Studies on the pyrolysis behavior of gasification and melting systems for municipal solid waste. Journal of Material Cycles and Waste Management. 2002;4:102-110.

[6] Smolders K, Van de Velden M, Baeyens J. Operating parameters for the bubbling fluidized (BFB) and circulating fluidized bed (CFB) processing of biomass. Proceedings of ‘‘use of renewables’’, Achema: Frankfurt. 2006.

[7] Bridgwater Anthony V. Review of fast pyrolysis of biomass and product upgrading. Biomass & Bioenergy. 2012;38:68-94.

[8] Engvall Klas, Kusar Henrik, Sjöström Krister, Pettersson Lars J. Upgrading of raw gas from biomass and waste gasification: Challenges and opportunities. Topics In Catalysis. 2011;54:949-959.

[9] Van der Drift A, Boerrigter Harold. Synthesis gas from biomass for fuels and chemicals: ECN Biomass, Coal and Environmental Research; 2006.

[10] Hauserman WB, Giordano N, Lagana M, Recupero V. Biomass gasifiers for fuel cells systems. La Chimica e l'industria. 1997;79:199-206.

[11] Walker Philip L, Rusinko Frank, Austin L Go. Gas reactions of carbon. Advances In Catalysis. 1959;11:133-221.

[12] Consonni Stefano, Viganò Federico. Waste gasification vs. conventional Waste-To-Energy: A comparative evaluation of two commercial technologies. Waste Management. 2012;32:653-666.

[13] Leckner Bo. Process aspects in combustion and gasification Waste-to-Energy (WtE) units. Waste Management. 2015;37:13-25.

[14] Malkow Thomas. Novel and innovative pyrolysis and gasification technologies for energy efficient and environmentally sound MSW disposal. Waste Management. 2004;24:53-79.

[15] Heermann C, Schwager FJ, Whiting KJ. Pyrolysis & Gasification of waste: A Worldwide Technology & Business Review. 2nd Edition: Juniper Consultancy Services Ltd.; 2001.

[16] Arena Umberto, Ardolino Filomena, Di Gregorio Fabrizio. A life cycle assessment of environmental performances of two combustion-and gasification-based waste-to-energy technologies. Waste Management. 2015;41:60-74.

[17] Okuwaki Akitsugu. Feedstock recycling of plastics in Japan. Polymer Degradation And Stability. 2004;85:981-988.

[18] Chen Tianju, Wu Jingli, Zhang Zhezi, Zhu Mingming, Sun Li, Wu Jinhu, et al. Key thermal events during pyrolysis and CO_2-gasification of selected combustible solid wastes in a thermogravimetric analyser. Fuel. 2014;137:77-84.

[19] Knoef Harrie, Ahrenfeldt Jesper. Handbook biomass gasification: BTG biomass technology group, The Netherlands; 2005.

[20] Zhao Wei, van der Voet Ester, Zhang Yufeng, Huppes Gjalt. Life cycle assessment of municipal solid waste management with regard to greenhouse gas emissions: Case study of Tianjin, China. Science Of The Total Environment. 2009;407:1517-1526.

[21] Consonni Stefano, Giugliano Michele, Massarutto Antonio, Ragazzi Marco, Saccani Cesare. Material and energy recovery in integrated waste management systems: Project

overview and main results. Waste Management. 2011;31:2057-2065.

[22] McKendry Peter. Energy production from biomass (part 3): gasification technologies. Bioresource Technology. 2002;83:55-63.

[23] Narvaez Ian, Orio Alberto, Aznar Maria P, Corella Jose. Biomass gasification with air in an atmospheric bubbling fluidized bed. Effect of six operational variables on the quality of the produced raw gas. Industrial & Engineering Chemistry Research. 1996;35:2110-2120.

[24] Doherty Wayne, Reynolds Anthony, Kennedy David. The effect of air preheating in a biomass CFB gasifier using ASPEN Plus simulation. Biomass & Bioenergy. 2009;33:1158-1167.

[25] Reed TBDA, Das Agua. Handbook of biomass downdraft gasifier engine systems: Biomass Energy Foundation; 1988.

[26] Habibi Rozita, Kopyscinski Jan, Masnadi Mohammad S, Lam Jill, Grace John R, Mims Charles A, et al. Co-gasification of biomass and non-biomass feedstocks: synergistic and inhibition effects of switchgrass mixed with sub-bituminous coal and fluid coke during CO_2 gasification. Energy & Fuels. 2012;27:494-500.

[27] Vamvuka D, Karouki E, Sfakiotakis S. Gasification of waste biomass chars by carbon dioxide via thermogravimetry. Part I: Effect of mineral matter. Fuel. 2011;90:1120-1127.

[28] Bruno G, Buroni M, Carvani L, Del Piero G, Passoni G. Water-insoluble compounds formed by reaction between potassium and mineral matter in catalytic coal gasification. Fuel. 1988;67:67-72.

[29] Nzihou Ange, Stanmore Brian, Sharrock Patrick. A review of catalysts for the gasification of biomass char, with some reference to coal. Energy. 2013;58:305-317.

[30] Parvez Ashak M, Mujtaba Iqbal M, Pang Chengheng, Lester Edward, Wu Tao. Effect of the addition of different waste carbonaceous materials on coal gasification in CO_2 atmosphere. Fuel Processing Technology. 2016;149:231-238.

[31] Ryu Changkook, Yang Yao Bin, Khor Adela, Yates Nicola E, Sharifi Vida N, Swithenbank Jim. Effect of fuel properties on biomass combustion: Part I. Experiments—fuel type, equivalence ratio and particle size. Fuel. 2006;85:1039-1046.

[32] Kumar Ajay, Jones David D, Hanna Milford A. Thermochemical biomass gasification: a review of the current status of the technology. Energies. 2009;2:556-581.

[33] Lv Pengmei, Chang Jie, Wang Tiejun, Fu Yan, Chen Yong, Zhu Jingxu. Hydrogen-rich gas production from biomass catalytic gasification. Energy & Fuels. 2004;18:228-233.

[34] Luo Siyi, Xiao Bo, Guo Xianjun, Hu Zhiquan, Liu Shiming, He Maoyun. Hydrogen-rich gas

from catalytic steam gasification of biomass in a fixed bed reactor: influence of particle size on gasification performance. International Journal Of Hydrogen Energy. 2009;34:1260-1264.

[35] Ruiz JA, Juárez MC, Morales MP, Muñoz P, Mendívil MA. Biomass gasification for electricity generation: review of current technology barriers. Renewable and Sustainable Energy Reviews. 2013;18:174-183.

[36] Wang Lijun, Weller Curtis L, Jones David D, Hanna Milford A. Contemporary issues in thermal gasification of biomass and its application to electricity and fuel production. Biomass and Bioenergy. 2008;32:573-581.

[37] Xiao Rui, Jin Baosheng, Zhou Hongcang, Zhong Zhaoping, Zhang Mingyao. Air gasification of polypropylene plastic waste in fluidized bed gasifier. Energy Conversion And Management. 2007;48:778-786.

[38] Zainal ZA, Rifau Ali, Quadir GA, Seetharamu KN. Experimental investigation of a downdraft biomass gasifier. Biomass and Bioenergy. 2002;23:283-289.

[39] He Maoyun, Hu Zhiquan, Xiao Bo, Li Jianfen, Guo Xianjun, Luo Siyi, et al. Hydrogen-rich gas from catalytic steam gasification of municipal solid waste (MSW): Influence of catalyst and temperature on yield and product composition. International Journal Of Hydrogen Energy. 2009;34:195-203.

[40] Sattar Anwar, Leeke Gary A, Hornung Andreas, Wood Joseph. Steam gasification of rapeseed, wood, sewage sludge and miscanthus biochars for the production of a hydrogen-rich syngas. Biomass and Bioenergy. 2014;69:276-286.

[41] Udomsirichakorn Jakkapong, Salam P Abdul. Review of hydrogen-enriched gas production from steam gasification of biomass: the prospect of CaO-based chemical looping gasification. Renewable and Sustainable Energy Reviews. 2014;30:565-579.

[42] Ahmed II, Gupta AK. Kinetics of woodchips char gasification with steam and carbon dioxide. Applied Energy. 2011;88:1613-1619.

[43] Sadhwani Narendra, Adhikari Sushil, Eden Mario R. Biomass Gasification Using Carbon Dioxide: Effect of Temperature, CO_2/C Ratio, and the Study of Reactions Influencing the Process. Industrial & Engineering Chemistry Research. 2016;55:2883-2891.

[44] Garcia L, Salvador ML, Arauzo J, Bilbao R. CO_2 as a gasifying agent for gas production from pine sawdust at low temperatures using a Ni/Al coprecipitated catalyst. Fuel Processing Technology. 2001;69:157-174.

[45] Kinoshita CM, Wang Y, Zhou J. Tar formation under different biomass gasification conditions. Journal Of Analytical And Applied Pyrolysis. 1994;29:169-181.

[46] Hernández JJ, Aranda G, Barba J, Mendoza JM. Effect of steam content in the air–steam flow on biomass entrained flow gasification. Fuel Processing Technology. 2012;99:43-55.

[47] Gupta Himanshu, Iyer Mahesh V, Sakadjian Bartev B, Fan Liang-Shih. Reactive separation of CO_2 using pressure pelletised limestone. International journal of environmental technology and management. 2004;4:3-20.

[48] Taba Leila Emami, Irfan Muhammad Faisal, Daud Wan Ashri Mohd Wan, Chakrabarti Mohammed Harun. The effect of temperature on various parameters in coal, biomass and CO-gasification: a review. Renewable and Sustainable Energy Reviews. 2012;16:5584-5596.

[49] Lahijani Pooya, Zainal Zainal Alimuddin. Gasification of palm empty fruit bunch in a bubbling fluidized bed: a performance and agglomeration study. Bioresource Technology. 2011;102:2068-2076.

[50] González JF, Román S, Bragado D, Calderón M. Investigation on the reactions influencing biomass air and air/steam gasification for hydrogen production. Fuel Processing Technology. 2008;89:764-772.

[51] Devi Lopamudra, Ptasinski Krzysztof J, Janssen Frans JJG. A review of the primary measures for tar elimination in biomass gasification processes. Biomass and Bioenergy. 2003;24:125-140.

[52] Wang Yin, Yoshikawa Kunio, Namioka Tomoaki, Hashimoto Yoshirou. Performance optimization of two-staged gasification system for woody biomass. Fuel Processing Technology. 2007;88:243-250.

[53] Turn S, Kinoshita C, Zhang Z, Ishimura D, Zhou J. An experimental investigation of hydrogen production from biomass gasification. International Journal Of Hydrogen Energy. 1998;23:641-648.

[54] Loha Chanchal, Chatterjee Pradip K, Chattopadhyay Himadri. Performance of fluidized bed steam gasification of biomass–modeling and experiment. Energy Conversion And Management. 2011;52:1583-1588.

[55] Li Jianfen, Liao Shiyan, Dan Weiyi, Jia Kuile, Zhou Xiaorong. Experimental study on catalytic steam gasification of municipal solid waste for bioenergy production in a combined fixed bed reactor. Biomass & Bioenergy. 2012;46:174-180.

[56] Acharya Bishnu, Dutta Animesh, Basu Prabir. An investigation into steam gasification of biomass for hydrogen enriched gas production in presence of CaO. International Journal Of Hydrogen Energy. 2010;35:1582-1589.

[57] Sørum Lars, Grønli MG, Hustad Johan E. Pyrolysis characteristics and kinetics of

municipal solid wastes. Fuel. 2001;80:1217-1227.

[58] Umeki Kentaro, Yamamoto Kouichi, Namioka Tomoaki, Yoshikawa Kunio. High temperature steam-only gasification of woody biomass. Applied Energy. 2010;87:791-798.

[59] Leung DYC, Wang CL. Fluidized-bed gasification of waste tire powders. Fuel Processing Technology. 2003;84:175-196.

[60] Ahmed I, Gupta AK. Syngas yield during pyrolysis and steam gasification of paper. Applied Energy. 2009;86:1813-1821.

[61] Lee Uisung, Chung JN, Ingley Herbert A. High-temperature steam gasification of municipal solid waste, rubber, plastic and wood. Energy & Fuels. 2014;28:4573-4587.

[62] Haykiri-Acma H, Yaman S. Interaction between biomass and different rank coals during co-pyrolysis. Renewable Energy. 2010;35:288-292.

[63] Lopez Gartzen, Erkiaga Aitziber, Amutio Maider, Bilbao Javier, Olazar Martin. Effect of polyethylene co-feeding in the steam gasification of biomass in a conical spouted bed reactor. Fuel. 2015;153:393-401.

[64] Edreis Elbager MA, Luo Guangqian, Li Aijun, Xu Chaofen, Yao Hong. Synergistic effects and kinetics thermal behaviour of petroleum coke/biomass blends during H_2O co-gasification. Energy Conversion And Management. 2014;79:355-366.

[65] Jakab E, Varhegyi G, Faix O1. Thermal decomposition of polypropylene in the presence of wood-derived materials. Journal Of Analytical And Applied Pyrolysis. 2000;56:273-285.

[66] Dong Changqing, Yang Yongping, Jin Baosheng, Horio Masayuki. The pyrolysis of sawdust and polyethylene in TG and U-shape tube reactor. Waste Management. 2007;27:1557-1561.

[67] Pinto F, Franco C, André RN, Miranda M, Gulyurtlu I, Cabrita I. Co-gasification study of biomass mixed with plastic wastes. Fuel. 2002;81:291-297.

[68] Luo Siyi, Xiao Bo, Hu Zhiquan, Liu Shiming. Effect of particle size on pyrolysis of single-component municipal solid waste in fixed bed reactor. International Journal Of Hydrogen Energy. 2010;35:93-97.

[69] He Maoyun, Xiao Bo, Liu Shiming, Hu Zhiquan, Guo Xianjun, Luo Siyi, et al. Syngas production from pyrolysis of municipal solid waste (MSW) with dolomite as downstream catalysts. Journal Of Analytical And Applied Pyrolysis. 2010;87:181-187.

[70] Grønli Morten Gunnar, Várhegyi Gábor, Di Blasi Colomba. Thermogravimetric analysis and devolatilization kinetics of wood. Industrial & Engineering Chemistry Research.

2002;41:4201-4208.

[71] Chen Shen, Meng Aihong, Long Yanqiu, Zhou Hui, Li Qinghai, Zhang Yanguo. TGA pyrolysis and gasification of combustible municipal solid waste. Journal of the Energy Institute. 2015;88:332-343.

[72] Lai ZhiYi, Ma XiaoQian, Tang YuTing, Lin Hai. Thermogravimetric analysis of the thermal decomposition of MSW in N_2, CO_2 and CO_2/N_2 atmospheres. Fuel Processing Technology. 2012;102:18-23.

[73] Ahmed I, Gupta AK. Characteristics of cardboard and paper gasification with CO_2. Applied Energy. 2009;86:2626-2634.

[74] Couto Nuno Dinis, Silva Valter Bruno, Rouboa Abel. Thermodynamic Evaluation of Portuguese municipal solid waste gasification. Journal of Cleaner Production. 2016.

[75] Mitta Narendar R, Ferrer-Nadal Sergio, Lazovic Aleksandar M, Perales José F, Velo Enric, Puigjaner Luis. Modelling and simulation of a tyre gasification plant for synthesis gas production. Computer Aided Chemical Engineering. 2006;21:1771.

[76] Niu Miaomiao, Huang Yaji, Jin Baosheng, Wang Xinye. Simulation of syngas production from municipal solid waste gasification in a bubbling fluidized bed using Aspen Plus. Industrial & Engineering Chemistry Research. 2013;52:14768-14775.

[77] Gungor Afsin, Yildirim Ugur. Two dimensional numerical computation of a circulating fluidized bed biomass gasifier. Computers & Chemical Engineering. 2013;48:234-250.

[78] Xiao Gang, Ni Ming-jiang, Chi Yong, Jin Bao-sheng, Xiao Rui, Zhong Zhao-ping, et al. Gasification characteristics of MSW and an ANN prediction model. Waste Management. 2009;29:240-244.

[79] Mikulandrić Robert, Lončar Dražen, Böhning Dorith, Böhme Rene, Beckmann Michael. Artificial neural network modelling approach for a biomass gasification process in fixed bed gasifiers. Energy Conversion And Management. 2014;87:1210-1223.

[80] Puig-Arnavat Maria, Hernández J Alfredo, Bruno Joan Carles, Coronas Alberto. Artificial neural network models for biomass gasification in fluidized bed gasifiers. Biomass and Bioenergy. 2013;49:279-289.

[81] Kuo Jia-Hong, Wey Ming-Yen, Chen Wei-Cheng. Woody waste air gasification in fluidized bed with Ca-and Mg-modified bed materials and additives. Applied Thermal Engineering. 2013;53:42-48.

[82] Yung Matthew M, Jablonski Whitney S, Magrini-Bair Kimberly A. Review of catalytic conditioning of biomass-derived syngas. Energy & Fuels. 2009;23:1874-1887.

[83] Shen Yafei, Yoshikawa Kunio. Recent progresses in catalytic tar elimination during

biomass gasification or pyrolysis—a review. Renewable and Sustainable Energy Reviews. 2013;21:371-392.

[84] Depner H, Jess A. Kinetics of nickel-catalyzed purification of tarry fuel gases from gasification and pyrolysis of solid fuels. Fuel. 1999;78:1369-1377.

[85] Schmidt S, Giesa S, Drochner A, Vogel H. Catalytic tar removal from bio syngas—catalyst development and kinetic studies. Catalysis Today. 2011;175:442-449.

[86] Milne Thomas A, Abatzoglou Nicolas, Evans Robert J. Biomass gasifier "tars": Their nature, formation, and conversion: National Renewable Energy Laboratory Golden, CO; 1998.

[87] Han Jun, Kim Heejoon. The reduction and control technology of tar during biomass gasification/pyrolysis: an overview. Renewable and Sustainable Energy Reviews. 2008;12:397-416.

[88] Abu El-Rub Z, Bramer EA, Brem G. Review of catalysts for tar elimination in biomass gasification processes. Industrial & Engineering Chemistry Research. 2004;43:6911-6919.

[89] Delgado Jesús, Aznar María P, Corella José. Calcined dolomite, magnesite, and calcite for cleaning hot gas from a fluidized bed biomass gasifier with steam: life and usefulness. Industrial & Engineering Chemistry Research. 1996;35:3637-3643.

[90] Moulijn Jacob A, Van Diepen AE, Kapteijn F. Catalyst deactivation: is it predictable?: What to do? Applied Catalysis A: General. 2001;212:3-16.

[91] Bartholomew Calvin H. Mechanisms of catalyst deactivation. Applied Catalysis A: General. 2001;212:17-60.

[92] Sun P, Grace JR, Lim CJ, Anthony EJ. The effect of CaO sintering on cyclic CO_2 capture in energy systems. Aiche Journal. 2007;53:2432-2442.

[93] Borgwardt Robert H. Calcium oxide sintering in atmospheres containing water and carbon dioxide. Industrial & Engineering Chemistry Research. 1989;28:493-500.

[94] Vassilatos V, Taralas G, Sjöström K, Björnbom E. Catalytic cracking of tar in biomass pyrolysis gas in the presence of calcined dolomite. The Canadian Journal of Chemical Engineering. 1992;70:1008-1013.

[95] Mudge LK, Baker EG, Mitchell DH, Brown MD. Catalytic steam gasification of biomass for methanol and methane production. Journal of solar energy engineering. 1985;107:88-92.

[96] Simell Pekka A, Hepola Jouko O, Krause A Outi I. Effects of gasification gas components on tar and ammonia decomposition over hot gas cleanup catalysts. Fuel.

1997;76:1117-1127.

[97] Baker Eddie G, Mudge Lyle K, Brown Michael D. Steam gasification of biomass with nickel secondary catalysts. Industrial & Engineering Chemistry Research. 1987;26:1335-1339.

[98] Arauzo Jesús, Radlein Desmond, Piskorz Jan, Scott Donald S. Catalytic pyrogasification of biomass. Evaluation of modified nickel catalysts. Industrial & Engineering Chemistry Research. 1997;36:67-75.

[99] Lammers G, Beenackers AACM. Catalytic tar removal from biomass producer gas with in situ catalyst regeneration. Fuel and Energy Abstracts1998. p. 35.

[100] Rong Nai, Wang Qinhui, Fang Mengxiang, Cheng Leming, Luo Zhongyang, Cen Kefa. Steam hydration reactivation of CaO-based sorbent in cyclic carbonation/calcination for CO_2 capture. Energy & Fuels. 2013;27:5332-5340.

[101] Raskin Neil, Palonen Juha, Nieminen Jorma. Power boiler fuel augmentation with a biomass fired atmospheric circulating fluid-bed gasifier. Biomass and Bioenergy. 2001;20:471-481.

[102] Rensfelt E, Everard D. Update on project ARBRE: wood gasification plant utilising short rotation coppice and forestry residues. VTT Symposium: Valtion Teknillinen Tutkimuskeskus; 1999. p. 103-118.

[103] Miccio F, Moersch O, Spliethoff H, Hein KRG. Gasification of two biomass fuels in bubbling fluidized bed. Consiglio Nazionale delle Ricerche ICR-CNR, Napoli (IT); 1999.

[104] Yan Feng, Luo Si-yi, Hu Zhi-quan, Xiao Bo, Cheng Gong. Hydrogen-rich gas production by steam gasification of char from biomass fast pyrolysis in a fixed-bed reactor: Influence of temperature and steam on hydrogen yield and syngas composition. Bioresource Technology. 2010;101:5633-5637.

[105] Butterman Heidi C, Castaldi Marco J. CO_2 as a carbon neutral fuel source via enhanced biomass gasification. Environmental Science & Technology. 2009;43:9030-9037.

[106] Tijmensen Michiel JA, Faaij Andre PC, Hamelinck Carlo N, van Hardeveld Martijn RM. Exploration of the possibilities for production of Fischer Tropsch liquids and power via biomass gasification. Biomass and Bioenergy. 2002;23:129-152.

[107] Ng Kok Leong, Chadwick D, Toseland BA. Kinetics and modelling of dimethyl ether synthesis from synthesis gas. Chemical Engineering Science. 1999;54:3587-3592.

[108] Panepinto Deborah, Tedesco Vita, Brizio Enrico, Genon Giuseppe. Environmental performances and energy efficiency for MSW gasification treatment. Waste and Biomass Valorization. 2015;6:123-135.

[109] Azapagic Adisa. Life cycle assessment and its application to process selection, design and optimisation. Chemical Engineering Journal. 1999;73:1-21.

[110] US Environmental Protection Agency. Life Cycle Assessment (LCA). 6 August 2010.

[111] Society of Environmental Toxicology and Chemistry (SATAC). Guidelines for life-cycle assessment: a code of practice: Pensacola; 1993.

[112] ISO. ISO 14040: Environmental management-Life cycle assessment-Principles and Framework. Geneva: ISP copyright office; 1997.

[113] ISO. ISO 14041: Environmental Management: Life Cycle Assessment: Goal and Scope Definition and Inventory Analysis: International Organization for Standardization; 1998.

[114] ISO. ISO 14042: environmental management—life cycle assessment—life cycle impact assessment. Geneva, Switzerland. 2000.

[115] ISO. ISO 14043: Environmental Management–Life Cycle Assessment–Life Cycle Interpretation. EN ISO. 2000;14043:18.

[116] ISO. ISO 14044: Environmental Management–Life Cycle Assessment–Requirements and Guidelines: ISO; 2006.

[117] Corominas Ll, Foley J, Guest JS, Hospido A, Larsen HF, Morera S, et al. Life cycle assessment applied to wastewater treatment: state of the art. Water Research. 2013;47:5480-5492.

[118] Peng Jinqing, Lu Lin, Yang Hongxing. Review on life cycle assessment of energy payback and greenhouse gas emission of solar photovoltaic systems. Renewable and Sustainable Energy Reviews. 2013;19:255-274.

[119] Plevin Richard J, Delucchi Mark A, Creutzig Felix. Using attributional life cycle assessment to estimate climate‐change mitigation benefits misleads policy makers. Journal of Industrial Ecology. 2014;18:73-83.

[120] Finnveden G. Methodological aspects of life cycle assessment of integrated solid waste management systems. Resources, Conservation and Recycling. 1999;26:173-187.

[121] Udo de Haes Helias A, Heijungs Reinout. Life-cycle assessment for energy analysis and management. Applied Energy. 2007;84(7-8):817-827.

[122] Tukker Arnold. Life cycle assessment as a tool in environmental impact assessment. Environmental Impact Assessment Review. 2000;20:435-456.

[123] Tonini Davide, Astrup Thomas. LCA of biomass-based energy systems: A case study for Denmark. Applied Energy. 2012;99:234-246.

[124] Arena Umberto, Mastellone Maria Laura, Perugini Francesco. The environmental performance of alternative solid waste management options: a life cycle assessment

study. Chemical Engineering Journal. 2003;96:207-222.

[125] Cherubini Francesco, Bargigli Silvia, Ulgiati Sergio. Life cycle assessment (LCA) of waste management strategies: Landfilling, sorting plant and incineration. Energy. 2009;34:2116-2123.

[126] Finnveden Göran, Johansson Jessica, Lind Per, Moberg Åsa. Life cycle assessment of energy from solid waste-part 1: general methodology and results. Journal of Cleaner Production. 2005;13:213-229.

[127] Wanichpongpan Wanida, Gheewala Shabbir H. Life cycle assessment as a decision support tool for landfill gas-to energy projects. Journal of Cleaner Production. 2007;15(18):1819-1826.

[128] Chen Dezhen, Christensen Thomas H. Life-cycle assessment (EASEWASTE) of two municipal solid waste incineration technologies in China. Waste Management & Research. 2010;28(6):508-519.

[129] Ou Xunmin, Zhang Xiliang, Chang Shiyan, Guo Qingfang. Energy consumption and GHG emissions of six biofuel pathways by LCA in (the) People's Republic of China. Applied Energy. 2009;86:S197-208.

[130] Kong Dung, Shan Jilei, Iacoboni Mario, Maguin Stephen R. Evaluating greenhouse gas impacts of organic waste management options using life cycle assessment. Waste Management & Research. 2012:0734242X12440479.

[131] Dahlbo Helena, Koskela Sirkka, Laukka Jari, Myllymaa Tuuli, Jouttijärvi Timo, Melanen Matti, et al. Life cycle inventory analyses for five waste management options for discarded newspaper. Waste Management & Research. 2005;23:291-303.

[132] Ekvall Tomas, Assefa Getachew, Björklund Anna, Eriksson Ola, Finnveden Göran. What life-cycle assessment does and does not do in assessments of waste management. Waste Management. 2007;27:989-996.

[133] Chaya Wirawat, Gheewala Shabbir H. Life cycle assessment of MSW-to-energy schemes in Thailand. Journal of Cleaner Production. 2007;15:1463-1468.

[134] Park Nyun-Bae, Yoo Jung-Hwa, Jo Mi-Hyun, Yun Seong-Gwon, Jeon Eui Chan. Comparative analysis of scenarios for reducing GHG emissions in Korea by 2050 using the low carbon path calculator. Journal of Korean Society for Atmospheric Environment. 2012;28:556-570.

[135] Khoo Hsien H. Life cycle impact assessment of various waste conversion technologies. Waste Management. 2009;29(6):1892-1900.

[136] Pa Ann, Bi Xiaotao T, Sokhansanj Shahab. A life cycle evaluation of wood pellet

gasification for district heating in British Columbia. Bioresource Technology. 2011;102:6167-6177.

[137] Ning Shu-Kuang, Hung Ming-Chien, Chang Ying-Hsi, Wan Hou-Peng, Lee Hom-Ti, Shih Ruey-Fu. Benefit assessment of cost, energy, and environment for biomass pyrolysis oil. Journal of Cleaner Production. 2013;59:141-149.

[138] Widyawati Meilina, Church Tamara L, Florin Nicholas H, Harris Andrew T. Hydrogen synthesis from biomass pyrolysis with in situ carbon dioxide capture using calcium oxide. International Journal Of Hydrogen Energy. 2011;36:4800-4813.

Chapter 2

Materials and Methods

This chapter is dedicated to the description of the materials, experimental and analysis methods, as well as mathematical modeling setups used for the study. It is divided into several sections as follows:

- **Section 2.1** presents the materials used, including both feedstock and catalyst properties;

- **Section 2.2** gives a description of the experimental capabilities for: pyro-gasification of typical MSW components, steam catalytic gasification of poplar wood and carbonation-calcination looping of CaO catalyst;

- **Section 2.3** is dedicated to the product sampling and analysis methods including: syngas and tar characterization, and solid analysis including TGA, Scanning Electron Microscopy (SEM) / Environmental Scanning Electron Microscope (ESEM), X-ray diffraction (XRD) and Brunauer-Emmett-Teller (BET).

- The mathematical modeling methods are presented in **Section 2.4**, which include: ANN used for the pyro-gasification prediction model, and the LCA used for pyro-gasification system analysis.

2.1 Materials characterization

2.2.1 Feedstock

Four MSW components, including wood, paper, food waste and plastic, are selected as feedstock for pyro-gasification in this study. They are representative of the most typical fractions in MSW. To ensure homogeneity of the feedstock in each test, clean materials are used instead of raw waste, namely, poplar wood, cardboard, bread and PE pellet, respectively. Graphs of these materials are depicted in **Figure 2. 1**.

Prior to the experiment, all these materials are crushed into sizes of ca. 4 mm × 4 mm; and then dried at 85 oC for 24 hours to lower the moisture content. **Table 2. 1** shows the proximate and ultimate analysis of these materials.

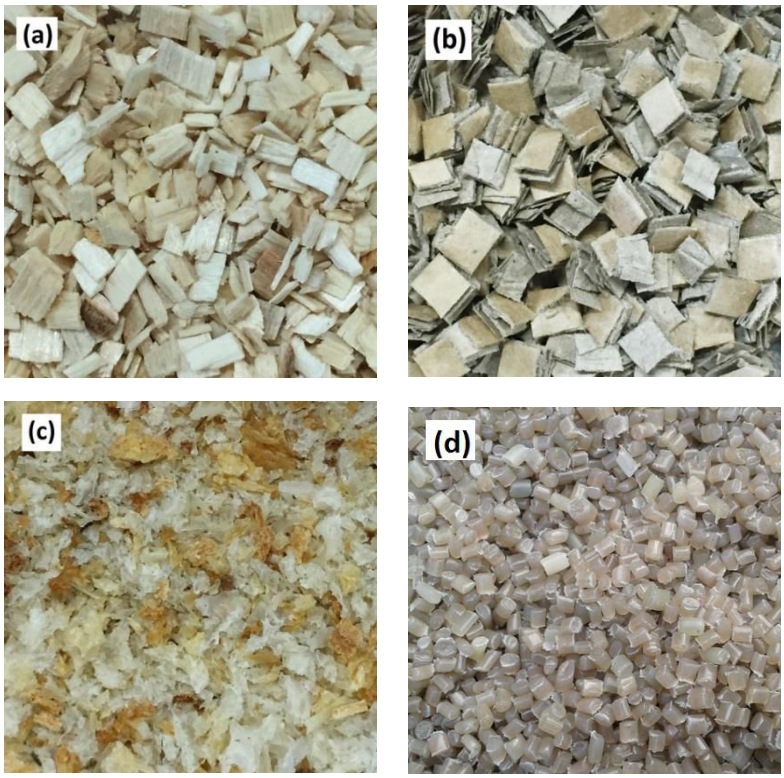

Figure 2. 1 Graphs of MSW components: (a), poplar wood; (b), cardboard; (c), food waste (bread); (d), PE pellet

Table 2. 1 Proximate and ultimate analysis of MSW components

	Proximate analysis [a] (ad, wt. %)				Ultimate analysis [a] (ad, wt. %)					LHV [a] (MJ/kg)
	M	V	FC	A	C	H	O	N	S	
Poplar wood	9.87	77.03	12.57	0.53	44.41	5.07	39.36	0.12	0.64	17.87
Cardboard	7.64	71.61	7.66	13.09	34.05	3.24	41.82	0.12	0.04	12.81
Bread	6.43	71.33	20.77	1.46	43.40	5.53	40.82	1.99	0.36	17.11
PE	0.14	98.47	0.09	1.3	83.08	11.2	4.07	0.01	0.2	45.48

[a] M: moisture; V: volatiles; FC: fixed carbon; A: ash; C: carbon; H: hydrogen; O: oxygen; N: nitrogen; S: sulfur; LHV: lower heating value.

These materials are used in different experiments. Details are listed in **Table 2. 2**.

Table 2. 2 Use of feedstock in different experiments

Feedstock used	Experiments
Poplar wood, cardboard, bread and PE	Pyro-gasification of typical MSW components (**Chapter 3**)
Poplar wood	Steam catalytic gasification for H_2-rich gas production (**Chapter 4**)

2.2.2 Catalyst

CaO powder is adopted as in-bed catalyst for steam catalytic gasification in **Chapter 4**; and, its reactivity during cyclic carbonation-calcination looping reaction is also examined in **Chapter 5**. CaO is received at 99% purity and with a calcination weight loss lower than 2%. After being sieved, a fraction of 0.28-0.45 mm is selected. Since CaO is hygroscopic, it is dried at 105 ^{o}C for 12 hours and stored in a sealed tank prior to experiments. Its specific surface area is measured at 2.37 m^2/g with a porosity of 0.00% (non detectable with the equipment used). The XRD pattern is shown in **Figure 2. 2**.

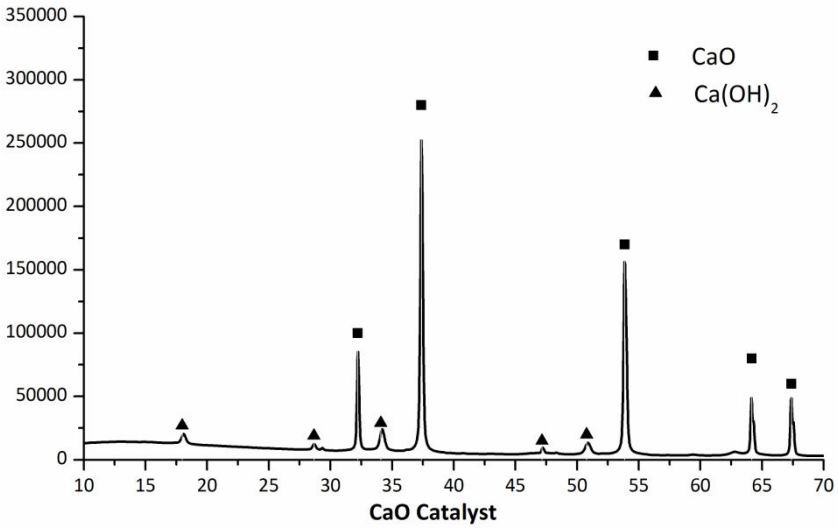

Figure 2. 2 XRD analysis of CaO catalyst

2.2 Experimental capabilities

2.2.1 Pyro-gasification of typical MSW components

2.2.1.1 Fluidized bed reactor

A laboratory batch-scale fluidized bed at RAPSODEE centre, Ecole des Mines d'Albi, is used to perform the pyro-gasification experiments. Schematic diagrams of the apparatus are depicted in **Figure 2. 3** and **Figure 2. 4**. Generally, the fluidized bed is composed of four parts:

- Main reaction chamber;

- Heating and temperature control system, which can be monitored by a computer;

- Inlet gas flow control system including two different sections: air/N_2/CO_2 gas control panel and steam generator; their flow can be set and monitored by computer;

- Gas and tar collection system.

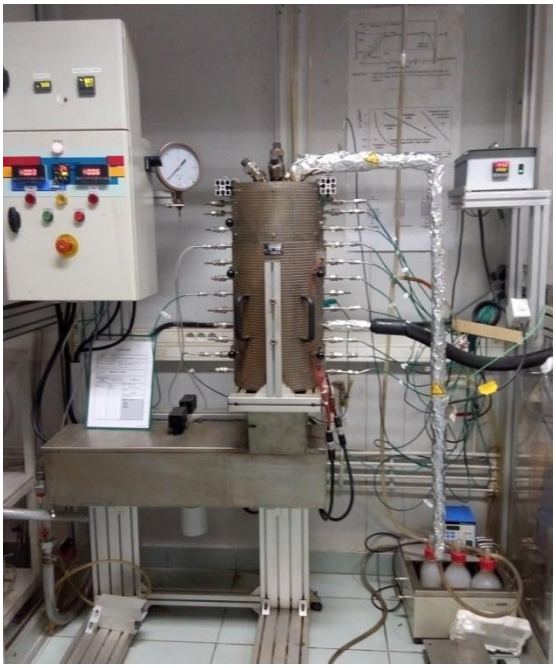

Figure 2. 3 Graph of the fluidized bed reactor

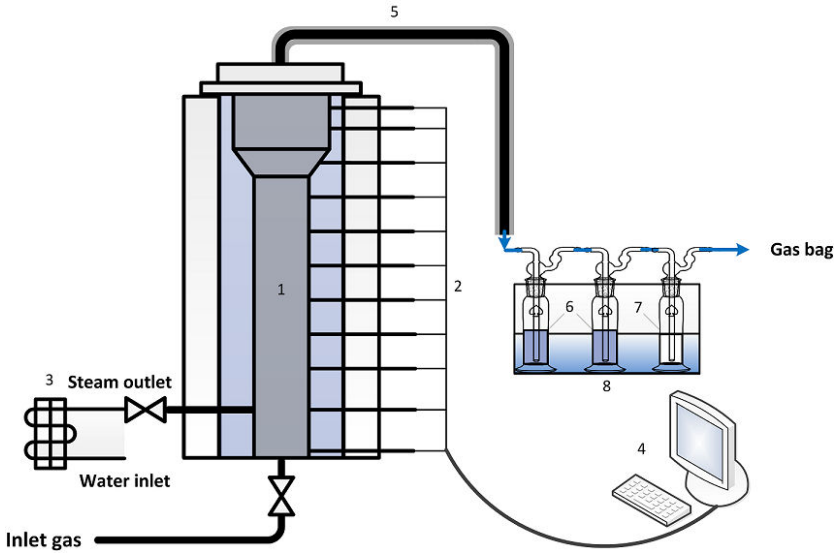

Figure 2. 4 Schematic diagram of the fluidized bed reactor: 1, reaction chamber; 2, thermocouples; 3, steam generator; 4, controller; 5, outlet pipe with heating tape; 6, tar condensation and removal; 7, empty impinger; 8, ice-water bath

The furnace is made of stainless steel, with the main reaction chamber 600 mm in height and 60 mm in inner diameter [1]. It is heated externally by electricity, and ten K-type thermocouples (IEC- KX-1) are positioned vertically to monitor the temperature profile throughout the reactor. The target temperature is controlled using a thermocouple placed close to the middle of the reactor. Two frits are equipped on the bottom and top of the

furnace, respectively. The bottom one is to hold the feedstock; while the top one is to prevent char escaping from the reactor. The gasifying agent is fed from the bottom of the furnace by a mass flow controller (BROOK instrument 5800 series). The flow is calibrated in advance between 0-15 Nm^3/h, 0-5 Nm^3/h and 0-1 Nm^3/h, respectively. Steam is supplied by a steam generator (BROOKS instrument), which uses water to generate the overheated steam vapor (150 ^oC) and its flow is controlled and set separately (0-1 NL/h). Prior to pyro-gasification, preliminary test is performed using minimum fluidization velocity to ensure particle fluidization during the experiments. More information regarding the qualification of fluidizing velocity in this reactor could be found by Ducousso [2] and Klinghoffer [3]. Note that, in this research, MSW itself is used as the bed material, while no inerts (such as silica sand) are additionally fed into the furnace.

Besides, to prevent tar condensation, a heating tape is installed on the outlet pipe to maintain the temperature above 200 ^oC. The raw product gas passes through a series of impingers immersed in an ice-water bath prior to its evacuation to the atmosphere, in order to remove the tars and purify the gas.

2.2.1.2 Operating conditions

The effects of MSW components and gasifying agent on pyro-gasification characteristics are investigated. **Table 2. 3** provides an overview of the experimental conditions. All combinations of the four materials, including both single- and multi-components, are considered; therefore a total of 15 tests ($C_4^1 + C_4^2 + C_4^3 + C_4^4 = 15$) are examined for each gasifying agent. For multi-components pyro-gasification, the mass ratio of each component is kept the same (e.g. a mixture of 50% poplar wood and 50% cardboard; a mixture of 33% bread, 33% PE and 33% poplar wood; etc.). The reaction atmosphere contains N_2, CO_2 and steam; therefore a total of 45 tests are conducted with the aforementioned varied MSW components and gasifying agent. For each trial, critical mass balance calculation is conducted to ensure the reliability of the test data. In addition, several replica are conducted under identical conditions to ensure the repeatability of the results.

Table 2. 3 Experimental conditions of MSW pyro-gasification

Effect of MSW components		Effect of gasifying agent
Single-component	- **(C_4^1 = 4):** poplar wood, cardboard, bread, PE	
Multi-components	- **Two-components (C_4^2 = 6):** wood/cardboard, wood/bread, wood/PE, cardboard/bread, cardboard/PE, bread/PE	- 100% N_2
	- **Three-components (C_4^3 = 4):** wood/cardboard/bread, wood/cardboard/PE, wood/bread/PE, cardboard/bread/PE	- 50 vol.% CO_2/50 vol.% N_2 - 50 vol.% steam/50 vol.% N_2
	- **Four-components (C_4^4 = 1):** wood/cardboard/bread/PE	
Total: (C_4^1 + C_4^2 + C_4^3 + C_4^4) × 3 = 45 runs		

For each experiment, the reaction temperature and inlet gas flow are kept constant at 650 °C and 0.6 Nm^3/h, respectively. The experimental procedures are as follows. At the beginning of each test, 80 g of feedstock is fed into the furnace, and N_2 is introduced continuously to the reactor at a steady flow rate of 0.6 Nm^3/h. Afterwards the furnace is heated to the desired temperature of 650 °C and maintains there, during which the sample actually go through partial decomposition. Once the pre-set temperature is reached, the inlet gas is switched to the gasifying agent (N_2, CO_2 or steam) for the pyro-gasification reaction. From this point on, the syngas begins to be collected by gas sampling bag at 0, 3, 5, 10 and 15 min. The reaction is maintained for a period of 15 min. After each experiment, the electrical heater is turned off, and the inlet gas is switched again to N_2 and the latter is supplied until the furnace reaches room temperature.

2.2.2 Steam catalytic gasification of poplar wood

Poplar wood is selected as feedstock for steam catalytic gasification. The experiments are conducted in a similar reactor, i.e., the lab-scale fluidized bed. The experimental procedures are also quite similar to the one mentioned previously, although CaO is added as

in-situ catalyst. At the beginning of the test, 80 g of poplar wood is mixed uniformly with the CaO catalyst at specified mass ratio and fed into the furnace. The furnace is then heated with N_2 introduced as the purge gas at 0.6 Nm^3/h. After the desired temperature is reached, steam has been injected hence starting the steam gasification step. The syngas is collected using gas sampling bag 5 times at 0, 3, 5, 10 and 15 min. At the end, the steam and electrical heater are turned off but N_2 is maintained following until the reactor reaches room temperature.

The effect of CaO/wood mass ratio, steam flowrate and reaction temperature on gasification characteristics is investigated. Detailed experimental conditions are listed in **Table 2. 4**. The amount of CaO additive loaded is set at 0, 16, 40 and 80 g, corresponding to the CaO/wood mass ratio of 0, 0.2, 0.5 and 1.0. Steam flowrate is varied from 80 to 320 g/h, and a temperature series of 600, 650, 700, 750 and 800 ^oC is examined. Besides, in order to verify the potential effect of CaO on reducing the gasification operating temperature, non-catalyst high-temperature steam gasification at 800 and 900 ^oC is carried out for comparison purpose. Also, mass balance and repeatable tests are conducted to ensure the reliability of the results.

Table 2. 4 Experimental conditions of steam catalytic gasification

No.	CaO/wood mass ratio	Steam flowrate (g/h)	Reaction temperature (^oC)
1#	0.2	80	700
2#		160	
3#		240	
4#		320	
5#	0	160	700
6#	0.5		
7#	1.0		
8#	0.2	160	600
9#			650
10#			750
11#			800
12#	0	160	800
13#			900

2.2.3 Carbonation-calcination looping of CaO catalyst

2.2.3.1 Experimental apparatus and procedures

Cyclic carbonation/calcination experiments on the CaO catalyst are conducted using two types of reactors: a TGA (951 Dupont Instrument) and a fluidized bed (same as what was described in **Section 2.2.1**). The use of the former one is to observe the weight variation characteristics of CaO during cyclic CO_2 capture and release reactions; while the latter is used to produce samples to study parameters such as morphology, specific surface area and sintering.

The experimental procedures of the TGA are as follows. The test is started with the carbonation of CaO in the reactor heated from room temperature to desired carbonation temperature at 20 ^{o}C/min under N_2 atmosphere. Once the pre-set temperature is reached, the gas stream is switch to 20 vol.% CO_2 (N_2 balance) and carbonation occurs. After 30 min the temperature is increased and the inlet gas is switched to 100% N_2 for calcination. The calcination step lasts for 10 min. The combined aforementioned steps account for one carbonation/calcination cycle. Then, a second cycle starts, and the furnace is cooled naturally to carbonation temperature again, which will be kept for 30 min for carbonation under 20 vol.% CO_2 before it is reheated to calcination temperature. The temperature program of the procedures is depicted in **Figure 2. 5**. For the whole reaction process, the total inlet gas is maintained at a constant flow of 3 L/h. Besides, calculation for the equilibrium temperature is also conducted in advance to ensure carbonation and calcination that occurs at specified condition.

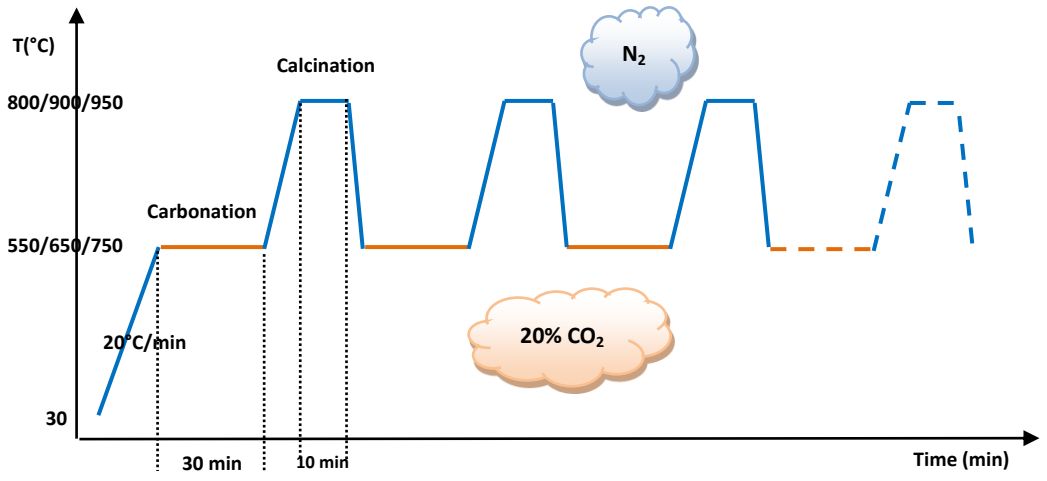

Figure 2. 5 Temperature program of the cyclic carbonation/calcination experiments

The experimental procedures conducted in the fluidized bed are similar to those of TGA, but the total inlet gas is set at 0.6 Nm^3/h. Besides, two extra kinds of experiments are designed: calcination at high temperature and long duration, and steam hydration for CaO re-generation. For the test aiming at high temperature and long periods of calcination, the calcination step is carried out at a higher temperature (1000 °C) for 2 hours, and the carbonation/calcination cycle is repeated only once. As for the CaO re-generation test, a separate hydration process is performed after each carbonation/calcination cycle. The furnace is cooled to 300 °C under N_2, and then maintained for 10 min using a mixture of 20 vol.% steam and 80 vol.% N_2. Afterwards the furnace is reheated to carbonation temperature under N_2, and prepared for the next carbonation process. Temperature program for these two experimental cases are illustrated in **Figure 2. 6**.

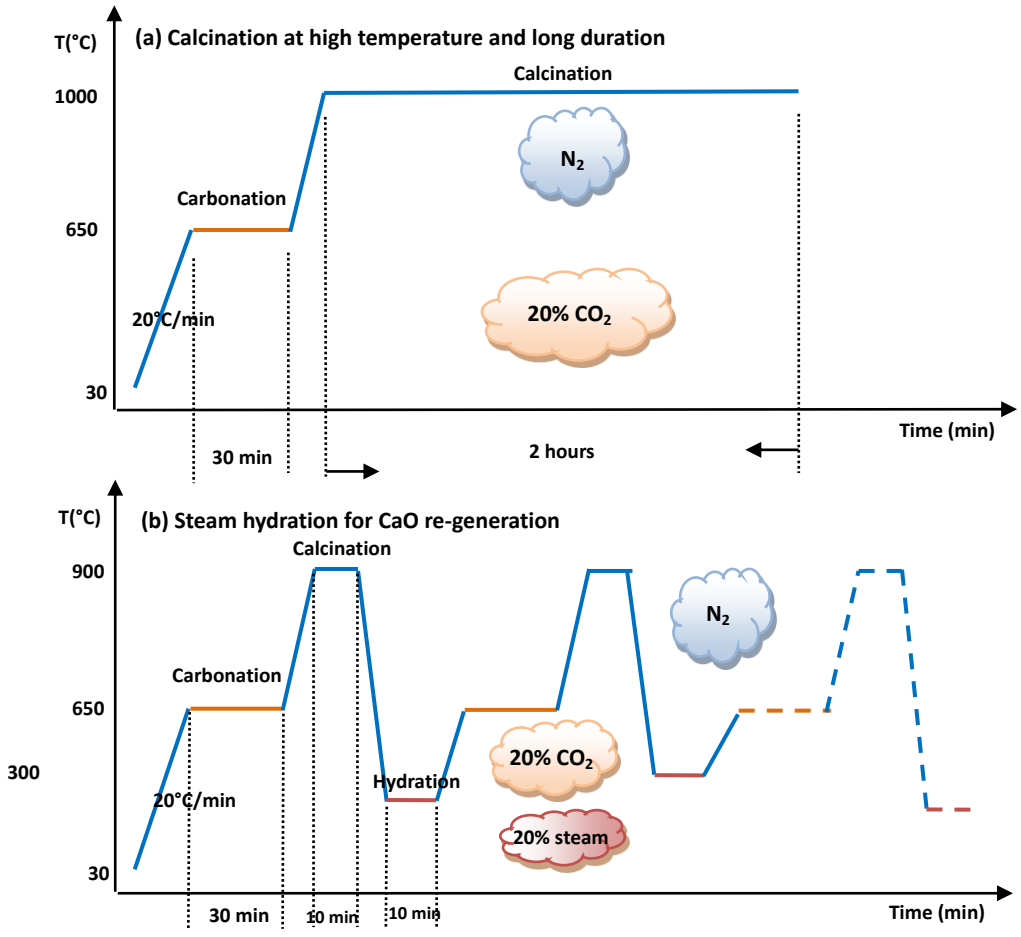

Figure 2. 6 Temperature program of cyclic carbonation/calcination reaction designed for: (a) Calcination at high temperature and long duration; (b) Steam hydration used for CaO re-generation

2.2.3.2 Operating conditions

The operating conditions for both TGA and fluidized bed experiments are listed in **Table 2. 5**. For TGA experiments, carbonation and calcination temperature is varied respectively at 10 cycles of reactions, in order to investigate the reactivity of CaO by checking its CO_2 adsorption capacity. For tests carried out in fluidized bed, different number of carbonation/calcination cycles (5/10/20) is conducted to examine the CaO reactivity during long series of cycles. In addition as mentioned above, high temperature and long duration of calcination, as well as steam hydration are conducted, to investigate the effect of sintering on CaO reactivity, and a potential CaO re-generation approach, respectively.

Table 2. 5 Experimental conditions of carbonation/calcination cycling of CaO catalyst

Reactor	Carbonation condition	Calcination condition	Cycle number	Aim
TGA	T = 550/650/750 °C, 20% CO_2, 30 min	T = 900 °C, 100% N_2, 10 min	10	Effect of carbonation temperature on CaO reactivity
	T = 650 °C, 20% CO_2, 30 min	T = 800/900/950 °C, 100% N_2, 10 min	10	Effect of calcination temperature on CaO reactivity
Fluidized bed	T = 650 °C, 20% CO_2, 30 min	T = 900 °C, 100% N_2, 10 min	5/10/20	Effect of long series cycles on CaO reactivity
	T = 650 °C, 20% CO_2, 30 min	T = 1000 °C, 100% N_2, 2 hours	1	Effect of sintering on CaO reactivity
	Carbonation at 650 °C, 20% CO_2 for 30 min; calcination at 900 °C, 100% N_2 for 10 min; after each cycle hydration at 300 °C, 20% steam for 10 min		5	Effect of steam hydration on CaO re-generation

2.3 Product sampling and analysis

2.3.1 Syngas characterization

Syngas obtained from both MSW pyro-gasification experiments (**Chapter 3**) and steam catalytic gasification experiments (**Chapter 4**) are characterized. The gas sampling is analyzed using gas chromatography (micro GC-3000A analyzer, Agilent). The measurement principle of micro-GC was reported by Ducousso [2]. The syngas components including H_2, CO, CO_2, CH_4 and N_2 are analyzed. Total syngas yield (Nm^3/h) is calculated according to N_2 balance, based on the known N_2 flowrate and the molar ratio of N_2 in the produced gas by Eq. (2.1) [4].

$$Y_{syngas,\,total} = \frac{100\% \times V_{N_2}}{x_{N_2}} \tag{2.1}$$

where, $Y_{syngas,\,total}$ represents the total yield of dry gas (Nm^3/h); V_{N2} stands for the pre-set N_2 flowrate (m^3/h); x_{N2} means the mole fraction of N_2 in the produced gas (%).

The net syngas yield ($Y_{syngas,\,net}$, N_2 free) could thus be quantified by deducting the inlet N_2, as illustrated by Eq. (2.2):

$$Y_{syngas,net} = \frac{100\% \times V_{N_2}}{x_{N_2}} - V_{N_2} \tag{2.2}$$

When CO_2 is used as gasifying agent (see **Chapter 3**), the net syngas yield is calculated by deducting both the inlet N_2 and CO_2 according to Eq. (2.3):

$$Y_{syngas,net} = \frac{100\% \times V_{N_2}}{x_{N_2}} - V_{N_2} - V_{CO_2} \tag{2.3}$$

It should be emphasized that compared with the actual situation, the method for calculating the syngas yield from CO_2 gasification would inevitably introduce deviation. This can be explained by the fact that the CO_2 inlet would be consumed by participating in gasification reactions such as Boudouard or dry reforming (see **Table 1. 1**); however the total amount of the inlet CO_2 is treated constant according to Eq. (2.3). Nevertheless, owing to the high gas velocity required for the fluidized bed reactor, the generated syngas only occupies a very small proportion of the total gas injected. Calculation based on Eq. (2.4) further verifies that, among all the CO_2 gasification cases, the proportion of the produced syngas is less than 10% of the total inlet gas. Hence, the calculation method is regarded acceptable.

$$X_{syngas,net}\,(vol.\%) = \frac{Y_{output\ gas} - Y_{inlet\,gas}}{Y_{inlet\,gas}} = \frac{Y_{syngas,net}}{V_{N_2} + V_{CO_2}} \quad (2.4)$$

where, $X_{syngas,\ net}$ stands for the proportion of net syngas yield to the total inlet gas (vol. %); $Y_{inlet\ gas}$ is the total quantity of inlet gas, which is the sum flowrate of N_2 and CO_2 (m^3/h).

2.3.2 Tar characterization

Tar obtained from steam catalytic gasification experiments (**Chapter 4**) are quantified. The liquid in the impingers are extracted by dichloromethane and separated into organic and inorganic fractions. The organic part is heated for dichloromethane evaporation and the remaining fraction is recorded as the tar yield [5, 6].

2.3.3 Solid characterization

The solid samples, including selected MSW feedstock, char (**Chapter 3** and **Chapter 4**) and CaO catalyst (**Chapter 5**), are characterized utilizing different analytical techniques. Those techniques include: TGA, SEM/ESEM, XRD and BET. Details are presented as follows.

2.3.3.1 TGA measurement

Apart from CaO catalyst, TGA is also used to give thermogravimetric and derivative thermogravimetric (TG/DTG) analysis of selected MSW feedstock. The experimental procedures are quite similar as described in **Section 2.2.3** with some modifications. The reactor is heated to 800 ^oC with a heating rate set at 30 ^oC/min. Two reaction agents are chosen: N_2 and CO_2. The aim of this analysis is to observe the differences in the thermal behavior of specified MSW component using different pyro-gasification agents.

2.3.3.2 SEM/ESEM measurement

SEM measurement for both selected char and catalyst samples are performed, in order to observe microscopic morphologies of the solid produced, such as porosity and surface structure.

Besides, ESEM experiment is also conducted to examine the effect of steam on CaO reactivity (**Chapter 5**). The advantage of using this equipment is that, it enables the sample to be heated and observed on a micrometer scale, so that the physical changes of the CaO structure throughout the reaction could be observed easily. The experimental program is set as follows: a piece of poplar wood, accompanied with several CaO particles on its surface, is placed inside the ESEM and heated at 20 ^{o}C/min to 800 ^{o}C under N_2 atmosphere. Once the desired temperature is reached, the inlet gas is switched to steam for gasification. Images are taken throughout the whole process.

2.3.3.3 XRD measurement

XRD measurement is carried out for the char obtained from steam catalytic gasification. The aim is to determine the main components and their crystallinity to help reveal more accurately the catalytic performance. Fundemental knowledge for the operating mechanism of XRD could be found by Ducousso [2]. The XRD equipment is a Phillips diffractometer type, with a θ-θ Bragg-Brentano configuration, a current of 45 kV and is operated at an intensity of 40 mA. Peaks could be recorded in 10-70 degrees in 2θ and a speed of 0.042 ^{o}/sec. JCPDS and COD databases are applied to assign the peaks.

2.3.3.4 BET measurement

BET measurement is used to determine the specific surface area and porosity of CaO catalyst before and after different designed carbonation/calcination cycles, in order to identify its reactivity and potential re-generation. Determination of the specific surface area is based on the adsorption isotherm. The used BET analyzer is an ASAP 2010 type from Micromeritics. Argon is used as the adsorption gas, and the Brunauer-Emmett-Teller model is used for the determination of specific surface area, since the isotherm is of type II. Based on the results, porosity, which represents the fraction of void space in a specified material, could be obtained by Eq. (2.5):

$$P(\%) = \frac{V_V}{V_T} \times 100\% \tag{2.5}$$

where, V_V stands for the volume of void-space; V_T is the total or bulk volume of material including the solid and void components; P denotes porosity.

2.3.4 Mass balance calculation

As aforementioned, mass balance of the pyro-gasification process is calculated to ensure the reliability of the data. A typical steam catalytic gasification experimental operated with a CaO/wood ratio of 0.2, steam flowrate of 160 g/h and temperature of 700 ^{o}C for 15 min (No. 2# as shown in **Table 2. 4**) is performed as example. **Figure 2. 7** illustrates the mass balance calculation result. The input contains the poplar wood sample, CaO catalyst, steam (as gasifying agent), and N_2 (as carrying gas). 80 g of wood is added at the beginning of experiment, and a total mass of 18.98 g of pyrolyzed char could be obtained as a result of the devolatilization during the heating stage. The remained pyrolyzed wood char then becomes the feedstock for steam catalytic gasification. Its mass is also measured by blank experiment. The output contains gas stream (H_2, CO, CO_2, CH_4, N_2 and O_2), solid residues (including the wood char and the reacted CaO catalyst), as well as the liquid condensate (including tar, condensed steam and generated water) leading to an overall mass balance of 96%.

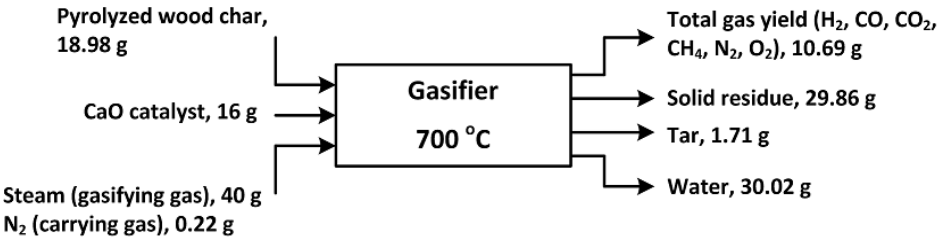

Figure 2. 7 Mass balance for steam catalytic gasification (Experimental run No. 2#, CaO/wood = 0.2, steam flowrate = 160 g/h, temperature = 700 ^{o}C)

Several possibilities may account for the deviation of the mass balance closure from 100%. Some tars may have condensed and deposited on the furnace walls, leading to the underestimation of the tar produced. The measurement uncertainties may lead to the inaccurate estimation of the syngas yield. Under all the test conditions in this study, the total mass balance closure is in the 88-98% range, which is quite acceptable to ensure the test quality.

2.4 Mathematical and modeling methods

2.4.1 ANN used for pyro-gasification prediction model

2.4.1.1 Concept of ANN

ANN, the artificial neural networks, is a mathematical method that could solve highly nonlinear and complex relationships [7]. The concept of ANN is to mimic the function of human brain based on the way that the brain performs operations and computations, which is able to map information between a set of input variables to related outputs.

In brain functions, millions of individual neurons are highly interconnected with one another. **Figure 2. 8** illustrates the basic structure of a biological neuron [8]. Generally, a biological neuron is composed of three main components: dendrites, soma and axon. Information, in the form of electrical pulses, is received by dendrites from other neurons as input paths. Soma occupies the function of summing up incoming signals; and then delivering them as output paths through its axons after receiving sufficient inputs. Synapse is the connection between the axon and dendrites of other neurons. The strength, also defined as synaptic efficiency, is determined by released chemicals from axon and the amount that is received by dendrites. The synaptic efficiency modifies the incoming signal and forms what the brain learns [9].

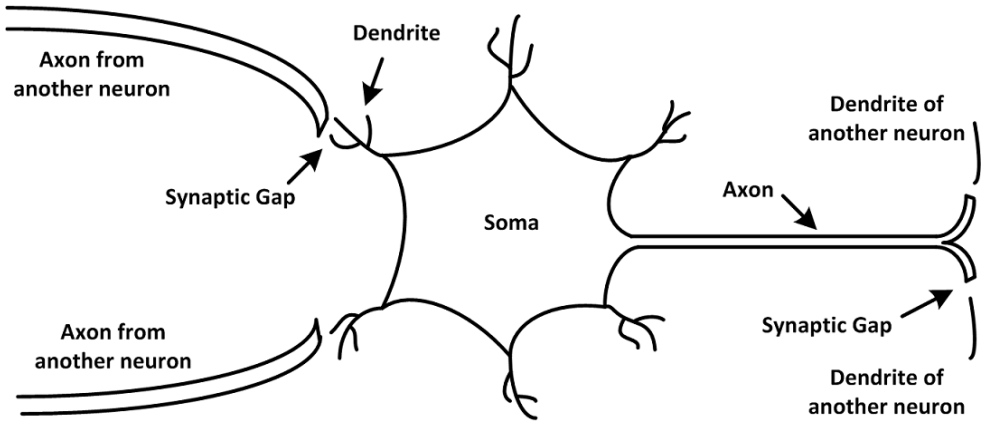

Figure 2. 8 Structure of the biological neuron [8]

The terminology of ANN is composed and operates in a similar way, with a typical diagram of ANN shown in **Figure 2. 9**. The basic processing unit in ANN is called a node, which acts as the function of a neuron to sum input information. There are input and output connections to the node, transferring the signals like dendrites and axon, respectively. The

synapse is referred to as 'the weight' in ANN; each comes with a numerical value to express the strength of the connection. By setting convertible weights, thresholds and mathematical functions [10], an ANN model could process information via dense interconnection of simple computation elements, which is related to the information processing functions of neurons.

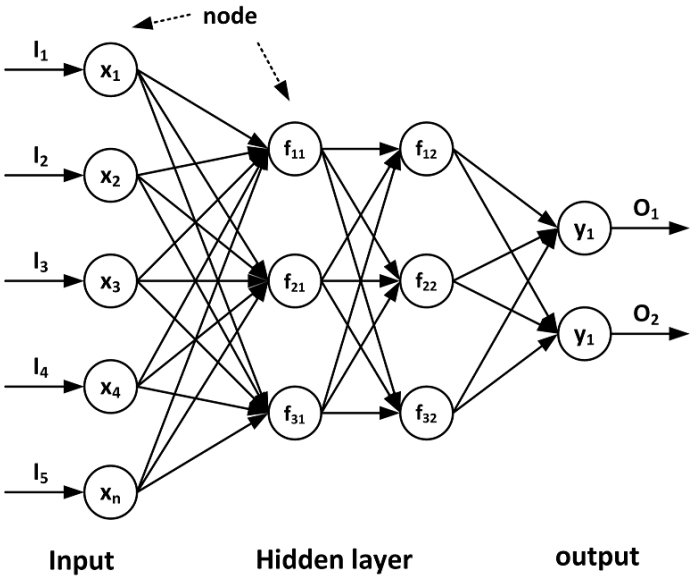

Figure 2. 9 Typical ANN structure

Owing to its structure, ANN has several major advantages over other mathematical models, with the most outstanding features outlined as follows:

- ANN has the ability to learn, recognize and generalize [11]. Once using a set of data to train an ANN, it could familiarize the trends in the data by adjusting the weights between its elements. This means that, a trained ANN could propose a specific target output from the input data, even if the data has never seen before. Such feature make ANN able to serve as a predictive model for specific applications, especially where traditional modeling methods fails to be productive, or in a case where cannot be described by simple mathematical formulae [10, 12].

- The creation of an ANN is a black box method where the user does not need to build a mathematical model to approximate the relationships among the data. Instead, ANN could self-adjust based on the information that the data contains [13, 14]. Due to its approximation capability as well as the inherent adaptive feature, ANN is especially suitable for addressing problems that contain complicated, non-linear relationships in a wide variety of inputs.

- Implementing an ANN can rely on software, providing flexibility to handle complex mathematical problems to a highly desired degree of accuracy [7].

2.4.1.2 Categorize and implementation of ANN

ANN was initially developed in the 1940s by McCulloch and Pitts [15]. Perceptron is the first artificial neural structure capable of learning by trial and error, which was developed by Rosenblatt in 1958, and was modified in 1961 to have multilayers to perform complex operations [16-18]. However, this technique remained dormant for several decades, mainly due to that the early applications faltered or quickly encountered constraints from limited computing power [14]. Thanks to the continuously improving hardware, ANN was received a revival in the 1980s. Over the past three decades more than 40 kinds of ANNs have been proposed and developed, and are widely used for risk analysis, emission control, function approximation, forecasting, strategy making, and various other application fields.

In general, ANN can be categorized as supervised or unsupervised according to the training method. For supervised training, any input vector in the training data set is related to an associated output, i.e., the weights are adjusted according to the target output. This method is most commonly applied to classification, prediction, and pattern association problems. Oppositely for unsupervised learning, no target outputs are specified for the input vector, i.e., the network is self-organized to modify the weights so that most similar input vectors form the same output unit. As a result, this method is suitable for handling data clustering problems [9].

Besides the classification method aforementioned, ANN could also be divided into two groups according to the network structure: feedforward and feedback neural networks. Typical ANN models include: backpropagation (BP), Hopfield and radial basis function [19].

The most widely used ANN method is the BP training algorithm, which is utilized in this study. BP algorithm is simply a gradient descent method to minimize the total squared error between the output computed by the network and a targeted output [20].

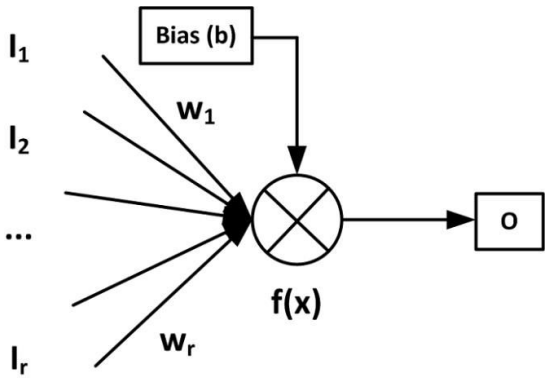

Figure 2. 10 Basic structure of a processing node

Figure 2. 10 shows the basic structure of a processing node. I_i (i = 1 to r) acts as an input vector, where each element is connected to the output with a proper weight (w_i). There is an additional bias value (b) included as input; therefore the output (O) could be presented as the result of a transfer function (f) over a summation of inputs multiplied by weight parameters and the bias value (Eq. (2.6)):

$$O = f\left(\sum_{i=1}^{r} I_i \times w_i + b\right) \tag{2.6}$$

The most common transfer functions in solving non-linear problems are sigmoid function and hyperbolic tangent. The sigmoid function is defined as:

$$f_s(x) = \frac{1}{1+e^{-x}} \tag{2.7}$$

As could be seen, the sigmoid function can map the real numbers into the interval (0, 1). Due to its ability of limiting values, sigmoid function is also called threshold function. If the input values are very low, the output tends to be 0; oppositely at very high input values, the output value tends to be 1.

Similarly, hyperbolic tangent is also a kind of threshold function (see Eq. (2.8)). This function varies between -1 and +1. Since both negative and positive regions exist, this function is particularly suited for data set including negative and positive range [21].

$$f_h(x) = \frac{e^{x} - e^{-x}}{e^{x} + e^{-x}} \tag{2.8}$$

ANNs are often far more complex than the one described above, and usually a BP network consists of one input layer, one output layer and a number of hidden layers, with

the typical structure depicted in **Figure 2. 9**. Input layer receives the information from external source. The hidden layers sum the information from the input layers, apply nonlinear function to the summed input vector and transfer them to the output layer. Output layer receives the processed information and sends them as output. With the introduction of hidden layers, ANN can approximate any desired function to any desired degree of accuracy [7].

Training a BP network involves three main stages: feedforward of the input training pattern, calculation and backpropagation of the associated error, and adjustment of the weights with respect to calculated error. The training algorithm involves the following steps [22]:

Step 0: Initialize weights;

Step 1: If the stopping condition is false, conduct steps 2-8; otherwise stop the training;

Step 2: For each training pair, do steps 3-7;

Feedforward phase:

Step 3: Each input unit (x_i, i = 1, ..., n) receives input value x_i, and distributes this value to all units in the input layer;

Step 4: Each hidden unit (z_j, j = 1, ..., p) sums its weighted inputs as Eq. (2.9):

$$zin_j = v_{0j} + \sum_{i=1}^{n} x_i v_{ij} \tag{2.9}$$

Where, V_{0j} stands for the bias on hidden unit j. Then the hidden unit applies activation function via Eq. (2.10), and sends this signal as outputs:

$$z_j = f(zin_j) \tag{2.10}$$

Step 5: Each output unit (y_k, k = 1, ..., m) sums its weighted inputs as Eq. (2.11):

$$yin_k = w_{0k} + \sum_{j=1}^{p} z_j w_{jk} \tag{2.11}$$

Where, w_{0k} stands for the bias on output unit k. Then the output unit applies its activation function to compute its output signal as Eq. (2.12):

$$y_k = f(yin_k) \tag{2.12}$$

Backpropagation of error:

Step 6: Each output unit (y_k, k = 1, ..., m) receives a target output corresponding to the input training pattern, computes its error information term as:

$$\delta_k = (t_k - y_k)f'(yin_k) \tag{2.13}$$

Where, δ_k represents the portion of error correction weight adjustment for w_{jk} due to an error at output unit y_k; t_k stands for the target output unit. As a result, the weighted correction term and biased correction term could be calculated as Eq. (2.14) and Eq. (2.15), respectively:

$$\Delta w_{jk} = \lambda \delta_k z_j \tag{2.14}$$

$$\Delta w_{0k} = \lambda \delta_k \tag{2.15}$$

Where, λ is the learning rate.

Step 7: Each hidden unit (z_j, j = 1, ..., p) sums its delta inputs as Eq. (2.16):

$$\delta in_j = \sum_{k=1}^{m} \delta_k w_{jk} \tag{2.16}$$

Then, δ_j, the portion of error correction weight adjustment for v_{ij} due to the backpropagation of error information from the output patterns to the hidden unit z_j, is calculated by multiplying δin_j by the derivative of its activation function, as Eq. (2.17):

$$\delta_j = \delta in_j f'(zin_j) \tag{2.17}$$

Based on the data, the weighted correction term and biased correction term of the hidden layer could be calculated as Eq. (2.18) and Eq. (2.19), respectively:

$$\Delta v_{ij} = \lambda \delta_j x_i \tag{2.18}$$

$$\Delta v_{0j} = \lambda \delta_j \tag{2.19}$$

Step 8: Verify the training stopping condition.

Training will stop if the total error is less than the error tolerance specified, or the maximum number of cycles is exceeded; otherwise continue training process.

Overall, the flowchart of BP network can be summarized as **Figure 2. 11**.

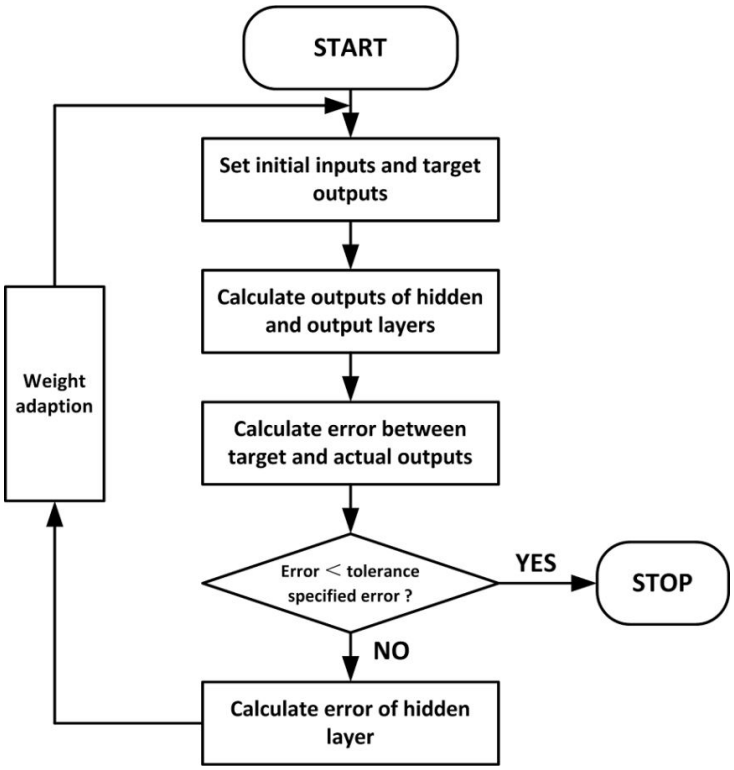

Figure 2. 11 Flowchart of BP network

2.4.1.3 MATLAB Neural Network Toolbox

Owing to the ability of organizing dispersed data into a nonlinear model [23], ANN has been proven as an ideal prediction tool. Especially, ANN is useful when the main goal is outcome prediction and the input data contain complex nonlinearities and interactions [24]. As a result, ANN is suitable to be used in predicting gasification characteristics, since they can approximate arbitrary nonlinear functions.

On the other hand, thanks to the developing software-based computing ability, in this study, the training and testing of ANN is applied with the assistance of MATLAB Neural Network Toolbox. The operation interface of this software is illustrated in **Figure 2. 12**. The network uses Levenberg-Marquardt BP algorithm (trainlm function). The function 'logsig' (sigmoid), 'tansig' (hyperbolic tangent) and 'purelin' (linear transfer) acts as transfer function

in the input layer, hidden layer and output layer, respectively. The performance of the ANN is measured by mean squared error and regression analysis. The outputs are compared with targets, and the system will adjust the weights of the internal connections to minimize errors.

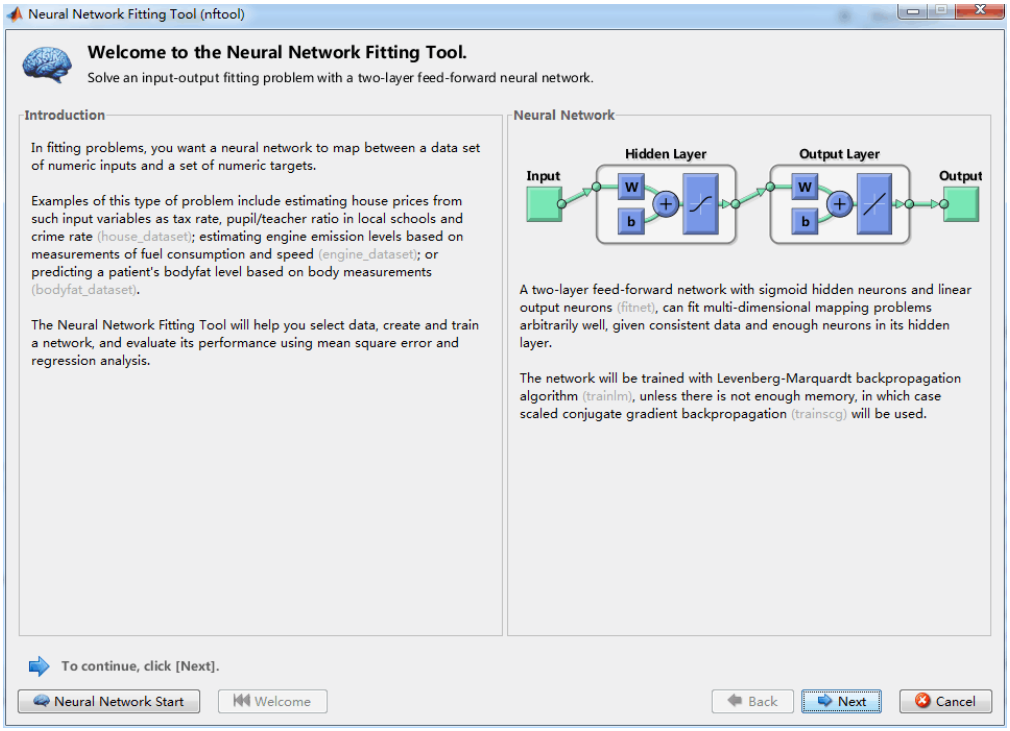

Figure 2. 12 Operation interface of MATLAB Neural Network Toolbox

2.4.2 LCA used for pyro-gasification system analysis

As it has been introduced in **Chapter 1**, the implementation of LCA consists of four phases: (1) goal and scope definition; (2) LCI; (3) LCIA; and (4) interpretation. In compliance with the framework, its utilization procedures in waste management field are illustrated in detail as follows.

2.4.2.1 Goal and scope definition

The aim of this step is to define unambiguously why the LCA has to be carried out, and what decision can be formulated from the results [25]. The scope of the study is expressed in terms of the *system boundary*, which quantifies the related processes and operations to be included. **Figure 2. 13** shows a general system boundary of a waste management system. To be specific, the system could be divided into several different waste activities: MSW

collection, transportation, material recycling, and various waste treatment methods such as landfill, thermal conversion, composting, final ash disposal, etc. When conducting a specified case study, those activities could be adjusted flexibly according to the aim of study estimated.

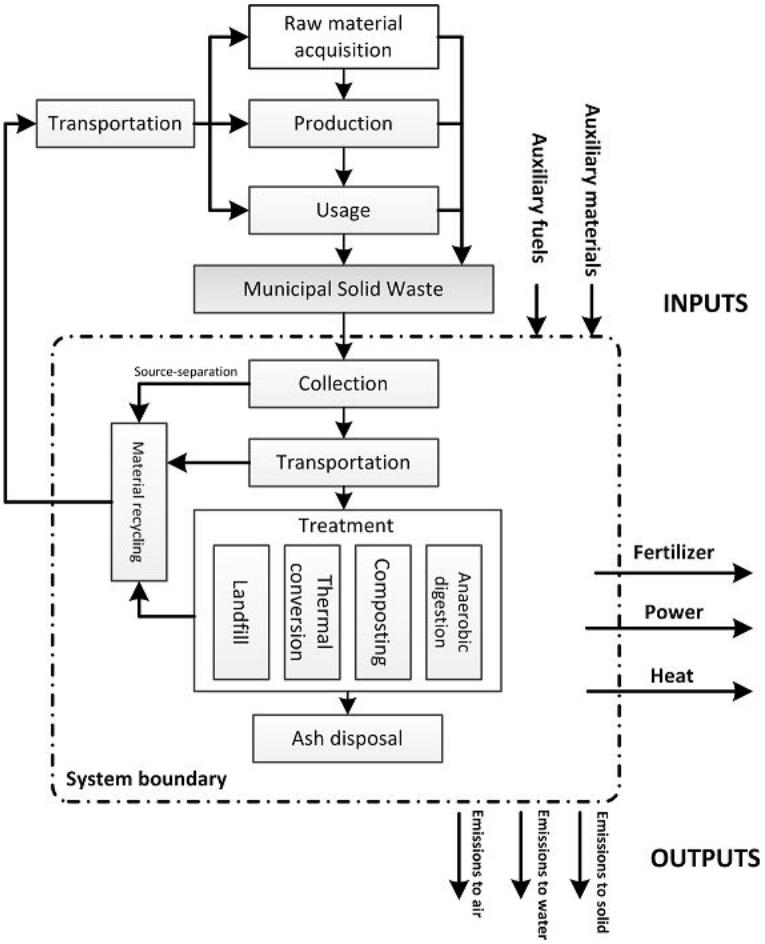

Figure 2. 13 A general system boundary of a waste management system

In addition to the waste processes introduced above, the background system is often defined to distinguish direct and indirect emissions from the life cycle perspective. Diagram of the foreground and background systems for waste management is illustrated in **Figure 2. 14**. According to the definition used explicitly in the UK Environment Agency [26], the emissions arising from the aforementioned waste activities (also defined as foreground system) are termed *direct burdens*. Conversely, background system defines the supply chain of materials and energy which are exchanged with the foreground waste management activities. For the specific example in **Figure 2. 13**, the supply of fuels should be traced back to their origins, i.e. from extraction and refining. The resources usages and emissions arising from the background activities are termed *indirect burdens*.

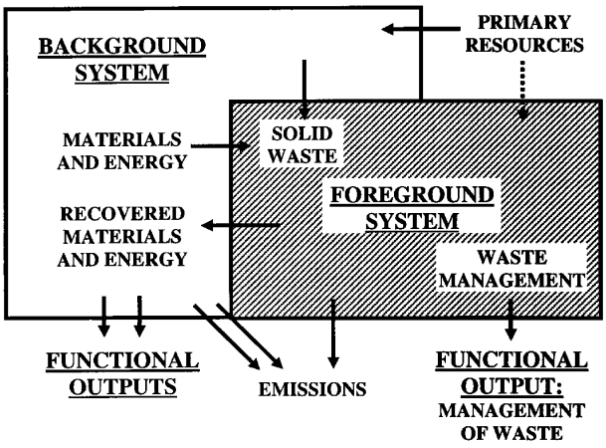

Figure 2. 14 Foreground and background systems for waste management, data source from Clift et al. [25]

The basis for comparison among alternatives is named the *functional unit*, which defines the same quantity of a specified operating parameter to be kept constant. In the waste management field, the functional unit is commonly chosen as a specified mass of waste, located at the premises where the material becomes 'waste'; for example one ton of MSW, or, the annual generation of MSW in one region.

2.4.2.2 Life cycle inventory

The aim of inventory analysis is to identify and quantify the materials and emissions crossing the system boundary. The complete set of burdens per functional unit constitutes the *inventory table*. As has been pointed out previously, all the inputs should be traced back to primary materials extracted from the earth.

Necessarily, one of the key challenges for inventory analysis is to gather relevant data associated with a specified process. Thanks to the developing database, numerical estimates for different background processes have already been quantified, which effectively save effort in compiling the inventory table.

Another key challenge of inventory analysis is related to allocation, which concerns how many of the processes within the system boundary will be shared with other supply chains, so that finding a rational basis for allocating the environmental impacts becomes necessary. A particular concern for waste management is WtE system, that not only treats waste, but also produces power or heat, thus providing a second function. To solve this multi-output problem, one method is to expand the system boundary to avoid allocation, which is

specifically recommended by ISO 14041 [27]. As shown in **Figure 2. 15**, the way of presenting the expanded system is to subtract the power-producing system using an alternative energy source from the WtE system [28]. In other words, it means that, the system is 'credited' with an equivalent amount of power being produced in an alternative manner. Those subtracted emissions are termed *avoided burdens*, which will probably result in a negative value of environmental burden of a specified system.

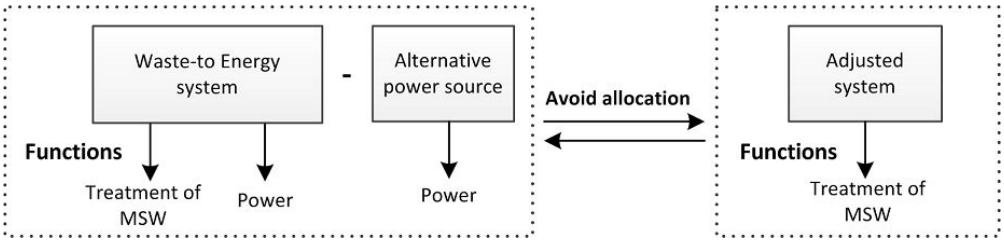

Figure 2. 15 Illustration of system expanding method for avoiding the allocation problem. Data source adapted from the research of Finnveden [28]

Accordingly the total LCI for the waste management scheme could be expressed as [25]:

Direct burdens - arising in the foreground waste management system

plus **Indirect burdens -** arising in the supply chains of materials and energy provided to the foreground

minus **Avoided burdens** - associated with activities displaced by material and/or energy recovered from the waste

2.4.2.3 Life cycle impact assessment

On basis of the inventory table, the next step of a LCA study terms is to quantify the magnitude and significance of the potential environmental impacts concerned. ISO 14042 [29] has regulated several steps for LCIA, in which some are mandatory but some are optional. Those elements included in the LCIA are illustrated in **Figure 2. 16**, with their conducting procedures and features introduced as follows [30].

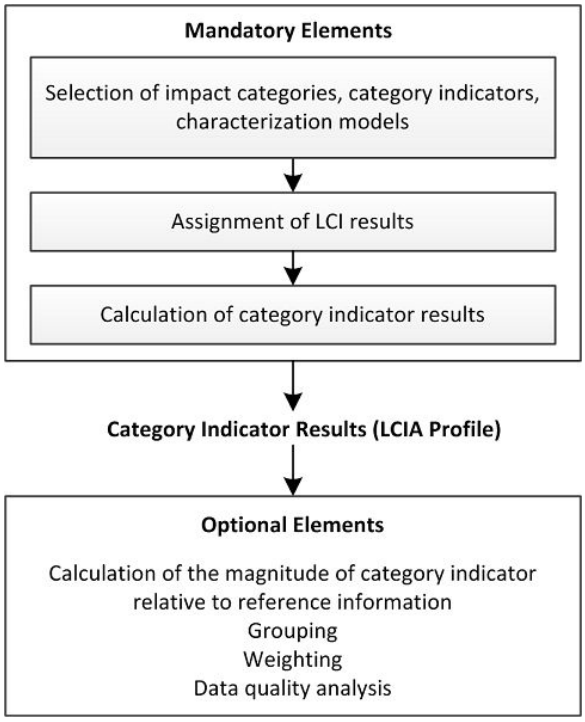

Figure 2. 16 LCIA procedures as regulated by ISO 14042 [29, 30]

- Selection of the impact categories of interest, indicators for the categories and models to quantify the contributions of different inputs and emissions to the impact categories;
- Assignment of the inventory data to the chosen impact categories (**classification**);
- Quantification of the contributions to the chosen impact indicators using characterization factors (**characterization**);
- Calculation of the magnitude of different impact categories relative to reference values (**normalization**, optional);
- **Grouping** and/or **weighting** the results, including sorting and possibly ranking of the indicators; aggregating indicator results across impact categories to a single result (optional);
- Data quality analysis.

Within the framework of LCIA, some reasonable impact assessment methods have been developed, which have been illustrated in **Chapter 1**. In this study, the EDIP 97 methodology (Environmental Development of Industrial Products), established by the Institute for Product Development at the Technical University of Denmark and is one of the most complete and

well-acceptable LCIA methodology in the world, is used to aggregate the environmental impact results [31]. EDIP 97 uses the midpoint approach for LCIA calculation, which covers almost the emission-related impacts, working environment impacts and resource use. The impact categories are illustrated in **Table 2. 6**. Besides characterization results, normalized LCIA values are also given, which is based on person equivalence (Pe, defined as one person by one year) to reflect the relative magnitude of different impacts. In EDIP 97 method, the normalization references are based on European standards.

Table 2. 6 Impact categories included in EDIP 97 methodology

Impact category	Characterization unit	Physical basis	Normalization references
Global warming (GW)	kg CO_2-equivalent	Global	8,700
Ozone depletion (OD)	kg CFC-11-equivalent	Global	25
Acidification (AC)	kg SO_2-equivalent	Regional	74
Nutrient enrichment (NE)	Kg NO_3^--equivalent	Regional	119
Photochemical ozone formation (POF)	kg C_2H_4-equivalent	Regional	25
Human toxicity via air (HTa)	m^3 air	Regional	2,090,000,000
Human toxicity via water (HTw)	m^3 water	Regional	179,000
Human toxicity via solid (HTs)	m^3 soil	Regional	157
Ecotoxicity via solid (ETs)	m^3 soil	Regional	964,000
Ecotoxicity via water chronic (ETwc)	m^3 water	Regional	352,000
Stored ecotoxicity in water (SETw)	m^3 water	Regional	11,400,000
Stored ecotoxicity in soil (SETs)	m^3 soil	Regional	506
Spoiled groundwater resources (SGWR)	m^3 water	Local	1200

2.4.2.4 Interpretation

Interpretation is the final stage of a LCA study. The obtained results both from LCI and LCIA phase could be used to seek for effective environmental improvements, or, served as scientific basis in the case of waste decision making or planning.

2.5 Bibliography

[1] Klinghoffer Naomi B, Castaldi Marco J, Nzihou Ange. Catalyst properties and catalytic performance of char from biomass gasification. Industrial & Engineering Chemistry Research. 2012;51:13113-13122.

[2] Ducousso Marion. Gasification biochar reactivity toward methane cracking. Albi, France: École Nationale Supérieure des Mines d'Albi-Carmaux conjointement avec l'INP Toulouse; 2015.

[3] Klinghoffer Naomi. Utilization of char from biomass gasification in catalytic applications: Columbia University; 2013.

[4] Zhou Chunguang, Stuermer Thomas, Gunarathne Rathnayaka, Yang Weihong, Blasiak Wlodzimierz. Effect of calcium oxide on high-temperature steam gasification of municipal solid waste. Fuel. 2014;122:36-46.

[5] Kihedu Joseph H, Yoshiie Ryo, Naruse Ichiro. Performance indicators for air and air–steam auto-thermal updraft gasification of biomass in packed bed reactor. Fuel Processing Technology. 2015.

[6] Van Paasen SVB, Kiel JHA, Neeft JPA, Knoef HAM, Buffinga GJ, Zielke U, et al. Guideline for sampling and analysis of tar and particles in biomass producer gases. Final report documenting the Guideline, R& D work and dissemination. 2002:95.

[7] Khashei Mehdi, Hejazi Seyed Reza, Bijari Mehdi. A new hybrid artificial neural networks and fuzzy regression model for time series forecasting. Fuzzy Sets And Systems. 2008;159:769-786.

[8] Fausett Laurene. Fundamentals of neural networks: architectures, algorithms, and applications: Prentice-Hall, Inc.; 1994.

[9] Afaghi Mahtab Khodaverdi. Application of artificial neural network modeling in thermal process calculations of canned foods. Montreal, Canada: McGill University; 2000.

[10] Ongen Atakan, Ozcan H Kurtulus, Arayıcı Semiha. An evaluation of tannery industry wastewater treatment sludge gasification by artificial neural network modeling. Journal Of Hazardous Materials. 2013;263:361-366.

[11] Pados Dimitris A, Papantoni-Kazakos P. A note on the estimation of the generalization error and the prevention of overfitting [machine learning]. Neural Networks, 1994 IEEE World Congress on Computational Intelligence, 1994 IEEE International Conference on: IEEE; 1994. p. 321-326.

[12] Xiao Gang, Ni Ming-jiang, Chi Yong, Jin Bao-sheng, Xiao Rui, Zhong Zhao-ping, et al. Gasification characteristics of MSW and an ANN prediction model. Waste Management.

2009;29:240-244.

[13] Bishop Christopher M. Neural networks for pattern recognition: Oxford university press; 1995.

[14] Hagan Martin T, Demuth Howard B, Beale Mark H, De Jesús Orlando. Neural network design: PWS publishing company Boston; 1996.

[15] Venkatasubramanian Venkat, Chan King. A neural network methodology for process fault diagnosis. Aiche Journal. 1989;35:1993-2002.

[16] Rosenblatt Frank. The perceptron: a probabilistic model for information storage and organization in the brain. Psychological Review. 1958;65:386.

[17] Rosenblatt Frank. Principles of neurodynamics. perceptrons and the theory of brain mechanisms. DTIC Document; 1961.

[18] Fierst Janna L, Phillips Patrick C. Modeling the evolution of complex genetic systems: The gene network family tree. Journal of Experimental Zoology Part B: Molecular and Developmental Evolution. 2015;324:1-12.

[19] Rao Valluru, Rao Hayagriva. C++ neural networks and fuzzy logic. New York: MIS: Press; 1995.

[20] Rumelhart David E, McClelland James L, Group PDP Research. Parallel distributed processing: IEEE; 1988.

[21] Swingler Kevin. Applying neural networks: a practical guide: Morgan Kaufmann; 1996.

[22] Kseibat Dawod S. Design of artificial neural network for food safety and quality during thermal processing in a can. Guelph: University of Guelph; 1999.

[23] Hecht-Nielsen Robert. Theory of the backpropagation neural network. Neural Networks, 1989 IJCNN, International Joint Conference on: IEEE; 1989. p. 593-605.

[24] Puig-Arnavat Maria, Hernández J Alfredo, Bruno Joan Carles, Coronas Alberto. Artificial neural network models for biomass gasification in fluidized bed gasifiers. Biomass and Bioenergy. 2013;49:279-289.

[25] Clift R, Doig A, Finnveden Göran. The application of life cycle assessment to integrated solid waste management: Part 1—Methodology. Process Safety And Environmental Protection. 2000;78:279-287.

[26] Nichols P, Aumônier S. Developing Life Cycle Inventories for Waste Management, Report No. CWM.128:97.

[27] ISO. ISO 14041: Environmental Management: Life Cycle Assessment: Goal and Scope Definition and Inventory Analysis: International Organization for Standardization; 1998.

[28] Finnveden G. Methodological aspects of life cycle assessment of integrated solid waste

management systems. Resources, Conservation and Recycling. 1999;26:173-187.

[29] ISO. ISO 14042: environmental management—life cycle assessment—life cycle impact assessment. Geneva, Switzerland. 2000.

[30] Pennington DW, Potting J, Finnveden Göran, Lindeijer E, Jolliet O, Rydberg Ty, et al. Life cycle assessment Part 2: Current impact assessment practice. Environment International. 2004;30:721-739.

[31] Wenzel H., Hauschild M.Z., Alting L. Environmental Assessment of Products, Volume 1: Methodology, tools and case studies in product development. London, UK: Chapman and Hall; 1997.

Chapter 3

Pyro-gasification of Typical MSW Components and Prediction Model

3.1 Introduction

As it has been indicated in **Chapter 1**, MSW pyro-gasification is a complex thermochemical process owing to the high complexity of MSW components and reaction agents. As a result, development of a general and practical pyro-gasification prediction model based on MSW physical composition is beneficial to help optimize high-quality syngas production considering the geographical differences in MSW properties. Accordingly, the structure of this chapter is presented as follows:

- **Section 3.2** investigates the pyro-gasification characteristics of MSW single-component. The effect of MSW components and reaction agent on high-quality syngas production is examined. Four typical MSW components, poplar wood, cardboard, food waste and PE are considered; and the pyro-gasification agent includes N_2, steam and CO_2.

- **Section 3.3** is dedicated to the pyro-gasification characteristics of MSW multi-components. All combinations of the four MSW components are considered, again using N_2/steam/CO_2 as reaction atmosphere. The syngas properties based on both experiment and theoretical linear calculation are examined, in order to investigate the interactions between these components.

- Based on the data obtained from **Section 3.2** and **Section 3.3**, a MSW pyro-gasification prediction model based on ANN mathematical method is established in **Section 3.4**. Proper training and validation processes are conducted to verify its feasibility and reliability.

- In **Section 3.5**, the established ANN model is then applied to compare MSW pyro-gasification characteristics between France and China, based on physical MSW composition in these two countries.

The characteristics of MSW feedstock and the experimental procedures are described in detail in **Chapter 2**, together with the structure and implementation of ANN model. The main findings are presented as follows.

3.2 Pyro-gasification characteristics of MSW single-component

With regard to MSW single-component, four MSW components (poplar wood, cardboard, food waste and PE) under three reaction atmosphere (N_2, steam and CO_2) are investigated. In the first section (**Section 3.2.1**), the pyro-gasification characteristics under N_2 atmosphere are analyzed in order to examine the effect of MSW component; and the other vector gases, i.e. steam and CO_2, are discussed in **Section 3.2.2**. Finally, potential utilizations of the produced syngas are discussed in **Section 3.2.3**.

3.2.1 Effect of MSW component

Figure 3. 1 shows the syngas composition of different MSW components under N_2 atmosphere, while the syngas yield is illustrated in **Table 3. 1**. The pyro-gasification has been carried out at 650 ^{o}C and maintained at this temperature for 15 min.

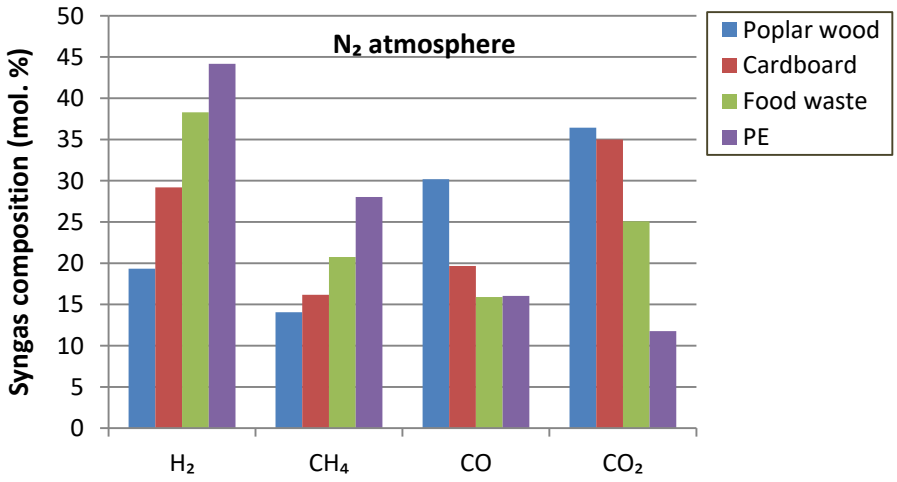

Figure 3. 1 Syngas composition from pyro-gasification of different MSW single-component under N_2 atmosphere (data obtained from lab-scale fluidized bed at 650 ^{o}C for 15 min)

Table 3. 1 Syngas yield from pyro-gasification of different MSW components under N_2 atmosphere (data obtained from lab-scale fluidized bed reactor at 650 °C for 15 min)

	Poplar wood	Cardboard	Food waste	PE
Syngas yield (Nm^3/kg)	0.070	0.135	0.141	0.058

Results reveal that PE produces the highest H_2 and CH_4 concentration; while the pyrolysis of wood contributes to more CO and CO_2. The difference would mainly be attributed to the different compositions and chemical bonds involved in the different materials [1]. PE, as a typical kind of plastic, contains primarily artificial polymers [2], which is relatively simple with high C and H content; together with a very low concentration of O coming from the charges and additives. As a consequence, the syngas is dominated by H_2 and CH_4, accounting for 44.2% and 28.0% volume percentage of the produced gas, respectively. The value is nearly 2-4 times higher than what is obtained for CO or CO_2. However, wood, cardboard and food waste are all biomass-like materials; the O content of these materials is relatively high, resulting in high CO and CO_2 concentration (the concentration of CO + CO_2 is in a range of 41.0-66.6% compared with 27.8% for PE). Among these three materials, wood and cardboard are mostly composed of cellulose, lignin and hemicellulose; and they exhibit similar syngas composition characteristics. The food waste, represented by bread in this study, is mainly composed with starch. It is a kind of polysaccharide, whose monomer is glucopyranose, and the produced gas is dominated by H_2 and CO_2, followed by CH_4 and CO.

However, although both wood and cardboard have similar major elements (as could be seen in **Table 2. 1**), their thermal behaviors differ a lot. Compared with wood, cardboard exhibits a much higher H_2 content, which is about 10% higher than that produced from wood pyrolysis. Meanwhile, CH_4 concentration from cardboard pyrolysis is also 2% higher than that of wood. Since CH_4 is mainly produced during the pyrolysis step [3], it could be speculated that the reactivity of cardboard is higher than wood. Research has indicated that for natural biomass, e.g. wood, cellulose occupies generally the largest fraction (40-50%) by weight; and that portion of hemicellulose is ca. 20-40% [4]. However for paper material, e.g. cardboard, the cellulose content reaches ca. 90% and is much higher than in the wood [2]. This could be justified by the paper processing step, where wood is firstly crushed and pulped, hence weakening the bonds between the fibres and lignin and finally results in the modification of its composition and characteristics to a large extent [5]. Research by Sorum et al. [6] proved that the degradation of cellulose occurs typically between 300 °C and 400 °C, while it is

observed above 400 °C for lignin. The structure of wood is quite dense that may inhibit the pyro-gasification reactions. However the re-processing step during cardboard manufacture could be responsible for the enhancement of cardboard reactivity.

The syngas yield for different components is shown in **Table 3. 1**, where the syngas yield from cardboard is found to be 0.135 Nm^3/kg, which is almost 2 times higher than that from wood pyrolysis. This again confirms that the reactivity of cardboard is higher than wood. Although their elemental composition is very similar, the special adhesion between cellulose and lignin in wood becomes one of the reasons for the lignin to degrade at a higher temperature in wood. This tight structure of wood makes it more difficult to be gasified.

0.141 Nm^3/kg of syngas could be generated from food waste, which is the highest among the MSW samples although the volatile matter of food waste is at the same level as that of wood and cardboard. It is also observed, despite the fact that the original particle size of each feedstock is comparable (ca. 4 mm × 4 mm), the char obtained from food waste exhibits a relatively smaller size, simultaneously porous and powder-like. Aguiar et al. [7] and Figueiredo et al. [8] revealed that there is a tendency for the syngas yield to increase with decreasing particle size. Therefore, the risen syngas production of food waste in this study could be due to the larger specific surface area of the char, which improves heat and mass transfer to produce more light gases. This speculation could be further verified by the high H_2 and CH_4 concentration from food waste pyrolysis in **Figure 3. 1**, since the char decomposition and secondary cracking reactions are effectively accelerated.

Besides, the syngas yield of PE is the lowest (0.058 Nm^3/kg) and represents only 40% of the value from food waste pyrolysis. The phenomenon is opposite to the research of Luo et al. [9]. They observed that during pyrolysis the syngas production of plastic (100% volatile, C/H = 6.62) is higher than wood and kitchen garbage, which could be attributed to the fact that the volatile content of plastic is high and its molecular chain structure is easy to break. However concerning the present study, the syngas starts to be collected when the furnace reaches the reaction temperature (650 °C). Buah et al. [10] declared that the degradation of plastic components mainly occurs at 410-500 °C. Therefore, it could be inferred that the pyrolysis of PE is nearly completed at the temperature studied, so that less gas could be released. Besides, since the volatile content of PE is relatively high, the remained fixed carbon and carbohydrates become too low to exhibit high enough reactivity.

3.2.2 Effect of reaction atmosphere

The effect of reaction atmosphere on syngas characteristics is examined, where N_2, steam and CO_2 are selected as the pyro-gasification agent. **Figure 3. 2**-**Figure 3. 5** show syngas composition under varied atmosphere for different MSW components, respectively; and **Table 3. 2** summarizes the data on syngas yield.

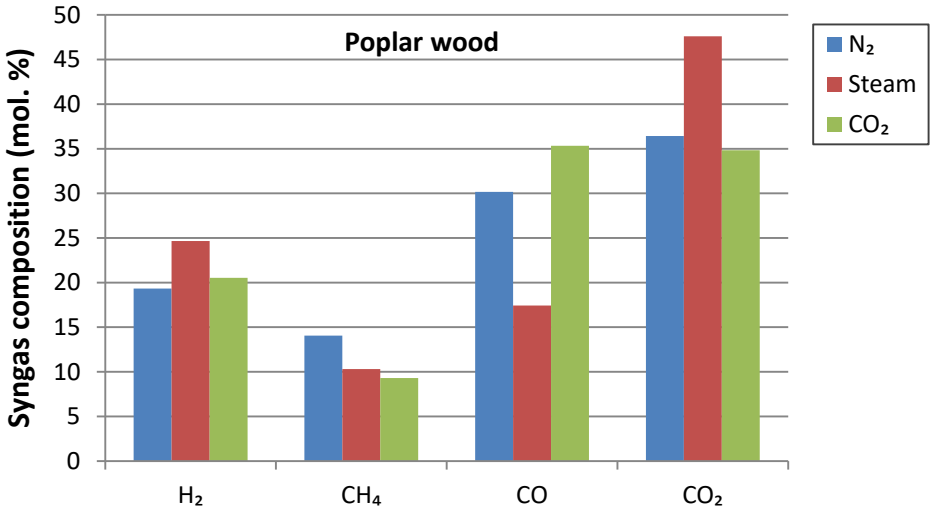

Figure 3. 2 Syngas composition under N_2/steam/CO_2 atmosphere following pyro-gasification of poplar wood

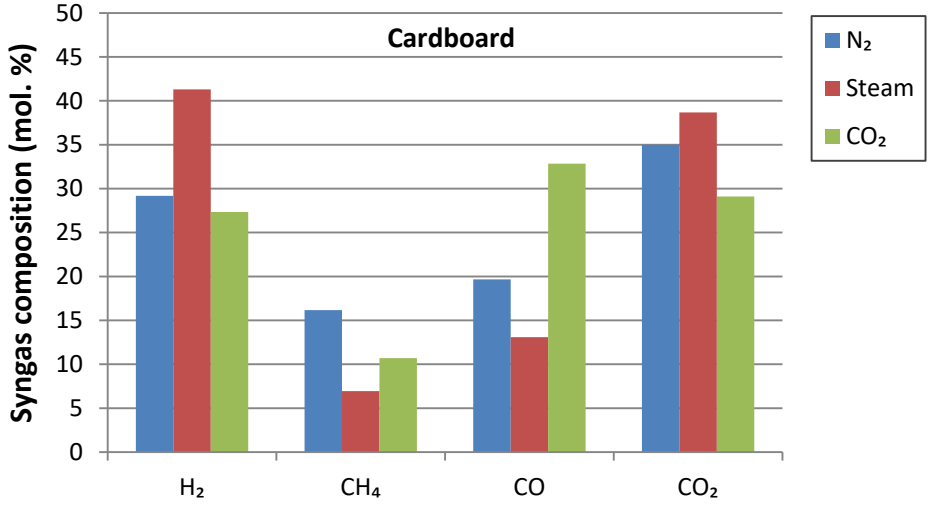

Figure 3. 3 Syngas composition under N_2/steam/CO_2 atmosphere following pyro-gasification of cardboard

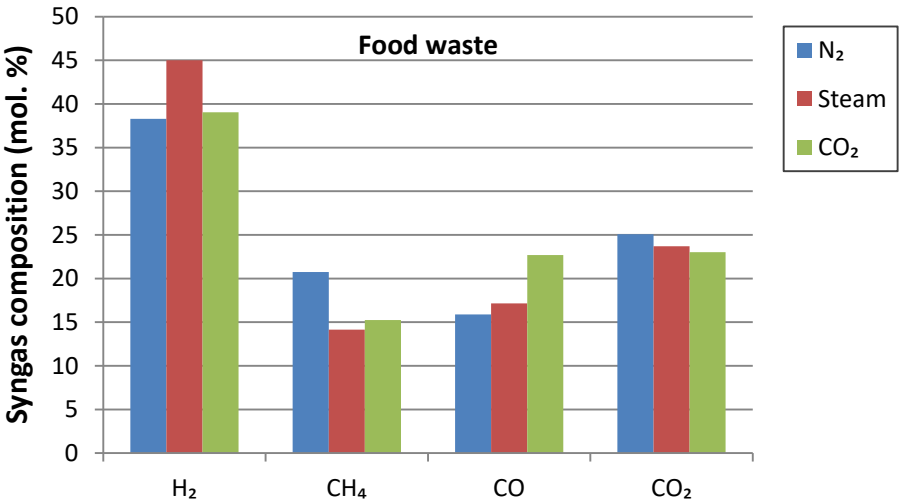

Figure 3. 4 Syngas composition under N_2/steam/CO_2 atmosphere following pyro-gasification of food waste

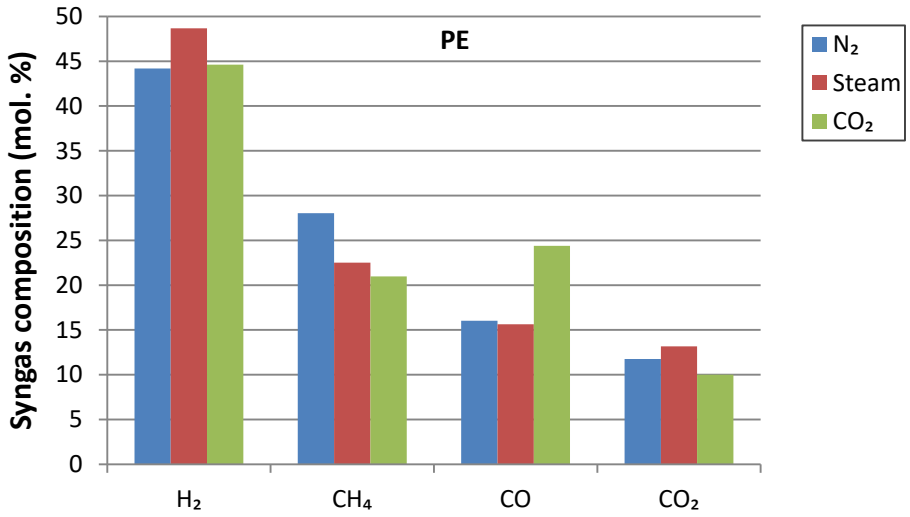

Figure 3. 5 Syngas composition under N_2/steam/CO_2 atmosphere following pyro-gasification of PE

Table 3. 2 Syngas yield under N_2/steam/CO_2 atmosphere for different MSW components (Unit: Nm^3/kg)

Reaction atmosphere	Poplar wood	Cardboard	Food waste	PE
N_2	0.070	0.135	0.141	0.058
Steam	0.088	0.151	0.153	0.070
CO_2	0.074	0.140	0.147	0.062

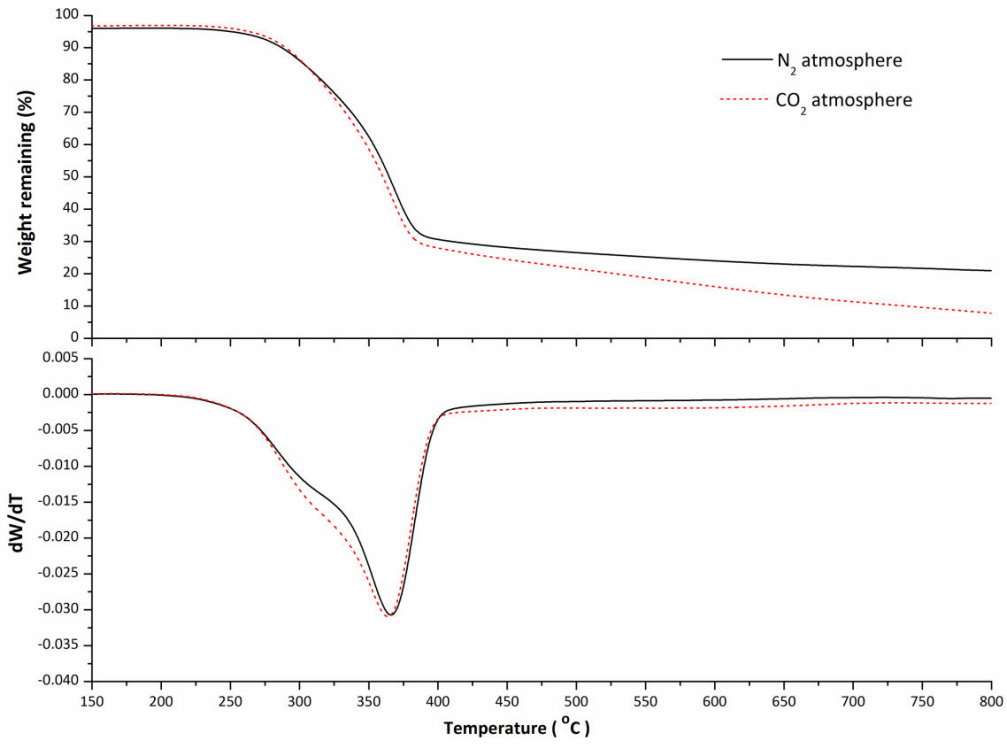

Figure 3. 6 TG and DTG curves of poplar wood under N_2 (solid line) and CO_2 (dashed line) atmosphere at a heating rate of 30 °C/min

Results reveal that both steam and CO_2 gasification are effective in enhancing syngas yields while simultaneously affect the syngas properties. A detailed discussion is given here for the case of poplar wood. When replacing N_2 with steam and CO_2, the syngas yield can be improved from 0.070 Nm^3/kg to 0.088 and 0.074 Nm^3/kg, respectively. This corresponds to an increasing rate of 26% and 6%, respectively. This phenomenon is in agreement with the mechanisms of the gasification reactions. It has been proven that the gasification process can be divided into two main sub-courses, primary pyrolysis followed by a sequence of hetero- and homogeneous reactions, including gaseous phase reactions and char gasification [11, 12]. **Figure 3. 6** illustrates the TG/DTG analysis of poplar wood under N_2 and CO_2 atmosphere. It could be seen that at temperature below ca. 380 °C, the general trend of the weight loss for CO_2 gasification is similar to that in N_2, suggesting that the shift of gasification atmosphere does not influence the behavior of pyrolysis significantly, i.e. pyrolysis step releasing volatile organic matter always occurs before the gasification step. However at temperature higher than 380 °C, the two TG curves show different decreasing rate. The weight loss under CO_2 atmosphere from 380 to 800 °C is 22.8%, which is significantly higher than 13.3% in N_2 atmosphere. This can be attributed to the gasification of complex char by CO_2 through the Boudouard and hydrocarbon CO_2 gasification reactions (Eq. (3.1) and Eq. (3.2)). As a consequence, the syngas yield is effectively improved.

Boudouard reaction:

$$C(s) + CO_2 \rightarrow 2CO + 173.5\,kJ/mol \quad (3.1)$$

Hydrocarbon CO_2 gasification reaction:

$$CH_mO_n(s) + (m - 2n + 4)/4\,CO_2 \rightarrow 2CO + m/2\,H_2O \quad (3.2)$$

It is also found that the gas yield from steam gasification is higher than that from CO_2 gasification. Ahmed et al. [13] observed that steam reactivity with char is about three times faster than that of CO_2. Therefore, the distinction in syngas production from steam and CO_2 gasification could primarily attributed to the reaction rate.

With regard to syngas composition, it is evident that the reaction atmosphere has a significant effect on syngas characteristics; not only by affecting the equilibrium of chemical reactions, but also in acting as reactant participating in the reactions. As presented in **Figure 3. 2**, the H_2 content for poplar wood steam gasification is favored by 5% when compared with its pyrolysis situation. It is because the water gas reaction (Eq. (3.3)), water gas shift reaction (Eq. (3.4)) and hydrocarbon reforming reaction (Eq. (3.5)) are enhanced in the presence of steam. As a result, CH_4 and CO concentration is both decreased while CO_2 increases. On the other hand, CO_2 gasification could considerably promote CO production, which is essentially due to the Boudouard reaction (Eq. (3.1)). It is also observed that the concentration of CH_4 and CO_2 exhibits a slight decrease as compared with those under pyrolysis condition. It can be speculated that the CH_4 dry reforming reaction (Eq. (3.6)) [14] probably occurs, which could be further verified by an increasing concentration of H_2 in the produced gas.

Water gas reaction:

$$C + H_2O \leftrightarrow CO + H_2 - 131\,kJ/mol \quad (3.3)$$

Water gas shift reaction:

$$CO + H_2O \leftrightarrow CO_2 + H_2 + 41\,kJ/mol \quad (3.4)$$

Hydrocarbon reforming reaction:

$$C_nH_m + nH_2O \leftrightarrow nCO + (n + m/2)H_2 - Q \quad (3.5)$$

Methane dry reforming reaction:

$$CH_4 + CO_2 \rightarrow 2CO + 2H_2 - 260\,kJ/mol \quad (3.6)$$

For the other three MSW components, the syngas composition under steam and CO_2 atmosphere exhibits a similar changed tendency as that of poplar wood. For steam gasification, results show that the H_2 content from cardboard, food waste and PE is increased by 12%, 7% and 4% compared with the tests under N_2 atmosphere, respectively. The figure confirms the high reactivity of cardboard and food waste as compared with wood. Besides, it is also noticed that for food waste, the CO concentration shows an increasing trend compared with its pyrolysis, which goes against the tendency observed for the other three MSW components. Realizing this fact, it is supposed that the secondary reaction is enhanced. The porous structure of food waste char makes the formed tar easier to be thermally cracked during transport in the pores of the particles, leading to an increased formation of CO and CH_4 due to tar reforming reaction (Eq. (3.7)).

Tar reforming reaction:

$$Tar + H_2O \rightarrow H_2 + CO_2 + CO + hydrocarbons + ... \quad (3.7)$$

As for CO_2 gasification, the CO concentration is increased by 13%, 7% and 8% for cardboard, food waste and PE, respectively, when compared with its counterpart pyrolysis case. However, looking at both the syngas property and syngas yield, it is found that the variation for PE is not as obvious as for the other components. The characteristics of PE, i.e. low-content of ash and fixed carbon, is the main contributor. Since the majority of volatile matter is released and swept away by the carrier gas during the heating step, the retained char could only exhibit a relatively low reactivity. Therefore, it could be concluded that the pyrolytic char from PE is not suitable as a recyclable to be re-used or recovered.

3.2.3 Utilization of syngas from pyro-gasification of MSW single-component

Table 3. 3 H_2/CO of the syngas from pyro-gasification of MSW single-component (Reaction condition: temperature = 650 °C; time = 15 min)

Reaction atmosphere	Poplar wood	Cardboard	Food waste	PE
N_2	0.64	1.53	2.49	3.07
Steam	1.57	3.90	2.77	3.14
CO_2	0.61	0.86	1.81	1.87

Considering the pyro-gasification data obtained using different MSW single-component and reaction atmosphere, it is supposed that the produced gas would probably have different end-use approaches [15]. As illustrated in **Table 3. 3**, using PE and food waste as raw materials generate syngas with a higher H_2/CO molar ratio. Steam gasification is effective to modify syngas property to high values of H_2/CO, which is required for chemical syntheses, or fuel cells [16]. With regard to this study, the obtained syngas from steam gasification exhibits the desired H_2/CO ratio for Fischer-Tropsch synthesis (target H_2/CO ratio at 1.5-3.0 [17]) for all four MSW components [18, 19]. On the contrary, using CO_2 as gasifying agent results in a lower H_2/CO of the syngas, which could be served as chemical raw material [20]. However, even under CO_2 atmosphere, the obtained syngas from food waste and PE gasification exhibits a H_2/CO ratio higher than 1.5. It infers that the end-use of the produced gas from these two materials should be determined carefully, or be modified through further upgrading process.

3.3 Pyro-gasification characteristics of MSW multi-components

Due to the complexity of MSW, the multi-components may not act independently during pyro-gasification. Nonlinear effects may occur during pyro-gasification of the MSW mixture, either synergy or inhibition. Therefore in order to gain a better understanding of their interactions, pyro-gasification characteristics of MSW multi-components are investigated. All combinations of the four components are considered, using N_2/steam/CO_2 as reaction atmosphere. As a consequence, this section is divided into three parts, where the pyro-gasification characteristics of the mixture involving two-components, three-components and four-components respectively for each case are discussed in details.

Apart from the experimental results, the theoretical linear calculation on both syngas yield and composition is also performed to better express the interactions. The linear calculation is based on a weighted average of the individual component according to Eq. (3.8):

$$Y_{linear\ calculation} = \sum (x_n \cdot Y_n) \quad (3.8)$$

where, $Y_{linear\ calculation}$ is the linear calculated syngas yield (or composition), x_n represents the mass ratio of each component n, which is kept identical in this study (i.e. 50% for two components mixture, 33% for three-components mixture, and 25% for four-components mixture); Y_n is the syngas yield (or composition) from the pyro-gasification of individual component n. If there is no interaction between the components, the calculated linear result would be identical as the obtained experimental result. Difference between the experimental and estimated yields should hence indicate any interaction.

3.3.1 Pyro-gasification of two-components mixture

To investigate the interactions of two-components during pyro-gasification, every two components of poplar wood, cardboard, food waste and PE are mixed at a 50:50 ratio by weight. As a result, a total of 6 mixtures are examined, which are named as: wood/cardboard, wood/food waste, wood/PE, cardboard/food waste, cardboard/food waste and food waste/PE. **Table 3. 4** presents both the linear calculation and experimental results on the syngas yield under N_2 atmosphere, together with the deviation between the two values.

Table 3. 4 Linear calculation and experimental results on the syngas yield of the two-components mixture under N_2 atmosphere

	Wood / Cardboard	Wood / Food waste	Wood / PE	Cardboard / Food waste	Cardboard / PE	Food waste / PE
Cal. [a] (Nm^3/kg)	0.103	0.105	0.064	0.138	0.097	0.100
Exp. [a] (Nm^3/kg)	0.100	0.109	0.069	0.141	0.107	0.106
Deviation [b] (%)	- 2.9%	+ 3.8%	+ 7.8%	+ 2.2%	+ 10.3%	+ 6.0%

[a] "Cal." and "Exp." is short for linear calculation and experimental result, respectively;

[b] Negative deviation means that the experimental-obtained syngas yield is less than the theoretical linear calculation value; vice versa, positive deviation represents a larger syngas yield value from the experiment.

Results reveal that nonlinear phenomena could commonly be observed for the pyrolysis of the mixtures, resulting in a deviated gas yield of 2-10%. Generally, interactions from the mixture of dissimilar components are much more significant than that of similar components. Wood, cardboard and food waste are all biomass-derived while PE is a nonbiogenic material, hence the results from the gas yield exhibit a much higher deviation when PE is evolved in the reaction. Synergistic effect is observed for the majority of co-pyrolysis cases since the syngas yield is increased, except for the syngas produced from the wood/cardboard mixture is decreased.

The syngas composition from both experiment and linear calculation is illustrated in **Figure 3. 7**. When wood is fed with cardboard, the concentration of CH_4 is slightly lower than the linear value, which again verifies that the co-pyrolysis restricts the devolatilization of wood/cardboard mixture. Actually during co-pyrolysis process, interactions might occur between volatile matters from the two materials; or between the volatile matter of one material and the fixed carbon of the other material or even both. With regards to the wood/cardboard mixture, the decreased reactivity could be explained by the cellulose-lignin interaction mechanism proposed by Hosoya et al. [21]. They indicated that, the lignin fraction might have an inhibiting effect on the anhydrosugar polymerization of cellulose, while the vapor phase carbonization of the low molecular weight products from lignin may also be inhibited by cellulose. As a result, they observed an increasing yield of tar fraction resulting from the mixing. In this study, since cardboard is mainly composed of cellulose but poplar wood contains considerable proportion of lignin, the interactions between cellulose and lignin might reduce the reactivity of cardboard. In addition, mass transport resistance might also be a second reason for the lowered reactivity [22, 23], which has been related essentially to the structure of wood char. **Figure 3. 8** presents the morphology of pyrolyzed wood char studied by SEM analysis. From the picture, the structure of wood in the char could be recognized clearly, which means that the treatment is not too destructive. It is thus supposed that the dense structure of wood would change the reaction kinetics and lower the conversion of the blends.

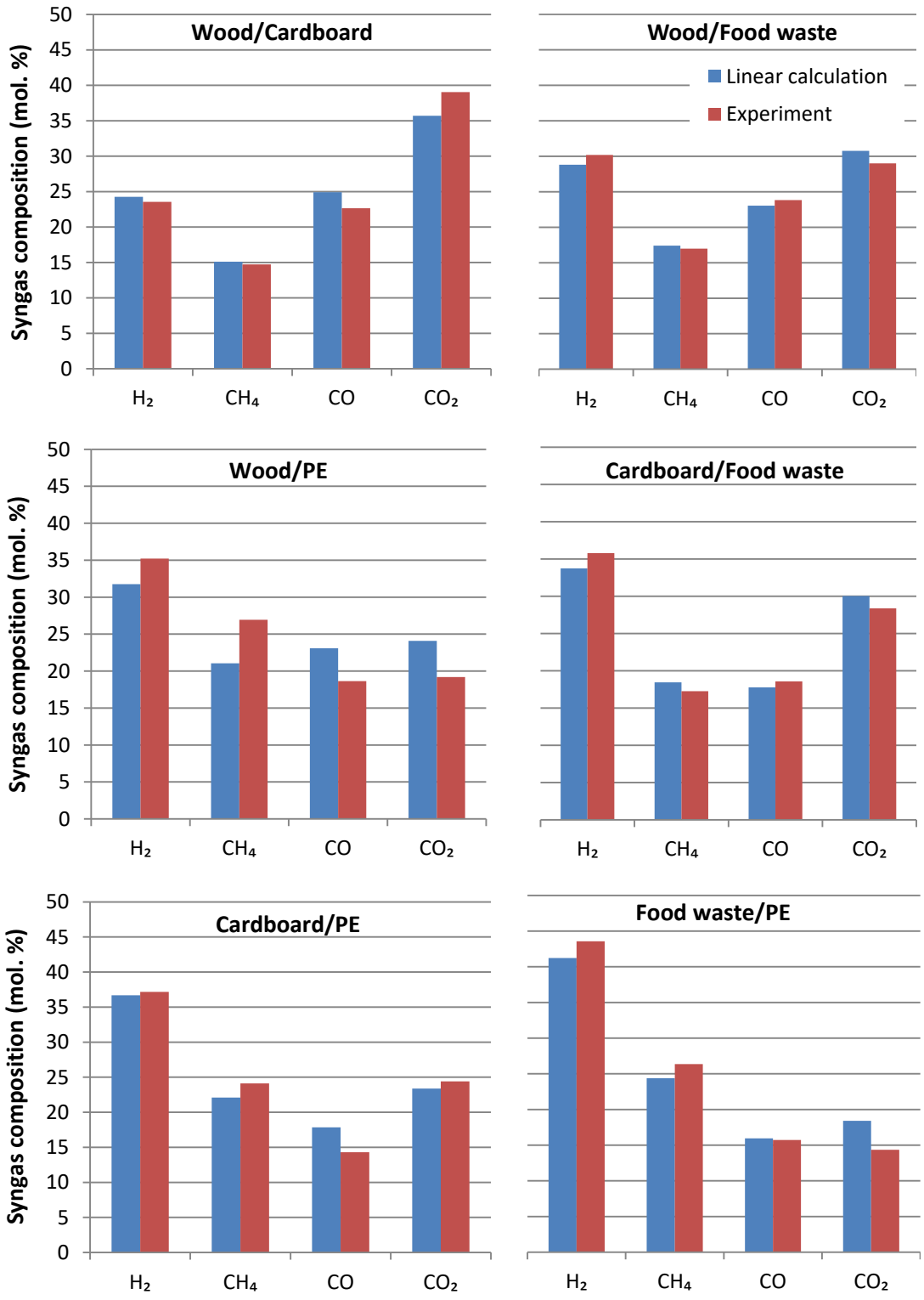

Figure 3. 7 Linear calculation and experimental results on the syngas composition of two-component mixtures under N_2 atmosphere

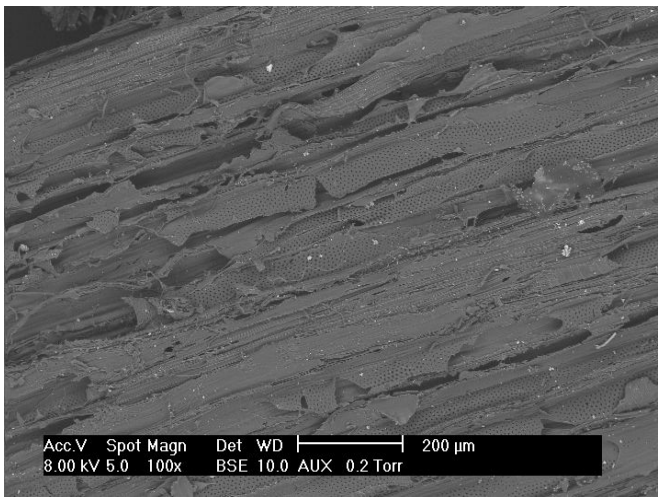

Figure 3. 8 Pyrolyzed wood char by SEM analysis. Working condition: poplar wood is heated under 100% N_2 to 800 ^oC at a heating rate of 20 ^oC/min

More obvious interactions are noticed concerning the co-pyrolysis of PE with other components. For the mixture of wood/PE, cardboard/PE and food waste/PE, deviations between linear average and experimental values of H_2, CH_4, CO, and CO_2 concentration are in a range of 1-11%, 8-28%, 1-20%, and 4-22%, respectively, as shown in **Figure 3. 7**. Interestingly, these three blends exhibit similar changed tendency of an increased concentration of H_2 and CH_4. Since both H_2 and CH_4 are dominating products from PE pyrolysis, it indicates that the synergistic effect of PE is enhanced when mixed with biomass. Previous studies also reported on the increased reactivity of co-feeding plastic and biomass [24-27]. Since the melting point of PE is relatively low (115-135 ^oC [28]), it is supposed that PE might melt and bind the particles of biomass when co-fed, protracting the permanence of these aggregates in the most reactive zone of the reactor and thus favoring their conversion into gaseous products [29]. Besides, Ahmed et al. [30] indicated that PE could act as H donor to the radicals formed in the biomass pyrolysis, thus stabilizing these radicals as hydrocarbon. On the other hand, biomass char could also pose a significant effect on catalyzing the reforming of volatiles. These mechanisms are connected, and therefore result in the increased synergistic interactions between the materials.

Besides, **Table 3. 4** also reveals that both food waste co-pyrolyzed with wood and cardboard accelerates the gas yield. The result confirms the speculation that the porous char obtained from food waste poses a positive effect on gas-solid phase reactions. The gas composition from **Figure 3. 7** further reveals that both the H_2 and CO content are improved compared with linear calculation values, proving that the secondary reaction of tar might probably be enhanced due to the high specific surface area of the food waste char.

With regard to co-gasification under steam and CO_2 atmosphere, nonlinear changes in the syngas yield are also observed, as illustrated in **Table 3. 5** and **Table 3. 6**. It is found that the values of deviation during CO_2 gasification are generally larger than those under steam gasification. To justify such behavior, it is speculated that since the reactions with CO_2 proceed more slowly than with steam, the porosity of the char may be changed. According to the study carried out by Klinghoffer et al. [31], char produced from CO_2 gasification exhibits a micro-pore network but is not observed for steam gasification. It is because CO_2 can diffuse into the pores of the char and modify its structure due to slower reaction kinetics. The high surface area of char could result in more interacted reactions between the components under CO_2 atmosphere.

Table 3. 5 Linear calculation and experimental results on the syngas yield of the two-components mixture under steam atmosphere

	Wood / Cardboard	Wood / Food waste	Wood / PE	Cardboard / Food waste	Cardboard / PE	Food waste / PE
Cal. (Nm^3/kg)	0.120	0.121	0.079	0.152	0.110	0.111
Exp. (Nm^3/kg)	0.129	0.131	0.093	0.170	0.118	0.125
Deviation (%)	+ 7.5%	+ 8.3%	+ 17.7%	+ 11.8%	+ 7.3%	+ 12.6%

Table 3. 6 Linear calculation and experimental results on the syngas yield of the two-components mixture under CO_2 atmosphere

	Wood / Cardboard	Wood / Food waste	Wood / PE	Cardboard / Food waste	Cardboard / PE	Food waste / PE
Cal. (Nm^3/kg)	0.107	0.110	0.068	0.144	0.101	0.104
Exp. (Nm^3/kg)	0.116	0.124	0.094	0.156	0.129	0.136
Deviation (%)	+ 8.4%	+ 12.7%	+ 38.2%	+ 8.3%	+ 27.7%	+ 30.8%

The mixture of wood and cardboard restrains the syngas yield under N_2 atmosphere (**Table 3. 4**); however it is shown beneficial both for steam and CO_2 gasification. This discrepancy could be probably attributed to the presence of alkali metals, which are mainly endogenous in the biomass and have proven to have a catalytic effect on the gasification process [24, 32]. As shown in **Figure 3. 8**, some bright spots are observed, which are quite dispersed at the surface of the char. Energy-dispersive X-ray spectroscopy (EDX) analysis further releases that these agglomerants are mainly composed of P, Ca, K, Na and Mg. During the pyrolysis step, volatiles are released while these endogenous minerals remain in the char. Moreover, it is also proven that the alkali-surface compounds could create a bigger gap between alkali metals and carbon to weaken the carbon-carbon bonds [33]. These behaviors therefore contribute to the promotion of the gasification reactivity. **Figure 3. 9** explores the impact of steam gasification that results in an increasing CH_4 and CO concentration by 2% and 5%, respectively, when compared with linear calculation, which may be due to secondary tar cracking (Eq. (3.7)). The enhanced reactivity also has a positive effect in improving the H_2 and CO content by 1% and 2% under CO_2 gasification case.

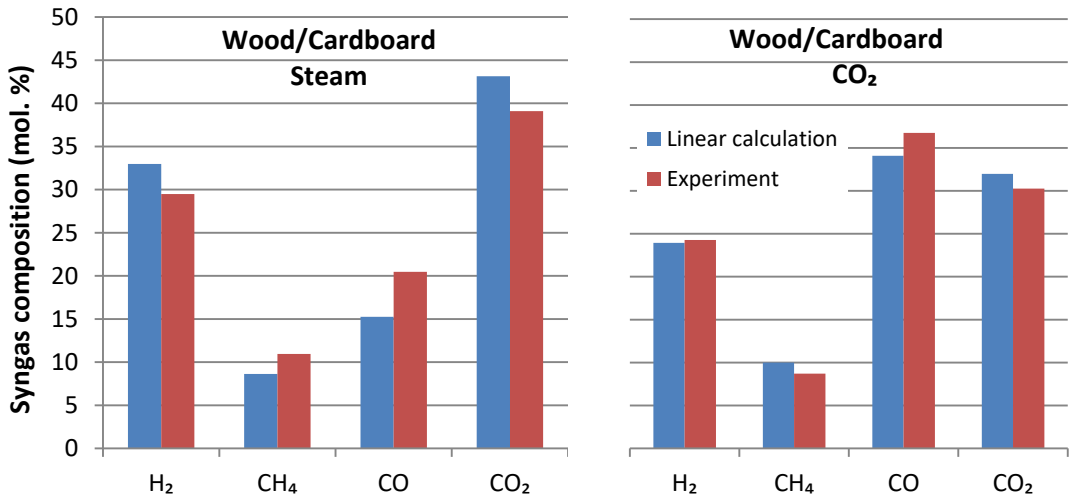

Figure 3. 9 Linear calculation and experimental results on the syngas composition of wood/cardboard under steam and CO_2 atmosphere

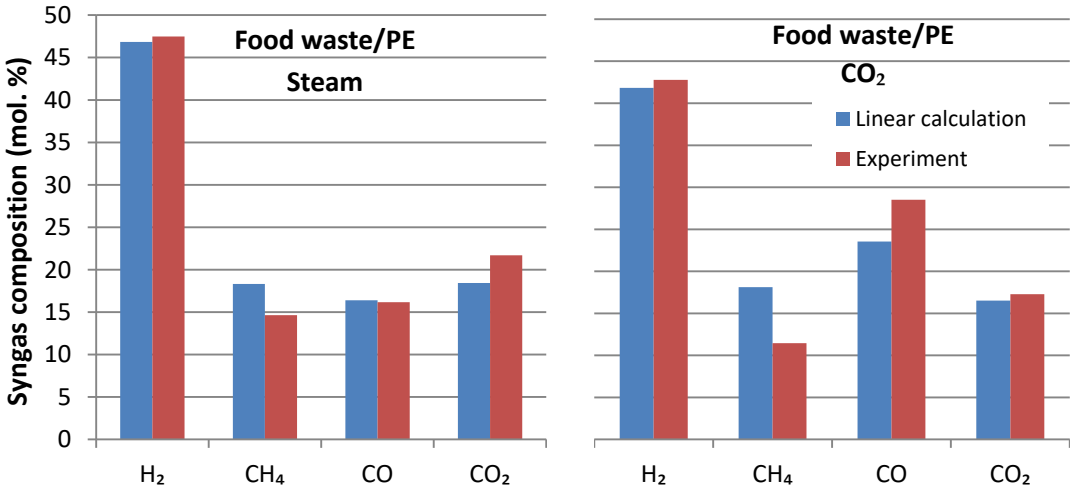

Figure 3. 10 Linear calculation and experimental results on the syngas composition of wood/cardboard and food waste/PE mixture under CO_2 atmosphere

Besides, similar as in pyrolysis cases, interactions between plastic and biomass co-gasification are more significant than those between biogenic materials. This phenomenon is especially obvious for food waste/PE mixture, which could be due to the porous characteristics of the food waste char. As shown in **Table 3.5** and **Table 3. 6**, the syngas yield could be improved by 12.6% and 30.8% under steam and CO_2 atmosphere, respectively. The syngas composition shown in **Figure 3. 10** further reveals that the reforming and tar cracking reactions (Eqs. (3.2), (3.5) and (3.6)) are enhanced, resulting in an increased H_2 and CO_2 concentrations when using either steam or CO_2 atmosphere.

3.3.2 Pyro-gasification of three-components mixture

The syngas yield for the mixture of three components is illustrated in **Table 3. 7**. Results reveal that the deviations between theoretical linear calculation and experiment are in a range of 6-36%. The values are significantly higher than the mixture of two-components, indicating much more obvious and complicated interactions among components.

Table 3. 7 Linear calculation and experimental results on the syngas yield of the three-components mixture under N_2/Steam/CO_2 atmosphere

		Wood / Cardboard /Food waste	Wood / Cardboard / PE	Wood / Food waste / PE	Cardboard / Food waste / PE
N_2 atmosphere	Cal. (Nm^3/kg)	0.115	0.088	0.090	0.112
	Exp. (Nm^3/kg)	0.123	0.083	0.115	0.127
	Deviation (%)	+ 7.0%	- 5.7%	+ 27.8%	+ 13.4%
Steam atmosphere	Cal. (Nm^3/kg)	0.131	0.103	0.104	0.124
	Exp. (Nm^3/kg)	0.144	0.115	0.125	0.137
	Deviation (%)	+ 9.9%	+ 11.7%	+ 20.2%	+ 10.5%
CO_2 atmosphere	Cal. (Nm^3/kg)	0.120	0.092	0.094	0.116
	Exp. (Nm^3/kg)	0.158	0.114	0.128	0.135
	Deviation (%)	+ 31.7%	+ 23.9%	+ 36.2%	+ 16.4%

Similar as the blending of two-components, more significant deviations are observed for reactions involving PE. Generally co-pyro-gasification is effective to promote syngas yield, except in the case of wood/cardboard/PE pyrolysis under N_2 atmosphere. By further examining the corresponding syngas composition (**Figure 3. 11**), it is found that the H_2 and CH_4 content is decreased by 15.3% and 11.6% respectively as compared with linear calculation result. It appears that the devolatilization process of these three materials inhibit each other. Habibi et al. [34] also observed such inhibition effect during the co-gasification of biomass and coal. This phenomenon is attributed to the inhibition effect of the ash which deactivates catalytic species such as P, Ca, K and Mg. A second reason for the decreasing reactivity might be due to the cellulose-lignin inhibiting effect and the tight structure of

wood char, as previous discussed. However, the syngas yield of the wood/cardboard/PE mixture is enhanced under steam and CO_2 gasification, which again verifies the catalytic effect of alkali metals on the gasification process as discussed above.

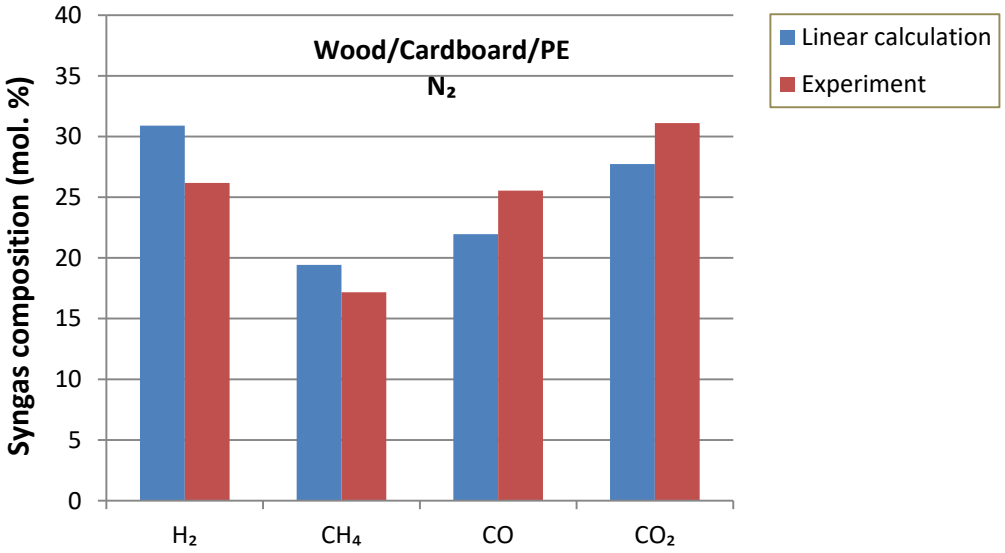

Figure 3. 11 Linear calculation and experimental results on the syngas composition of wood/cardboard/PE mixture under N_2 atmosphere

Meanwhile, CO_2 gasification again exhibits higher interactions than the N_2 and steam atmosphere. **Figure 3. 12** plots the syngas composition of three-components mixture under CO_2 atmosphere. Different blending exhibits varied changed tendency of the gas proportion. However compared with the pure material gasification data in **Figure 3. 2**-**Figure 3. 5**, it is observed that the gas composition of the food waste-involved mixtures is in much more comparable to the gasification of pure food waste. It therefore seems that the influence of other materials becomes less dominant. Two reasons could probably account for such phenomenon: 1) Food waste shows the highest gas production among the MSW samples and therefore its gasification property poses significant influence in determining the overall gas composition. 2) The porous structure of food waste char might be the second reason, which verifies the speculation that it has effectively enhanced the gasification reactivity of the mixtures through reforming and cracking reactions.

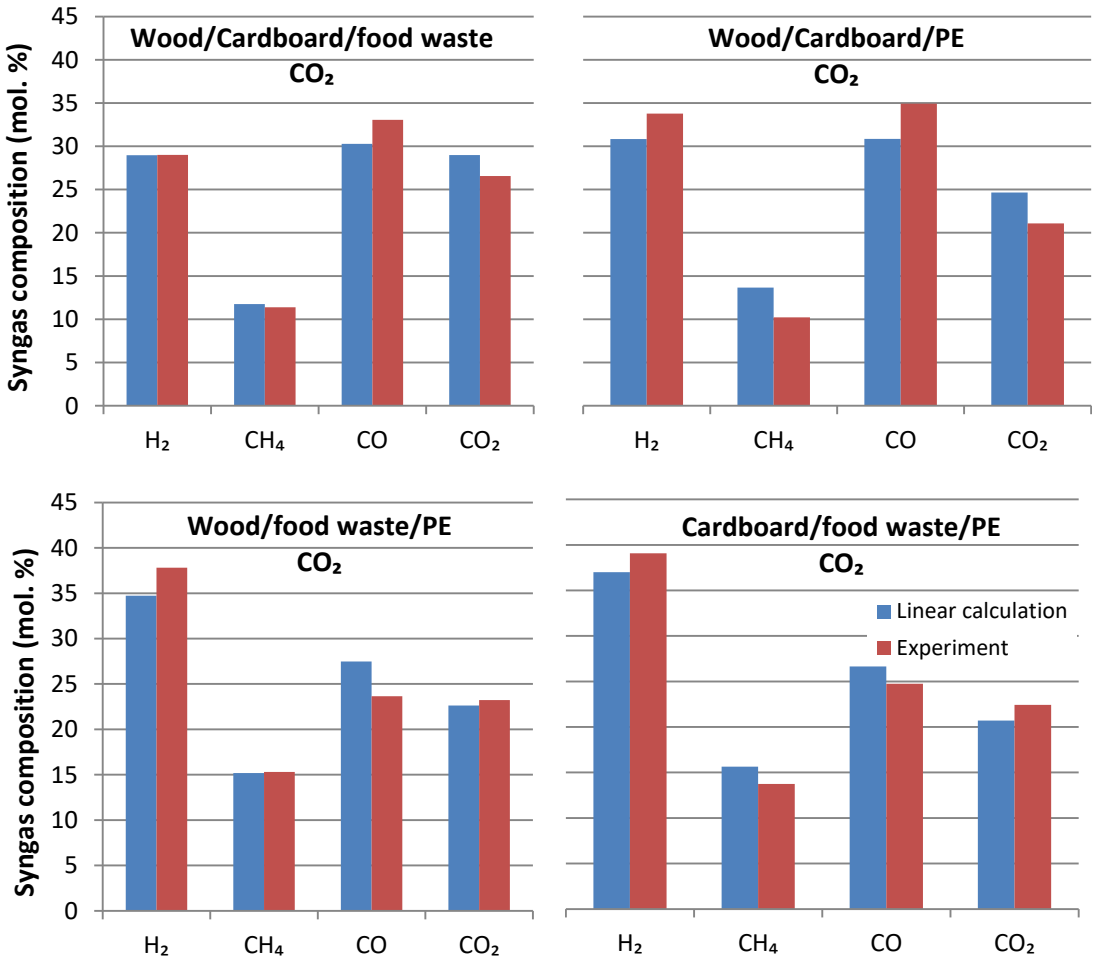

Figure 3. 12 Linear calculation and experimental results on the syngas composition of three-components mixture under CO_2 atmosphere

3.3.3 Pyro-gasification of four-components mixture

Linear interpolation underestimates the gas yield for four-components mixture cases, as illustrated in **Table 3. 8**. The gas yields under N_2/steam/CO_2 atmosphere are all considerably promoted, indicating that the interactions among MSW components are effective to enhance the gasification reactivity. Various factors, such as the characteristics of MSW components, char structure, presence of alkali metals and reaction atmosphere, are responsible for the interactions; the final gas properties are seen as a result of competitive reactions.

Table 3. 8 Linear calculation and experimental results on the syngas yield of the four-components mixture under N_2/Steam/CO_2 atmosphere

	N_2 atmosphere	Steam atmosphere	CO_2 atmosphere
Cal. (Nm^3/kg)	0.101	0.115	0.106
Exp. (Nm^3/kg)	0.112	0.140	0.131
Deviation (%)	+ 10.9%	+ 21.7%	+ 23.6%

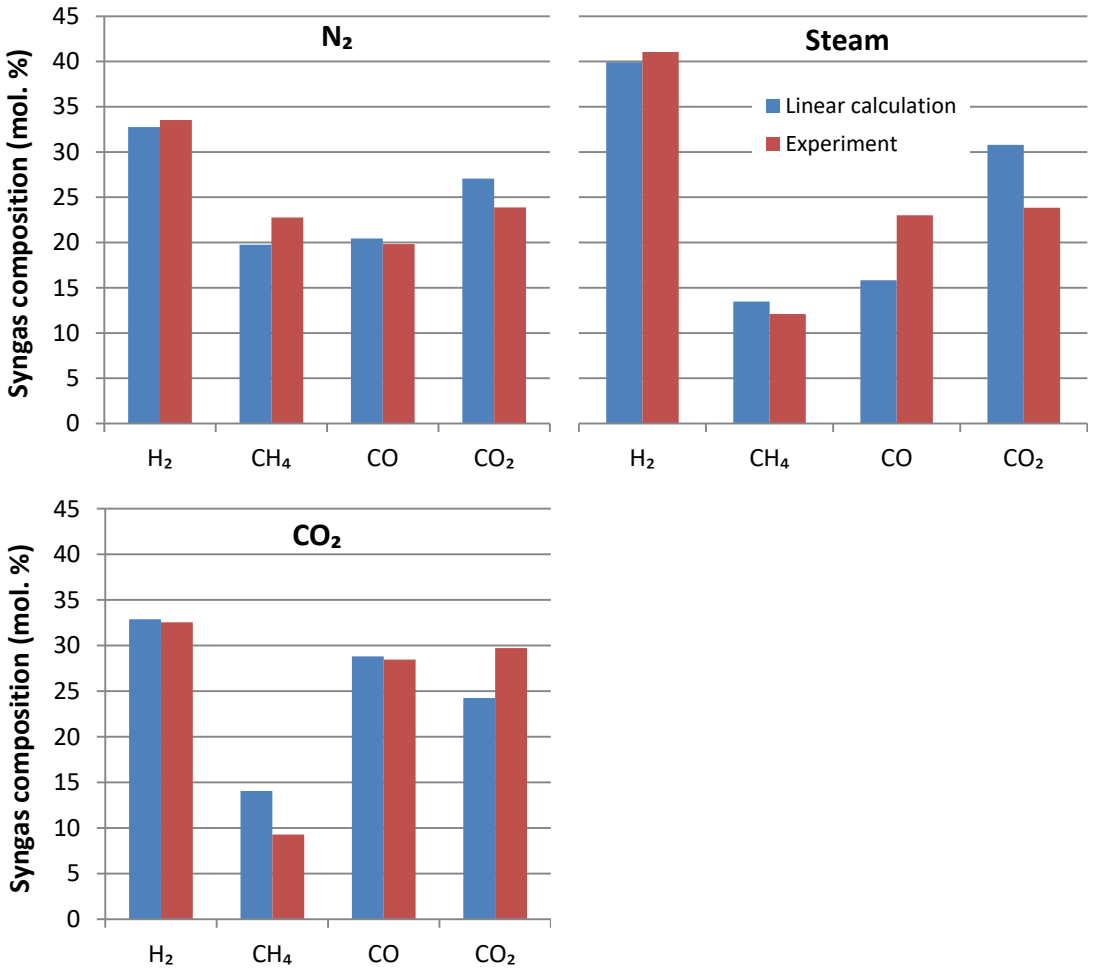

Figure 3. 13 Linear calculation and experimental results on the syngas composition of four-components mixture under N_2/Steam/CO_2 atmosphere

The syngas composition of the four-components mixture is shown in **Figure 3. 13**. Compared with the gas composition obtained from the two-components mixture, results show that some interactions are offset while some are not, as a result of complicated interaction mechanisms as discussed previously. Coupling with the result from MSW single component, the pyro-gasification characteristics are more related to food waste, due to their high reactivity as well as the high specific surface area of char produced. It could also be

concluded that, although pyro-gasification of pure PE char exhibits limited reactivity, the mixture of biomass and non-biomass materials generates significant synergistic effect to the pyro-gasification process. Overall, the results reveal that the pyro-gasification reactions are enhanced, indicating the increasing char decomposition and secondary cracking reactions.

3.3.4 Utilization of syngas from pyro-gasification of MSW multi-components

Table 3. 9 Linear calculation and experimental H_2/CO molar ratio of the syngas from pyro-gasification of four-components mixture

H_2/CO molar ratio	N_2 atmosphere	Steam atmosphere	CO_2 atmosphere
Cal.	1.93	2.85	1.29
Exp.	1.70	1.79	1.14

The interactions among MSW multi-components during pyro-gasification process have resulted changes in the syngas quality. As a result, the syngas properties as well as its potential utilization approaches are investigated. The four-components mixture is taken as an example, with the H_2/CO molar ratio of the obtained syngas from both linear calculation and experimental results shown in **Table 3. 9**.

Results from **Table 3. 8** and **Figure 3. 13** show that the gain in syngas yield have at the same time, impacted the syngas composition. When comparing the experimental results to the linear calculation values, the H_2 content is actually not affected significantly; while great changes are observed for the CO_2 and CH_4 concentration. CO is especially affected only in steam atmosphere. The changes in syngas composition thus lead to:

- In N_2 atmosphere, the H_2/CO ratio is quite the same for both theoretical and experimental results (1.93 and 1.70, respectively). At the same time less CO_2 is generated, which indicates less amount of GHG emissions.

- In steam atmosphere, the H_2/CO ratio is declined from 2.85 (linear calculation) to 1.79 (experimental value) mainly due to an increase in CO concentration. It infers a decrease of syngas quality, despite the fact that the total syngas yield is increased.

- In CO_2 atmosphere, the H_2/CO ratio does not change greatly (1.29 vs. 1.14); however more CO_2 is produced and special attention for the alleviation of GHG emissions is essential.

In realizing the properties of syngas obtained, the potential utilization approaches are examined. Syngas from steam gasification shows the highest H_2/CO value; it, together with the syngas produced in N_2 atmosphere, exhibits the desired H_2/CO ratio for Fischer-Tropsch synthesis. CO_2 gasification produces the syngas with lowest H_2/CO; and although it is still, as the other gasification medium, suitable for energy generation.

3.4 MSW pyro-gasification ANN model establishment

3.4.1 Structure of the model

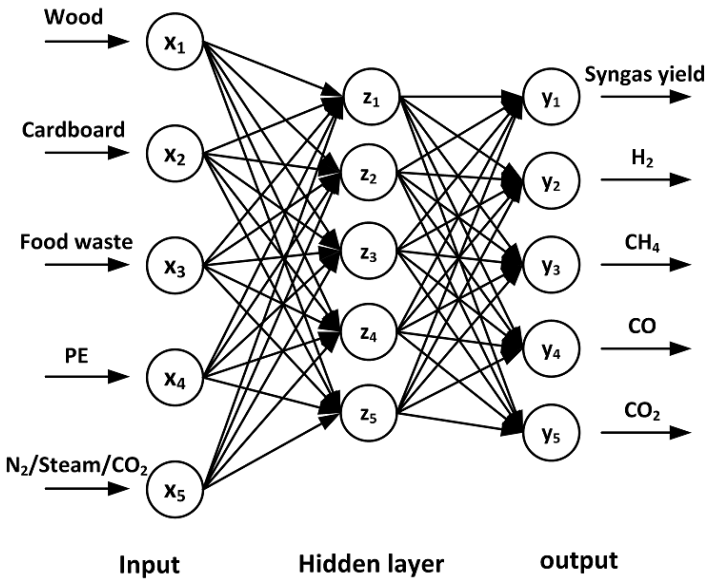

Figure 3. 14 MSW pyro-gasification ANN model structure

The ANN model described in **Chapter 2** is used to establish MSW pyro-gasification characteristics using a BP (backpropagation) network (see **Figure 3. 14**). The model consists of three layers: an input layer, an output layer and one hidden layer. The data obtained from **Section 3.2** and **Section 3.3** are used to meet the requirements for establishing the ANN model. As aforementioned, the main objective of this study is to predict the MSW pyro-gasification characteristics based on physical composition, hence five neurons related to the proportion of wood, cardboard, food waste and PE, as well as the specified reaction atmosphere (N_2, steam or CO_2) are set as input variables. Output layer involves five neurons: syngas yield, and the syngas composition including H_2, CH_4, CO and CO_2. In addition, five neurons are included in the hidden layer.

As mentioned in **Chapter 2**, MATLAB Neural Network Toolbox is applied for ANN calculation. The input data are divided into three sets: training data, validation data and testing data; each of them occupies 70%, 15% and 15% of the total input data, respectively. To ensure the robustness of the model, those different kinds of data are randomly selected from the available database. Overall, the parameters set for the MSW pyro-gasification ANN model is summarized in **Table 3. 10**.

Table 3. 10 ANN parameters used in MSW pyro-gasification model

Model type	Model structure	Algorithm	Transfer fuction	Sample category and proportion
3-layer BP network	5 × 5 × 5	Trainlm	Logsig Tansig Purelin	Training 70% Validation 15% Testing 15%

3.4.2 Training ANN

A total of 45 experimental results from **Section 3.2** and **Section 3.3** are provided from the ANN prediction model, with the detailed input and output database listed in **Table 3. 11**. The input data include the pyro-gasification of MSW single- and multi-components, using N_2, steam and CO_2 as reaction atmosphere, respectively. As a result, the input matrix for MATLAB software could be expressed as Eq. (3.9):

$$\text{Input matrix} = (\text{wt.\% wood}, \text{wt.\% cardboard}, \text{wt.\% food waste}, \text{wt.\% PE}, \text{reaction atmosphere}) \quad (3.9)$$

In order to express all the inputs in numeral form, the reaction atmosphere of N_2, steam and CO_2 is defined to be number 1, 3, 5, respectively. Therefore, all the inputs could be presented as vector. For example, gasification of wood under N_2 atmosphere (sample No. 1#) could be described as (100, 0, 0, 0, 1); while the gasification of cardboard/food waste/PE mixture under CO_2 atmosphere (sample No. 42#) could be presented as (0, 33.33, 33.33, 33.33, 5). A total of 31 experimental results are selected as training samples, and the other 14 samples are distributed equally as validation and testing samples.

Table 3. 11 Experimental results from MSW pyro-gasification as ANN input and output database

No.	Input					Output				
	Wood (wt.%)	Cardboard (wt.%)	Food waste (wt.%)	PE (wt.%)	Reaction atmosphere [a]	Syngas yield (m^3/kg)	H_2 (vol.%)	CH_4 (vol.%)	CO (vol.%)	CO_2 (vol.%)
1	100	0	0	0	1	0.070	19.33	14.06	30.17	36.43
2	0	100	0	0	1	0.135	29.18	16.17	19.66	34.99
3	0	0	100	0	1	0.141	38.29	20.74	15.89	25.08
4	0	0	0	100	1	0.058	44.18	28.03	16.03	11.76
5	100	0	0	0	3	0.088	24.66	10.30	17.43	47.60
6	0	100	0	0	3	0.151	41.30	6.94	13.08	38.68
7	0	0	100	0	3	0.153	45.01	14.14	17.15	23.70
8	0	0	0	100	3	0.070	48.67	22.51	15.64	13.18
9	100	0	0	0	5	0.074	20.53	9.31	35.33	34.84
10	0	100	0	0	5	0.140	27.34	10.70	32.85	29.11
11	0	0	100	0	5	0.147	39.05	15.25	22.69	23.01
12	0	0	0	100	5	0.062	44.62	20.97	24.40	10.01
13	50	50	0	0	1	0.100	23.56	14.73	22.65	39.05
14	50	0	50	0	1	0.109	30.19	16.99	23.82	29.00
15	50	0	0	50	1	0.070	35.22	26.95	18.64	19.20
16	0	50	50	0	1	0.141	35.78	17.26	18.58	28.38
17	0	50	0	50	1	0.107	37.18	24.11	14.30	24.40
18	0	0	50	50	1	0.106	43.58	26.35	15.72	14.35
19	50	50	0	0	3	0.129	29.49	10.96	20.47	39.09
20	50	0	50	0	3	0.131	26.61	10.64	21.01	41.74
21	50	0	0	50	3	0.093	38.13	14.39	14.82	32.67
22	0	50	50	0	3	0.170	39.89	8.82	18.04	33.25
23	0	50	0	50	3	0.118	46.38	11.01	14.35	28.26
24	0	0	50	50	3	0.125	47.48	14.64	16.17	21.71
25	50	50	0	0	5	0.116	24.27	8.72	36.74	30.27
26	50	0	50	0	5	0.124	30.70	10.08	32.61	26.61
27	50	0	0	50	5	0.094	33.39	11.65	32.09	22.87
28	0	50	50	0	5	0.156	28.15	10.82	33.10	27.93

29	0	50	0	50	5	0.129	38.73	12.25	34.62	14.40
30	0	0	50	50	5	0.136	42.77	11.45	28.51	17.27
31	33.33	33.33	33.33	0	1	0.123	31.42	16.88	18.30	33.40
32	33.33	33.33	0	33.33	1	0.083	26.18	17.17	25.54	31.10
33	33.33	0	33.33	33.33	1	0.115	35.42	22.24	18.04	24.29
34	0	33.33	33.33	33.33	1	0.127	37.13	20.11	15.38	27.38
35	33.33	33.33	33.33	0	3	0.144	38.94	7.60	23.08	30.38
36	33.33	33.33	0	33.33	3	0.115	40.13	13.51	11.81	34.55
37	33.33	0	33.33	33.33	3	0.125	41.70	14.17	18.48	25.64
38	0	33.33	33.33	33.33	3	0.137	44.45	11.93	19.25	24.37
39	33.33	33.33	33.33	0	5	0.158	29.01	11.37	33.06	26.56
40	33.33	33.33	0	33.33	5	0.114	33.78	10.21	34.92	21.08
41	33.33	0	33.33	33.33	5	0.128	37.81	15.32	23.65	23.22
42	0	33.33	33.33	33.33	5	0.135	39.08	13.75	24.75	22.42
43	25	25	25	25	1	0.112	33.53	22.76	19.83	23.88
44	25	25	25	25	3	0.140	41.05	12.10	23.01	23.85
45	25	25	25	25	5	0.131	32.54	9.28	28.46	29.72

[a] The number 1, 3, 5 represents the reaction atmosphere of N_2, steam and CO_2, respectively.

The outputs of the ANN model calculation results are presented in **Figure 3. 15-Figure 3. 18**. As indicated in **Figure 3. 15**, the validation performance attains its best at epoch 200 (epoch means the number of iterations). The mass squared error of the function curves decreases significantly over the first 10 iterations; after that stably declines to the minimum values. **Figure 3. 16** shows that the gradient and Mu value attains 9.98E-08 and 1E-09 at epoch 200, respectively, which are within the pre-set values and demonstrate that the ANN model has been properly trained and validated.

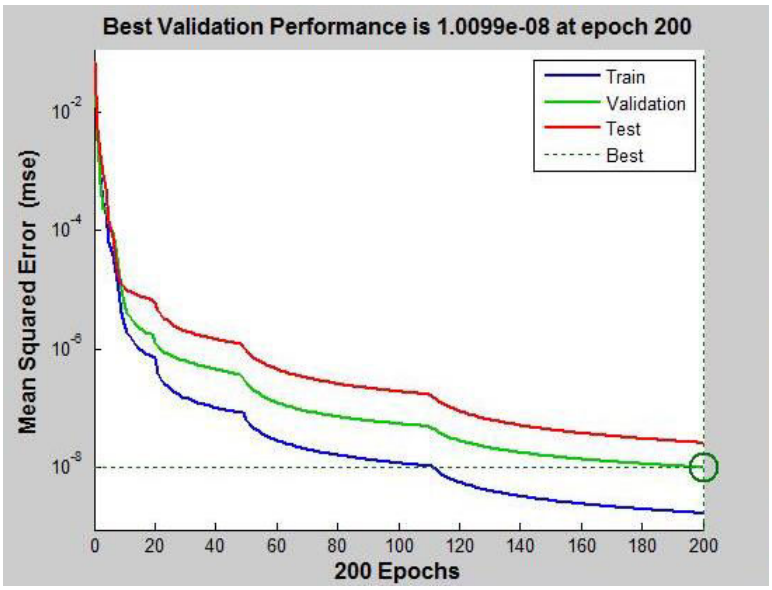

Figure 3. 15 MATLAB ANN modeling result: training performance

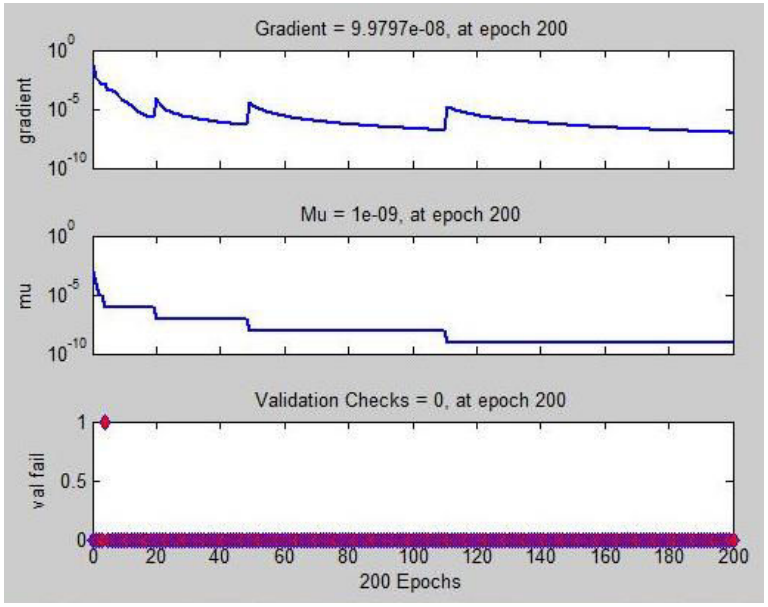

Figure 3. 16 MATLAB ANN modeling result: gradient, Mu and validation checks at epoch 200

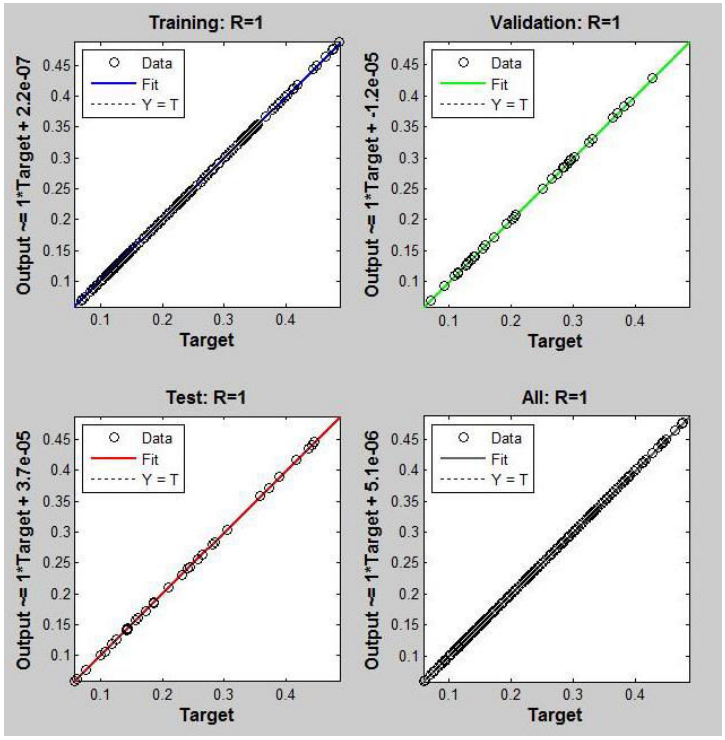

Figure 3. 17 MATLAB ANN modeling result: regression analysis

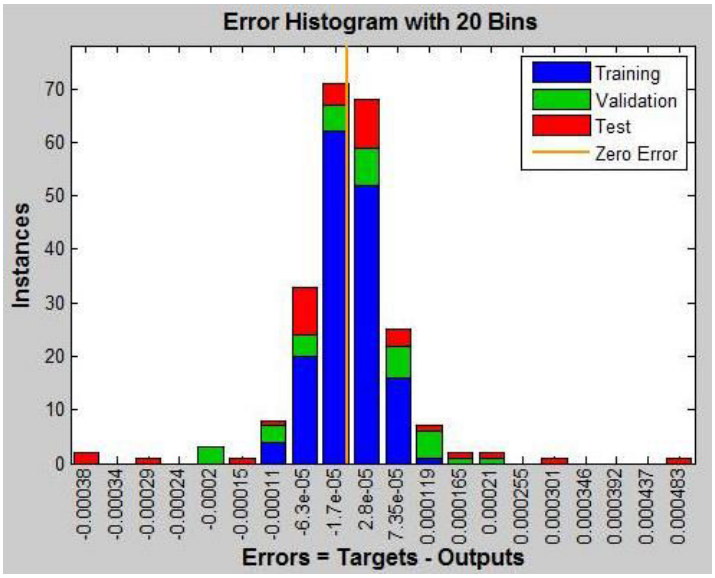

Figure 3. 18 MATLAB ANN modeling result: error histogram

Figure 3. 17 illustrates the regression analysis of the modeling result. The training and validation determination co-efficient (R) of 1 indicates that the ANN has learned well between input parameters and output syngas properties. Similarly, R value from testing data is also relatively high, indicating that the model is able to accurately predict the data that have not been used in the training. Thus, the overall dataset performance of the ANN is very good, with errors between targets and outputs illustrated in **Figure 3. 18**.

3.4.3 Validating ANN

In order to further validate the model, two extra experiments are conducted and compared with the prediction results, using a four-components MSW blend at different mixing rate and different reaction atmosphere. **Table 3. 12** shows the test conditions, and the output results from both experiment and prediction are illustrated in **Figure 3. 19**. To analyze the prediction results comprehensibly, relative error (RE) is used, which is defined as Eq. (3.10):

$$\text{Relative error (RE)} = \frac{\text{Prediction result} - \text{experimental result}}{\text{Experimental result}} \times 100\% \quad (3.10)$$

Table 3. 12 MSW pyro-gasification experimental conditions as validating samples in ANN prediction model

No.	Wood (%)	Cardboard (%)	Food waste (%)	PE (%)	Reaction atmosphere
1	15	15	50	20	N_2
2	20	20	40	20	Steam

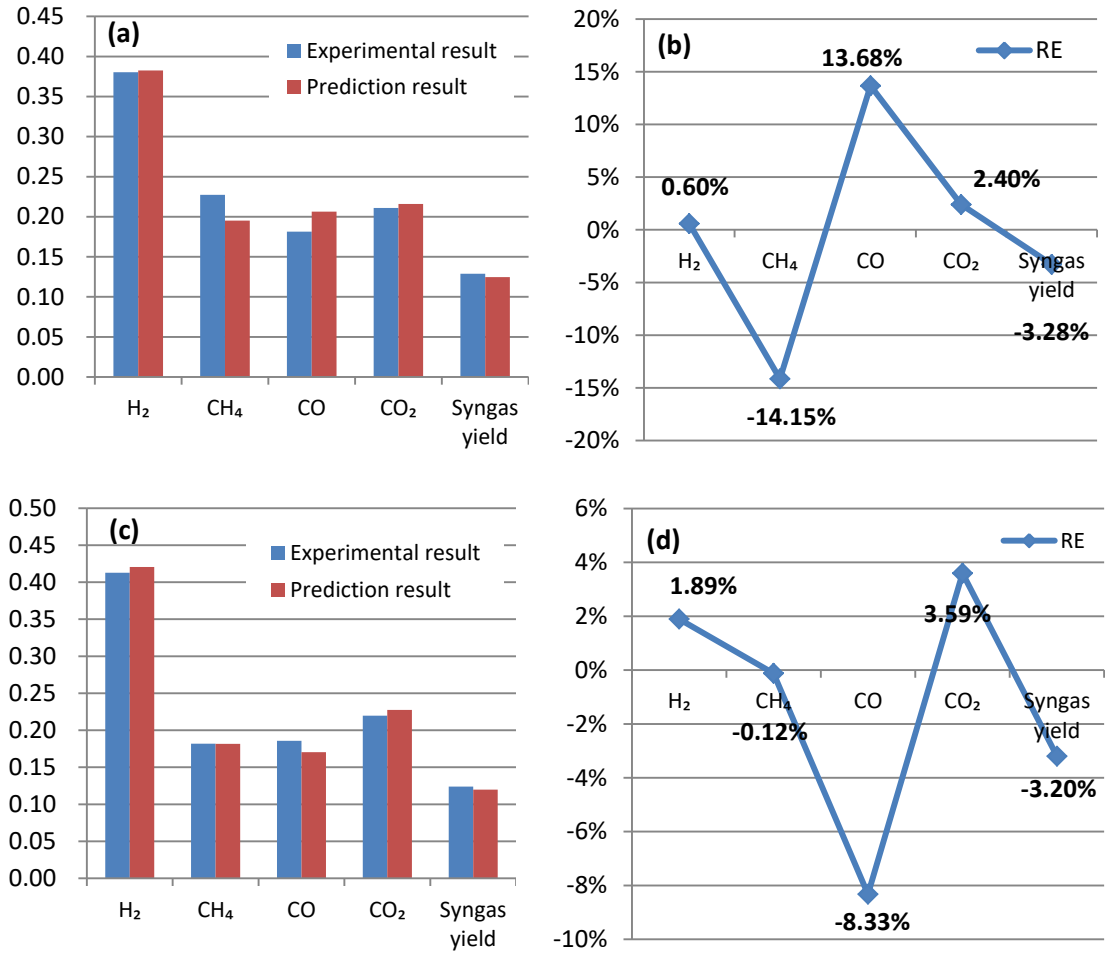

Figure 3. 19 Experimental results, ANN prediction and relative error of MSW pyro-gasification characteristics: (a) and (b): wood/cardboard/food waste/PE = 15/15/50/20 under N_2 atmosphere; (c) and (d): wood/cardboard/food waste/PE = 20/20/40/20 under steam

As shown in **Figure 3. 19**, most of the prediction data are very close to the experimental results. The RE values of the two samples are in the -14% to +14% range, which is quite acceptable in terms of the reliability. Interactions among different MSW components, endogenous minerals, their catalytic effect, and varying conditions inside the reactor could be possible reasons explaining the complexity of the process. However, the accuracy of the model could be further improved by adding more training samples based on experimental results and literature data. Overall, the results demonstrate that the established ANN model is able to properly and accurately predict the syngas yield and composition characteristics during MSW pyro-gasification process.

3.5 Comparison MSW pyro-gasification characteristics between France and China

After carrying out the training and validation step, the established ANN is utilized to forecast the pyro-gasification characteristics of MSW both in France and China. The aim is to compare the differences in syngas properties, as well as to identify their potential efficient utilization approaches.

3.5.1 Comparison of MSW quantities and composition

As it has been pointed out in the General Introduction, the quantity and composition of MSW are closely related to the degree of economic development, lifestyle of the residents and the energy source [35]. In France, 48.7 million tons of MSW were generated in 2010, which corresponded to ca. 740 kg per capita per year [36]. The waste generation per capita has more than doubled in the latest 40 years, although it was reported that the increasing rate has slowed since 2002 [37]. By comparison, in China, 158.1 million tons of MSW were collected in 2010 [38], which is more than 3 times higher than that in France. According to the World Bank [39], China has become the world's largest MSW generator since 2005. The annual MSW increasing rate in China attains ca. 5.5% and keeps on rapidly increasing; with the most recent data showing that the MSW generation reaches 178.6 million tons in 2014 [40]. In average, the waste generation in China equals to 238 kg per capita per year, significantly lower than in France which can be related to the huge population as well as the level of development.

Similarly in both countries, a large quantity of MSW is produced by the population in their daily activities, which mainly consists of food waste, paper, plastic, textiles, glass, metal, wood and residual inorganics (such as ash and dust produced by cooking and heating). **Table 3. 13** and **Figure 3. 20** present a comparison of MSW composition and characteristics between France and China; while data from the USA and global average are set as reference. Some major differences and general trends exist when comparing the waste composition in the two countries:

- China has higher organic fraction, which occupies more than half of the total MSW and is 16% higher than in France. This is primarily attributable to the diet habit.
- The content of recyclables in France, especially paper and cardboard, is relatively high compared with that in China. The level of development would be one reason; besides, the effect of informal activities in China would be another important

reason. There is a tradition for Chinese residents to accumulate and sell higher value recyclables to the announced and regularly appearing collectors [41], which occurs before the municipal collection and thus reduce the quantity of recyclables flowing into the municipal collection system.

- Due to the distinction in the contents of organics and recyclables, MSW in China exhibits high moisture content and lower caloric value, when compared with the MSW characteristics of France.

Table 3. 13 MSW composition and characteristics in selected countries and regions [42, 43]

	Composition (wt.% of total wet waste) [a]							Moisture	LHV
	Organic	Paper	Plastic	Wood	Textile	Metal	Other	(%)	(MJ/kg)
France	39.6	16.2	11.7	2.6 [b]	12.9	3.0	14.0	36.7	9.3
China	55.9	8.5	11.2	2.9	3.2	n.m. [c]	18.4	48.1	5.3
USA [d]	21.1	14.8	17.6	8.2	11.2	9.0	18.1	27.9	11.8
Global average [d]	46.0	17.0	10.0	n.m.	n.m.	4.0	18.0	n.m.	n.m.

[a] The fraction of "other" mainly includes glass, composite waste, and inorganics (e.g. gravel, ceramics, etc.);

[b] The fraction of "wood" in France may include other combustibles, but here we suppose it only consists of pure wood;

[c] n.m.: not mentioned;

d Data from USA and global average are set as reference; source from US EPA [44] and the World Bank [45].

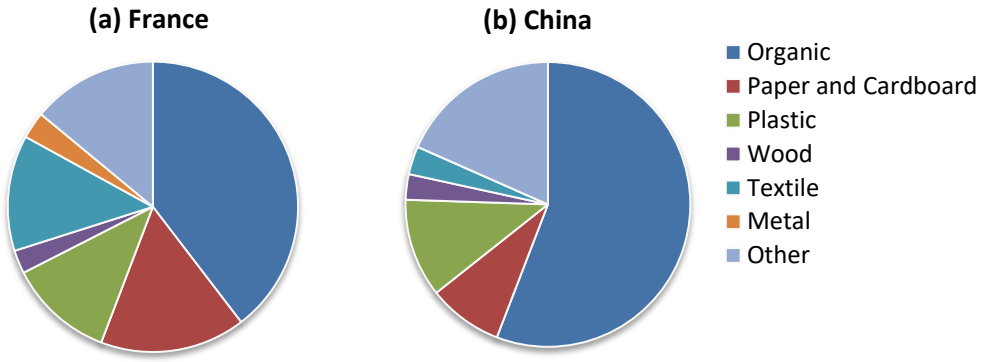

Figure 3. 20 Comparison of MSW composition between France and China

3.5.2 Prediction of MSW pyro-gasification characteristics based on ANN model

Based on the MSW composition data, MSW pyro-gasification characteristics in both France and China are predicted and compared using the established ANN model. The comparison is based on 1 ton of wet MSW. Besides, some assumptions are made to fit the data adjustable as ANN model input:

- ✓ Only fractions of organic, paper & cardboard, plastic and wood are considered to be contributable for pyro-gasification process. In fact, fractions of metals, glass and other inorganics are inert materials and will not take part in the thermo-chemical reactions. However, this hypothesis ignores the pyro-gasification of textile which should necessarily cause deviations. This could be improved in the future by adding extra data on textile.
- ✓ Organic, paper & cardboard, plastic and wood are supposed to be pure food waste, cardboard, PE and poplar wood, respectively.
- ✓ To unify the data into ANN model input, MSW fractions are converted to dried basis and the relative proportions are calculated, as illustrated in **Table 3. 14**.

Table 3. 14 Relative MSW composition calculated as ANN model input

	Organic	Paper and Cardboard	Plastic	Wood
France	29.62%	36.74%	27.00%	6.64%
China	44.31%	20.43%	27.40%	7.85%

The prediction results are illustrated in **Figure 3. 21**, which has been converted to a 1 ton of wet MSW basis. Results reveal that, a much higher syngas yield could be obtained from the pyro-gasification of MSW in France. The syngas yield under N_2, steam and CO_2 atmosphere attains 68.1, 73.7 and 68.7 m^3/t-MSW, respectively; which is 14%, 11% and 10% higher compared with those in China. Several reasons could explain such results. First, MSW in France has a lower moisture content, thus its total combustible amount is higher since the comparison is based on the same amount of wet waste. Second, cardboard occupies a relatively high ratio in the French MSW, which shows potential to generate more gas according to the previously reported pyro-gasification results. As a result, the total gas yield has been increased by the characteristics of the French MSW.

With regard to MSW composition, it is generally found that, pyro-gasification of MSW in China could result in higher proportion of H_2 and CH_4. This could mainly be attributed to the effect of food waste, which occupies a higher frction of the Chinese MSW and exhibits higher H_2 and CH_4 content consulting its pyro-gasification characteristics (see **Figure 3. 4**). Besides, it is speculated that the interactions could also be an important reason. Food waste exhibits higher reaction activity based on the analysis reported in **Section 3.2** and **Section 3.3**; thus the interactions between plastic and biomass may be enhanced considering the relatively high content of food waste of MSW in China.

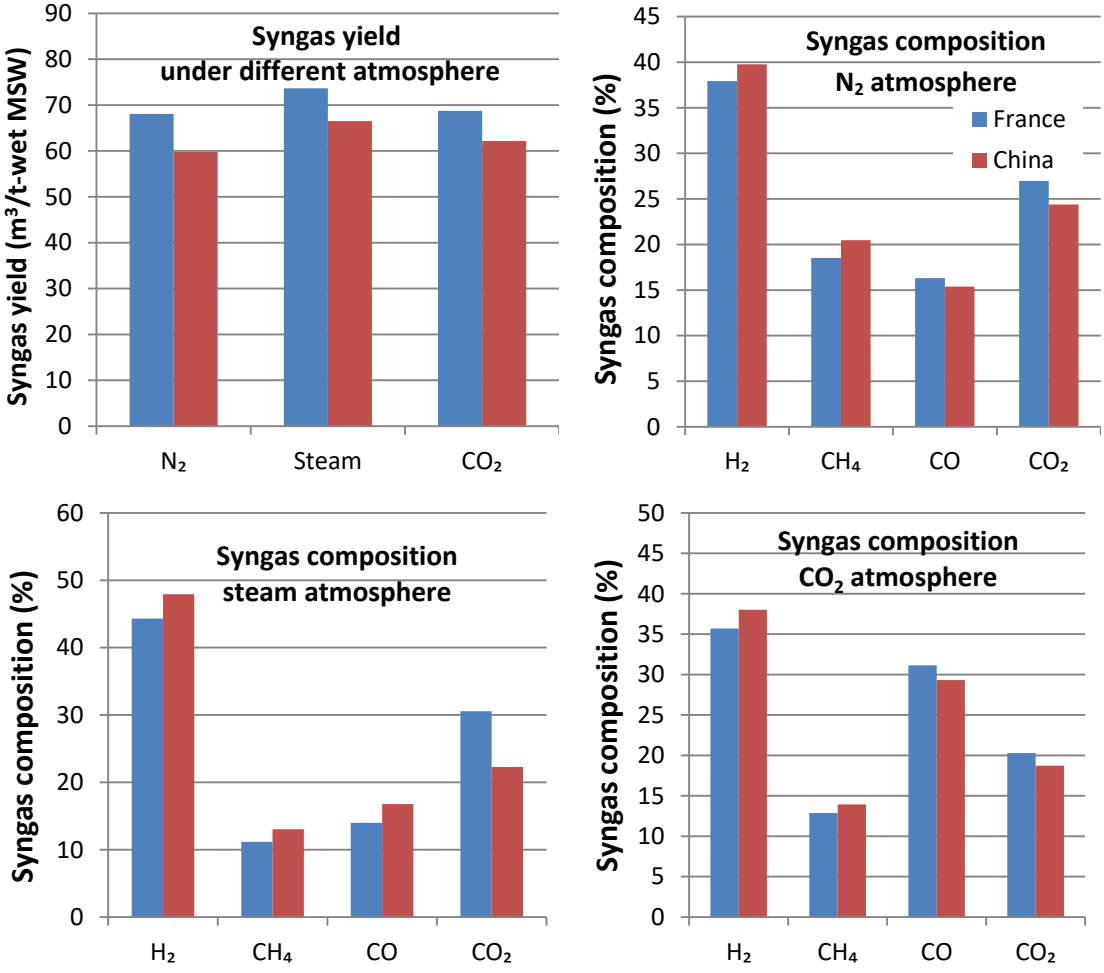

Figure 3. 21 Comparison syngas yield and composition from MSW pyro-gasification between France and China based on an ANN prediction model

An estimation is also made by simply hypothesizing if the annually generated MSW could all be utilized for pyro-gasification. **Table 3. 15** reveals that, 9448, 10517 and 9829 million m^3 of syngas could be obtained from the pyro-gasification of MSW in China under N_2, steam and CO_2 atmosphere, respectively. The values are about 3 times higher than in France due to the large quantity of MSW generated in China. The H_2/CO ratio of the obtained syngas in both France and China is in a range of 1.2-3.2, which is quite suitable for utilization in Fischer-Tropsch processes, or used for energy recovery. Overall, although it is impossible to use all the generated MSW for pyro-gasification, this technique provides a promising approach for the efficient energy utilization of MSW.

Table 3. 15 Estimated annually syngas yield and properties from MSW pyro-gasification based on ANN prediction model

	N_2 atmosphere		steam atmosphere		CO_2 atmosphere	
	Syngas yield, Mm^3	H_2/CO	Syngas yield, Mm^3	H_2/CO	Syngas yield, Mm^3	H_2/CO
France	3314.78	2.32	3587.45	3.17	3347.14	1.15
China	9447.99	2.59	10517.09	2.86	9829.079	1.30

3.6 Summary of chapter

- The pyro-gasification of MSW single-component is carried out. The effect of feedstock characteristics and reaction atmosphere (N_2, steam and CO_2) is investigated, with several major findings drawn as follows:

  - ✓ Due to the distinction in compositions and chemical bonds, different MSW components exhibit varied syngas composition. PE shows the highest H_2 and CH_4 concentration; while pyrolysis of wood contributes to more CO and CO_2. Wood and cardboard have similar major elements; however the reactivity of cardboard is higher than wood due to the tight structure of wood. Food waste shows the highest gas production, its char is porous with larger specific surface area which effectively improves cracking reactions. PE char exhibits limited reactivity, since the remained fixed carbon and carbohydrates are relatively low.

- ✓ Both steam and CO_2 gasification are effective to enhance syngas yield while simultaneously affecting syngas properties. Steam gasification exhibits a noticeably higher gas yield when compared with CO_2 atmosphere, which could be attributed to the higher reaction rate. Using steam as gasifying agent could considerably promote H_2 production, and the obtained syngas would exhibit the desired H_2/CO ratio suitable for Fischer-Tropsch synthesis processes for all the four MSW components. CO_2 gasification is effective for CO enhancement. For poplar wood and cardboard, the lower H_2/CO of the syngas is suitable as chemical raw material.

- The pyro-gasification characteristics of MSW multi-components are then examined to better understand the interaction mechanisms. The mixture of two-components, three components and four-components are all considered, and the following conclusions could be drawn based on the data obtained:

- ✓ Nonlinear phenomena are commonly observed for mixtures. Interactions from the mixture of dissimilar components are much more significant than those of similar components. Plastic co-pyro-gasified with biomass promotes reactivity, resulting in an increased syngas yield compared with theoretical calculation.

- ✓ Co-pyrolysis restricts the devolatilization of the wood/cardboard mixture due to the cellulose-lignin inhibiting effect and the tight structure of wood char. However synergistic effect is obtained under steam and CO_2 co-gasification cases, attributed to the catalytic effect of alkali metals in the biomass on the gasification process.

- ✓ Due to slower reaction kinetics, the char from CO_2 gasification might be more porous with high surface area; thus contributes to the promotion of the gasification reactivity and resulted in higher interactions during CO_2 gasification than steam gasification.

- ✓ The mixture of three-components and four-components shows much more obvious and complicated interactions compared with the blending of two-components as a result of various interaction mechanisms. Generally interactions between different components are effective to strengthen pyro-gasification reactions.

- To improve the syngas quality, some best conditions could be summarized as:

Table 3. 16 A summary of conditions for high-quality syngas production

	MSW component	Atmosphere	Syngas characteristics	
			Syngas yield	H_2/CO
Single-component	Food waste	All tested atmosphere	√	
	PE	All tested atmosphere		√
	All tested components	Steam		√
Multi-component	Biomass-derived components	CO_2	√	
	PE + biomass-derived components	Steam	√	√

- ANN model is developed to predict the MSW pyro-gasification characteristics. The model is based on BP network, with the assistance of MATLAB Neural Network Toolbox. The basic parameters set could be summarized as:

  - ✓ Three-layer structure: an input layer, an output layer and one hidden layer. Five neurons including four MSW components (wood, cardboard, food waste and PE) and the reaction atmosphere are set as input variables; output layer involves five neurons as syngas yield and the composition (H_2, CH_4, CO and CO_2). Five neurons are set for the hidden layer.
  - ✓ 'logsig' (sigmoid), 'tansig' (hyperbolic tangent) and 'purelin' (linear transfer) are set as transfer function for input layer, hidden layer and output layer, respectively. Levenberg-Marquardt BP algorithm is applied as trainlm function.
  - ✓ 70% of the input data are set as training samples; with the remaining 15% and 15% set as validation and testing samples, respectively. Different kinds of data are randomly selected to ensure the robustness of the model.
  - ✓ A total of 45 experimental data obtained from MSW pyro-gasification are used to meet the requirements of ANN model establishment. The performance of training shows good generalization capacity of the model. When used to validate the model, the relative error between experimental and prediction results are within ±14%, which indicates high feasibility of the model to be served in MSW pyro-gasification characteristics prediction.

- The established ANN model is then applied to compare MSW pyro-gasification characteristics between France and China based on physical composition. Results indicate that, on basis of the same amount of MSW, more syngas could be produced from MSW in France considering its higher cardboard content as well as the lower moisture content. MSW in China exhibits higher H_2 and CH_4 concentration, due to the higher food waste proportion and the probable enhanced interactions. The H_2/CO ratio of the syngas both in France and China is in a range of 1.2-3.2, suitable for utilization in a Fischer-Tropsch process or energy recovery. Overall, ANN is an appropriate means to predict pyro-gasification characteristics of MSW.

3.7 Bibliography

[1] Chen Tianju, Wu Jingli, Zhang Zhezi, Zhu Mingming, Sun Li, Wu Jinhu, et al. Key thermal events during pyrolysis and CO_2-gasification of selected combustible solid wastes in a thermogravimetric analyser. Fuel. 2014;137:77-84.

[2] Chen Shen, Meng Aihong, Long Yanqiu, Zhou Hui, Li Qinghai, Zhang Yanguo. TGA pyrolysis and gasification of combustible municipal solid waste. Journal of the Energy Institute. 2015;88:332-343.

[3] Gómez-Barea Alberto, Leckner Bo. Modeling of biomass gasification in fluidized bed. Progress In Energy And Combustion Science. 2010;36:444-509.

[4] McKendry Peter. Energy production from biomass (part 1): overview of biomass. Bioresource Technology. 2002;83:37-46.

[5] Merrild H., Damgaard A., Christensen T. H. Recycling of paper: accounting of greenhouse gases and global warming contributions. Waste Management & Research. 2009;27:746-753.

[6] Sørum Lars, Grønli MG, Hustad Johan E. Pyrolysis characteristics and kinetics of municipal solid wastes. Fuel. 2001;80:1217-1227.

[7] Aguiar L, Márquez-Montesinos F, Gonzalo A, Sánchez JL, Arauzo J. Influence of temperature and particle size on the fixed bed pyrolysis of orange peel residues. Journal Of Analytical And Applied Pyrolysis. 2008;83:124-130.

[8] Figueiredo JL, Valenzuela C, Bernalte A, Encinar JM. Pyrolysis of holm-oak wood: influence of temperature and particle size. Fuel. 1989;68:1012-1016.

[9] Luo Siyi, Xiao Bo, Hu Zhiquan, Liu Shiming. Effect of particle size on pyrolysis of single-component municipal solid waste in fixed bed reactor. International Journal Of

Hydrogen Energy. 2010;35:93-97.

[10] Buah WK, Cunliffe AM, Williams PT. Characterization of products from the pyrolysis of municipal solid waste. Process Safety And Environmental Protection. 2007;85:450-457.

[11] Consonni Stefano, Viganò Federico. Waste gasification vs. conventional Waste-To-Energy: A comparative evaluation of two commercial technologies. Waste Management. 2012;32:653-666.

[12] Kwak Tae-Heon, Maken Sanjeev, Lee Seungmoon, Park Jin-Won, Min Byoung-ryul, Yoo Young Done. Environmental aspects of gasification of Korean municipal solid waste in a pilot plant. Fuel. 2006;85:2012-2017.

[13] Ahmed II, Gupta AK. Kinetics of woodchips char gasification with steam and carbon dioxide. Applied Energy. 2011;88:1613-1619.

[14] Chubb Talbot A. Characteristics of CO_2-CH_4 reforming-methanation cycle relevant to the solchem thermochemical power system. Solar Energy. 1980;24:341-345.

[15] Gil Javier, Corella José, Aznar María P, Caballero Miguel A. Biomass gasification in atmospheric and bubbling fluidized bed: effect of the type of gasifying agent on the product distribution. Biomass and Bioenergy. 1999;17:389-403.

[16] De Filippis Paolo, Borgianni Carlo, Paolucci Martino, Pochetti Fausto. Prediction of syngas quality for two-stage gasification of selected waste feedstocks. Waste Management. 2004;24:633-639.

[17] Butterman Heidi C, Castaldi Marco J. CO_2 as a carbon neutral fuel source via enhanced biomass gasification. Environmental Science & Technology. 2009;43:9030-9037.

[18] Riggs James B. Method for controlling H_2/CO ratio of in-situ coal gasification product gas. United States Patent, Patent number 4,476,927; 1984.

[19] Sattar Anwar, Leeke Gary A, Hornung Andreas, Wood Joseph. Steam gasification of rapeseed, wood, sewage sludge and miscanthus biochars for the production of a hydrogen-rich syngas. Biomass and Bioenergy. 2014;69:276-286.

[20] Mitsuoka Keiichirou, Hayashi Shigeya, Amano Hiroshi, Kayahara Kenji, Sasaoaka Eiji, Uddin Md Azhar. Gasification of woody biomass char with CO_2: the catalytic effects of K and Ca species on char gasification reactivity. Fuel Processing Technology. 2011;92:26-31.

[21] Hosoya T, Kawamoto H, Saka S. Cellulose–hemicellulose and cellulose–lignin interactions in wood pyrolysis at gasification temperature. Journal Of Analytical And Applied Pyrolysis. 2007;80:118-125.

[22] Haykiri-Acma H, Yaman S. Interaction between biomass and different rank coals during

co-pyrolysis. Renewable Energy. 2010;35:288-292.

[23] Völker S, Rieckmann Th. Thermokinetic investigation of cellulose pyrolysis—impact of initial and final mass on kinetic results. Journal Of Analytical And Applied Pyrolysis. 2002;62:165-177.

[24] Lopez Gartzen, Erkiaga Aitziber, Amutio Maider, Bilbao Javier, Olazar Martin. Effect of polyethylene co-feeding in the steam gasification of biomass in a conical spouted bed reactor. Fuel. 2015;153:393-401.

[25] Mastellone Maria Laura, Zaccariello Lucio, Arena Umberto. Co-gasification of coal, plastic waste and wood in a bubbling fluidized bed reactor. Fuel. 2010;89:2991-3000.

[26] Pinto F, Franco C, André RN, Miranda M, Gulyurtlu I, Cabrita I. Co-gasification study of biomass mixed with plastic wastes. Fuel. 2002;81:291-297.

[27] Ruoppolo G, Ammendola P, Chirone R, Miccio F. H_2-rich syngas production by fluidized bed gasification of biomass and plastic fuel. Waste Management. 2012;32:724-732.

[28] Batra Kamal. Role of Additives in Linear Low Density Polyethylene (LLDPE) Films. Project Report 2013-14. Kharagpur, West Bengal: Department of Chemistry, Indian Institute of Technology Kharagpur; 2014.

[29] Zaccariello Lucio, Mastellone Maria Laura. Fluidized-Bed Gasification of Plastic Waste, Wood, and Their Blends with Coal. Energies. 2015;8:8052-8068.

[30] Ahmed II, Nipattummakul N, Gupta AK. Characteristics of syngas from co-gasification of polyethylene and woodchips. Applied Energy. 2011;88:165-174.

[31] Klinghoffer Naomi B, Castaldi Marco J, Nzihou Ange. Catalyst properties and catalytic performance of char from biomass gasification. Industrial & Engineering Chemistry Research. 2012;51:13113-13122.

[32] Kaewpanha Malinee, Guan Guoqing, Hao Xiaogang, Wang Zhongde, Kasai Yutaka, Kusakabe Katsuki, et al. Steam co-gasification of brown seaweed and land-based biomass. Fuel Processing Technology. 2014;120:106-112.

[33] Parvez Ashak M, Mujtaba Iqbal M, Pang Chengheng, Lester Edward, Wu Tao. Effect of the addition of different waste carbonaceous materials on coal gasification in CO_2 atmosphere. Fuel Processing Technology. 2016;149:231-238.

[34] Habibi Rozita, Kopyscinski Jan, Masnadi Mohammad S, Lam Jill, Grace John R, Mims Charles A, et al. Co-gasification of biomass and non-biomass feedstocks: synergistic and inhibition effects of switchgrass mixed with sub-bituminous coal and fluid coke during CO_2 gasification. Energy & Fuels. 2012;27:494-500.

[35] Huang Qifei, Wang Qi, Dong Lu, Xi Beidou, Zhou Binyan. The current situation of solid

waste management in China. Journal of Material Cycles and Waste Management. 2006;8:63-69.

[36] Agence de l'Environnement et de la Maîtrise de l'Energie (ADEME). ITOM: Les installations de traitement des ordures ménagères en France. 2010.

[37] Agence de l'Environnement et de la Maîtrise de l'Energie (ADEME). Waste figures for France. 2009.

[38] Chinese Statistics Yearbook Compiling Committee. Chinese statistics yearbook 2012. Beijing: Chinese Statistics Press; 2012.

[39] Hoornweg Dan, Lam Philip, Chaudhry Manisha. Waste Management in China: Issues and Recommendations. Washington DC: East Asia Infrastructure Development, The World Bank; 2005.

[40] Chinese Statistics Yearbook Compiling Committee. Chinese statistics yearbook 2014. Beijing: Chinese Statistics Press; 2014.

[41] Tai Jun, Zhang Weiqian, Che Yue, Feng Di. Municipal solid waste source-separated collection in China: A comparative analysis. Waste Management. 2011;31:1673-1682.

[42] Beylot Antoine, Villeneuve Jacques. Environmental impacts of residual Municipal Solid Waste incineration: A comparison of 110 French incinerators using a life cycle approach. Waste Management. 2013;33:2781-2788.

[43] Zhou Hui, Meng AiHong, Long YanQiu, Li QingHai, Zhang YanGuo. An overview of characteristics of municipal solid waste fuel in China: physical, chemical composition and heating value. Renewable and Sustainable Energy Reviews. 2014;36:107-122.

[44] United States Environmental Protection Agency. Advancing sustainable materials management: facts and figures 2012. 2014.

[45] Hoornweg Daniel, Bhada-Tata Perinaz. What a waste: a global review of solid waste management. Washington DC: The World Bank; 2012.

Chapter 4

Steam Catalytic Gasification for Hydrogen-rich Gas Production

4.1 Introduction

Based on the results reported in **Chapter 3**, the aim of this chapter is mainly focused on the optimization of MSW pyro-gasification process to produce high-quality syngas. As discussed in **Chapter 1**, among the various syngas utilization routes, H_2 production is particularly attractive because of its high efficiency and pollution-free ability. Unfortunately at present, over 96% of the H_2 production in the world comes from steam reforming of natural gas and oil, and coal gasification [1]. Taking into account the fossil fuel depletion and emissions on global warming, H_2 production from renewable and clean resources is of significant importance.

MSW has been considered to be such a potential material for H_2 production [2-6], since it contains a high proportion of renewable and biogenic-derived components, which are CO_2 neural and make MSW a rather attractive feedstock to produce H_2. Results from **Chapter 3** showed the possibility and feasibility to produce H_2 from MSW, while steam gasification is the most favorable for enhancing H_2 content compared with pyro-gasification under N_2 or CO_2 atmosphere. Poplar wood is selected as the feedstock for steam catalytic gasification, aiming at a more accurate investigation of the characteristics of H_2-rich gas production as potential optimization approach for the pyro-gasification process. Besides, the use of wood as feedstockis also due to the fact that it is one of the most representative components in MSW and occupies ca. 2-15% mass ratio of MSW according to the statistical report of the World Bank [7]. As a result, effective treatment of this material is of significant importance.

In addition, as it has been highlighted in **Chapter 1**, CaO exhibits the ability to enhance H_2 production from tar cracking. Considering the catalytic effect of CaO, it is thus proposed that in-situ CaO additive could serve as an efficient approach to reduce the steam gasification temperature when compared with the non-catalytic situation. Actually, current steam gasification is mostly carried out at a relatively high temperature (above 1000 °C) to ensure the gasification performance [8]. Such high reaction temperature leads to a lower energy efficiency and as well poor economy. However, CaO catalytic gasification offers the possibility to obtain as high quality as the syngas produced by non-catalytic gasification. This approach could thus substantially lower the required gasification temperature, and will finally increase the system efficiency and reduce the operation cost. Ohtsuka et al. [9] studied the reactivity of coal by steam gasification, indicating that the reaction temperature could be decreased by 110-150 °C in the presence of calcium hydroxide ($Ca(OH)_2$). Also, Dalai et al. [10] revealed that the gasification temperature could be lowered by ca. 150 °C, when using CaO as catalyst for biomass steam gasification. However in the field of MSW catalytic steam gasification, study on the reaction temperature reduction potential is still limited.

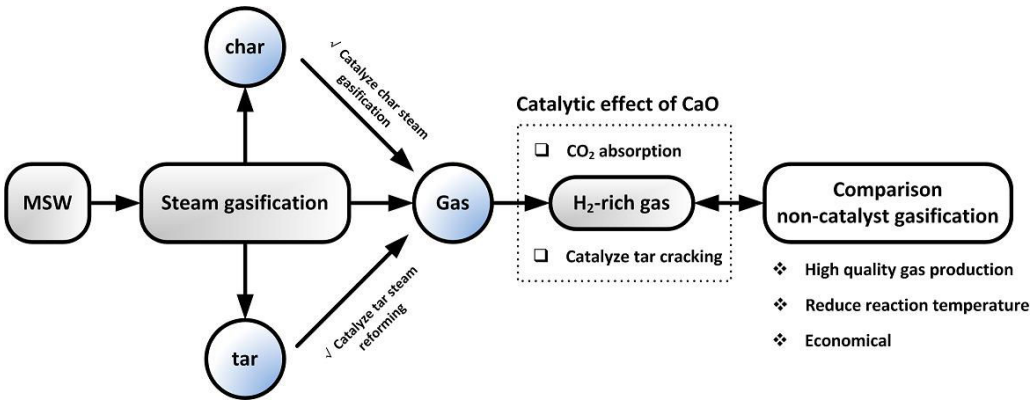

Figure 4. 1 Potential catalytic effect of CaO on optimizing the steam gasification of MSW to produce H_2-rich gas

Accordingly in this chapter, steam gasification of MSW has been investigated for H_2-rich gas production, using CaO as in-bed catalyst. The purpose of the study is briefly illustrated in **Figure 4. 1**, which could be expressed as follows:

I. Evaluate the steam catalytic gasification performance: the influence of steam flowrate, CaO addition ratio and reaction temperature is studied, with emphasis on H_2-rich and high quality gas production. Based on the data, the optimal working condition is determined.

II. Optimize the steam gasification process at lower temperature: high-temperature gasification under non-catalyst condition is also carried out. By comparing the syngas property and products characteristics between catalytic and non-catalytic cases, the potential of reducing the gasification temperature by using CaO catalyst is examined.

The knowledge acquired could represent the foundation for potential pyro-gasification optimization approach, and to develop a more effective and economical MSW pyro-gasification process. The feedstock used and experimental procedures related to this work has been described in detail in **Chapter 2**, and the main experimental results are discussed below. The structure of this part will be presented as follows: **Section 4.2** investigates the effect of operating conditions on the performance of catalytic steam gasification, where the catalyst activity and steam flowrate is examined. Based on the results obtained, **Section 4.3** mainly focuses on process optimization under different temperatures. The results are further compared with non-catalyst gasification cases in **Section 4.4**, to verify the potential of reducing the gasification temperature as another potential optimization approach.

4.2 Effect of operating conditions on catalytic steam gasification

4.2.1 Effect of CaO/wood mass ratio

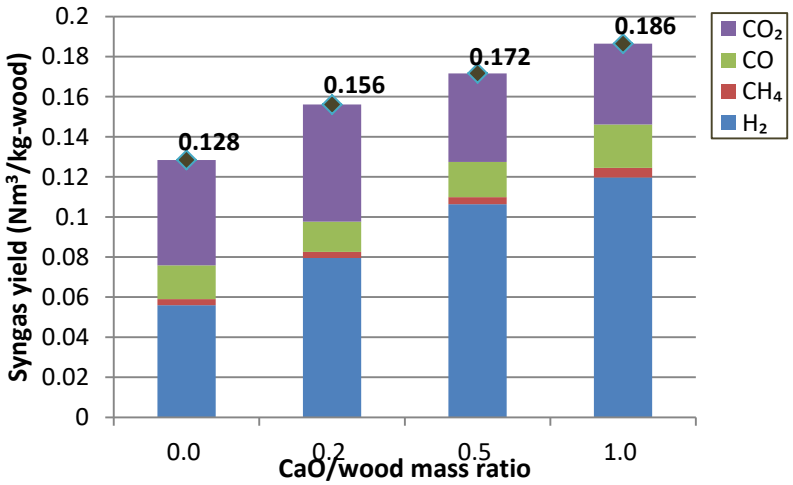

Figure 4. 2 Effect of CaO/wood mass ratio on syngas yield (steam flowrate = 160 g/h; temperature = 700 °C; reaction = 15 min)

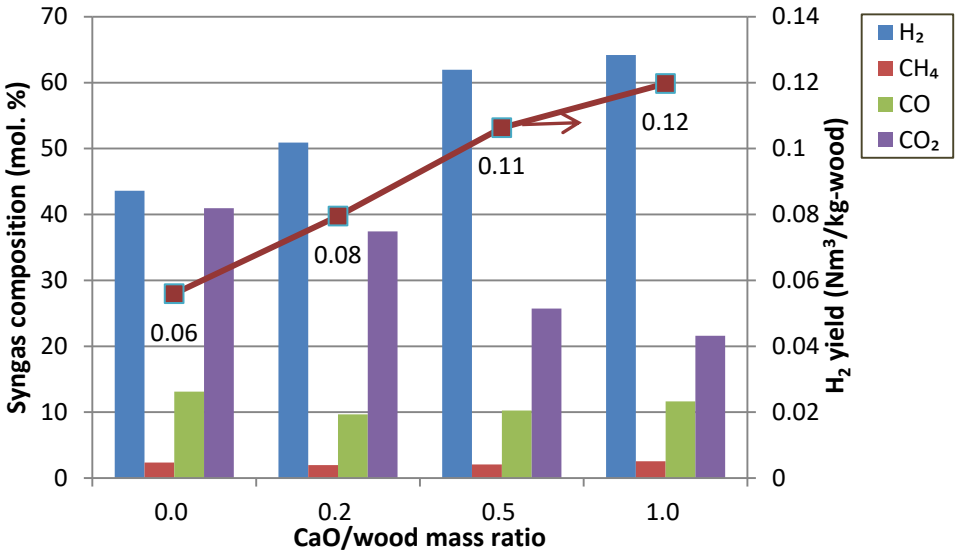

Figure 4. 3 Effect of CaO/wood mass ratio on H_2 yield and syngas composition (steam flowrate = 160 g/h; temperature = 700 °C; reaction = 15 min)

The first operating conditions investigated are focused on the effect of catalyst loading. The effect of CaO/wood mass ratio (varying from 0 to 1) has been studied at a steam flowrate of 160 g/h and temperature of 700 °C. Syngas yield and composition are shown in **Figure 4. 2** and **Figure 4. 3**, respectively. **Figure 4. 2** illustrates that the total gas yield is remarkably enhanced after the addition of CaO, revealing the obviously catalytic effect of CaO on steam gasification. H_2 yield is increased rapidly from 0.06 Nm^3/kg of wood in the absence of CaO to 0.12 Nm^3/kg of wood at a CaO/wood mass ratio of 1, corresponding to an elevated H_2 concentration going from 43.6% to 64.2% (**Figure 4. 3**). It could also be noticed that the H_2 yield is increased quite linearly with the increase of the ratio up to 0.5. The results indicate that CaO catalyst enhances the H_2 production (volume produced) and increases the quality of the syngas (higher H_2 concentration in the gas), as expected.

It has been proven that during the steam gasification process, the final gas composition is a result of several complex and competing reactions. **Table 4. 1** shows the properties of the pyrolyzed char after heating the furnace to the reaction temperature (700 °C) before injecting the steam, which is quanlified as blank test in advance. The important reactions involved in steam gasification are listed as follows, considering the actual elemental composition of the pyrolyzed char according to **Table 4. 1**.

Table 4. 1 Proximate and ultimate analysis of pyrolyzed poplar char at 700 °C

	Proximate analysis (ad, wt. %)				Ultimate analysis (ad, wt. %)					LHV (MJ/kg)
	M	V	FC	A	C	H	O	N	S	
Pyrolyzed wood char [a]	6.33	10.84	80.42	2.41	79.23	2.77	9.02	0.24	0	30.52

[a] Poplar wood char is produced through pyrolysis in N_2 atmosphere to a temperature of 700 °C at a constant heating rate of 20 °C/min.

Stoichiometric steam reforming reaction:

$$C_{6.60}H_{2.77}O_{0.56} + 6.04\,H_2O \leftrightarrow 6.60\,CO + 7.425\,H_2 \quad (4.1)$$

Water gas reaction:

$$C + H_2O \leftrightarrow CO + H_2 \text{ - } 131\,kJ/mol \quad (4.2)$$

Water-gas shift reaction:

$$CO + H_2O \leftrightarrow CO_2 + H_2 + 41\,kJ/mol \quad (4.3)$$

Boudouard reaction:

$$C + CO_2 \rightarrow 2CO + 173.5\,kJ/mol \quad (4.4)$$

Tar reforming reaction:

$$Tar + H_2O \xrightarrow{CaO} H_2 + CO_2 + CO + hydrocarbons + ... \quad (4.5)$$

According to the stoichiometric reaction as Eq. (4.1), complete steam gasification of the pyrolyzed char should result in high amount of CO and H_2, and a H_2/CO ratio of 1.125. **Figure 4. 3** verifies the high H_2 concentration of 43.6% without catalyst. Yet the CO concentration is quite low, representing one third of CO_2 value, which can mainly be attributed to the water gas shift reaction (Eq. (4.3)). In the presence of excessive water during steam gasification, CO_2 could be produced in higher amount as a result of CO oxidation. **Figure 4. 3** shows also that with the increasing CaO loading, the increase in H_2 concentration is accompanied with a significant decrease in CO_2 concentration. This decrease is also quite linear, indicating that the CaO concentration is involved in the amount of CO_2 measured in the gas phase.

To better verify the catalytic mechanism, CO_2 equilibrium test is conducted. According to the involved reactions, the production of CO_2 could be attributed to the water gas shift reaction (Eq. (4.3)) and the tar reforming reaction (Eq. (4.5)); while the Boudouard reaction (Eq. (4.4)) could be the main contributor to CO_2 consumption. The mechanism of CO_2 adsorption by CaO is via the carbonation reaction Eq. (4.6), which could further lower the CO_2 partial pressure and enhance the water gas shift reaction hence producing more H_2 [11]. Previous studies have indicated that the catalytic effect of CaO is two-folds: to serve as CO_2 acceptor, as well as to participate in the tar reforming reactions. This is indicated by the decreased concentrations of CO and CH_4 from **Figure 4. 3**, which could be attributed to the facilitated tar reforming reaction. Nevertheless, the changed tendency is not as obvious as the linearly decreased CO_2 concentration. Thus, it could be speculated that the dominant catalytic mechanism of CaO at the reaction conditions is via CO_2 adsorption, mainly due to that the contact frequency between CO_2 gas and CaO sorbents is improved with the increasing CaO amount, and in the fluidized bed.

Carbonation reaction:

$$CaO + CO_2 \rightarrow CaCO_3 + 178\,kJ/mol \quad (4.6)$$

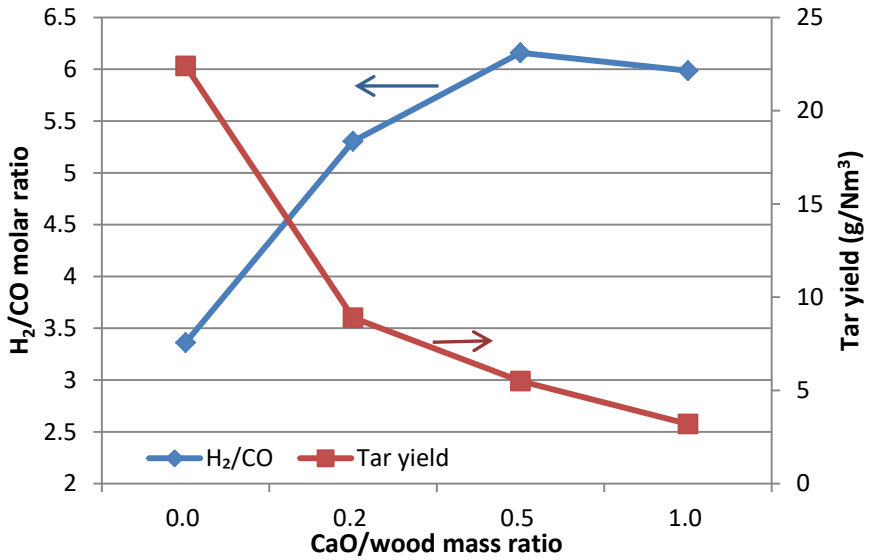

Figure 4. 4 Effect of CaO/wood mass ratio on H_2/CO ratio and tar yield (steam flowrate = 160 g/h; temperature = 700 °C; reaction = 15 min)

The H_2/CO and tar yield under different CaO/wood mass ratios are presented in **Figure 4. 4**. By increasing the CaO/wood mass ratio from 0 to 1, the H_2/CO ratio shows an increasing trend from 3.36 to 5.99. The peak value of 6.16 appears at CaO/wood mass ratio of 0.5; after

what the H_2/CO ratio exhibits a slight decrease since the increase in H_2 production is not as obvious as in CO. Meanwhile, the tar yield is declined continuously from 22.4 to 3.2 g/Nm^3. Overall, the concentration of tar could be effectively reduced by 60% under CaO/wood mass ratio of 0.2 compared with that in absence of CaO. It is also observed that the color of the collected tars turns from deep brown into light yellow when increasing the CaO/wood ratio from 0 to 1 (**Figure 4. 5**). This shows that the tar reforming reaction (Eq. (4.4)) is indeed enhanced by the CaO catalyst. Supporting this observation, research by Han et al. [12] proved that CaO could catalyze the reduction reactions of tar species such as toluene, phenol and formic acid. Besides, recent studies also reported that the O^{2-} ions formed as the active sites on CaO could provide spatially diffuse electron clouds that overlap the orbitals of the incoming molecules and disrupt the stability of the π-electron cloud of tar species finally leading to the splitting of the aromatic rings [8, 13, 14]. For practical application, it is evident that the tar content should be down to a lower level in order to avoid any damage to the downstream energy conversion device or fouling of the gas purification system. Elimination of tar inside the gasifer seems to be an optimal method, since removing the tar from the syngas by means of a wet physical method owes the drawback of losing chemical energy of the syngas [15]. In this sense, the utilization of CaO as catalyst could serve as a potential approach for both H_2-rich and tar-free gas production.

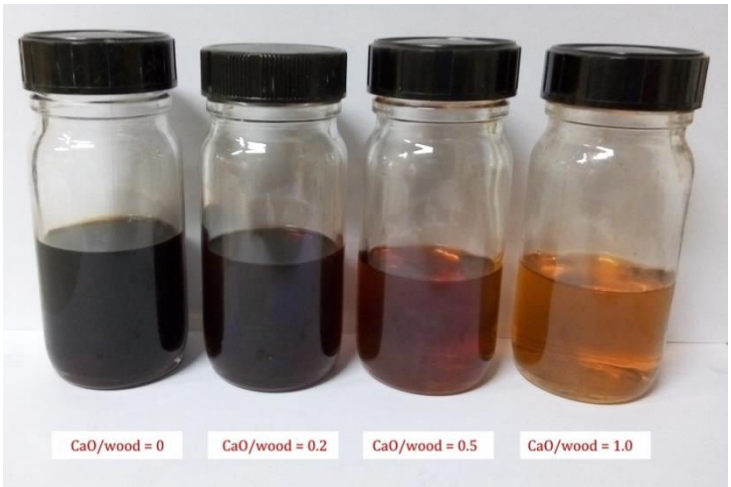

Figure 4. 5 Effect of CaO/wood mass ratio on the characteristics of collected tar (steam flowrate = 160 g/h; temperature = 700 °C; reaction = 15 min); from left to right: CaO/wood mass ratio of 0, 0.2, 0.5 and 1

4.2.2 Effect of steam flowrate

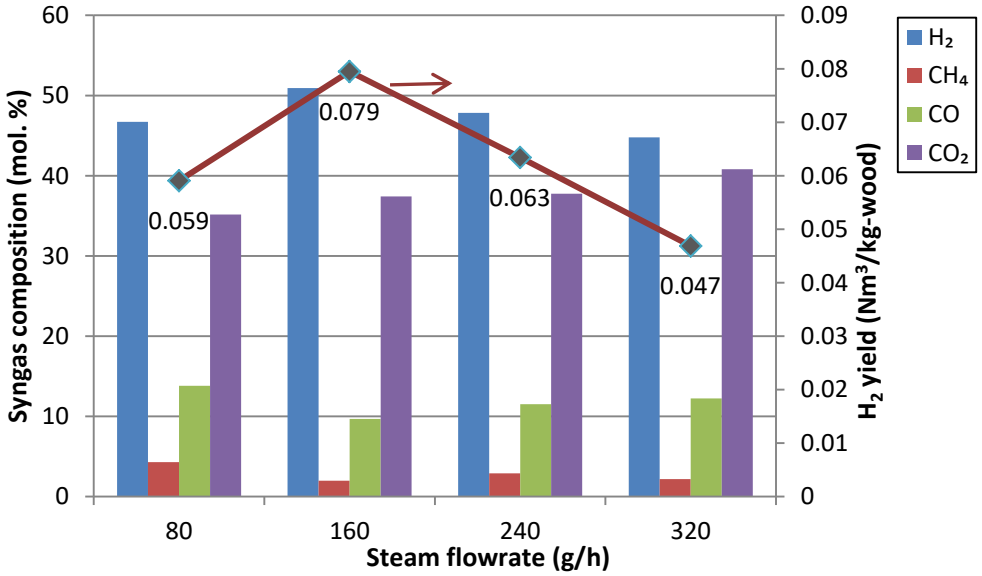

Figure 4. 6 Effect of steam flowrate on H_2 yield and syngas composition (CaO/wood = 0.2; temperature = 700 ^oC; reaction = 15 min)

In order to enhance H_2 production from steam catalytic gasification, the influence of steam flowrate is investigated. Four different steam flowrates of 80, 160, 240 and 320 g/h are studied at a CaO/wood ratio of 0.2 and a temperature of 700 ^oC. The syngas composition and H_2 yield are presented in **Figure 4. 6**. Results reveal that with an initial increase in steam flowrate from 80 to 160 g/h, the H_2 yield is remarkably increased from 0.059 to 0.079 Nm^3/kg of fed wood. However the H_2 yield drop to 0.063 and 0.047 Nm^3/kg of fed wood when the steam flowrate is further increased to 240 and 320 g/h, respectively; which corresponds to a decreased rate of 20% and 41% as compared with the peak value obtained at a steam flowrate of 160 g/h. Regarding the syngas composition, the H_2 concentration exhibits a similar trend of first increase and then decrease; the maximum H_2 content reaches 50.9% at a steam flowrate of 160 g/h. The evolution of CH_4 is completely at the opposite although in a relatively low concentration (ca. 4.3%-2.2%).

By increasing the amount of steam in the reactor, it should facilitate the steam reforming reactions (Eqs. (4.1)-(4.3)), which improves the H_2 yield and concentration in the syngas. It is also suggested that CaO reveals better catalytic performance with an adequate presence of steam. Manovic et al. [16] concluded that steam hydration would efficiently promote the carbonation reactivity of CaO, which would be helpful to further shift the thermodynamic equilibriums of water gas (Eq. (4.2)) and water-gas shift (Eq. (4.3)) reactions

towards the formation of H_2. Nevertheless when the steam flowrate exceeds 160 g/h, a declined trend of H_2 yield and concentration is observed. Li et al. [17] and Acharya et al. [11] also observed a decreased H_2 production at higher steam flowrates (H_2O/MSW mass ratio of 1.33-2.66 and H_2O/C mass ratio of 0.83-1.58 in their studies, respectively). This phenomenon could probably due to that at higher steam flowrate, the amount of steam is sufficient inside the furnace and is no longer the rate limiting step. Then the further increase in steam flowrate would not facilitate the reaction; and could result in a decrease of the available heat in the reactor by the absorption of excessive steam.

Table 4. 2 exhibits the product characteristics as a function of steam flowrate. Results indicate that the product distribution of syngas, tar and solid residue exceeds 100% due to the reaction with steam. With steam flowrate increasing from 80 to 160 g/h, the solid yield declines from 86.7% to 85.4%, which is explained by Paviet et al. [18] who hypothesized that a higher steam molar fraction has resulted in a lower diffusion resistance of the char. However, the production of solid residue turns to have a slight rise when the steam flowrate is further increased to 240 and 320 g/h, since the primary decomposition of char is inhibited at a lower reaction temperature. Similarly, the tar concentration reaches its minimum of 8.9 g/Nm^3 at a steam flowrate of 160 g/h; and then slightly increases to 9.6 g/Nm^3.

Table 4. 2 Effect of steam flowrate on gasification products distribution and characteristics (CaO/wood = 0.2; temperature = 700 °C; reaction = 15 min)

Steam flowrate (g/h)	80	160	240	320
Product distribution (wt. %)				
Syngas	24.80	29.93	26.35	22.15
Tar	7.99	4.90	5.12	5.17
Solid residue	86.68	85.36	86.13	86.59
Product characteristics				
Syngas yield (Nm^3/kg-wood)	0.126	0.156	0.133	0.105
Tar yield (g/Nm^3)	14.7	8.9	9.4	9.6
H_2/CO	3.41	5.30	4.24	3.73

The H_2/CO ratio shows an increasing trend, in agreement with the results of He et al. [5]. Maximum H_2/CO value of 5.30 is reached at a steam flowrate of 160 g/h, attributed to the gradually decreasing CO concentration as well as the increasing H_2 content. Regarding the high range of H_2/CO ratio obtained in this research, syngas could serve in chemical industry for ammonia synthesis or for fuel cell applications [19].

Figure 4. 7 plots the H/C and O/C atomic molar ratio of the syngas at different steam flowrates. It appears that the H/C atomic ratio ranges between 1.68 and 2.10, with the peaking value obtained at steam flowrate of 160 g/h. The O/C atomic ratio increases slightly from 1.57 to 1.68 mainly due to the increased amount of CO_2 produced. Compared with the H/C and O/C atomic molar ratio of the feedstock (1.37 and 0.66, respectively), it appears that the steam catalytic gasification is effective to increase those values due to the decomposition of hydrocarbon and the formation of H_2-rich gas [6].

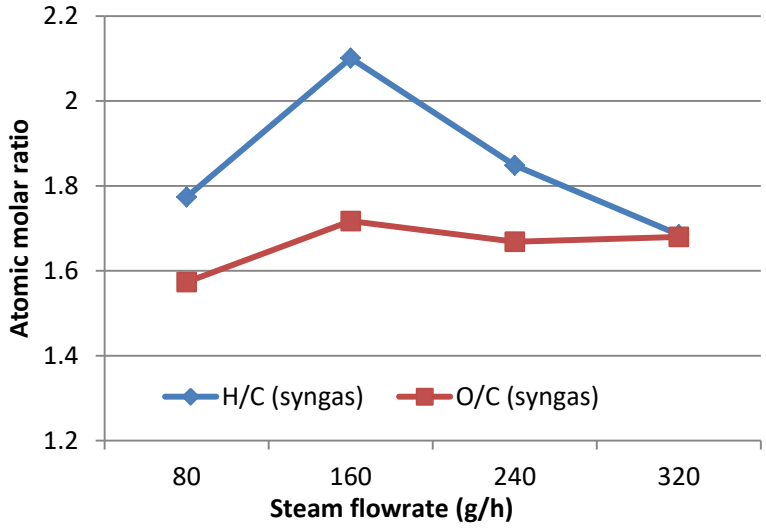

Figure 4. 7 Effect of steam flowrate on H/C and O/C atomic molar ratio of the syngas (CaO/wood = 0.2; temperature = 700 °C; reaction = 15 min)

4.3 Process optimization: selecting proper temperature

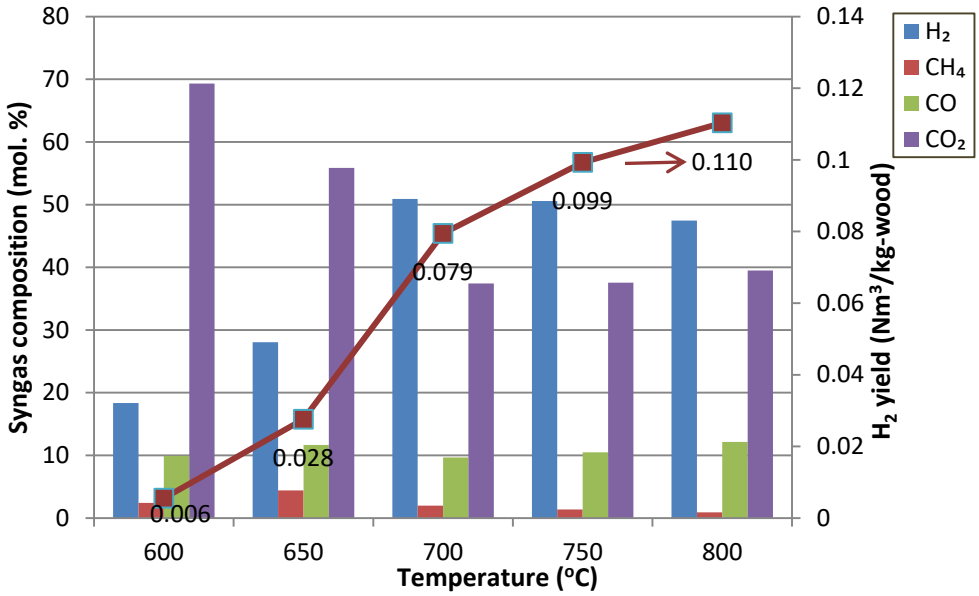

Figure 4. 8 Effect of temperature on H_2 yield and syngas composition (CaO/wood = 0.2; steam flowrate = 160 g/h; reaction = 15 min)

Based on the previous results, the next step involving the use of CaO as a catalyst is to focuse on process optimization. First, catalytic steam gasification under different temperatures is examined. **Figure 4. 8** illustrates the influence of reaction temperature on H_2 yield and syngas composition at a CaO/wood of 0.2 and a steam flowrate of 160 g/h. It is obvious that temperature has played a crucial role on the gasification process. With the increasing temperature, the H_2 yield and concentration in the syngas is significantly increased from 0.006 Nm^3/kg of wood and 18.3% at 600 ^oC to 0.079 Nm^3/kg of wood and 50.9% at 700 ^oC, respectively. According to Le Chatelier's principle, higher temperature provides more favorable conditions for the endothermic reactions such as the steam reforming reaction (Eq. (4.1)) and water gas reaction (Eq. (4.2)), resulting in an accelerated H_2 production and concentration output. This speculation could be evidenced by the increasing CO concentration with temperature. Meanwhile, it is found that with a temperature increase from 600 to 700 ^oC, CO_2 concentration drops remarkably from 69.3% to 37.4%, corresponding to a decreasing rate of 46%. The enhanced tar cracking reaction (Eq. (4.5)) at a higher temperature could be the second reason for the promoted H_2 production, which is effectively indicated by the decreased concentration of CH_4 in the syngas.

However, it is found that the H_2 concentration tends to decrease when the reaction temperature rises from 700 to 800 ^oC. This is accompanied by a gradually increasing CO_2

concentration to 39.5% at 800 °C. Previous studies have revealed that the adsorption ability of CaO catalyst is related to the reaction temperature and CO_2 equilibrium partial pressure, hence, the carbonation reaction and its reverse calcination reaction occurs under different thermodynamic limitations of the system [20-22]. Baker et al. [23] has presented the chemical equilibrium of the reaction as:

$$\log P_{CO_2}[atm] = 7.079 - 8308 / T[k] \quad (4.6)$$

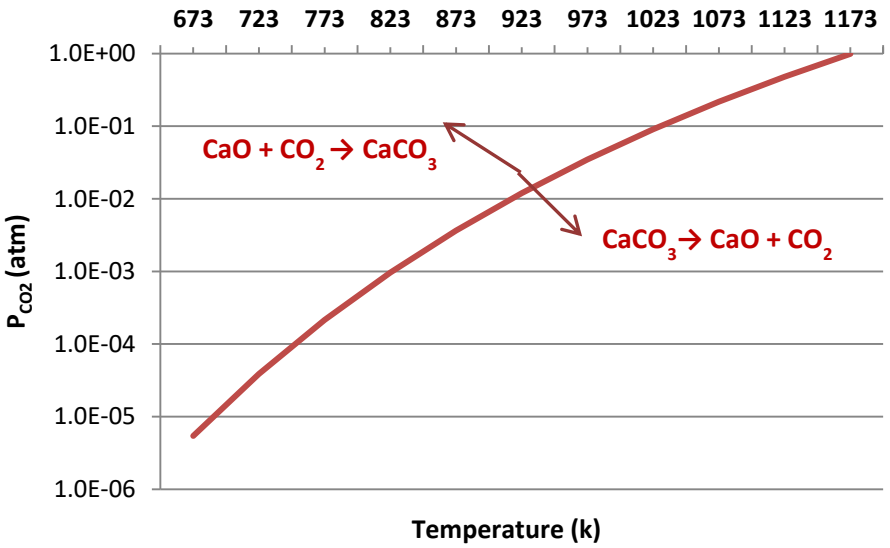

Figure 4. 9 CO_2 equilibrium partial pressure as a function of temperature for carbonation/calcination reactions

The equilibrium data are depicted in **Figure 4. 9** for a range of temperatures from 673 to 1173 K and for pressures up to 1 atm. For a given P_{CO2}, CaO carbonation takes place when the temperature is lower than the corresponding equilibrium value of this partial pressure. But if the temperature continuously increases and exceeds the equilibrium value, carbonation reaction is inhibited and $CaCO_3$ calcination reaction occurs. With regard to the present study, the average CO_2 concentration in the reactor is around 1-2%, corresponding to the $CaCO_3$ calcination temperature of ca. 650-700 °C. The theoretical calculation agrees well with the experimental results. When the temperature reaches 750 or 800 °C, the catalytic effect of CaO sorbent is unfavorable and little CO_2 is absorbed. As a consequence, H_2 concentration drops when the temperature is higher than 700 °C. H_2 yield keeps rise due to the tar cracking reaction (Eq. (4.5)); however, its increasing rate is declined owing to the weakening of water-gas shift reaction (Eq. (4.3)).

It is also worth to mention that by comparison, He et al. [6] reported an increase in H_2 yield and concentration when operating at 950 ^oC. The primary difference is due to the fact that their experimental apparatus is a fixed bed and the CO_2 concentration at 950 ^oC reaches 22%. However by using a fluidized bed, the inlet gas flow should be maintained at a higher level to guarantee the fluidizing condition. This would result in a dilution of the CO_2 in the syngas and subsequently, would reduce the CO_2 equilibrium partial pressure. Therefore, it could be concluded that the reaction temperature should be controlled at an adequate level, not only to achieve effective CO_2 adsorption by CaO, but also to adapt to different types of reactors.

Table 4. 3 Effect of the temperature on gasification products distribution and characteristics (CaO/wood = 0.2; steam flowrate = 160 g/h; reaction = 15 min)

Temperature (^oC)	600	650	700	750	800
Product distribution (wt. %)					
Syngas	9.01	25.92	29.93	39.23	50.29
Tar	7.97	6.92	4.90	3.57	3.49
Solid residue	95.74	91.59	85.36	84.32	82.20
Product characteristics					
Syngas yield (Nm^3/kg-wood)	0.030	0.098	0.156	0.196	0.232
Tar yield (g/Nm^3)	16.3	13.3	8.9	6.2	5.7
H_2/CO	1.87	2.45	5.30	4.86	3.98

The effect of temperature on gasification products characteristics is illustrated in **Table 4. 3**. The data indicates that with the temperature increasing from 600 to 800 ^oC, the syngas yield is raised about 8 times from 0.030 to 0.232 Nm^3/kg of wood, equal to an increased mass distribution percentage varying from 9.01% to 50.29%. The solid and tar yield decrease accordingly; the concentration of tar reaches its minimum of 5.7 g/Nm^3 at 800 ^oC. It is proven that more favorable thermal cracking and steam reforming reactions occur at higher temperatures, which then result in the accelerated secondary cracking reactions into the gas fraction. However, the H_2/CO ratio experiences first increase and then decrease, reaching an peak value of 5.30 at a temperature of 700 ^oC. It could be concluded that the reaction temperature should be balanced to an adequate level by considering both the CO_2 adsorption ability of CaO catalyst and the gasification performance. Regarding the data, the optimal operating temperature should be 700 ^oC so that the formation of $CaCO_3$ could be enhanced at the presence of CaO catalyst leading to an improved H_2 production.

4.4 Process optimization: comparison with non-catalyst high-temperature steam gasification

Considering the combined effects of catalyst loading and steam flowrate on increasing both the H_2 yield and concentration, it is worth investigating if catalytic steam gasification could be served as a potential approach to reduce the gasification temperature. To verify its effect, the results are compared with non-catalyst high-temperature steam gasification. **Table 4. 4** shows the products characteristics both for catalytic and non-catalytic steam gasification. Comparing the syngas composition, results show that using CaO as catalyst is effective for H_2 improvement. As depicted in **Figure 4. 10**, 20% CaO addition at 700 ^{o}C could generate as much H_2 content (ca. 50%) as a 900 ^{o}C gasification without catalyst. This value is higher than the one obtained for non-catalyst gasification at 800 ^{o}C; and obviously, any further increase in CaO proportion in the mixture will continue to raise the H_2 concentration. As a result, a much higher H_2/CO ratio could be obtained under catalytic gasification, which represents about 1.4-2 times more than the cases without catalyst. Meanwhile, results also indicate that the tar yield after adding the CaO catalyst could be declined significantly (**Figure 4. 11**), which would mainly be attributed to the greater activity of CaO on tar cracking. The tar yield after 20% CaO addition at 700 ^{o}C drops to 8.9 g/Nm^3, which is 39% lower than non-catalytic gasification at 900 ^{o}C (14.5 g/Nm^3).

Table 4. 4 Comparison syngas composition and products characteristics between catalytic and non-catalytic steam gasification [a]

Gasification condition	Syngas composition (mol. %)				H_2 yield	H_2/CO	Tar yield
	H_2	CH_4	CO	CO_2	(Nm^3/kg)		(g/Nm^3)
800 ^{o}C, non-catalyst	46.07	0.96	13.21	39.76	0.104	3.76	20.9
900 ^{o}C, non-catalyst	50.33	1.33	18.23	30.11	0.156	3.02	14.5
700 ^{o}C, CaO/wood = 0.2	50.92	1.98	9.68	37.42	0.079	5.30	8.9
700 ^{o}C, CaO/wood = 0.5	61.96	2.07	10.25	25.73	0.106	6.16	5.5
700 ^{o}C, CaO/wood = 1.0	64.20	2.56	11.64	21.60	0.120	5.99	3.2

[a] Catalytic steam gasification represents the working conditions under temperature = 700 ^{o}C, steam flowrate = 160 g/h while varying the CaO/wood mass ratio; while non-catalytic gasification is also conducted at steam flowrate = 160 g/h with varied temperatures.

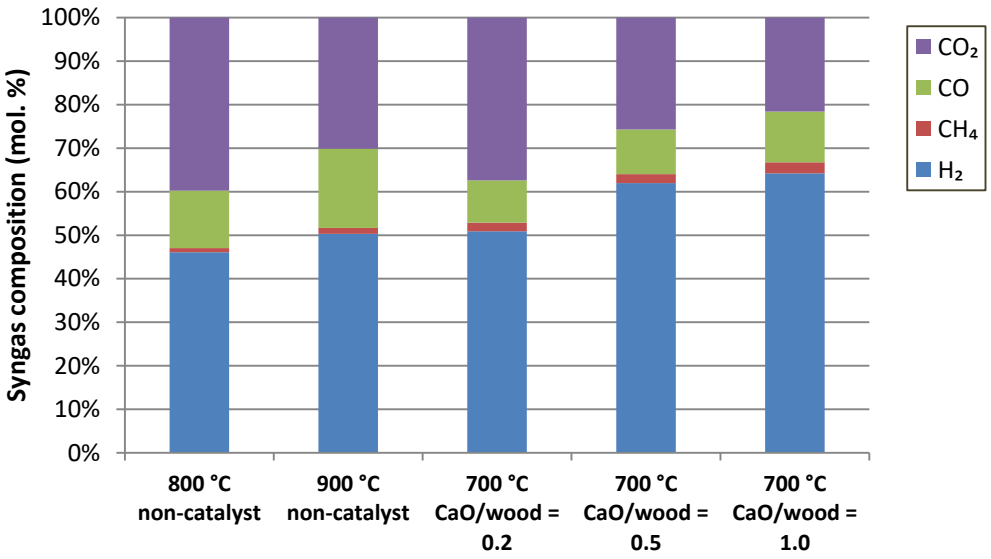

Figure 4. 10 Syngas composition of catalytic and non-catalytic steam gasification

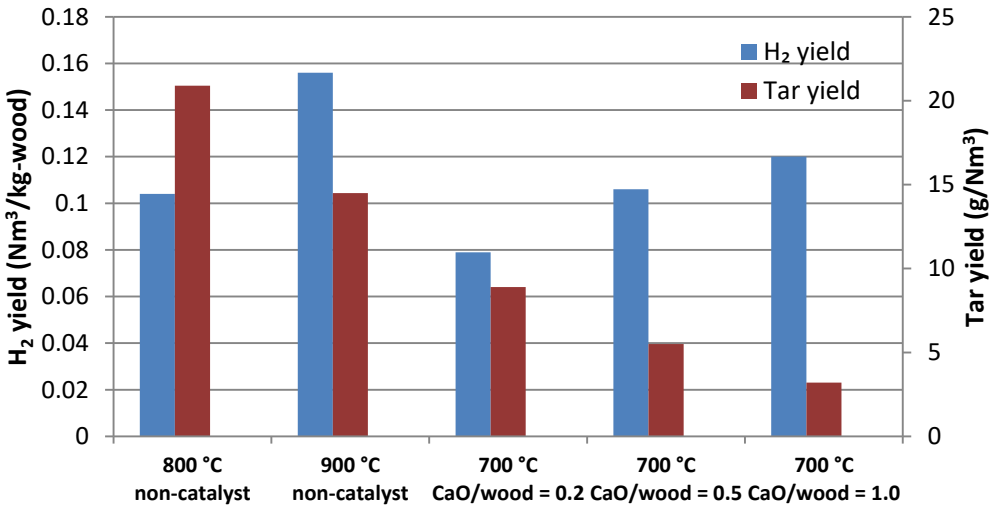

Figure 4. 11 H_2 and tar yield of catalytic and non-catalytic steam gasification

With regard to the H_2 yield, 50% CaO addition at 700 °C allows the production of H_2 yield of 0.106 m^3/kg-wood, which is equivalent to that gasified at 800 °C without catalyst (0.104 m^3/kg-wood). By further investigating syngas properties, it is found that the H_2 concentration could be improved by 16% with 50% CaO addition at 700 °C compared with a 800 °C non-catalyst gasification. Meanwhile, CO and CO_2 content decrease significantly following the addition of CaO, and the H_2/CO ratio is thus elevated to a higher level (6.16 at 50% CaO addition at 700 °C vs. 3.76 at 800 °C without catalyst). Therefore, it could be concluded that using CaO as catalyst is an effective approach to reduce the reaction temperature of steam gasification. 50% CaO addition could effectively reduce the reaction temperature of ca. 100 °C, which could be a measument showing benefits in energy saving.

4.5 Solid analysis

To study the performance of steam catalytic gasification, the solid residues obtained at different reaction conditions are examined with SEM, XRD and EDX analyses. **Figure 4. 12** shows the SEM photograph of the reacted char at CaO/wood = 0.0, steam flowrate = 160 g/h and temperature = 700 ^{o}C; with the EDX of selected points illustrated in **Table 4. 5**. As shown in **Figure 4. 12**, the bright particle represents the endogenous alkali matals in the wood, since no CaO catalyst has been added during this test. EDX analysis (point 1 in **Table 4. 5**) further reveals that the elements are mainly composed of Ca, Mg, S and K. On the other hand, point 2 and 3 in **Table 4. 5**, which represent the main skeleton of wood char, are mainly composed of C and O. Compared with the original char before tests (as shown in **Table 4. 1**), the atom ratio of C/O decreases, indicating that carbon is consumed during the gasification phase.

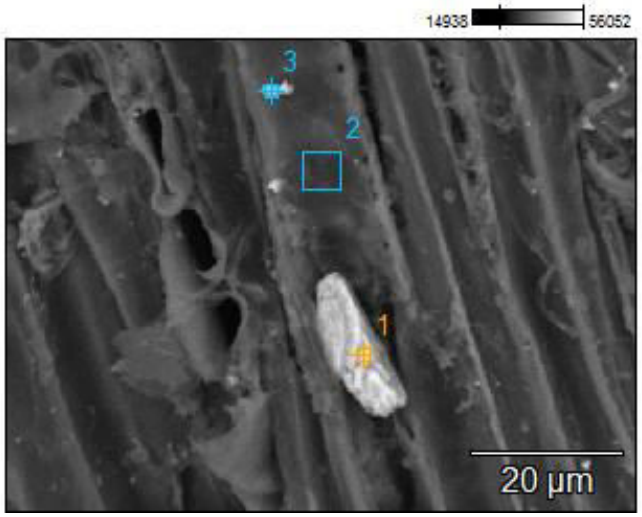

Figure 4. 12 SEM analysis of the solid products. Working condition: CaO/wood = 0.0; steam flowrate = 160 g/h; temperature = 700 ^{o}C

Table 4. 5 EDX analysis of the solid products. Working condition: CaO/wood = 0.0; steam flowrate = 160 g/h; temperature = 700 ^{o}C

	Elements (Atom %)						
	C	O	Ca	Mg	Si	S	K
Point 1	9.13	71.54	16.78	2.23	0.16	0.09	0.07
Point 2	75.74	19.83	2.05	0.46	0.33	-	1.02
Point 3	43.31	51.37	4.72	0.20	0.18	-	0.22

SEM and EDX results of the solid products at CaO/wood = 0.2, steam flowrate = 160 g/h and temperature = 700 ^{o}C are illustrated in **Figure 4. 13** and **Table 4. 6**, respectively. As shown in the SEM morphology, when CaO is added as catalyst, a large number of white particles are scattered on the surface of solid products. EDX result reveals that, the atom ratio of Ca : C : O is about 1 : 3.1 : 0.9, proving the generation of $CaCO_3$ as a result of CO_2 adsorption.

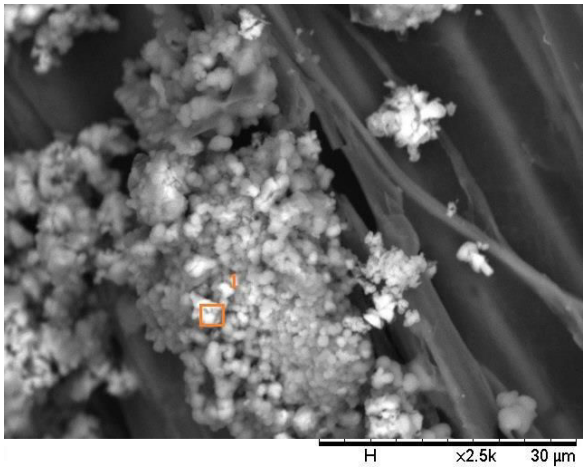

Figure 4. 13 SEM analysis of the solid products. Working condition: CaO/wood = 0.2; steam flowrate = 160 g/h; temperature = 700 ^{o}C

Table 4. 6 EDX analysis of the solid products. Working condition: CaO/wood = 0.2; steam flowrate = 160 g/h; temperature = 700 ^{o}C

Elements	C	O	Ca	Si
Atom, %	17.80	61.96	20.06	0.19

Besides, XRD analysis of the solid product is conducted at different CaO addition, steam flowrate and temperature. Results at varied CaO addition (**Figure 4. 14**) reveal that, the intensity of CaO and $CaCO_3$ increases with increasing CaO/wood mass ratios from 0.2 to 1.0. The result accords well with the experimental observation, which verifies the enhanced catalytic effect of CaO at higher loading quantity. On the contrary, the intensity of $CaCO_3$ decreases with increasing steam flowrate (**Figure 4. 15**); while the intensity of $Ca(OH)_2$ is raised. This again proves the speculation that the reactivity of CaO will decrease at excessive high steam flowrate due to the decreased available heat inside the reactor.

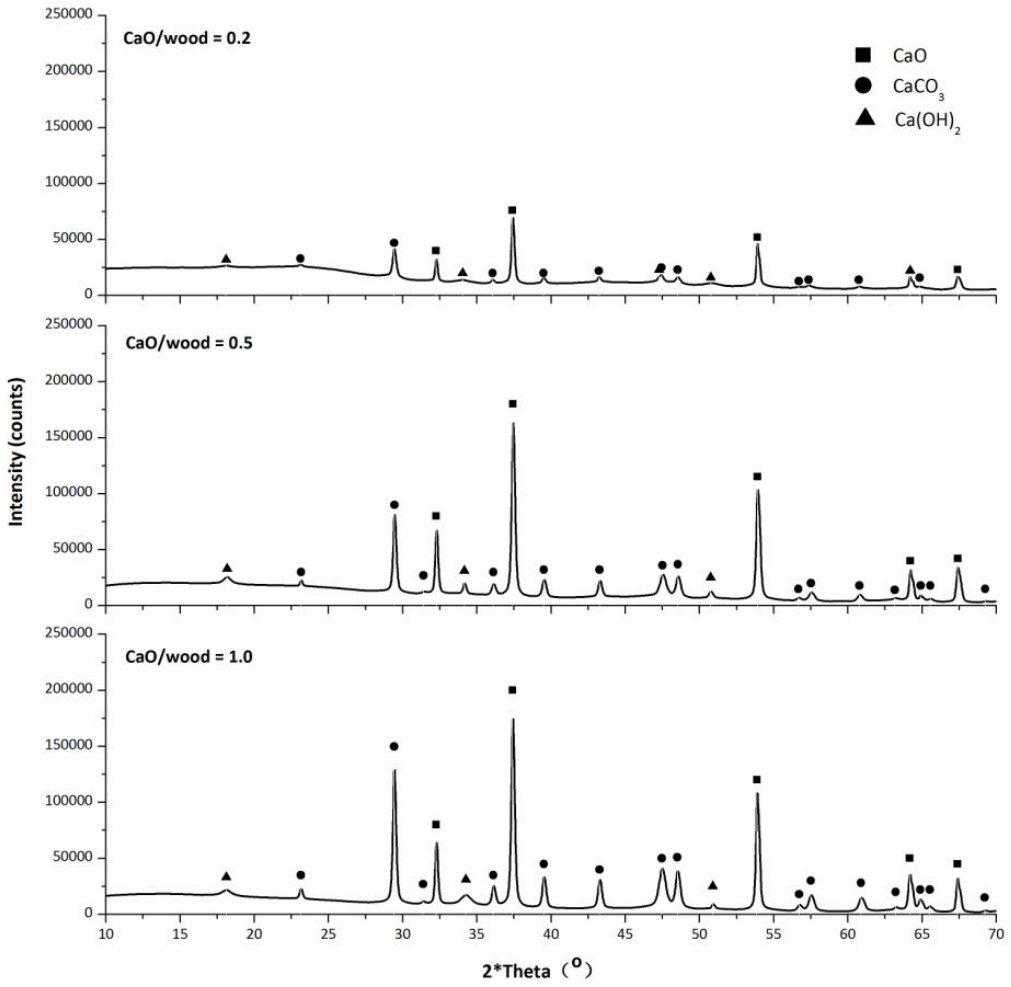

Figure 4. 14 XRD analysis of the solid products at varied CaO/wood mass ratios (steam flowrate = 160 g/h; temperature = 700 °C)

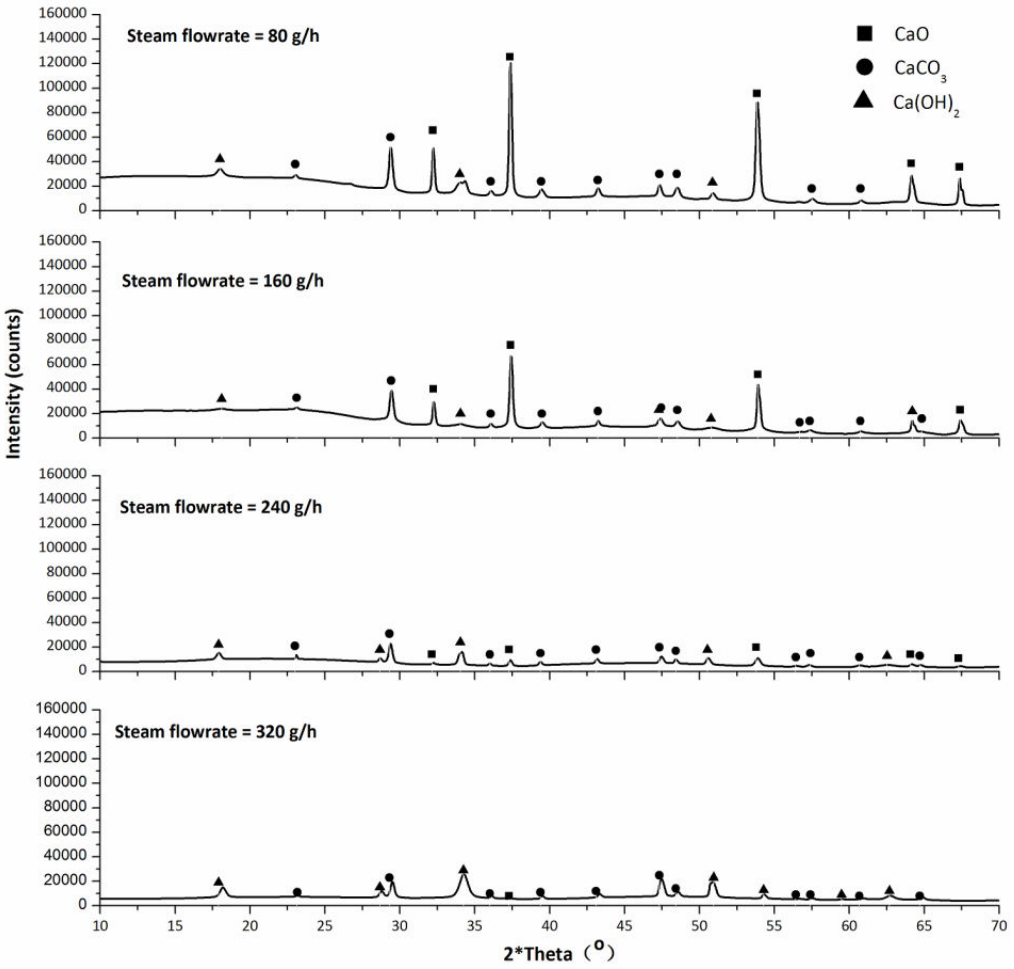

Figure 4. 15 XRD analysis of the solid products at varied steam flowrate (CaO/wood = 0.2; temperature = 700 °C)

With regard to the effect of temperature at 600/700/800 °C, the main peaks at 600 °C correspond to $CaCO_3$, CaO and $Ca(OH)_2$, with the intensity of $CaCO_3$ dominants over other compounds, as shown in **Figure 4. 16**. The diffraction peaks of $CaCO_3$ are significantly dropped when the temperature is increased to 700 °C, indicating that the decomposition of $CaCO_3$ starts to take place and less CO_2 is captured. It is also found that no $CaCO_3$ is observed at 800 °C; however, it is surely converted to CaO or $Ca(OH)_2$ in presence of steam, resulting in strong peaks for these compounds. Literature further revealed that CaO obtained at high temperature is of more perfect crystal phase, and this will cause a poor catalytic activity due to fewer crystal defects [24].

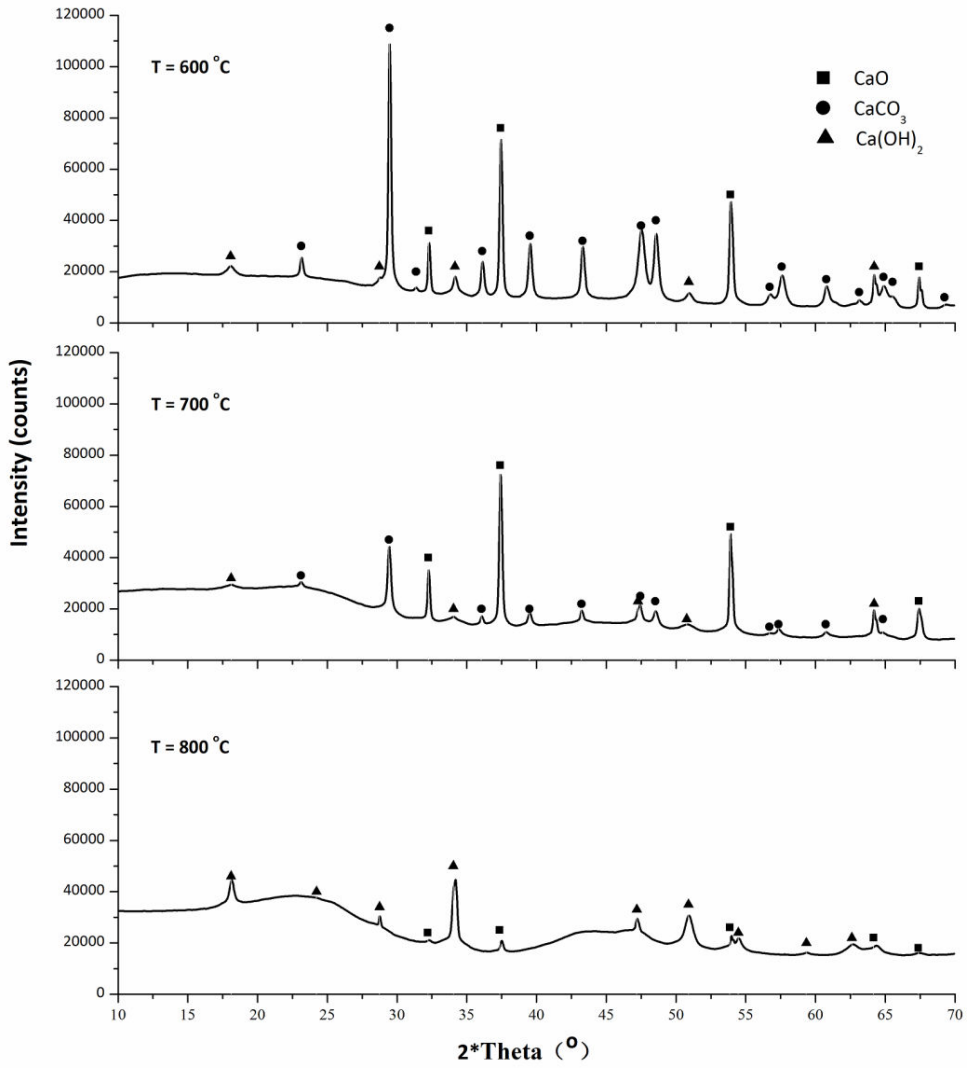

Figure 4. 16 XRD analysis of the solid products at 600/700/800 °C (CaO/wood = 0.2; steam flowrate = 160 g/h)

4.6 Summary of chapter

In this chapter, the catalytic effect of CaO on steam gasification is experimentally investigated in a fluidized bed reactor aiming at the optimization of the MSW pyro-gasification process. The purpose of the study is two-folds: (i) to identify the optimal working condition aiming at H_2-rich gas production; (ii) to investigate the potential of reducing the gasification temperature by using the catalyst. The influence of the CaO/wood mass ratio, steam flowrate and reaction temperature is studied; and the results are further compared with non-catalyst high-temperature gasification situations. The following conclusions have been drawn:

- The addition of CaO shows obvious catalytic effect allowing H_2 improvement in the syngas. Simultaneously increasing the mass ratio of CaO/wood from 0 to 1 could remarkably reduce the tar yield due to the enhanced reforming reactions.
- Increasing the steam flowrate is beneficial to shift the water gas shift reactions towards H_2 production. However, an excessive steam injection leads to an opposite effect, and a maximum H_2 concentration and yield is achieved at steam flowrate of 160 g/h.
- Higher temperature enhances the H_2 production and tar reduction due to the favored water gas shift and reforming reactions. The H_2 concentration is however decreased when temperature exceeds 700 ^{o}C. Therefore the optimal reaction temperature should be determined by a comprehensive consideration both of the gasification performance and the CaO carbonation ability according to the results obtained from XRD analysis.
- Compared with non-catalyst high-temperature gasification, 50% CaO addition at 700 ^{o}C could produce as much H_2 as from a non-catalyzed gasification at 800 ^{o}C. Meanwhile, a much higher H_2 concentration and H_2/CO ratio could be obtained from catalytic gasification. Therefore, it could be concluded that 50% CaO addition as catalyst at 700 ^{o}C is effective to reduce the steam gasification reaction temperature of ca. 100 ^{o}C.
- There is a strong potential for producing H_2-rich gas from MSW by catalytic steam gasification with inexpensive and abundant CaO as catalyst. The decreased gasification reaction temperature could also be a measurement showing benefits in energy saving.

Overall, the main findings from this chapter could be resumed in **Figure 4. 17**.

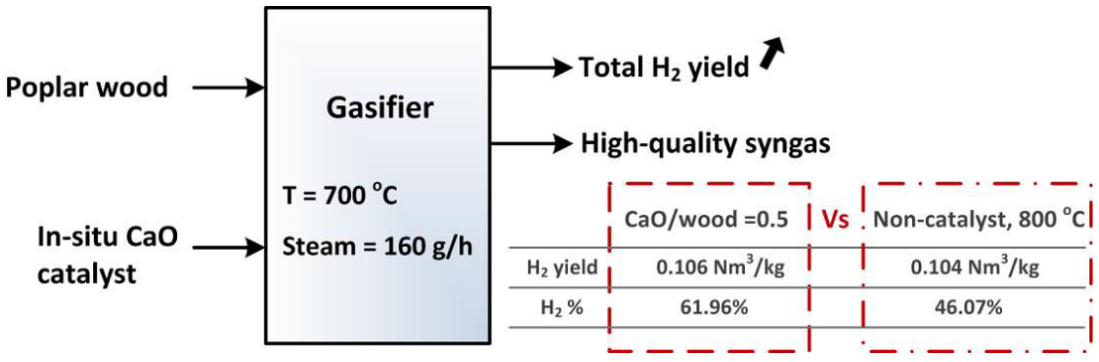

Figure 4. 17 Structure and main findings of Chapter 4

4.7 Bibliography

[1] Ewan BCR, Allen RWK. A figure of merit assessment of the routes to hydrogen. International Journal Of Hydrogen Energy. 2005;30:809-819.

[2] Min TJ, Yoshikawa K, Murakami K. Distributed gasification and power generation from solid wastes. Energy. 2005;30:2219-2228.

[3] Björklund Anna, Melaina Marc, Keoleian Gregory. Hydrogen as a transportation fuel produced from thermal gasification of municipal solid waste: an examination of two integrated technologies. International Journal Of Hydrogen Energy. 2001;26:1209-1221.

[4] Ni Meng, Leung Dennis YC, Leung Michael KH, Sumathy K. An overview of hydrogen production from biomass. Fuel Processing Technology. 2006;87:461-472.

[5] He Maoyun, Xiao Bo, Liu Shiming, Guo Xianjun, Luo Siyi, Xu Zhuanli, et al. Hydrogen-rich gas from catalytic steam gasification of municipal solid waste (MSW): influence of steam to MSW ratios and weight hourly space velocity on gas production and composition. International Journal Of Hydrogen Energy. 2009;34:2174-2183.

[6] He Maoyun, Hu Zhiquan, Xiao Bo, Li Jianfen, Guo Xianjun, Luo Siyi, et al. Hydrogen-rich gas from catalytic steam gasification of municipal solid waste (MSW): Influence of catalyst and temperature on yield and product composition. International Journal Of Hydrogen Energy. 2009;34:195-203.

[7] Hoornweg Daniel, Bhada-Tata Perinaz. What a waste: a global review of solid waste management. Washington DC: The World Bank; 2012.

[8] Shuai Chao, Hu Song, He Limo, Xiang Jun, Sun Lushi, Su Sheng, et al. The synergistic effect of $Ca(OH)_2$ on the process of lignite steam gasification to produce hydrogen-rich gas. International Journal Of Hydrogen Energy. 2014;39:15506-15516.

[9] Ohtsuka Yasuo, Asami Kenji. Steam gasification of coals with calcium hydroxide. Energy & Fuels. 1995;9:1038-1042.

[10] Dalai AK, Sasaoka E, Hikita H, Ferdous D. Catalytic gasification of sawdust derived from various biomass. Energy & Fuels. 2003;17:1456-1463.

[11] Acharya Bishnu, Dutta Animesh, Basu Prabir. An investigation into steam gasification of biomass for hydrogen enriched gas production in presence of CaO. International Journal Of Hydrogen Energy. 2010;35:1582-1589.

[12] Han Long, Wang Qinhui, Ma Qiang, Yu Chunjiang, Luo Zhongyang, Cen Kefa. Influence of CaO additives on wheat-straw pyrolysis as determined by TG-FTIR analysis. Journal Of Analytical And Applied Pyrolysis. 2010;88:199-206.

[13] Jordan C Andrea, Akay Galip. Effect of CaO on tar production and dew point depression

during gasification of fuel cane bagasse in a novel downdraft gasifier. Fuel Processing Technology. 2013;106:654-660.

[14] Udomsirichakorn Jakkapong, Basu Prabir, Salam P Abdul, Acharya Bishnu. Effect of CaO on tar reforming to hydrogen-enriched gas with in-process CO_2 capture in a bubbling fluidized bed biomass steam gasifier. International Journal Of Hydrogen Energy. 2013;38:14495-14504.

[15] Arena Umberto. Process and technological aspects of municipal solid waste gasification. A review. Waste Management. 2012;32:625-639.

[16] Manovic Vasilije, Lu Dennis, Anthony Edward J. Steam hydration of sorbents from a dual fluidized bed CO_2 looping cycle reactor. Fuel. 2008;87:3344-3352.

[17] Li Jianfen, Liao Shiyan, Dan Weiyi, Jia Kuile, Zhou Xiaorong. Experimental study on catalytic steam gasification of municipal solid waste for bioenergy production in a combined fixed bed reactor. Biomass & Bioenergy. 2012;46:174-180.

[18] Paviet Frédéric, Bals Olivier, Antonini Gérard. The effects of diffusional resistance on wood char gasification. Process Safety And Environmental Protection. 2008;86:131-140.

[19] De Filippis Paolo, Borgianni Carlo, Paolucci Martino, Pochetti Fausto. Prediction of syngas quality for two-stage gasification of selected waste feedstocks. Waste Management. 2004;24:633-639.

[20] Florin Nicholas H, Harris Andrew T. Enhanced hydrogen production from biomass with in situ carbon dioxide capture using calcium oxide sorbents. Chemical Engineering Science. 2008;63:287-316.

[21] Florin Nicholas H, Harris Andrew T. Hydrogen production from biomass coupled with carbon dioxide capture: the implications of thermodynamic equilibrium. International Journal Of Hydrogen Energy. 2007;32:4119-4134.

[22] Blamey J, Anthony EJ, Wang J, Fennell PS. The calcium looping cycle for large-scale CO_2 capture. Progress In Energy And Combustion Science. 2010;36:260-279.

[23] Baker EH. The calcium oxide–carbon dioxide system in the pressure range 1—300 atmospheres. Journal of the Chemical Society. 1962:464-470.

[24] Feng Bo, Bhatia Suresh K, Barry John C. Variation of the crystalline structure of coal char during gasification. Energy & Fuels. 2003;17:744-754.

Chapter 5

Investigation CaO Catalyst De-activation and Re-generation during Carbonation-calcination Looping Cycles

5.1 Introduction

Results from **Chapter 4** have revealed that CaO exhibits a strong potential to be served as an in-situ catalyst for MSW pyro-gasification. Accordingly, a gasification-based catalyst recycling system is designed, aiming at achieving CaO recycling to facilitate its industrial application, as depicted in **Figure 5. 1**.

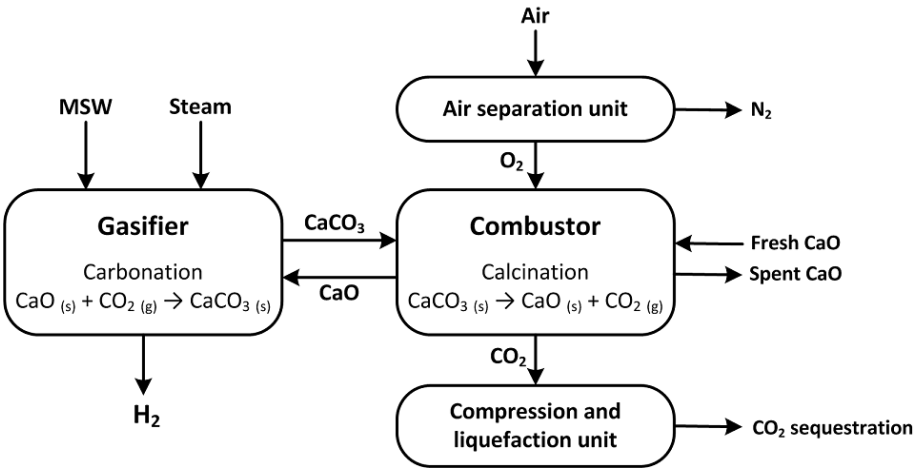

Figure 5. 1 Design of the gasification-based CaO catalyst recycling system

The principle of the system is based on the concept of carbonation/calcination looping [1, 2]. CaO is repeatedly cycled between two reactors via the reversible carbonation reaction

according to Eq. (5.1). In the gasifier, catalytic gasification takes place, where CO_2 is captured by CaO and converted to $CaCO_3$ hence producing H_2-rich syngas. The used catalyst, consisting mainly of $CaCO_3$, is then conveyed to the secondary reactor (combustor), where calcination reaction occurs and the formed CaO is fed back to the gasifier. In the combustion chamber, O_2 could be applied as the oxidant instead of air, so that the flue gas released from the calcinator consists of pure CO_2, which is suitable for sequestration as carbon capture and storage (CCS) technology. This cycle is continued and spent, unreactive CaO is continuously replaced by fresh, reactive sorbent.

$$CaO + CO_2 \rightarrow CaCO_3 + 178\,kJ/mol \tag{5.1}$$

This proposed system provides a viable approach for the recycling and re-generation of CaO catalyst, which could serve as potential optimization of catalytic pyro-gasification in light of industrial application. However, the most thoroughly issue resulting from the use of CaO is the loss of catalyst reactivity over a number of cycles of reaction with CO_2. **Chapter 1** has indicated some possible paths for catalyst decay; with several recent researches showed that sintering accompanied with the decrease of the sorbent surface area, may become important contributors for CaO de-activation [3-6].

Regarding the fact, investigation of the CaO catalyst reactivity during a series of carbonation/calcination cycles is essential. The aim of the study is two-folds, to reduce the reactivity decay rate through process parameters optimization, as well as to boost the catalyst reactivity via re-generation. It is expected that, in-depth examination of the catalyst reactivity could be helpful for a better design of the MSW pyro-gasification process towards a more effective and cleaner industrial-scale syngas production route. Accordingly, the structure of this chapter is presented as follows. The mechanism and kinetics of CaO de-activation is discussed in **Section 5.2**. Based on the results, operating variables with regard to CaO reactivity and potential re-generation method are proposed and tested, which are presented in **Section 5.3**. CaO powder is used as the feedstock. The experiments are conducted in two types of reactors: a TGA is used to observe the weight variation characteristics of CaO during carbonation/calcination cycles; while samples produced from a fluidized bed is used for solid analysis such as morphology and specific surface area. Detailed feedstock and experimental conditions have been described in detail in **Chapter 2**, and the main findings are presented as follows.

5.2 Mechanism and kinetics of CaO de-activation

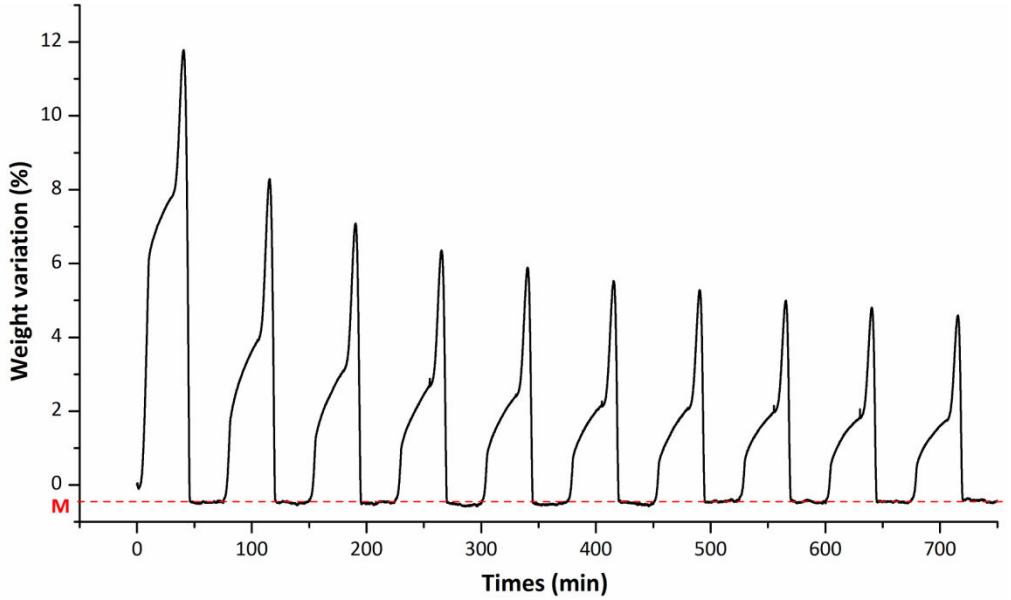

Figure 5. 2 10 repeated carbonation/calcination cycles of CaO in TGA experiment. Experimental condition: calcination at 900 ^{o}C for 10 min; carbonation at 550 ^{o}C and 20 vol. % CO_2 for 30 min

Figure 5. 2 shows the weight variation of CaO during carbonation/calcination cycles in a TGA. By checking the mass of the CaO catalyst (represented by line M in **Figure 5. 2**), it is observed that the final mass after cyclic carbonation/calcination reaction is equal to its initial value, indicating that there is no mass loss of the sample during the cyclic test. However, whilst the mass of CaO after each calcination process remains almost constant, the mass change upon carbonation process is reduced dramatically with the increasing number of cycles. The maximum weight variation reaches approximately 12% from the first carbonation cycle, however that value after 10 carbonation/calcination cycles is degraded to less than 5%. The finding infers that the CO_2 adsorption capacity of the CaO catalyst is reduced, meaning that its reactivity decays over long series of reaction with CO_2.

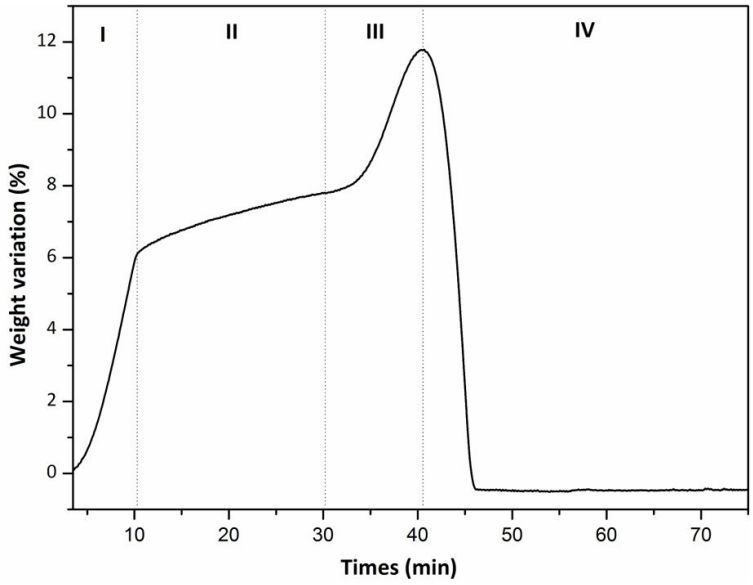

Figure 5. 3 1st carbonation/calcination cycle of CaO in TGA experiment: I, fast initial carbonation period; II, slow carbonation period; III, temperature programming stage to the pre-set calcination temperature; IV, fast calcination period

With regard to each cycle, the carbonation/calcination process could be divided into three regions (**Figure 5. 3**): the fast initial carbonation period (I, up to 10 min), the slow carbonation period (II, 10-30 min; before the temperature is increased to calcination temperature in III), and the fast calcination period (IV, up to completion). According to reaction kinetics, the fast initial carbonation period (I) is a kinetic-control stage, where the process is controlled by the reaction between CaO and CO_2. The reaction product is $CaCO_3$, which occupies a higher molar volume (36.9 cm^3/g) than CaO (16.9 cm^3/g) [7]. As a result, a product layer of $CaCO_3$ will be formed with the reaction progress on the surface of CaO and impedes CO_2 transport. The carbonation reaction then follows a diffusion-control period, i.e., slow carbonation period (II), which proceeds much slower and is governed by the diffusion of CO_2 through the built-up compact layer of $CaCO_3$. The following calcination period (IV) proceeds fast, and it has been reported by Barker et al. [8] that, complete calcination could be rapidly achieved in less than 1 min. Dissociation of the $CaCO_3$ proceeds gradually from the outer surface of the particle inward, and a porous layer of CaO, remains.

According to literature, the loss in reactivity of the CaO catalyst could be attributed to numerous factors. To better understand its degradation mechanism, several experiments are designed, including long series of carbonation/calcination at different number of cycles, as well as high temperature calcination. The sample definition and test conditions are listed in **Table 5. 1**, and their properties are measured both by SEM and BET analysis.

Table 5. 1 Test definition and conditions conducted in a fluidized bed

No.	Sample definition	Test conditions	Research aim
0#	Original CaO	-	-
1#	Carbonation/calcination for 5 cycles	Carbonation: 650 ^{o}C, 20% CO_2, 30 min; calcination: 900 ^{o}C, 100% N_2, 10 min; repeated for 5/10/20 cycles	Effect of long series cycles on CaO reactivity
2#	Carbonation/calcination for 10 cycles		
3#	Carbonation/calcination for 20 cycles		
4#	High temperature and long reaction time calcination	Carbonation: 650 ^{o}C, 20% CO_2, 30 min; calcination: 1000 ^{o}C, 100% N_2, 2 hours; repeated for only 1 cycle	Effect of sintering on CaO reactivity

The particle morphology of the different samples is illustrated in **Figure 5. 4**. The original CaO occupies different sizes. There are some variations in the structure showing irregular shapes for particles; their active surfaces are quite rough. The surface of particles cycled 5 times (1#) appears to be smoother. Some particles are aggregated, resulting in an increase of the particle size. The transition from the rough surface to the smooth surface indicates a loss of fine structure for the CaO. If the cycled times are further increased, the size of particle keeps on increasing. As seen in samples 2# and 3#, small pores are amalgamated to form larger pores, it is clear that there is a loss in the total porosity of the CaO particles. The results infer that, one reason for the drop-off in CaO reactivity could be attributed to the closure of small pores during carbonation-calcination cycles that do not reopen [9]. The results accord well with the CaO degradation mechanism proposed by Lysikov et al. [10]. As illustrated by the schematic diagram in **Figure 5. 5**, the newly formed CaO, upon the first calcination process, is porous and highly reactive. Over the course of several recarbonation-decomposition cycles, the necks between adjacent CaO grains thicken and reinforce, which leads to pore blocking in the CaO particles leading to the incomplete carbonation. The amount of unreacted CaO increases from cycle to cycle, leading to the formation of a rigid unreactive outer layer of CaO.

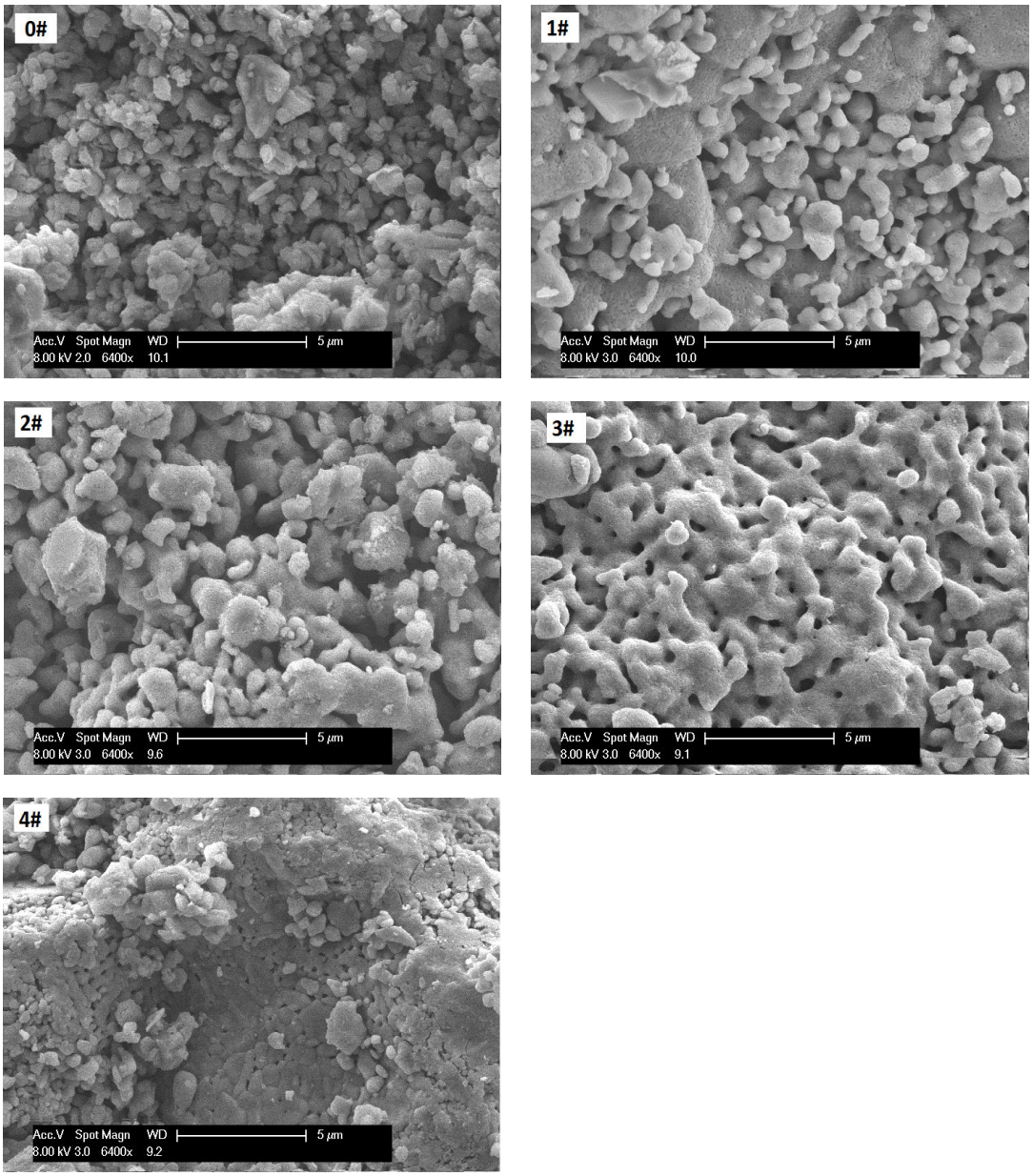

Figure 5. 4 SEM images of CaO after specified carbonation/calcination cycles: 0#, original CaO; 1#, CaO after 5 cycles; 2#, CaO after 10 cycles; 3#, CaO after 20 cycles; 4#, CaO after 1 cycle at high temperature and long time calcination

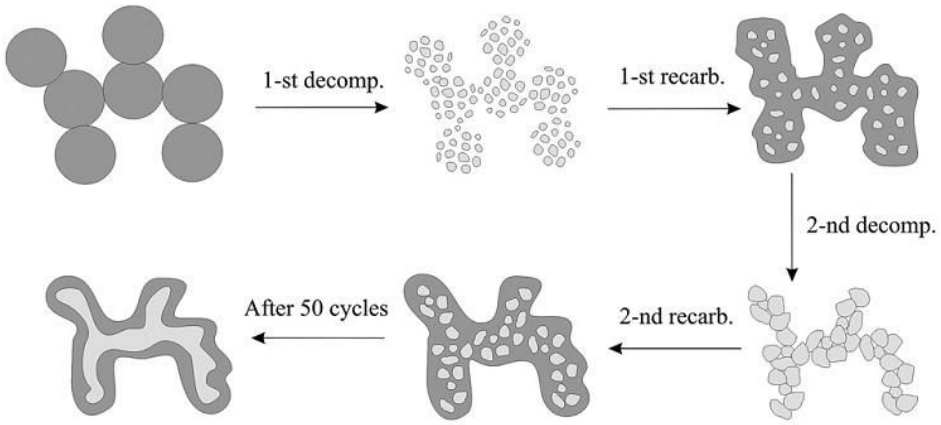

Figure 5. 5 Mechanism for the textural transformation of CaO during carbonation/calcination cycles. The CaO phase is shown by light grey, and $CaCO_3$ is shaded dark grey [10]

On the other hand, sintering could be regarded as another important mechanism for the de-activation of CaO. Sample 4# is a typical example of this phenomenon. As clearly seen from the SEM images in **Figure 5. 4**, the CaO particles are aggregated to form a relatively large and flat surface. No visible obvious pores can be found, even if the carbonation/calcination process has cycled only once. The results indicate that sintering is sensitive to higher temperature and duration of calcination, which is set at 1000 ^{o}C and 2 hours under this experimental condition, respectively. Actually, the mechanism of sintering is often accompanied with changes in pore shape and pore shrinkage, which is proven to be occurring primarily during calcination process [11]. Research by Borgward et al. [12] reveals that calcination temperatures above 900 ^{o}C will cause a remarkable increase of sintering. This temperature would even shift to a lower value if the reactions are conducted under a higher partial pressure of CO_2 or H_2O. As expected, more highly sintering environment will lead to sharp decrease in surface area and porosity of CaO particles, resulting in a faster rate of CaO de-activation.

Table 5. 2 Specific surface area and porosity of the samples by BET analysis

	0#	1#	2#	3#	4#
S_{BET}, m^2/g	2.37	3.24	3.03	2.09	2.02
Porosity, %	0.00	7.33	5.78	4.88	0.00

The specific surface area and porosity of different samples is shown in **Table 5. 2**. The 0.00% value reported for the porosity of sample 0# and 4# is to be understood as non detectable with the quipment used. The results are well in accordance with the speculated CaO de-activation mechanisms. Sample 1# exhibits a higher specific surface area than the original sample 0#. It is also accompanied by the increasing of porosity from 0% to 7.33%, which indicates that pores are created upon CO_2 release during calcination, since CaO derived from $CaCO_3$ has a much faster initial reaction rate than crystalline CaO [8]. The surface area and porosity of CaO continuously decreases from sample 1# to 3# when the number of carbonation/calcination cycles is increased. The phenomenon is in agreement with the SEM pictures, proving that the de-activation of CaO might be due to the closure of small pore channels. The specific surface area of sample 4# is the lowest among the samples. For the latter, a porosity of 0.00% is also observed, which indicates the significant role of sintering in determining the CaO carrying capacity.

Sun et al. [11] have further proposed the effect of pore size on the reactivity of CaO. According to their research, the pores are divided into two types: Type 1 as the smaller pores (< 220 nm) and Type 2 as the larger ones (> 220 nm). During the calcination process, the calcination of $CaCO_3$ will create Type 1 pores; while Type 2 pores are affected by sintering together with Type 1 pores. Therefore, the surface area of Type 1 pores is seen to decrease upon several carbonation/calcination cycles, while the one associated with Type 2 pores increases. As a result, the pores size of CaO exhibits increasing trend upon cycling, causing the loss in reactivity of CaO.

To summarize, there are two main determining factors affecting the de-activation of CaO: the clogging of small pores during carbonation, and the sintering mechanism occurring during calcination. To better utilize CaO as in-bed gasifier catalyst and for the design of carbonation-calcination looping cycle, the process condition should be optimized to ensure its high reactivity upon continual cycling.

5.3 Study operating variables on CaO reactivity and re-generation

As discussed in **Section 5.2**, de-activation is a considerable problem for the long-term use of CaO as catalyst. To improve its performance upon cycling, two options are feasible, either by alteration of the process conditions, or by sorbent enhancement. It has been

proven that during industrial application of CaO using various feedstock and reactors, loss in CaO reactivity can be affected by a number of factors, such as: pressure, temperature, CO_2 concentration of carbonation/calcination process [13-15]; competing sulphation and sulphidation reactions; presence of steam; and ash fouling [16]. Among those parameters, the carbonation/calcination temperature could be a critical design parameter for optimizing catalytic gasification reaction, since it directly relates to the determination of gasification reaction temperature and the subsequent downstream combustion stage. As a consequence, their effects on the rate of CaO decay during multicycle carbonation/calcination are worth to be investigated.

On the other hand, some potential options are currently proven viable to re-activate the CaO sorbent. Thermal pretreatment and preactivation has been investigated [10, 17]; results indicate that treating sorbent at high temperature with N_2 could improve the long-term reactivity of CaO. Sorbent synthesis is also developed, which includes $CaCO_3$ precipitation to enhance the reactive surface area [18, 19]; and CaO dispersal with inert porous matrix to improve mechanical stability [20]. Other re-generation methods include natural limestone doping and chemical pretreatment; however steam hydration is likely to be the most feasible approach considering the superior availability of steam and convenience of hydration or steam addition [21]. It has been proven that steam hydration after calcination under low temperature could pose a positive effect to modify the pore structure of the spent CaO so as to recover its CO_2 carrying capacity. Hence, more explorations become essential in order to better reveal the influence of steam hydration on the re-generation performance of CaO.

Accordingly, the effects of carbonation/calcination temperature and steam hydration are studied to optimize the carbonation-calcination process parameters. The effect of temperature is examined using TGA. Carbonation is studied at a temperature series of 550, 650 and 750 ^{o}C; while calcination temperature of 800, 900 and 950 ^{o}C is considered. The carbonation process is conducted in a 20 vol.% CO_2 concentration for 30 min, while calcination is performed under N_2 atmosphere for 10 min. The number of carbonation/calcination cycles is set at 10. The CaO activity is measured by carbonation conversion efficiency (CCE, %), which is an indicator of CO_2 capture capacity as defined by Eq. (5.2):

$$CCE_N = \frac{m_N - m_0}{m_0} \frac{\bar{M}_{CaO}}{\bar{M}_{CO_2}} \times 100\% \qquad (5.2)$$

Where, N represents the N^{th} number of cycle; m_N and m_0 stands for the mass of the sample after Nth carbonation process and the initial sample mass, respectively; $\bar{M}_{CaO}$ and $\bar{M}_{CO2}$ is the molar mass of CaO and CO_2, respectively.

The effect of steam hydration is studied in the fluidized bed and the particle morphology and specific surface area is detected by SEM and BET analysis. Carbonation is conducted at 650 °C, using a 20 vol. % CO_2 for 30 min, while calcination is proceessed at 900 °C, 100 vol. % N_2 for 10 min. The carbonation-calcination cycle is repeated 5 times, with steam hydration conducted after each cycle. Detailed descriptions of the experimental conditions are presented in **Chapter 2**.

5.3.1 Effect of carbonation temperature

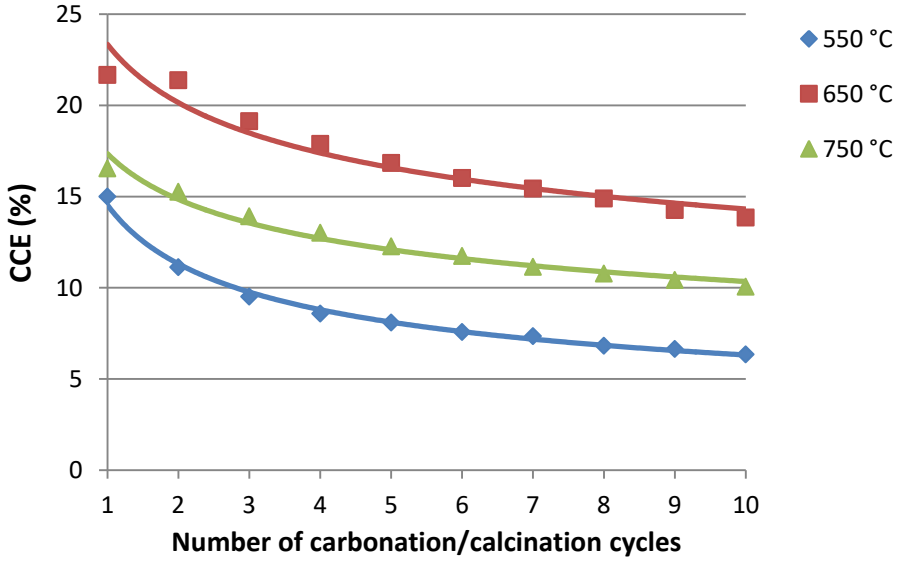

Figure 5. 6 Effect of carbonation temperature on carbonation conversion efficiency (%) during 10 repeated carbonation/calcination cycles. Experimental condition: calcination at temperature 900 °C for 10 min; carbonation at CO_2 concentration of 20 vol.% for 30 min

Carbonation conversion efficiency during 10 cycles of carbonation/calcination process under different carbonation temperature is plotted in **Figure 5. 6**, which is conducted under a constant calcination temperature of 900 °C. Result at 550 °C represents the same experimental run as that performed in **Figure 5. 2**. For different temperatures, all values of CCE exhibit a continuous decay trend with the increasing number of cycles. The maximum conversion capacity appears at first cycle (15.0-21.7%), while that value is reduced to

6.4-13.9% at the 10th cycle. The results are consistent with the CaO de-activation mechanisms as discussed above. The CO_2 capture capacity of CaO deactivates significantly with the increasing series of cycles, mainly caused by sintering accompanied with the decrease of the catalyst surface area as well as the loss of porosity [3, 6].

Among the analyzed carbonation temperatures, 650 ^oC exhibits the highest CCE value. The lower CCE value at 550 ^oC could be attributed to kinetic limitation. According to the chemical carbonation/calcination reaction equilibrium as discussed in **Chapter 4**, the equilibrium value for calcination temperature under an experimental CO_2 partial pressure of 20% is approximately 795 ^oC. At temperature lower than the equilibrium value, increasing the reaction temperature is effective for CaO carbonation, which could be attributed to the increased CO_2 capture capacity at 650 ^oC. Conversely, increase temperature higher than 750 ^oC causes a drop in CaO conversion efficiency. It could be speculated that, since the sintering temperature of $CaCO_3$ attains at 527 ^oC [13], the sintered $CaCO_3$ might grow over the mouths of pores and seal them off. This mechanism is remarkably enhanced at higher temperature and will thus result in the deterioration of CaO.

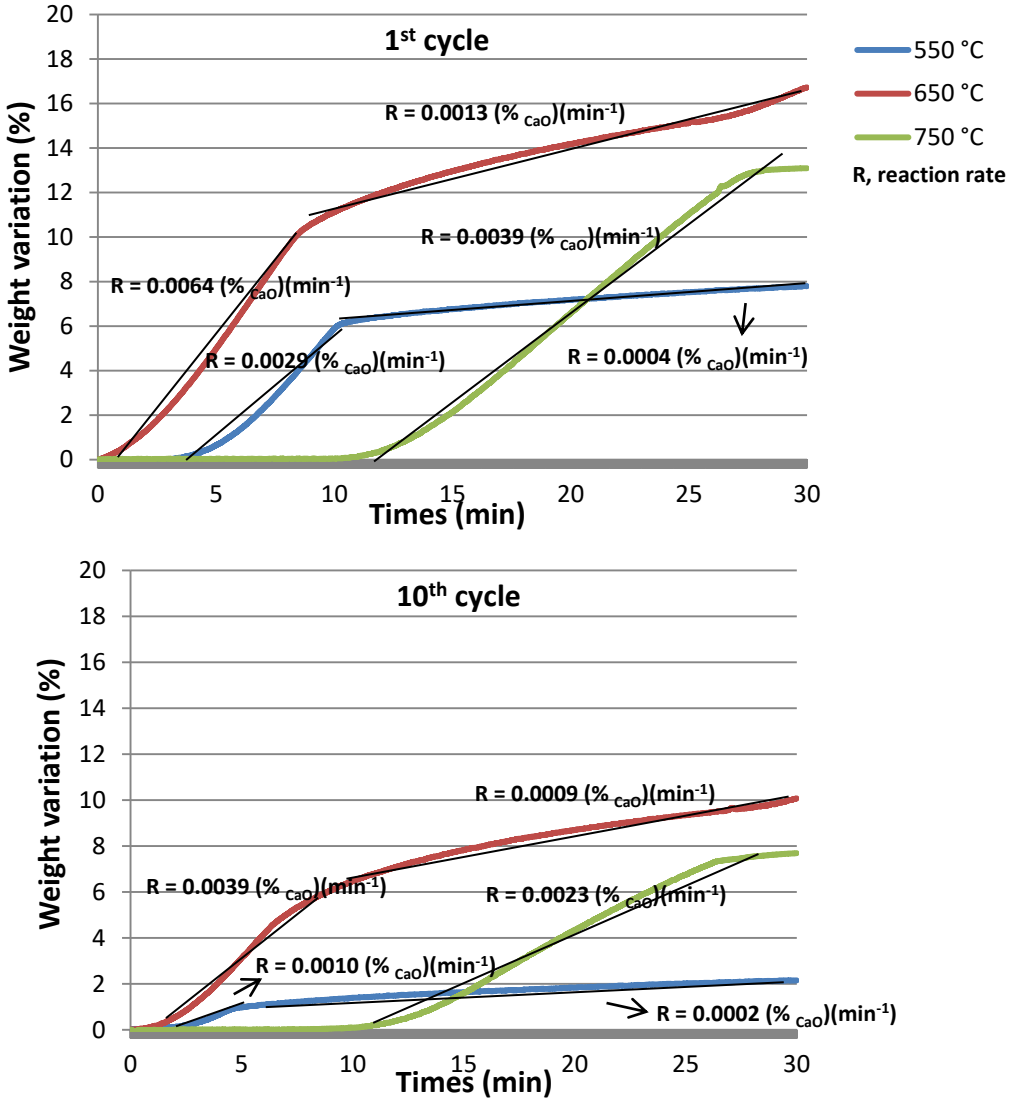

Figure 5. 7 Comparison 1st and 10th carbonation process as a function of time under different carbonation temperatures. Experimental condition: calcination at temperature 900 °C for 10 min; carbonation at 20 vol.% CO_2 for 30 min

Figure 5. 7 shows the comparison of CaO weight variation and reaction rate during the carbonation process between the 1st and 10th cycle. It is found that, at 550 and 650 °C, kinetic-control region contribute to the majority of CaO conversion. The reaction rate under fast initial carbonation period is 5-7 times higher than that of slow carbonation period, proving that the reaction is largely controlled by the reaction between CaO and CO_2. The reaction rate at 650 °C is much higher than the one at 550 °C (0.0064 vs. 0.0029 $\%_{CaO}$/min). However, no obvious conversion occurs during the kinetic-control phase under temperature of 750 °C, carbonation seems to be retarded after 10 min that mostly belongs to the diffusion-control stage. This verifies the decreased reactivity of CaO at high temperature, which may cause significant decreased contact frequency between CaO and CO_2. With regard

to the 10th cycle, the CO_2 capture capacity of CaO decreases to a large extent. Especially, the boundary between the kinetic-control phase and diffusion-control stage becomes not as clear as for the 1st cycle. This is accompanied by a decreased reaction rate both for kinetic-control and diffusion-control phases, which again proves a reduction in CaO reactivity after a series of cycles.

Therefore, it could be concluded that 650 ^{o}C is the most suitable carbonation temperature under the present experimental conditions. If further applied for industrial utilization, the carbonation time could be shorted within the fast carbonation stage considering conversion efficiency and economic factors.

5.3.2 Effect of calcination temperature

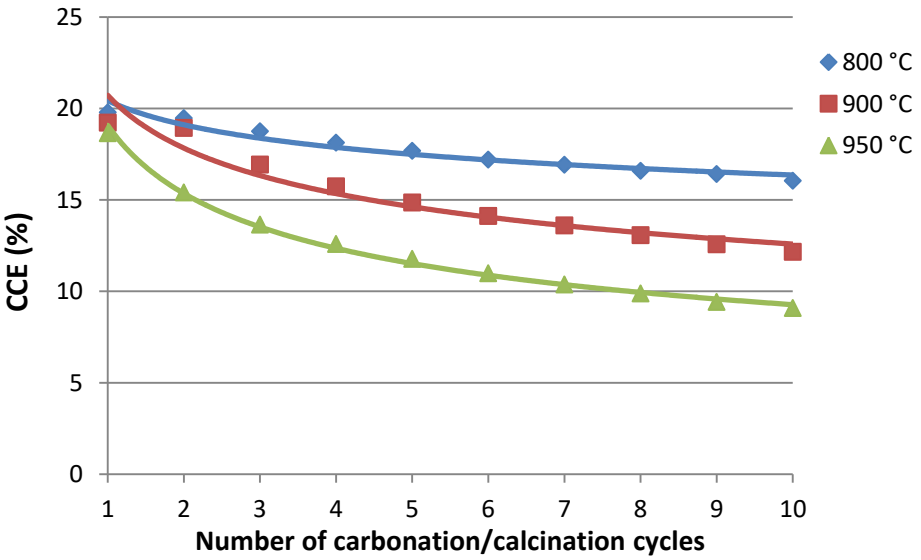

Figure 5. 8 Effect of calcination temperature on carbonation conversion efficiency (%) during 10 repeated carbonation/calcination cycles. Experimental condition: carbonation at temperature 650 ^{o}C, CO_2 concentration of 20 vol.% for 30 min; calcination at specified temperature for 10 min

Figure 5. 8 shows the effect of calcination temperature on the CaO performance, which is conducted under a constant carbonation temperature of 650 ^{o}C. Again the decay in CaO activity with the increasing carbonation/calcination cycles is observed. The carbonation conversion efficiency of the 1st cycle under different tested calcination temperatures does not differ significantly; however this distinction is continuously enlarged during long-time

CaO looping cycles. This supports the phenomenon of sintering during the reactions, which is accompanied by the agglomeration of particles and closure of pore channels and has gradually deteriorated the CaO performance [14, 22]. When comparing different calcination temperatures, it is found that 800 °C exhibits the highest carbonation conversion efficiency, which is in a range of 16.1-19.8% during the 10 cycles and is 1-7% higher than the values under 950 °C. This is consistent with the results discussed above. Increasing the calcination temperature above 900 °C has clearly accelerated the decay in CO_2 adsorption capacity. The sintering mechanism responsible for the poor sorbent performance is drastically enhanced at higher calcination temperatures.

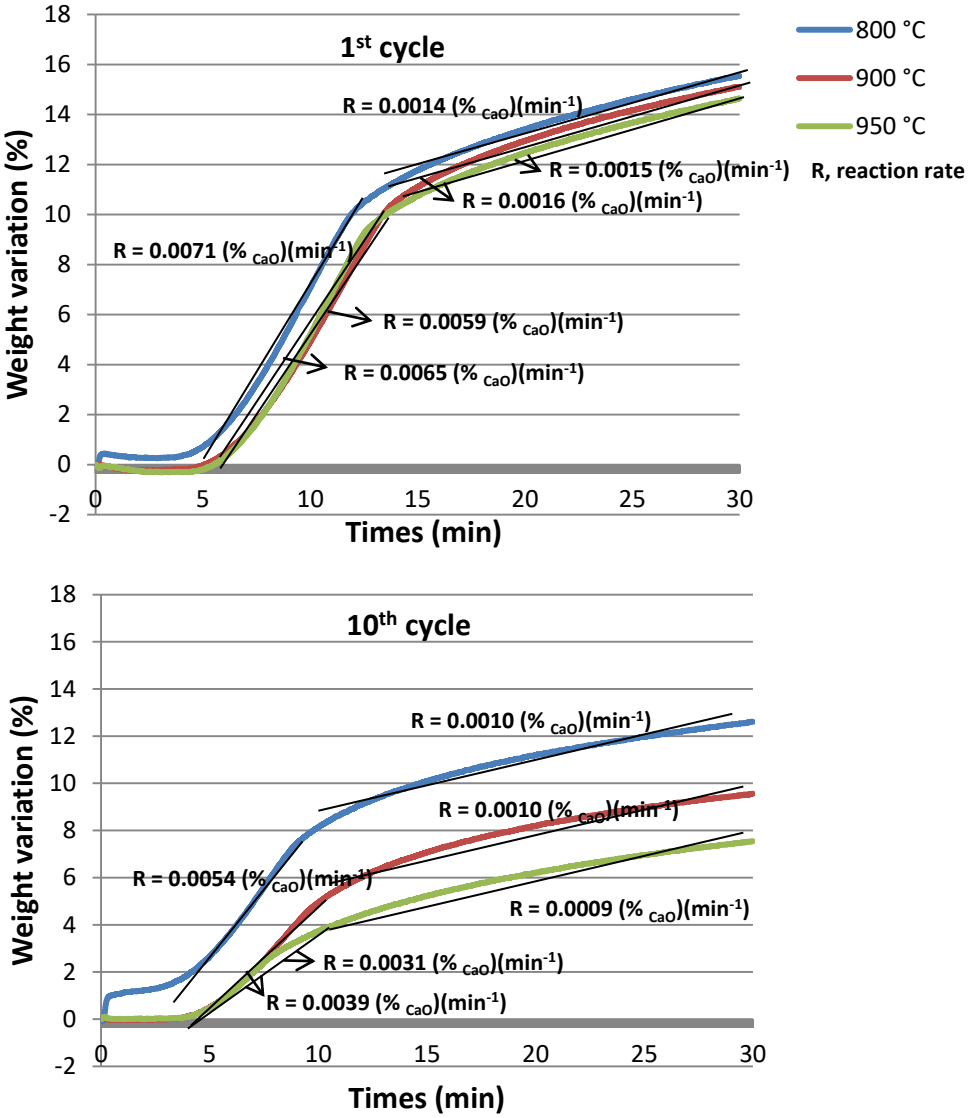

Figure 5. 9 Comparison between the 1st and 10th carbonation process as a function of time under different calcination temperature. Experimental condition: carbonation at 20 vol.% CO_2 for 30 min; calcination at specified temperature for 10 min

The comparison of CaO weight variation and reaction rate between the 1st and 10th cycle under different calcination temperatures is illustrated in **Figure 5. 9**. As can be seen, kinetic-control stage again dominates the CaO conversion. For cases under different temperatures, the reaction rate of kinetic-control stage differs significantly; while they exhibit a similar reaction rate during the slow carbonation stage. With increasing number of cycles, the distinction of CO_2 capture capacity under different temperatures is obviously enlarged. Again, the kinetic-control stage at the 10th cycle is weaker, especially for temperature of 950 ^oC. The reaction rate of kinetic-control stage decreases from 0.0059-0.0071 $\%_{CaO}$/min to 0.0031-0.0054 $\%_{CaO}$/min. This again verifies the decreased of the amount of small pores caused by sintering. Under this circumstance, the carbonation process is more likely to proceed via diffusion other than through the surface area or internal pores of CaO particle, which then results in a remarkably poor performance with the increasing of carbonation-calcination cycles.

Overall, it could be concluded that a calcination temperature of 800 ^oC exhibits the highest CaO conversion efficiency under the tested conditions. To ensure the sorbent performance, calcination temperatures should be controlled below 900 ^oC to reduce sintering, which is hypothesized to be the main cause in the reduction of the CO_2 adsorption capacity.

5.3.3 Steam hydration for CaO re-generation

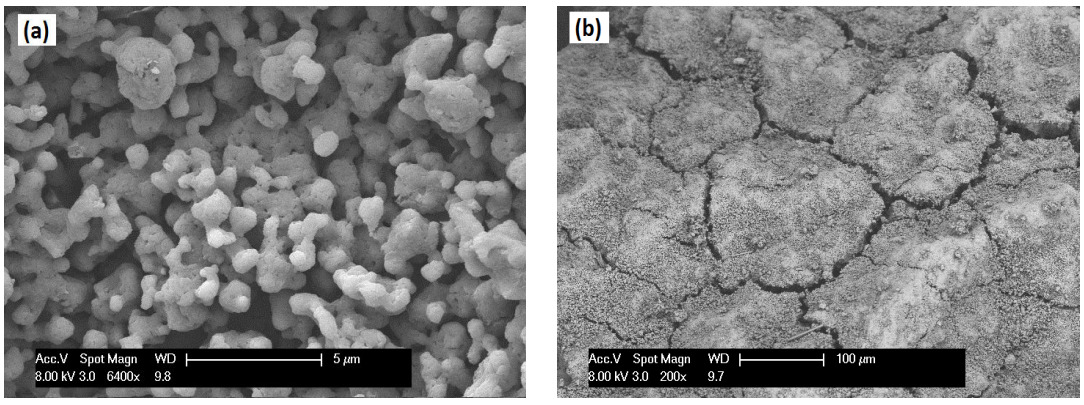

Figure 5. 10 SEM images of CaO with steam hydration after 5 carbonation/calcination cycles: (a) 6400×; (b) 200×

Table 5. 3 Specific surface area and porosity of CaO with steam hydration

	5 cycles with steam hydration	Original CaO (0#)	5 cycles without steam hydration (1#)
S_{BET}, m^2/g	4.70	2.37	3.24
Porosity, %	7.33	0.00	12.38

The characteristics of CaO particle with steam hydration as re-generation method after 5 carbonation/calcination cycles are measured by SEM and BET analysis, with results shown in **Figure 5. 10** and **Table 5.3**, respectively. It is evident that steam hydration has a positive effect on CaO reactivity re-generation. BET analysis (**Table 5.3**) shows that, the specific surface area of the hydration sample is increased to 4.70 m^2/g, which is higher than both the original sample (0#) and the sample after 5 cycles without steam hydration (1#). Similarly, porosity of the hydration sample attains 12.38%, which is 69% higher than that of sample 1#. SEM results from **Figure 5. 4** further confirm that, compared with the morphology of the CaO particles without re-generation, steam hydration after every carbonation-calcination cycle could effectively maintain the sorbent morphology and structure. Particles from **Figure 5. 10 (a)** exhibit small sizes than those without hydration addition after 5 cycles (Sample 1# in **Figure 5. 4**). At the same time, it is also found from **Figure 5. 10 (b)** that the particle surface has been divided into several small cracks.

The effect of steam on CaO re-generation could be explained by the advancing interface mechanism proposed by Glasson et al. [23, 24]. It has been proved that the benefit is mainly brought by $Ca(OH)_2$, which is formed as the product of the hydration reaction between CaO and steam. Since the mole volume of $Ca(OH)_2$ (ca. 33 cm^3/mol) is larger than that of CaO (ca. 17 cm^3/mol) and much close to $CaCO_3$ (ca. 37 cm^3/mol) [21, 25], the size of the CaO sorbent will increase during the hydration process. Cracks are formed on the hydrated sorbent surface, leading to the generation of new reaction surfaces. Subsequently during the dehydration stage, $Ca(OH)_2$ decomposes to CaO again, the particle size shrink and pores are thus reopened. As a result, the hydration re-generation of CaO could be attributed to crystalline texture recrystallization and pore structure reorganization [26], which restrains the decrease of sorbent surface area and the loss of porosity [27] and, thus, maintains the reactivity of the cyclic CaO sorbent at a higher level.

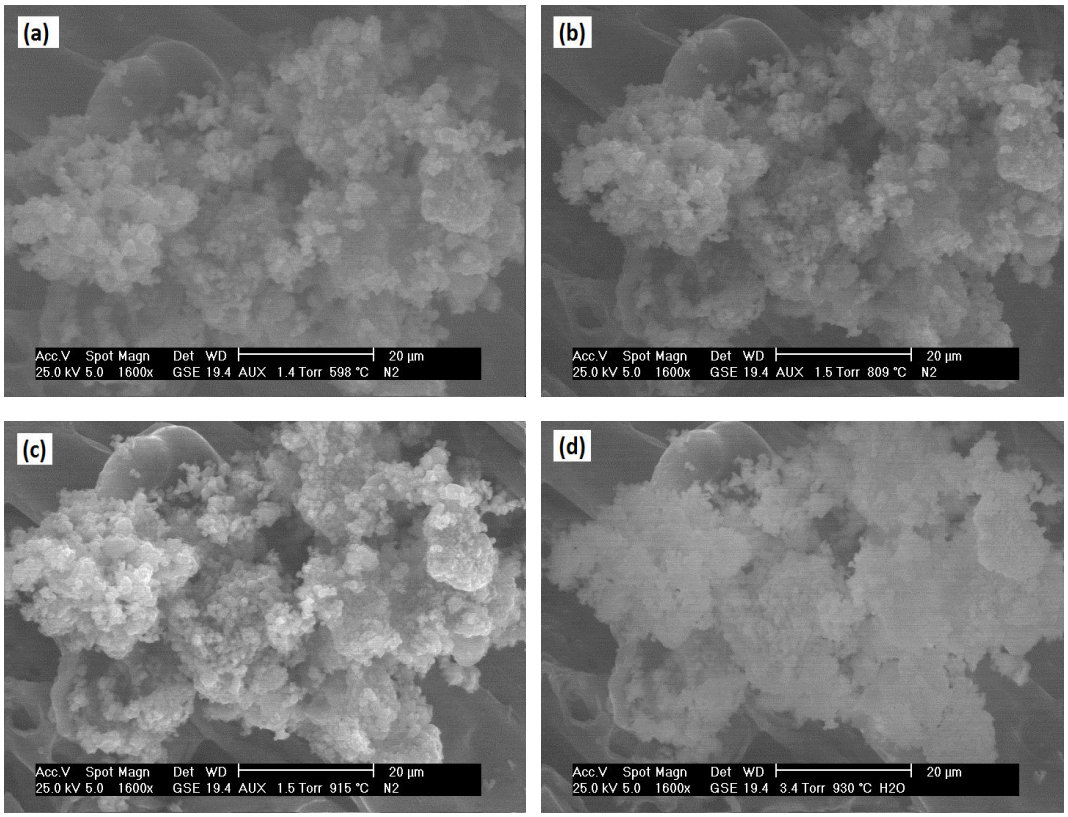

Figure 5. 11 Structure of CaO during gasification of poplar wood in ESEM using the following heating stage: (a) 500 °C under N_2; (b) 700 °C under N_2; (c) 800 °C under N_2; (d) 800 °C under steam

The influence of high-temperature steam is also investigated. The aim is two-folds: 1) to examine its effect on CaO reactivity, and 2) to check if steam gasification could serve as a potential option to retain CaO catalytic effect based on the results of **Chapter 4**. Accordingly, steam catalytic gasification of poplar wood is conducted in an ESEM instrument to see in-situ evolving. The experimental procedures are reported in **Chapter 2**. **Figure 5. 11** shows N_2 atmosphere leads to no significant changes in the morphological structure of CaO during the heating stage, but after the injection of steam the surface of CaO becomes relatively flat. Donat et al. [28] also reported an increased CaO pore size in the presence of high-temperature steam during carbonation/calcination cycles. They indicated that steam is effective to enhance the reactivity of CaO in two ways. It promotes sintering that produce a CaO morphology with larger pores, which are more stable and less sensitive to pore blockage. The diffusion resistance during carbonation is also reduced and thus allows for a higher conversion. Overall, the use of steam is an effective approach for CaO catalyst re-generation. This can be achieved by low-temperature hydration reaction after carbonation-calcination cycle, or, steam gasification is also beneficial to retain CaO reactivity.

5.4 Summary of Chapter

Due to the catalytic effect of CaO both on CO_2 adsorption and syngas quality improvement as discussed in **Chapter 4**, a gasification-based catalyst recycling system based on carbonation/calcination looping is proposed. The latter uses the reversible reaction of CaO to achieve H_2-rich syngas production as well as catalyst recycling. Unfortunately, CaO sorbent is far from reversible in practice; its reactivity shows significant decrease over multiple CO_2 capture and release cycles. To better facilitate its industrial application, experiments are conducted to analyze the CaO de-activation mechanism, to reduce its rate of decay in reactivity, as well as to re-generate the sorbent. The main findings are as follows:

- The CO_2 adsorption capacity of CaO is continuously reduced during carbonation/calcination cycles. Its degradation is primarily related to two causes. One could be attributed to the clogging of small pores during carbonation that do not reopen. Sintering is another important mechanism for the de-activation of CaO, which mainly occurs during calcination resulting in a decrease of the CaO surface area and porosity.

- The effects of carbonation/calcination temperature are studied to optimize the carbonation-calcination process parameters. 650 ^{o}C is shown to be the most suitable carbonation temperature considering both reaction kinetics and CaO reactivity; while calcination temperature above 800 ^{o}C accelerates sintering and the decay in CO_2 adsorption capacity.

- The presence of steam has a positive impact on CaO re-generation. This can be achieved by steam hydration after carbonation-calcination cycle, which is proven effective to maintain the surface area and morphology of CaO. Besides, steam gasification is also beneficial to retain CaO reactivity.

Overall, the main findings from this chapter are summarized in **Figure 5. 12**.

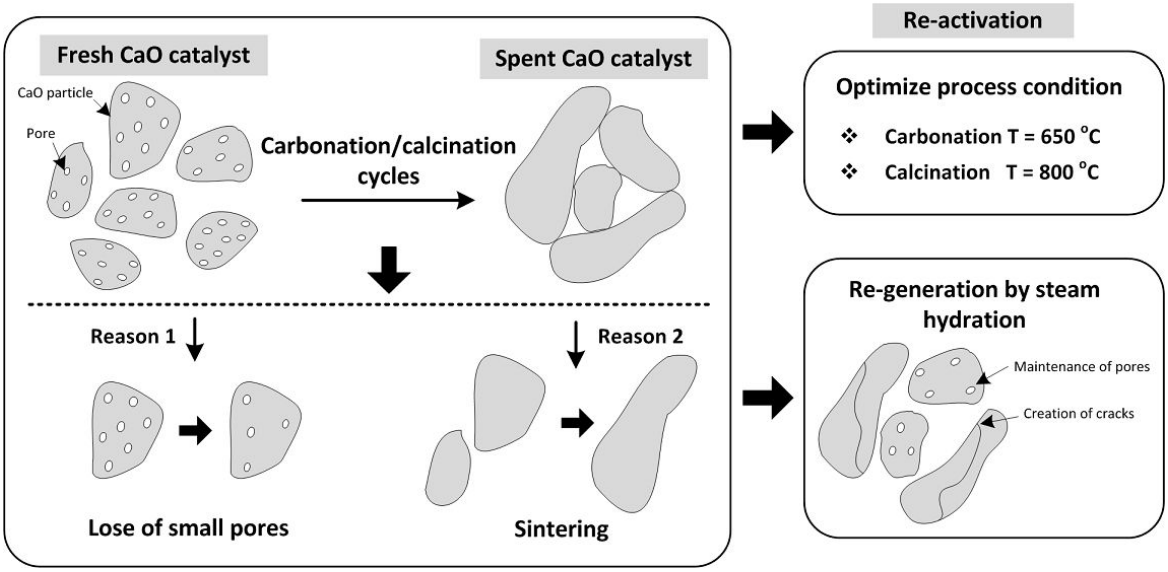

Figure 5. 12 De-activation and re-activation of CaO catalyst as main findings of Chapter 5

5.5 Bibliography

[1] Shimizu T, Hirama T, Hosoda H, Kitano K, Inagaki M, Tejima K. A twin fluid-bed reactor for removal of CO_2 from combustion processes. Chemical Engineering Research and Design. 1999;77:62-68.

[2] Gorin E. Gasification of carbonaceous solid fuels. Google Patents; 1953.

[3] Abanades J Carlos, Alvarez Diego. Conversion limits in the reaction of CO_2 with lime. Energy & Fuels. 2003;17:308-315.

[4] Sun Ping, Grace John R, Lim C Jim, Anthony Edward J. Investigation of attempts to improve cyclic CO_2 capture by sorbent hydration and modification. Industrial & Engineering Chemistry Research. 2008;47:2024-2032.

[5] Wu Y, Blamey J, Anthony EJ, Fennell PS. Morphological changes of limestone sorbent particles during carbonation/calcination looping cycles in a thermogravimetric analyzer (TGA) and reactivation with steam. Energy & Fuels. 2010;24:2768-2776.

[6] Grasa Gemma S, Abanades J Carlos. CO_2 capture capacity of CaO in long series of carbonation/calcination cycles. Industrial & Engineering Chemistry Research. 2006;45:8846-8851.

[7] Blamey J, Anthony EJ, Wang J, Fennell PS. The calcium looping cycle for large-scale CO_2 capture. Progress In Energy And Combustion Science. 2010;36:260-279.

[8] Barker Ronald. The reversibility of the reaction $CaCO_3 \rightleftarrows CaO + CO_2$. Journal of applied Chemistry and biotechnology. 1973;23:733-742.

[9] Fennell Paul S, Pacciani Roberta, Dennis John S, Davidson John F, Hayhurst Allan N. The effects of repeated cycles of calcination and carbonation on a variety of different limestones, as measured in a hot fluidized bed of sand. Energy & Fuels. 2007;21:2072-2081.

[10] Lysikov Anton I, Salanov Aleksey N, Okunev Aleksey G. Change of CO_2 carrying capacity of CaO in isothermal recarbonation-decomposition cycles. Industrial & Engineering Chemistry Research. 2007;46:4633-4638.

[11] Sun P, Grace JR, Lim CJ, Anthony EJ. The effect of CaO sintering on cyclic CO_2 capture in energy systems. Aiche Journal. 2007;53:2432-2442.

[12] Borgwardt Robert H. Calcium oxide sintering in atmospheres containing water and carbon dioxide. Industrial & Engineering Chemistry Research. 1989;28:493-500.

[13] Bhatia SK, Perlmutter DD. Effect of the product layer on the kinetics of the CO_2 ‐ lime reaction. Aiche Journal. 1983;29:79-86.

[14] Chen Huichao, Zhao Changsui, Li Yingjie, Chen Xiaoping. CO_2 capture performance of calcium-based sorbents in a pressurized carbonation/calcination loop. Energy & Fuels. 2010;24:5751-5756.

[15] Sun Ping, Grace John R, Lim C Jim, Anthony Edward J. Determination of intrinsic rate constants of the CaO–CO_2 reaction. Chemical Engineering Science. 2008;63:47-56.

[16] Dean Charles C, Blamey John, Florin Nicholas H, Al-Jeboori Mohamad J, Fennell Paul S. The calcium looping cycle for CO_2 capture from power generation, cement manufacture and hydrogen production. Chemical Engineering Research and Design. 2011;89:836-855.

[17] Manovic Vasilije, Anthony Edward J. Thermal activation of CaO-based sorbent and self-reactivation during CO_2 capture looping cycles. Environmental Science & Technology. 2008;42:4170-4174.

[18] Florin Nicholas H, Harris Andrew T. Preparation and characterization of a tailored carbon dioxide sorbent for enhanced hydrogen synthesis in biomass gasifiers. Industrial & Engineering Chemistry Research. 2008;47:2191-2202.

[19] Gupta Himanshu, Iyer Mahesh V, Sakadjian Bartev B, Fan Liang-Shih. Reactive separation of CO_2 using pressure pelletised limestone. International journal of environmental technology and management. 2004;4:3-20.

[20] Li Zhen-shan, Cai Ning-sheng, Huang Yu-yu. Effect of preparation temperature on cyclic CO_2 capture and multiple carbonation-calcination cycles for a new Ca-based CO_2 sorbent. Industrial & Engineering Chemistry Research. 2006;45:1911-1917.

[21] Rong Nai, Wang Qinhui, Fang Mengxiang, Cheng Leming, Luo Zhongyang, Cen Kefa.

Steam hydration reactivation of CaO-based sorbent in cyclic carbonation/calcination for CO_2 capture. Energy & Fuels. 2013;27:5332-5340.

[22] Manovic Vasilije, Charland Jean-Pierre, Blamey John, Fennell Paul S, Lu Dennis Y, Anthony Edward J. Influence of calcination conditions on carrying capacity of CaO-based sorbent in CO_2 looping cycles. Fuel. 2009;88:1893-1900.

[23] Glasson DR. Reactivity of lime and related oxides. II. Sorption of water vapour on calcium oxide. Journal of Applied Chemistry. 1958;8:798-803.

[24] Glasson DR. Reactivity of lime and related oxides. III. Sorption of liquid water on calcium oxide ('wet'hydration). Journal of Applied Chemistry. 1960;10:38-42.

[25] Zeman Frank. Effect of steam hydration on performance of lime sorbent for CO_2 capture. International Journal of Greenhouse Gas Control. 2008;2:203-209.

[26] Ramachandran Vangipuram Seshachar, Sereda Peter J, Feldman RF. Mechanism of hydration of calcium oxide. Nature. 1964;201:288-289.

[27] Gullett BK, Bruce KR. Pore distribution changes of calcium‐based sorbents reacting with sulfur dioxide. Aiche Journal. 1987;33:1719-1726.

[28] Donat Felix, Florin Nicholas H, Anthony Edward J, Fennell Paul S. Influence of high-temperature steam on the reactivity of CaO sorbent for CO_2 capture. Environmental Science & Technology. 2012;46:1262-1269.

Chapter 6

Life Cycle Assessment and Optimization of MSW Pyro-gasification Technology

6.1 Introduction

Chapter 1 has pointed out the necessary and current gaps in research regarding the systematic evaluation of MSW thermal treatment technologies. As a result, this chapter is mainly focused on the assessment and optimization of MSW pyro-gasification technology using LCA methodology. The aim would be to guide for its further appropriate development worldwide, while providing the scientific basis for decision makers regarding the improvement of local waste management plan. With this overall objective, two LCA studies are performed:

- **Section 6.2** is mainly dedicated to give a systematic and holistic comparison between MSW gasification and conventional incineration technologies. Besides, the geographic distinctions are also considered to identify potential improvements.

- **Section 6.3** is mainly focused on the potential optimization of the pyro-gasification process, where different syngas utilization approaches are quantitatively modeled to seek for an energy-efficient and environmental-sound application route.

It needs to emphasize that only energy generation schemes will be discussed in this chapter, which is mainly due to the current technological and data limitation. However, as pointed out in **Chapter 1**, different alternative cycles are basically available for the utilization of syngas. The implementation and procedures for LCA have been introduced in **Chapter 2**.

The application of LCA is in compliance with the ISO standards [1]; and EDIP 97, which is a well-acceptable impact assessment method, is used to aggregate the environmental impact results [2].

6.2 MSW gasification vs. incineration: Comparative assessment of commercial technologies

As regulated by ISO 14040 [1], the LCA framework can be divided into four phases: (1) goal and scope definition, (2) LCI, (3) LCIA, and (4) interpretation. These four steps are implemented in this study, as described separately below.

6.2.1 Goal and scope definition

Due to the potential benefits brought by MSW pyro-gasification, its applications based on commercial scale started to be organized. Although the operating experience is still limited, as many as 100 plants around the world have already emerged so far [3], and the majority are located in Japan, generally based on gasification process; or to a smaller scale, on pyrolysis. In Europe, the presence of gasification also increased during the last decades, such as Lahti in Finland, Norrsundet in Sweden, Averoy in Norway. Among those applications, the gasification stage is in most cases linked to a downstream energy recovery device, i.e., as a pre-stage for a successive complete combustion process, known as “two-step oxidation” WtE scheme. Compared with conventional MSW incineration, the combustion stage, burning the syngas, is cleaner and more efficient than the direct incineration of heterogeneous waste. And, the potential benefits are also related to a lower generation of some pollutants (NO_x, dioxin), reduced excess air, recovery of metals in non-oxidized form and emission control [4]. However, using this novel technology does not imply an absolute environmental sustainability. The whole gasification-based plant tends to be more complicated; besides, the feedstock needs to be pre-treated, which consumes more energy and may thus vary the overall energy efficiency and environmental effects. Therefore, it is essential to have a comprehensive and quantitative comparison between gasification and conventional incineration, to help guide for the further appropriate development of WtE technologies.

Nevertheless and as pointed out by McDougall et al. [5], the behavior of waste management systems varies as a result of geographic differences in waste characteristics, energy sources or availability of treatment schemes. Consulting WtE technologies worldwide,

it is observed that the majority of existing MSW incineration plants in EU countries is mechanical-grate type [6]. However in Asia countries especially China, fluidized bed incinerators occupy a large share of the market due to advantages of their great thermal capacity to treat low-grade MSW characterized with high moisture and low LHV [7]. Besides, the composition of MSW also differs a lot among regions, as an example for the more dominant role of paper (newspapers and packages) in EU countries compared with relatively larger proportion of organic in Asian countries [8]. Those different MSW characteristics and operating conditions may significantly affect the quantity of the energy recovered and the emissions discharged. In this sense, a comparison between different regions is also meaningful, in order to obtain a transparent and in-depth understanding of the WtE technologies worldwide.

Keeping these in mind, the goal of this LCA study is to give a comparative assessment of MSW gasification and conventional incineration WtE technologies, taking into account the geographic distinctions between developed and developing countries. As a result, a total of three systems are evaluated, using the LCA system boundary illustrated in **Figure 6. 1**. S1 represents the gasification-based WtE system, in which MSW is first gasified and then fully oxidized in the secondary combustion chamber for energy recovery. A commercial operated plant in EU (Kymijärvi II power plant, Finland) is selected as analysis basis. S2 and S3 stand for the conventional MSW incineration cases, of which industrial operating data for French or Chinese conditions are selected for the calculation.

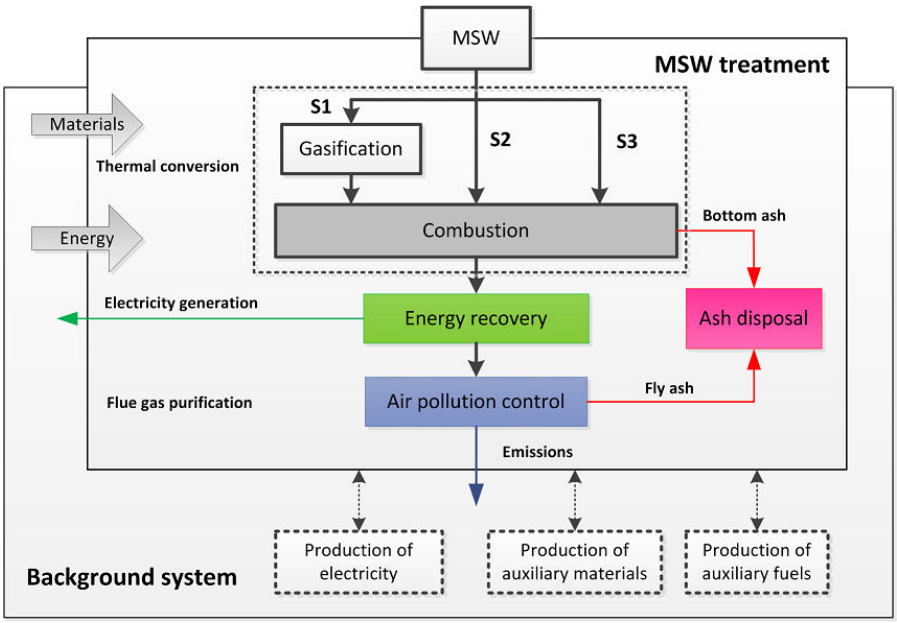

Figure 6. 1 System boundary for the comparison of MSW gasification and conventional incineration technologies

Energy and material flows presented as inputs and outputs are shown with arrows in **Figure 6. 1**. In general, the system boundary is divided into foreground and background system in order to distinguish direct and indirect environmental burdens. The foreground system is process-specific, which begins at the moment when the waste enters the incineration plant; and attains the limit when waste becomes inert materials, or else emissions to the environment, or useful energy again. Hence, the study includes MSW pre-treatment (for S1), thermal treatment, flue gas treatment, solid residue management, and energy recovery. Processes used for MSW collection and transportation before entering the incineration gate are excluded, as they are identical in all systems. Wastewater effluent generated during treatment is not considered due to the lack of data; however this assumption will not cause significant deviations since modern incinerators are designed with wastewater treatment, recycling and reused equipment so that the plant can meet a 'zero discharge' target [7, 9]. Besides, emission from plant construction is also omitted, as it is negligible when compared to the total impacts [5].

Background system accounts for the relevant upstream and downstream processes interacting with the system. Production of auxiliary materials and energy, such as diesel, lime, etc., is all considered apart from their consumption phase, hence leading to a 'cradle to grave' calculation method. Besides, since useful commodity as electricity is produced, allocation of the profit becomes necessary. In this study, substitution by system expansion is performed [10]. The same amount of 'avoided' emissions generated by conventional electricity production is subtracted from those produced during waste treatment. Two sets of electricity production data are considered, either as European average power grid data, or based on the specific country's local condition to reflect the effect of energy structure on the final results in the sensitivity analysis.

One ton of MSW is set as the functional unit, which means that all input and output data are converted to this basis. Data are mainly taken from site-specific measurements, either by operation report or by field survey; the detailed process description will be presented in the following section. Background data related to raw material production are mainly obtained from the Gabi software.

6.2.2 Process description and data source

6.2.2.1 Gasification-based WtE process (S1)

Kymijärvi II power plant, located in Lahti region, Finland, is selected for calculation in this part of the work. It is the first gasification plant in the world that utilizes only solid recovered fuel (SRF) for the combined heat and electricity (CHP) production, without adding auxiliary fuels [11]. The raw material of the SRF is energy-containing waste. As a result of the gasification technology, the waste itself is not directly burned, but instead turned into syngas, and after purification, combusted in an ordinary boiler for the recovery of energy. The commercial operation of the plant started in 2012, and consists of 2 × 80 MW fluidized bed gasification lines with a total plant capacity of 50 MW of electricity and 90 MW of district heat. Annually, the plant could handle approximately 250,000 tons of SRF [12].

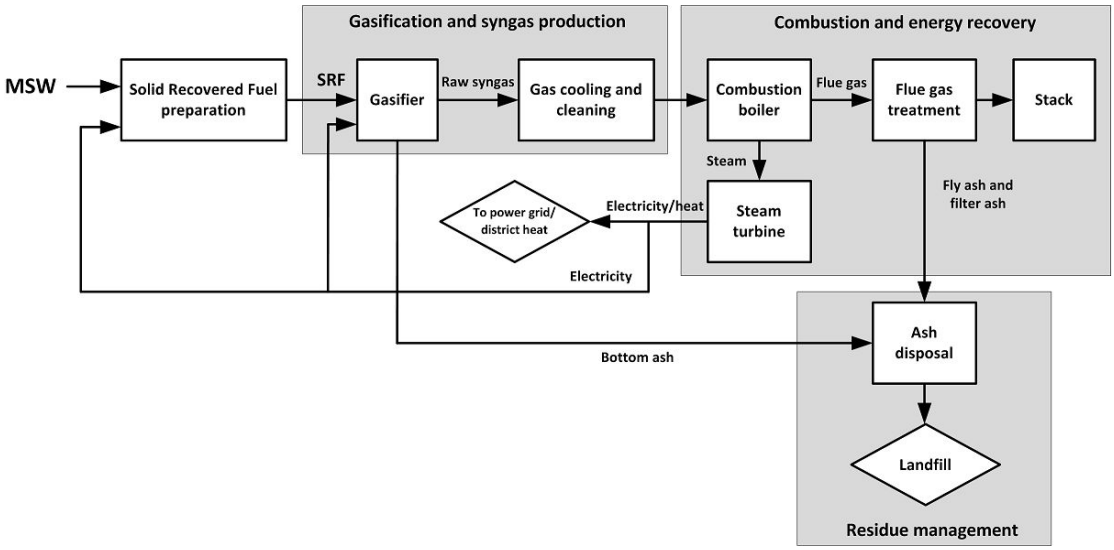

Figure 6. 2 Flowchart of the gasification-based WtE process (S1)

The flowchart of the plant is shown in **Figure 6. 2**. The plant consists of six basic unit operations: the gasification system, the syngas cooling and cleaning system, the boiler, the flue gas treatment system, the energy recovery system and the ash disposal system. More specifically, the gasifier is a circulating fluidized bed runned at atmospheric pressure, with a 25 m height and a 5 m outer diameter. Oxygen acts as gasifying agent, and the operating temperature is 850-900 ^{o}C. The bed material consists of sand and lime. After gasification, the SRF, which has been turned into combustible gas, undergoes the gas cooling and cleaning process; while the sand, lime and ash are separated and returned to the gasifier.

The product gas is cooled to 400 ^{o}C for impurities removal, so that materials causing corrosion, such as alkali chlorides, turn from gas into solid particles. This temperature is

chosen to prevent tar condensation. During the gas cooling process, the heat is recovered for preheating the feedwater conducted to the boiler. The syngas containing solids then flows through the hot filter for particle removal, after what it is fully combusted in the boiler. The boiler is a natural-circulation steam boiler with a water tube structure. The gas is burned at 850 ^{o}C to produce superheated steam (540 ^{o}C and 121 bar), which is then utilized in turbine and generator for energy recovery. The electricity goes into the national grid; and the district heat produced is transferred along the trunk network to residents in the Lahti and Hollola region.

The flue gas treatment system includes a NO_x catalyst to reduce the nitrogen oxides into nitrogen, a bag filter for the capture of ash, $NaHCO_3$ to neutralize the acid gases, as well as the activated carbon to bind heavy metals and dioxin. The plant produces three kinds of ashes: bottom ash, filter ash and fly ash. While the bottom ash is sent for landfill, the filter and fly ash as contains carbon and impurities which requires safety treatment.

6.2.2.2 Incineration process under condition of France (S2)

S2 system reflects the conventional incineration process under local conditions in France. Data from Beylot et al. [13] are used, in which the environmental performance of 110 French incinerators are reported, corresponding to 85% of the total number of incineration plants currently operate in France. Therefore, the calculation of scenario S2 in this study is actually based on the average emission and energy consumption level of incinerators in France.

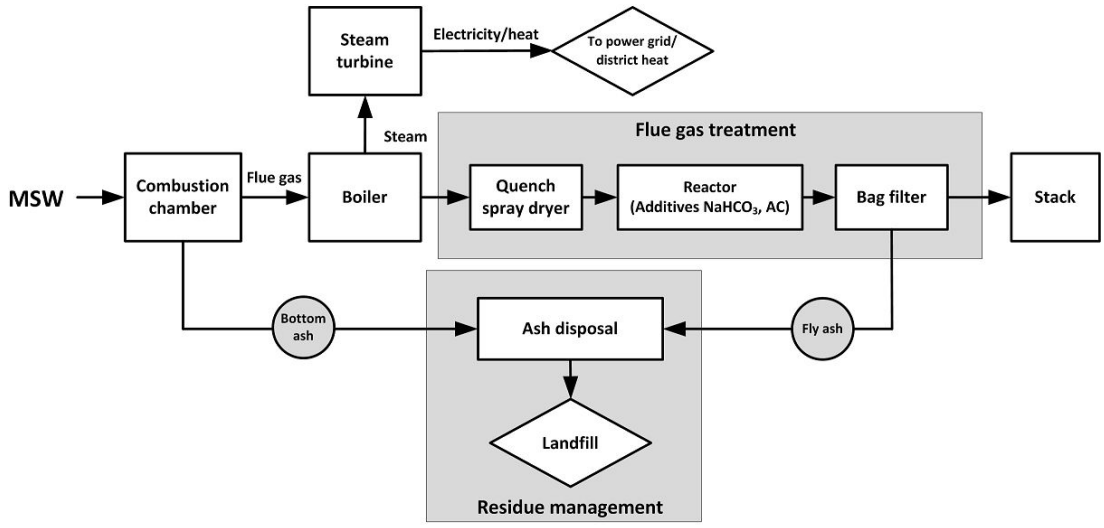

Figure 6. 3 Flowchart of the incineration process

Incinerators in France are mostly grate type, with the typical process flowchart shown in **Figure 6. 3**. Generally, the plant is composed of four sections: combustion (typically by moving grate technology in S2), energy recovery, flue gas treatment and ash disposal. One major characteristic of the grate furnace is its ability to swallow an unsorted MSW fed. The primary air is supplied from the bottom section. As the MSW enters through the fuel chute, it undergoes drying, devolatilization, and combustion when moving along the sloping grate. The bottom ash forms at the end of the grate, which then is turned down into an ash quench. The secondary air is provided above the bed to ensure complete combustion, and the total excess air usually varies between 1.6 and 2.2 [6, 14]. Flue gas treatment system typically consists of quenching spray dryers, electrostatic precipitators, acid scrubbers, desulfurization with lime, DeNO$_x$ with ammonia and finally a bag filter [15]. All the French incineration plants are complied with the European Directive 2000/76/EC on waste incineration emission limit standard. Especially, two thresholds on NO$_x$ emissions (200 and 400 mg/m^3, respectively; as daily average values) are distinguished until 2010, permitting a less stringent limit for small-scale incinerators [16].

The energy is then recovered by the steam turbine and generator. Among all the incineration plants investigated in France, 37% uses the recovered energy for electricity generation only, with an average net efficiency of 14%. 26% of the plants use the energy for CHP generation at an average efficiency of 33%. The remaining plants are for heat production only at a net efficiency of 43%. The energy recovered is assumed to satisfy the plant's internal energy consumption. This value is estimated at 172 kWh electricity per ton of MSW by Beylot et al. [13], and the remaining amount is delivered to the grid to substitute for the French mixes.

6.2.2.3 Incineration process under condition of China (S3)

The S3 system represents the conventional incineration process under the local condition of China. As aforementioned, fluidized bed incinerators are widely applied in China considering specific MSW properties; therefore, one typical full-scale fluidized bed incineration plant is assessed as comparison. The selected plant is located in Hangzhou, one of the most developed cities in China. The data for this analysis could be found in the work by Dong et al. [17]. By the end of 2014, approximately 9050 tons of MSW is generated per day in the city, with an annual growth rate of more than 7% [18]. Currently four incineration plants are in operation, and another new plant is under construction. The selected plant has

a treatment capacity of 1200 ton/day. The flowchart of the plant bears great similarities with the grate furnace, as illustrated in **Figure 6. 3**. However, the MSW should be pretreated, and the fed needs to be crushed and shredded to lower its size prior to its introduction in the fluidized bed. Because the heating value of MSW in the city is low (4.31 MJ/kg), the fresh waste is stored for 1-2 days for dehydration prior to firing. Besides, to keep stable burning, coal is added as auxiliary fuel at a ratio of 50 kg per ton of fed MSW.

After complete stirring, the shredded MSW is fed into the furnace and mixes with the bed material, which consists of sand-like particles of about 0.5 mm in size. The fluidizing velocity in this type of furnace is high, so that the bed particles can be carried outside the furnace with the flue gas, and then separated by a cyclone and recycled to the bed again. The most obvious advantage of fluidized bed is that it increases the contact among the waste, the combustion air and the hot sand bed, thus facilitating complete combustion. To this regard, the excess air ratio could be lowered to around 1.4-1.5.

A series of flue gas treatment units, including a semi-dry scrubber and a baghouse filter are installed as air pollution control system. Part of the acid gases, particulate matters, heavy metals and toxic organic pollutants especially dioxin produced by the incineration process can be effectively removed. The discharged flue gas is in compliance with the environmental regulations; the concentration of emissions is monitored on-line so that the average emissions are available. The recovered energy is used for electricity generation and the average energy recovery efficiency is estimated at 27%. 80% of the total generated electricity is sent to the power grid, while the remaining 20% is used for self-consumption such as for waste pre-treatment and leachate treatment. Bottom ash and fly ash, accounting for about 22% mass weight, are disposed by landfill.

6.2.2.4 Waste composition

MSW physical and chemical properties under local condition of different analyzed scenarios are used for calculation. Conventional incineration systems of S2 and S3 use mixed MSW as feedstock and therefore MSW composition data from statistical measurements of France and China are adopted, which are taken from ADEME and Hangzhou Municipal Solid Waste Disposal Supervision Center [13, 19], respectively (see **Table 6. 1**).

Table 6. 1 Statistical MSW composition in France (S2) and Hangzhou, China (S3)

	Composition (wt.% of total wet waste)							
	Organic	Paper	Plastic	Wood	Textile	Glass	Metal	Inert
France (S2)	39.6	16.2	11.7	2.6 [a]	12.9	6.3	3.0	7.0
Hangzhou, China (S3)	58.5	13.3	18.8	2.6	1.5	2.7	1.0	2.0

[a] The fraction of "wood" in France may include other combustibles, but here we suppose it only consists of pure wood.

In Finland, the waste management system mainly includes materials recycling, incineration, gasification, organic waste composting and landfill. **Figure 6. 4** illustrates the changing tendency of waste treatment options in the Lahti region in 2004 and 2012. Results show that the proportion of MSW gasification has been dramatically increased. As in the case of S1, SRF is used as the feedstock instead of unsorted MSW. It mainly consists of combustible waste that is not suitable for material recycling, such as unclean plastic, paper, cardboard and wood. The refining process for SRF has specified stringent quality standards, which agrees with the CEN/TC 343 regulation, promulgated by the European Committee for Standardization [20]. As a result, the heating value of the feedstock can be increased to a higher level, while its moisture content can be lowered. **Table 6. 2** summarizes the characteristics of the SRF, as well as the MSW used in S2 and S3.

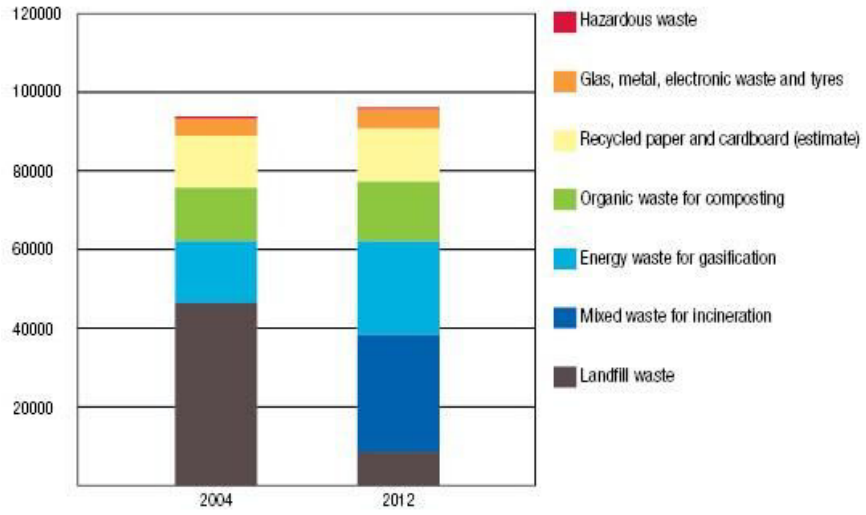

Figure 6. 4 Comparison waste management system in Lahti region between 2004 and 2012. Data obtained from the official website of Lahti gasification plant (https://www.lahtigasification.com)

Table 6. 2 Characteristics of the MSW applied in S1, S2 and S3

	LHV (ar, MJ/kg)	Moisture (ar, %)	Ash (ad, %)	Carbon (ad, %)
Finland (S1) [a]	14.2	26.8	9.4	50.2
France (S2)	9.3	36.7	17.1	52.3
China (S3)	4.3	53.3	8.7	41.6

[a] Data based on monthly combined samples and average values are used [12].

6.2.2.5 Pretreatment of MSW

Since SRF is used in S1, its production process from raw MSW will be considered. After separating, the waste is shredded to a particle size of about 6 cm, reduce the moisture content to below 20-30%, then pelletized to form SRF. The energy consumption in the SRF production process mainly includes electricity and fuels. Relevant data from literature [21] estimated the demand at 804 MJ of electricity [21] and 32.3 MJ of diesel [22] per ton of MSW.

Pretreatment of MSW is also introduced in S3 in order to help homogenize the MSW while improveing its heating value. As aforementioned, this includes storage for drying and shredding for size reduction, which essentially requires electricity. No accurate value of electricity consumption could be obtained; however it is part of the total internal electricity consumption that has been measured as a whole.

6.2.2.6 Energy recovery

Energy is recovered in all scenarios (S1, S2 and S3). Three options to this effect exist: as electricity only, as heat only, or as CHP production. Those three types are all available in France (S2); while S3 plant is designed for electricity production and S1 plant operated in CHP mode. In order to give a reasonable and transparent comparison between different systems, the energy is considered as electricity recovery only, nevertheless the CHP mode will be discussed later in sensitivity analysis (**Section 6.4**).

6.2.3 Life cycle inventory

Considering all input and output data of the aforementioned processes, detailed energy and material flows are compiled, as displayed in **Table 6. 3**. In addition, some key assumptions are made to fulfill the calculation:

- Only fossil-derived CO_2 emission is considered as a contributor to GW, while biogenic CO_2 emission is regarded to be carbon neural.
- Due to the lack of data, heavy metals to the air are not contained in this study. For S1 and S3, data related to gaseous dioxin emission are taken from on-site measurement; as for S2, the relevant value is obtained based on EC standard due to the lack of data.
- Chemical additives used for air pollution control usually include lime, NaOH, activated carbon, etc. Only lime is calculated due to the data unavailability of the others, however this assumption is considered acceptable because of the small amount used in each case.
- Emissions during the ash disposal process are obtained from literature, in which statistical data that are currently used for dealing with MSW in the UK and in Europe are applied as calculation basis [23].

Table 6. 3 Material and energy flows for different analyzed systems (data are presented based on 1 t/MSW)

	Unit	S1	S2	S3
Input streams				
Electricity for MSW pretreatment	kWh	223.33		
Diesel for MSW pretreatment	L	0.84		
Coal as auxiliary fuel	kg			50.00
Electricity for ash treatment	kWh	2.95	1.28	4.01
Diesel for ash treatment	L	3.28	3.17	4.76
Lime for flue gas purification	kg	13.50	10.20	9.60
Output streams				
Electricity output [a]	kWh	1079.41	361.04	294.33
Bottom ash [b]	Kg	69.71	118.00	110.00
Air pollution control residues [b]	kg	81.12	34.30	110.00
Air emissions				
CO	mg/Nm^3	2.00	51.00	94.30
SO_2	mg/Nm^3	7.00	51.20	247.30
NO_x	mg/Nm^3	161.00	927.00	200.00
HCl	mg/Nm^3	1.00	18.30	46.90
Dust	mg/Nm^3	2.00	8.70	30.50
Dioxin	mg/Nm^3	2.00E-09	1.00E-07	1.50E-07

[a] Data are given as net electricity output, i.e., the internal electricity consumption inside the plant has been deducted from the gross electricity generation;

[b] For S1, the amount of bottom ash and air pollution control residues is obtained from the operation report. For S2, the values are derived from literature [10]; for S3, the amount of air pollution control residues generated is obtained by the measurement data from a similar scale fluidized bed plant [7], and the total amount of solid residues is obtained from the operation report.

The generated electricity is assumed to substitute the same amount of electricity that is produced by conventional means. As aforementioned, two sets of electricity mix are considered, which are either following EU basis, or based on the specific condition of the local country. The relevant distribution of the electricity grid is presented in **Table 6. 4** [24], which serves as calculation basis for the emissions generated from conventional electricity

production. Specifically, the French electricity mix is dominated by nuclear energy; the Chinese electricity is mainly relied on fossil fuels, while the Finnish electricity mix is considered more balanced between the former two countries.

Table 6. 4 Distribution of electricity of EU average, Finland, France and China (Unit: %) [24]

	Fossil fuels	Nuclear	Hydroelectric	Geothermal	Solar	Tide and wave	Wind	Biomass and waste
EU average	47.20	24.09	16.64	0.33	1.99	0.01	5.92	4.14
Finland	25.49	32.68	24.72	0.00	0.01	0.00	0.73	16.36
France	8.42	76.40	10.90	0.00	0.75	0.09	2.80	0.98
China	77.07	1.94	17.96	0.00	0.13	0.00	2.01	0.94

6.2.4 Life cycle impact assessment

As presented in **Chapter 2**, the EDIP 97 methodology is used to aggregate the LCI results [2]. The pollutants investigated include CO_2, CO, SO_2, NO_x, HCl, dust, dioxin and heavy metals to the soil (Cd, Cr, Cu, Pb, Ni and Zn) caused by solid residue solidification and stabilization. Seven impact categories are considered, including both non-toxic and toxic impacts: GW, AC, NE, POF, HTa, HTs and ETs. Toxic impacts via water are omitted, since they are mainly caused by leachate pollutants, in addition to the fact that the relevant data are lacking. Results based on characterized values are used. In addition, normalized LCIA values are also used to quantify the relative magnitude of different impacts in terms of person equivalence, i.e., Pe. Detailed characterization unit and normalization references have been indicated in **Chapter 2** (as in **Table 2. 6**).

6.2.5 Interpretation and discussion

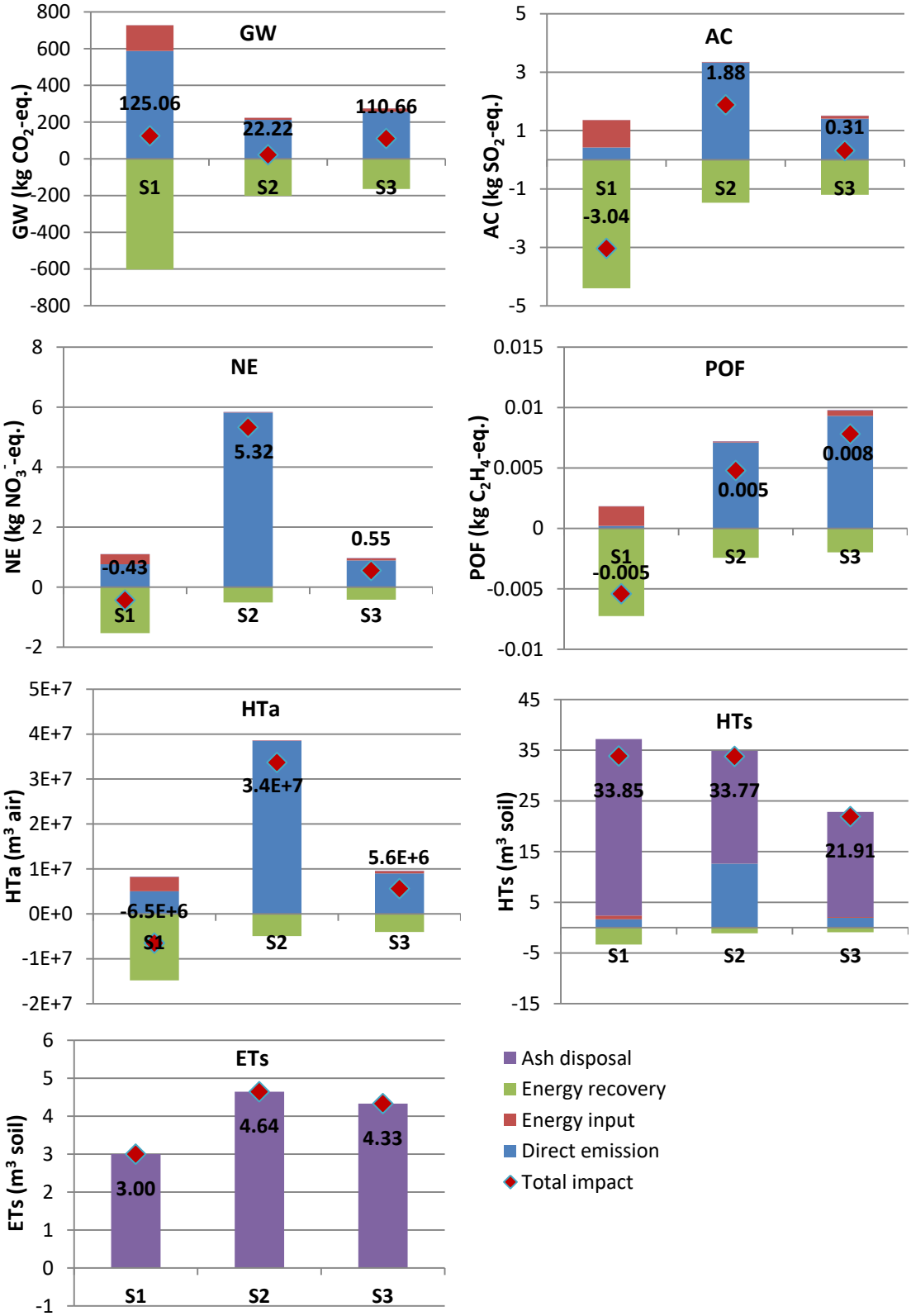

Figure 6. 5 Characterized environmental impacts of different systems: S1, gasification-based plant in Finland; S2, conventional MSW incineration plant in France; S3, conventional MSW incineration plant in China

Figure 6. 5 illustrates the environmental impacts related to each category including GW, AC, NE, POF, HTa, HTs and ETs. Emissions and their contribution to each impact are distributed over four stage-wise contributions: energy input, direct emission, energy recovery and ash disposal. In general, gasification scenario (S1) exhibits the lowest impact on the majority categories (AC, NE, POF, HTa and ETs). Especially, negative values appear for AC, NE, POF and HTa of S1, indicating a net environmental benefit from using gasification-based WtE technology. Oppositely, conventional MSW incineration under French condition (S2) mostly contributes to AC, NE, HTa and ETs; however this system is the most preferable to GW. With respect to each stage, the impacts are primarily compensated by energy recovery, which avoids a significant part of emissions generated by fossil fuel-based energy production. Direct emission released during treatment is the main contributor to the total impact; while the toxic-related impacts to the soil as HTs and ETs are mostly affected by the ash disposal phase. Emissions from energy input pose insignificant impacts to S2 and S3; however its effect is more obvious in the case of S1.

CO_2 and CO are elements that contribute to GW, however CO_2 is a crucial factor since the concentration of CO is low in all systems (**Table 6. 3**). Results show that S2 system leads to the least impact. It appears that the direct GW emission from S2 is the lowest. Compared with S1, it is because in this study, the calculation is based on one ton of the wet waste. Since the MSW used in S1 contains the lowest moisture content, its combustible matter content is high so that more CO_2 is released as a result of incineration. As for S3, coal is co-fired as an auxiliary fuel, the latter contains a large amount of fossil-derived carbon that becomes another contributor to CO_2 emission. Besides, the higher GW impact of S1 but lower GW value of S2 could also be related to the input energy. Pretreatment of MSW for SRF production is required in S1, which is quite energy intensive at a consumption of 223 kwh of electricity and 0.84 liter of diesel. However this process is not necessary in S2 and S3. Although significant higher electricity can be recovered in S1, this benefit could not be comparable to the overall emissions caused by waste pretreatment and direct emission; thus leads to the highest GW impact in S1.

The principal contributors for AC are SO_2, HCl and NO_x. Compared to the direct incineration cases of S2 and S3, 162% and 110% decreases in AC have been achieved in S1, respectively. This environmental improvement can be explained by two reasons. First, a drastic reduction of direct emission has been achieved. In fact, the homogeneous gas-gas reaction in the combustor allows realizing pre-mixed flames, which can pose positive effect to limit NO_x production [4]. As seen in **Table 6. 3**, the concentration of NO_x released from S1

is 161 mg/Nm^3; while that value in S2 and S3 system attains 927 and 200 mg/Nm^3, respectively. Moreover, since syngas purification process is performed prior to combustion, acid gases such as HCl and SO_2 have also been effectively removed. Meanwhile, the environmental advantage brought by S1 is also coupled with a substantial increase in the energy recovery amount. In fact, in contrast to the heterogeneous solid-gas oxidation by conventional incineration, the "two-step" scheme allows achieving impurities removal before its fully oxidation; so that the quality of superheated steam can be improved to a higher level (540 ^oC, 121 bar in Lahti gasification plant compared with 400 ^oC, 40 bar in conventional incineration plant [25]) and the electricity generation efficiency is effectively increased.

Results from both NE and POF show that S1 leads to the least impact. Generally, NE is mainly caused by NO_x; while POF is affected by CO and dioxin emissions. Similar to AC, reduced process emissions as well as an increased electricity generation are the main reasons for the environmental benefit of S1. However, the incineration process of S2 leads to a relatively high NO_x concentration, so that the NE load from S2 is the highest among the scenarios. In view of POF, S3 exhibits the worst performance, mainly owing to that more dioxin is released, and the amount of energy recovered is the lowest among the three analyzed systems.

HTa reflects health risk on humans due to environmentally toxic substances such as dust, NO_x, SO_2 and CO. It appears that direct emission from S2 provides a significant effect to the total toxic impact. NO_x emission is the main source, which occupies not only a large generation amount, but also a high HTa equivalent factor. Once again the HTa from S1 is the lowest, due to the dual-advantages of a cleaner gas production and efficient energy generation. However, the impacts of heavy metals on the soil are elements that decisively contribute to HTs and ETs. These impacts contribute greatly to the ash disposal phase, since heavy metals contained in the ash will transfer to the soil after landfill, or will be released during the solidification/stabilization treatment.

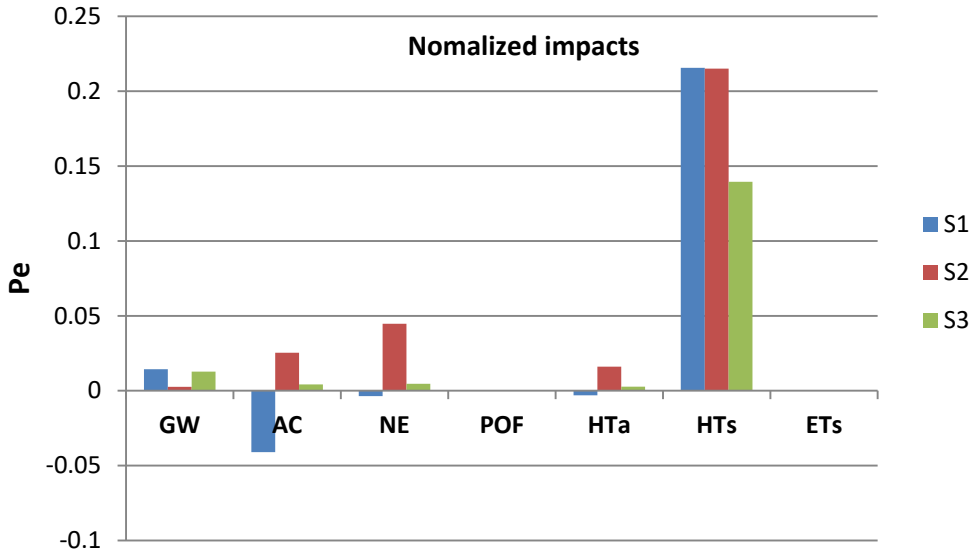

Figure 6. 6 Normalized environmental impacts of different systems: S1, gasification-based plant in Finland; S2, conventional MSW incineration plant in France; S3, conventional MSW incineration plant in China

Figure 6. 6 illustrates the normalized environmental impacts of different systems. Results reveal that HTs exhibits the highest person equivalence. Consulting its caused reasons as discussed, it could be concluded that the ash disposal process needs to be improved for decreasing the environmental loads. NE, AC and HTa are the main contributors affected by S2. Thus, effective measurements, especially for the reduction of NO_x released during incineration, become essential and inevitable.

6.2.6 Summary of the section

Based on the LCA analysis of three commercial operated WtE plants, an environmental comparison of MSW gasification and conventional incineration technologies are conducted. Results reveal that, compared with conventional MSW direct incineration, gasification-based WtE system exhibit the lowest environmental loads for the majority of impacts, i.e., AC, NE, POF, HTa and ETs. The environmental improvements are mainly due to two reasons. The energy recovery efficiency is effectively increased when using this technology, since emissions (especially HCl) are removed from the syngas before full oxidation, hence the quality of superheated steam can be improved to a higher level. A significantly increased amount of electricity can be recovered, which therefore avoids more emissions generated by fossil fuel-based energy production. Besides, the environmental advantage brought by

gasification could also be attributed to the dramatic reduction of direct emissions. In contrast to the heterogeneous solid-gas oxidation by conventional incineration, the "two-step" combustion scheme achieves a homogeneous gas-gas reaction, which is effective to limit NO_x production. Noteworthy that the syngas cleaning step before entering the combustion chamber also achieves HCl and SO_2 removal.

While taking a closer look at the two conventional incineration scenarios, plants based on the French conditions lead to an inferior performance regarding AC, NE and HTa impacts. NO_x released during incineration process is the main contributor, and therefore effective measurements to control its emission are essential. Incineration plant in China has a higher impact on GW, since the heating value of MSW is lower and coal is added as auxiliary fuel. Besides, POF under Chinese incineration plant also exhibits a higher load, since more dioxin is released, and the amount of energy recovered is lower than plants in EU countries. Regarding this fact, more strict dioxin emission limit could be regulated. Improving the level of MSW source-separated collection could also be one approach to increase the MSW calorific value. Meanwhile, increasing attentions should be paid to the ash disposal methods from both gasification and incineration systems to avoid heavy metal emissions to the soil.

Overall, the main structure of this section is presented in **Figure 6. 7**, and the determining factors as well as their degree causing each environmental impact are summarized in **Table 6. 5**.

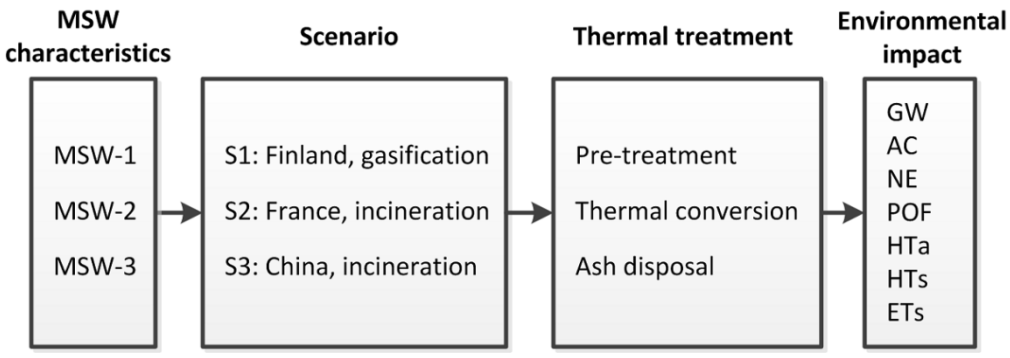

Figure 6. 7 Main research structure for the LCA comparison of MSW gasification and incineration technologies

Table 6. 5 Main factors and their degree causing different environmental impacts

		S1	S2	S3
Non-toxic impacts	GW	**+++** [a] (MSW characteristics, pre-treatment) [b]	**+** (Thermal conversion)	**++** (MSW characteristics, thermal conversion)
	AC	**+** (Pre-treatment)	**+++** (Thermal conversion)	**++** (Thermal conversion)
	NE	**+** (Thermal conversion, pre-treatment)	**+++** (Thermal conversion)	**++** (Thermal conversion)
	POF	**+** (Pre-treatment)	**++** (Thermal conversion)	**+++** (MSW characteristics, thermal conversion)
Toxic impacts	HTa	**+** (Thermal conversion, pre-treatment)	**+++** (Thermal conversion)	**++** (Thermal conversion)
	HTs	**+++** (Ash disposal)	**++** (Ash disposal, thermal conversion)	**+** (Ash disposal)
	ETs	**+** (Ash disposal)	**+++** (Ash disposal)	**++** (Ash disposal)

[a] The symbol of '+' and '-' represents the degree of the related environmental impact for different scenarios. '+++' means that the scenario exhibits the highest environmental load related to the specified impact; while '+' means that the scenario exhibits the lowest impact.

[b] Processes inside the bracket mean the determining factors causing the related environmental impact.

6.3 Pyro-gasification optimization: emphasis on energy efficient and environmental sound applications

Results from **Section 6.2** prove that, the "two-stage" gasification-based WtE scheme is able to reduce environmental emissions and improve the energy recovery efficiency compared to conventional MSW incineration. On the other hand, one outstanding advantage of the pyro-gasification process is its potential to generate a syngas fitting different applications. As presented in **Chapter 1**, syngas could be combusted in a gas boiler combined with a steam turbine; or after a more or less advanced purification step, used in devices with higher energy efficiency such as gas turbine or internal combustion engine. It could even be served as feedstock for chemicals such as ammonia or methanol or bio-fuels production [26, 27]. The most common configuration nowadays is to burn the syngas in a boiler for power/heat generation (e.g. as the Lahti plant that was analyzed in this study); since the steam cycle is easy to handle and a gas pre-treatment following tar removal is not required. However, one example using the IGCC has already appeared in the SVZ gasification plant in Germany [3]. Considering the continuously developing syngas cleaning and catalytic tar reduction technologies, it is believed that more approaches for the utilization of syngas will be available in a near future. Regarding this fact, a quantitative assessment of the different pyrolysis and gasification utilization approaches is conducted using LCA methodology, with the aim to help guide and optimize an energy-efficient and environmental-sound application route.

6.3.1 Scenarios definition

Based on the main aim of the study, the LCA system boundary is drawn in **Figure 6. 8**. In general, the investigation includes both MSW pyrolysis/gasification conversion and the subsequent downstream products utilization phase. Three types of energy utilization options are considered, hence a total of six scenarios are evaluated: S1, S2 and S3 represents pyrolysis combined with steam turbine, gas turbine, and internal combustion engine, respectively; while similarly their counterparts under gasification condition are defined as S4, S5 and S6. Our study is mainly focused on WtE routes, thus other potential applications such as Fischer-Tropsch or chemicals production are not included.

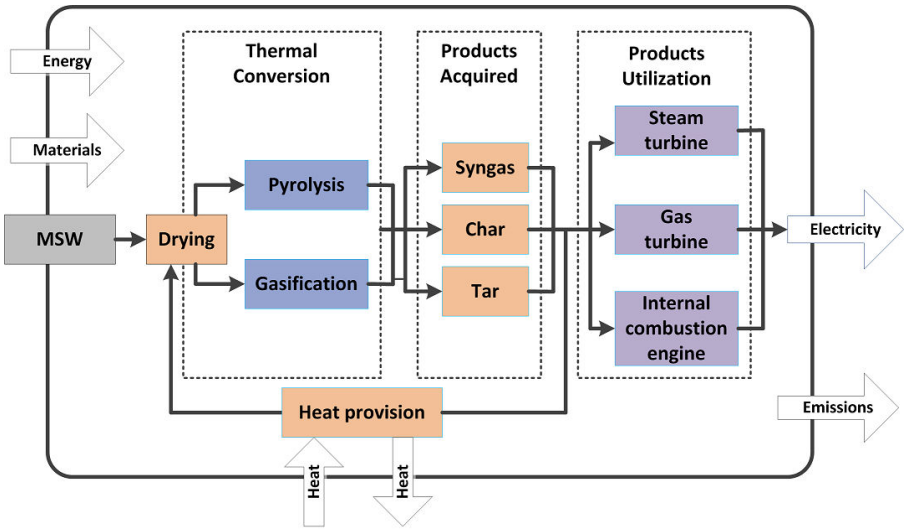

Figure 6. 8 System boundary for the evaluation of pyro-gasification syngas utilization approaches

As for the previous part of the study, one ton of MSW is set as the functional unit. Energy and material flows as inputs and outputs are shown with arrows in **Figure 6. 8**. A drying step is performed prior to the pyrolysis/gasification process to lower the MSW moisture content [28]. The heat required for drying and reaction is assumed to be supplied by char and/or tar combustion, which is typical in industrial applications. Similarly as the evaluation mode in **Section 6.2**, MSW collection and transportation are excluded since they are identical in all scenarios. Again, emissions from plant construction are omitted. From the life cycle perspective, the production of the used energy and materials is included apart from their consumption phase. The relevant data is derived from the Gabi software database. Allocation of the recovered electricity is again considered on the same substitution basis as in the **Section 6.2** adopted here.

6.3.2 Life cycle inventory and assessment indicator

MSW physical and chemical properties based on local condition in China, as given in **Table 6. 1**-**Table 6. 2**, are used as calculation basis. It needs to be emphasized that, the assessment presented in **Section 6.2** is based on industrial-scale operating, while the analysis in this section is a theoretical calculation, i.e., the data are mostly obtained from literature. It is on one hand due to the data unavailability because of the lack of relevant industrial practice; on the other hand, this calculation method provides a convenient and transparent basis for the comparison of different scenarios.

Data on pyrolysis and gasification conversion phase are obtained from our previous experiments in a fluidized bed. N_2 and air acts as fluidization agent for pyrolysis and gasification, respectively. MSW is dried beforehand to adjust the moisture content to ca. 10%. A series of tests under different temperatures and equivalent ratios are investigated to identify the most optimal working condition. The temperature ranges from 550 to 850 ^{o}C in 100 ^{o}C increments; and ERs under each temperature vary from 0 to 0.8. Under each test, the three-phase product yield, gas composition and energy distribution are acquired. More detailed experimental procedures and results could be found in Dong et al. [29].

The energy conversion efficiency, which represents the total quantity of energy escaping the furnace (syngas + tar), is set as the evaluation index for different tests. Experimental results show that gasification under a temperature of 650 ^{o}C and an equivalent ratio of 0.4 achieves the highest efficiency, while 850 ^{o}C is the most suitable temperature for pyrolysis. Therefore, the features of these two working conditions are employed in the LCA, with the detailed information listed in **Table 6. 6**.

Table 6. 6 Products features of pyrolysis and gasification process used in LCA study

Working condition	Pyrolysis	Gasification
	Temperature: 850 ^{o}C Equivalent ratio: 0	Temperature: 650 ^{o}C Equivalent ratio: 0.4
Syngas yield, m^3/kg-MSW	1.20	2.32
Syngas LHV, MJ/m^3	7.64	4.50
Tar yield, kg/kg-MSW [a]	0.15	0.07
Tar LHV, MJ/kg	21.04	20.69
Char yield, kg/kg-MSW	0.22	0.18
Char LHV, MJ/kg	14.06	10.52

[a] Moisture content is excluded.

[b] Data source from Dong et al. [29].

Three energy conversion devices are considered: steam turbine, gas turbine, and internal combustion engine; their efficiencies are obtained from typical operating values. **Table 6. 7** summarizes the plant efficiencies when used in different energy utilization cycles. The efficiency of the gas boiler-steam turbine cycle (S1, S4) is set at 27.8%, which is higher than the efficiency from conventional MSW incineration plant since the homogenous, gas-phase combustion is more controllable and effective [4]. Meanwhile, syngas from

pyrolysis/gasification can also be used in gas turbine combined cycle (S2, S5) or internal combustion engine (S3, S6), and an efficiency of 35.5% and 25.0% can be reached [30, 31], respectively.

Table 6. 7 Plant efficiency of different power generation systems

	Gas boiler-steam turbine [a]	Gas turbine combined cycle [a]	Internal combustion engine [b]
Power output efficiency, %	27.8	35.5	25.0

[a] Data source: [31]

[b] Data source: [30]

For gas boiler-steam turbine cycle scenarios (S1, S4), syngas and tar are fully oxidized in the secondary combustion chamber for heat recovery; while for scenarios of S2, S3, S5 and S6, the syngas is cooled and purified for tar removal to meet the stringent gas quality requirement needed for gas turbine or internal combustion engine. According to the theoretical calculation and experimental observation, autothermal gasification could be achieved under temperature of 650 ^{o}C and equivalent ratio of 0.4, hence no additional heat source is required for the gasification scenarios (S4-S6). However, since pyrolysis is an endothermic process, external energy source is necessary. In this study, the energy required for pyrolysis is assumed to be provided by char and/or tar combustion, which is supposed to take place in a separate furnace. The process thermal efficiency is set at 75%, which is a typical value for industrial heating boilers in operation [22]. And for gasification process, since the quality of produced tar and char is normally quite low, they are not treated as by-products and their utilization is not considered.

Besides, since the moisture content of the raw MSW is relatively high (53.3%, as shown in **Table 6. 2**), the MSW needs to be dried prior to pyrolysis and gasification [28]. The MSW is assumed to be pre-treated to a moisture content of ca. 10%, which is in agreement with the experimental condition. For steam turbine scenarios of S1 and S4, exhaust steam from the turbine is used to offset the energy demand for drying, with the surplus sent for electricity production. For scenarios of S2, S3, S5 and S6, the heat recovered from the syngas cooling phase is assumed as the heating source. A thermal utilization efficiency of 90% is set for the drying process [22]. The quantity of energy needed in each sector is verified in the calculation to ensure the energy balance.

As for the environmental emissions, both the air pollutions discharged from thermal treatment and the pollutions to the soil from ash disposal are considered. The pollutants investigated include CO_2, CO, SO_2, NO_x, HCl, dust, dioxin and heavy metals contaminations both for air and soil. Since MSW pyrolysis and gasification technologies are not yet commercially applied in China, the national pollution control standards are used to determine the emission factors. The emitted pollutants from gas boiler and gas turbine meet the corresponding required emission limits of Air Pollution Standard for Thermal Power Plant (GB 13223-2011) [32]. Since no limit standards are currently available for the emissions from internal combustion engine, limits of the oil power plant are adopted, which are also regulated by GB 13223-2011 [32]. Toxic-related emissions as heavy metals and dioxin are assumed to be in agreement with Standard for Pollution Control on MSW Incineration (GB 18485-2001) [33]. The relevant emission factors are summarized in **Table 6. 8**.

Table 6. 8 Emission factors used for the syngas utilized in steam turbine, gas turbine, and internal combustion engine

Device	Gas boiler-steam turbine	Gas turbine	Internal combustion engine
Scenario	S1, S4	S2, S5	S3, S6
CO, mg/Nm^3 [a]	150	150	150
SO_2, mg/Nm^3	35	35	50
NO_x, mg/Nm^3	100	50	120
HCl, mg/Nm^3 [b]	75	0	0
Dust, mg/Nm^3	5	5	20
Dioxin, ng TEQ/Nm^3	1.0	1.0	1.0
Hg, mg/Nm^3	0.2	0.2	0.2
Pb, mg/Nm^3	1.6	1.6	1.6
Cd, mg/Nm^3	0.1	0.1	0.1

[a] No limit standard is regulated for CO from the three devices, therefore the standard from incineration plant is used;

[b] HCl emitted from gas boiler-steam turbine is set as the same from incineration plant; while this value is set at 0 for gas turbine and internal combustion engine because HCl is considered to be removed during syngas purification process.

Similarly as in **Section 6.2**, EDIP 97 method is used as the LCIA basis. Both the life cycle environmental and energetic impacts are analyzed. Environmental indicators considered include GW, AC, NE, HTa, HTs and ETs. Results are presented in normalized values, i.e., Pe.

Life cycle energy performance is measured by energy conversion efficiency, which is defined as the sum of output electricity and heat divided by the total input energy. The calculation method is shown in Eqs. (6.1) and (6.2):

$$\text{Energy conversion efficiency} = \frac{E_{Heat} + E_{Elec}}{E_{total}} \quad (6.1)$$

$$E_{total} = E_{MSW} + E_{Thermal\,conversion} + E_{Ash\,disposal} + E_{Energy\,production} \quad (6.2)$$

6.3.3 Life cycle interpretation

6.3.3.1 Environmental impacts

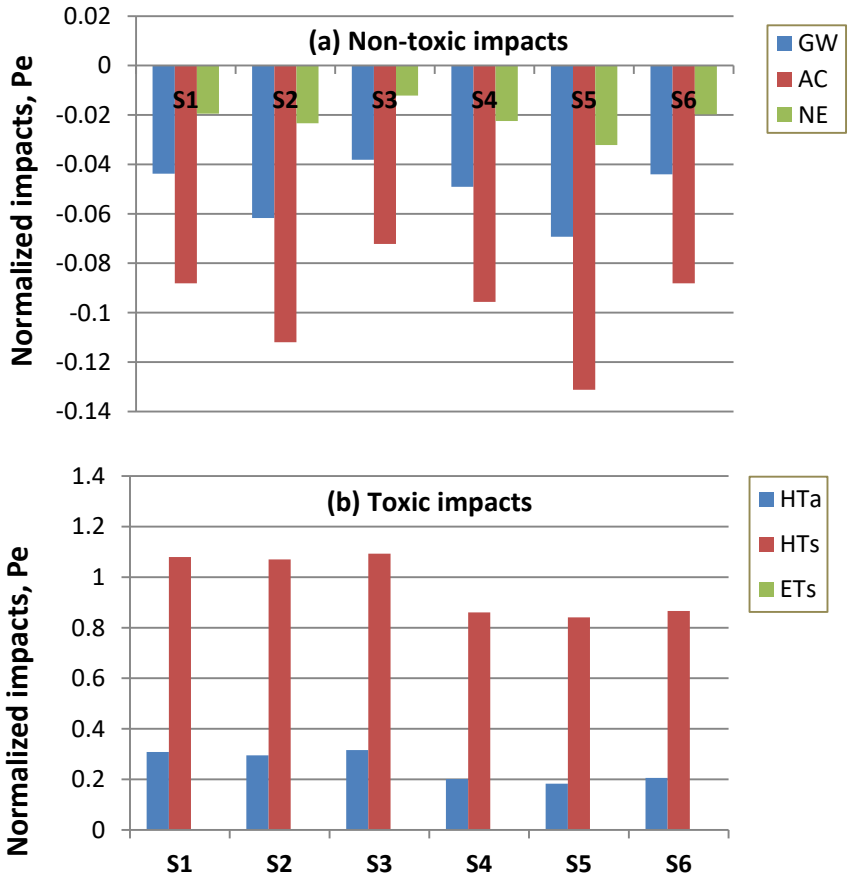

Figure 6. 9 Normalized environmental impacts of different systems: (a) non-toxic impacts; (b) toxic impacts. S1, pyrolysis + steam turbine; S2, pyrolysis + gas turbine; S3, pyrolysis + internal combustion engine; S4, gasification + steam turbine; S5, gasification + gas turbine; S6, gasification + internal combustion engine

The normalized environmental impacts from different scenarios are illustrated in **Figure 6. 9**. Results reveal that all the non-toxic impacts (GW, AC and NE) are given in negative values. It indicates that the environmental benefits from the recovered energy have surpassed the sum of emissions generated during the life cycle, and therefore net environmental savings can actually be achieved. Nevertheless, toxic-related impacts such as HTa, HTs and ETs show positive values, which indicate the net environmental loadings. When giving a parallel comparison of different pyrolysis and gasification cycles, gasification equipped with gas turbine (S5) leads to the least impact. S2 (pyrolysis + gas turbine) also exhibits a good performance, which reveals that using a more efficient energy conversion device like gas turbine allows counterbalancing more emissions by substituting more of the conventional energy production. Gas boiler-steam turbine systems (S1, S4) rank after; the same reason could be responsible for the environmental benefits in that case. However, S3 and S6 (internal combustion engine systems) rank the last. Although direct emissions during thermal treatment could be controlled at a lower level, this benefit is at the sacrifice of the energy recovery efficiency. As shown in **Table 6. 8**, the plant efficiency using internal combustion engine is the lowest, since the syngas has to be cooled for purification and part of the energy is lost. However, results also reveal that pyrolysis systems are inferior to those of gasification, due to the higher input energy required for the pyrolysis process.

Based on the results, the contribution of different unit stages to the overall impacts is further investigated, with the aim to seek for potential improvements. The total impacts are divided into four processes: direct emission, energy input, energy recovery and ash disposal. Their contribution to each impact category is illustrated in **Figure 6. 10**, with their detailed underlying effects analyzed as follows.

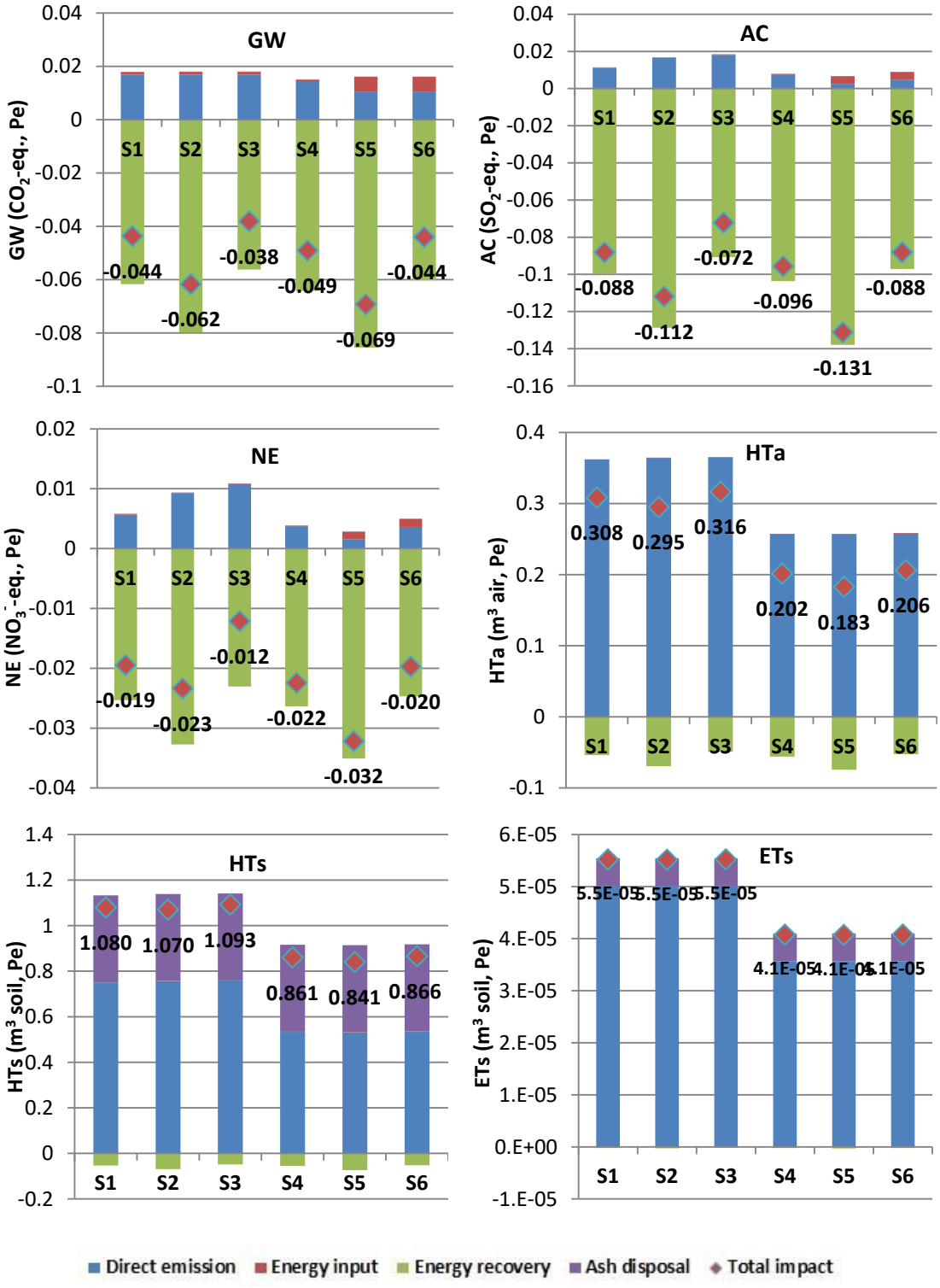

Figure 6. 10 Effect of different unit processes to the normalized environmental impacts: S1, pyrolysis + steam turbine; S2, pyrolysis + gas turbine; S3, pyrolysis + internal combustion engine; S4, gasification + steam turbine; S5, gasification + gas turbine; S6, gasification + internal combustion engine

For different systems, the distinctions for the non-toxic impacts (GW, AC and NE) are primarily attributed to energy recovery, which compensates a significant part of emissions generated by fossil fuel-based energy production. However, the differences in the scores of toxic-related impacts are mostly affected by direct emissions. It appears that the S5 system, which represents gasification combined with gas turbine, exhibits the lowest environmental loadings of all the analyzed impact categories. The reduced emissions as well as the increased energy generation are responsible for the environmental improvement. Actually, the purification of syngas prior to combustion could lead to acid gases removal; especially for HCl and SO_2, which are the main causes for equipment erosion and AC potential. The combustion technique inside the gas turbine is also an important aspect to limit NO_x generation as a result of the pre-mixed flames. Besides, increased amount of electricity can be recovered since the efficiency of the gas turbine is higher (35.5%) than steam turbine and internal combustion engine. Given these reasons, effective syngas purification coupled with gas turbine cycle could be an effective improvement optimization for the current gasification technique.

However, it is also important to emphasize that some issues are fairly vital regarding the gasification-gas turbine cycle. First, the recovery of heat that occurs during syngas cooling phase is important; otherwise the sensible heat of the syngas will lose and decrease the overall plant efficiency. Besides, careful attentions should be paid to the heavy metal leaching during the ash disposal phase, since it occupies a significant proportion of HTs and ETs potential among all the analyzed systems.

6.3.3.2 Energy conversion efficiency

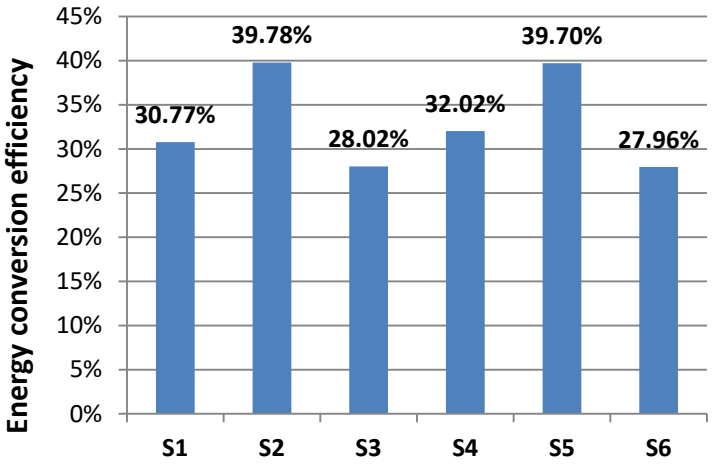

Figure 6. 11 Life cycle energy conversion efficiency of different thermochemical conversion/combustion systems: S1, pyrolysis + steam turbine; S2, pyrolysis + gas turbine; S3, pyrolysis + internal combustion engine; S4, gasification + steam turbine; S5, gasification + gas turbine; S6, gasification + internal combustion engine

The life cycle energy indicator, represented by energy conversion efficiency, is illustrated in **Figure 6. 11**. Similar to the environmental results, energy conversion efficiency of the different utilization cycles is: (S2, S5) ＞ (S1, S4) > (S3, S6), which is mainly determined by the efficiency of the energy conversion device. The energy conversion efficiency of gas turbine systems reaches approximately 40%, while that value of steam turbine cycles reaches ca. 31-32%. It is observed that, a much higher efficiency could be achieved by using these technologies, in comparison with the typical MSW incineration plant (19-27%) [3]. Also, unlike environmental assessment results, pyrolysis coupled with gas turbine and internal combustion engine exhibit as high energy conversion as their counterpart gasification systems. The results highlight the importance for the utilization of pyrolysis by-products, which could effectively be served as energy source to offset process energy demand, such as the heat required for MSW pre-drying, and to maintain pyrolysis reactions.

6.3.4 Summary of the section

Syngas obtained from pyro-gasification could be used via various approaches, which enlarges the application routes. However, the different energy utilization options downstream of the gasifier will significantly vary the overall energy efficiency and environmental effects. Regarding the fact, pyrolysis and gasification coupled with three types of energy utilization cycles, i.e., gas boiler-steam turbine, gas turbine and internal combustion engine, is analyzed by LCA. The main structure of this section could be illustrated by **Figure 6. 12**, and the environmental and energetic performance of different pyrolysis/gasification scenarios is summarized in **Figure 6. 13**.

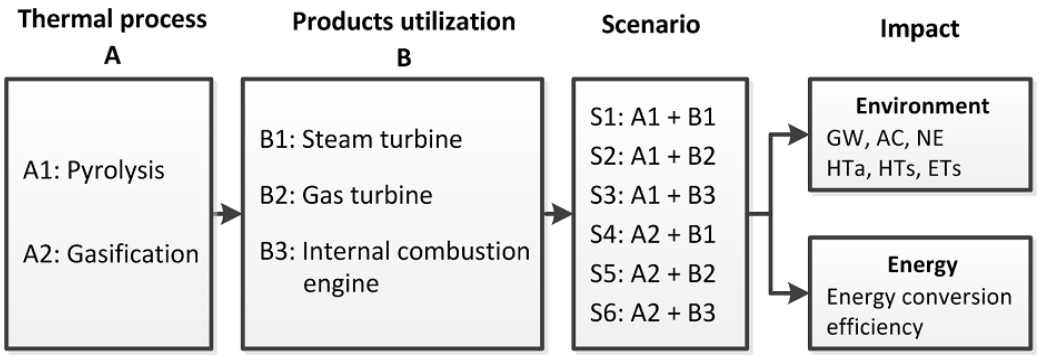

Figure 6. 12 Main research structure for the LCA comparison of MSW pyro-gasification products utilization approaches

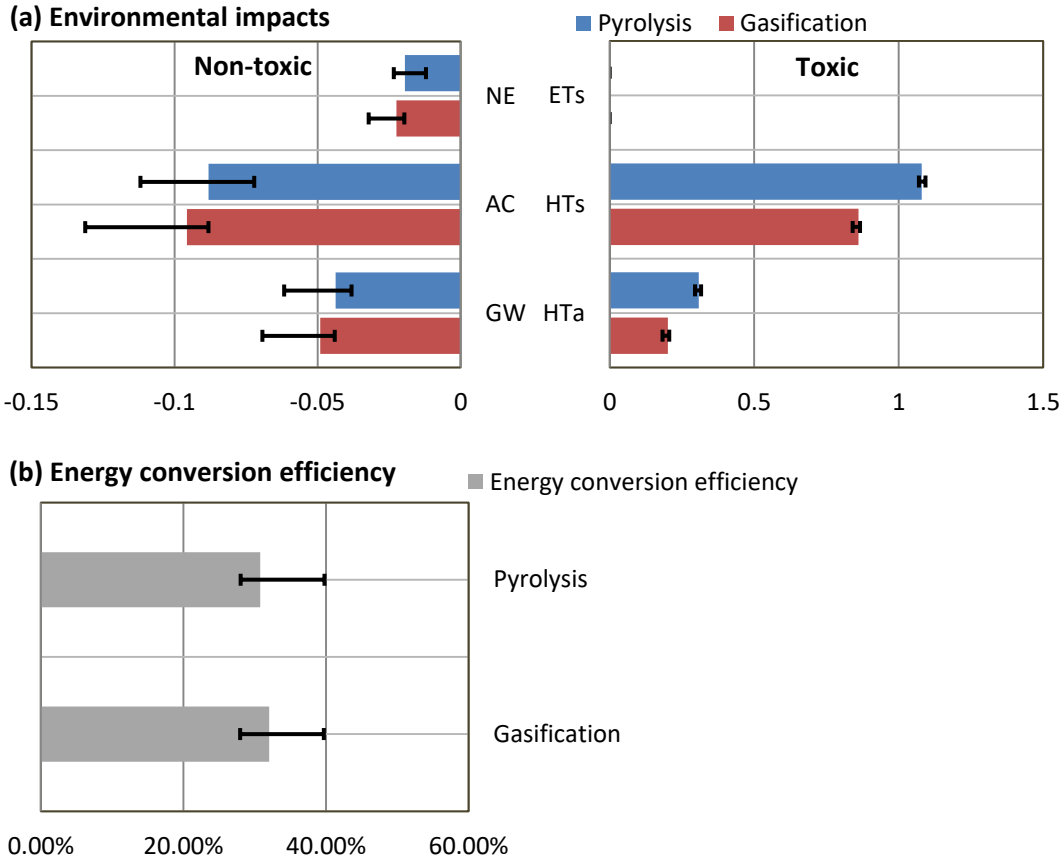

Figure 6. 13 Summary for the environmental and energetic performance of different pyrolysis/gasification scenarios (lowest value, default value and highest value in the figure represents the utilization of gas turbine, steam turbine and internal combustion engine, respectively)

Environmental results show that gasification equipped with a gas turbine leads to the least impacts. The environmental benefits are primarily attributed to the energy recovery, revealing that using a more efficient energy conversion device allows counterbalancing more emissions by substitution of conventional energy production. Meanwhile, the direct emissions are also reduced to a large extent, thanks to the acid gases removal prior to syngas combustion. Pyrolysis systems are inferior to gasification, due to the higher energy required for their processes. Results from life cycle energy conversion efficiency exhibit a similar trend, with steam turbine systems rank after and internal combustion engine systems tread on the heels. Given these reasons, an effective syngas purification coupled with gas turbine cycle could be an effective optimization for the current gasification technique; while more attentions should be paid to efficient heat recovery during syngas cooling phase as well as to prevent heavy metal leaching during the ash disposal.

6.4 Sensitivity analysis

During LCA calculation, the problem of data uncertainty may limit the reliability of the final performance [9]. To determine the significance of some key parameters on the overall environmental impact, as well as to seek for improvement measurements, sensitivity analysis is conducted. The baseline scenario in **Section 6.2** and **Section 6.3** is compared with three variations: the use of CHP production, the effect of energy substitution, and the source of emission factors, with their influence discussed in detail as follows.

6.4.1 Use of combined heat and electricity production

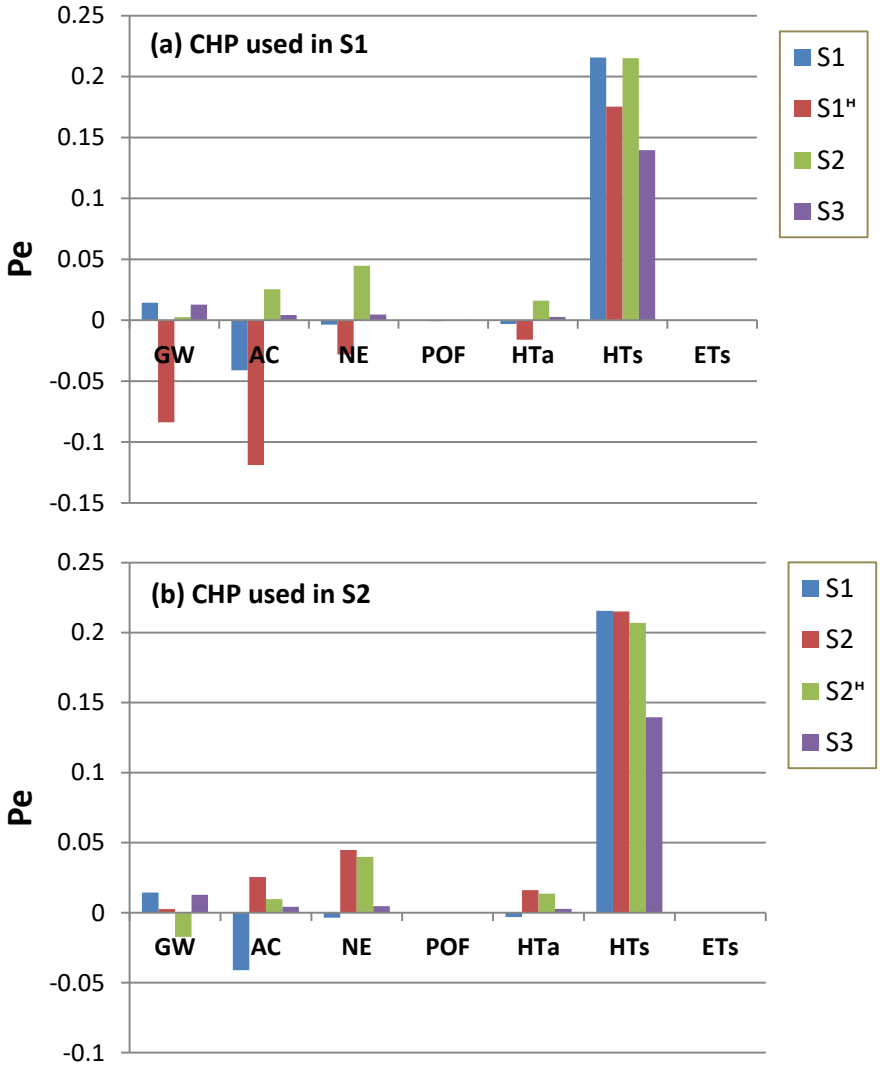

Figure 6. 14 Sensitivity analysis of different WtE technologies. Results are presented as normalized environmental impacts: S1, gasification-based plant in Finland; S2, conventional MSW incineration plant in France; S3, conventional MSW incineration plant in China; superscript letter 'H' represents the use of CHP production in specified plant

As mentioned in **Section 6.2**, the gasification plant in Finland (S1) is actually operated with CHP production, while approximately 26% French incinerators are also CHP type. To investigate their effect, the energy of the gasification plant and French incineration plant is assumed to be recovered by CHP mode, respectively, and the corresponding environmental impacts are shown in **Figure 6. 14**. Results from both $S1^{H}$ and $S2^{H}$ systems show that the use of CHP has significant benefits for all the environmental impacts. Since CHP is more efficient, these environmental savings are due to the increasing substitution of fossil fuels to generate electricity and the associated emissions. It demonstrates the importance of maximizing the efficiency of energy recovery. CHP could be regarded as a feasible option, if the specified region requires a constant demand for process heating [34].

6.4.2 Effect of energy substitution

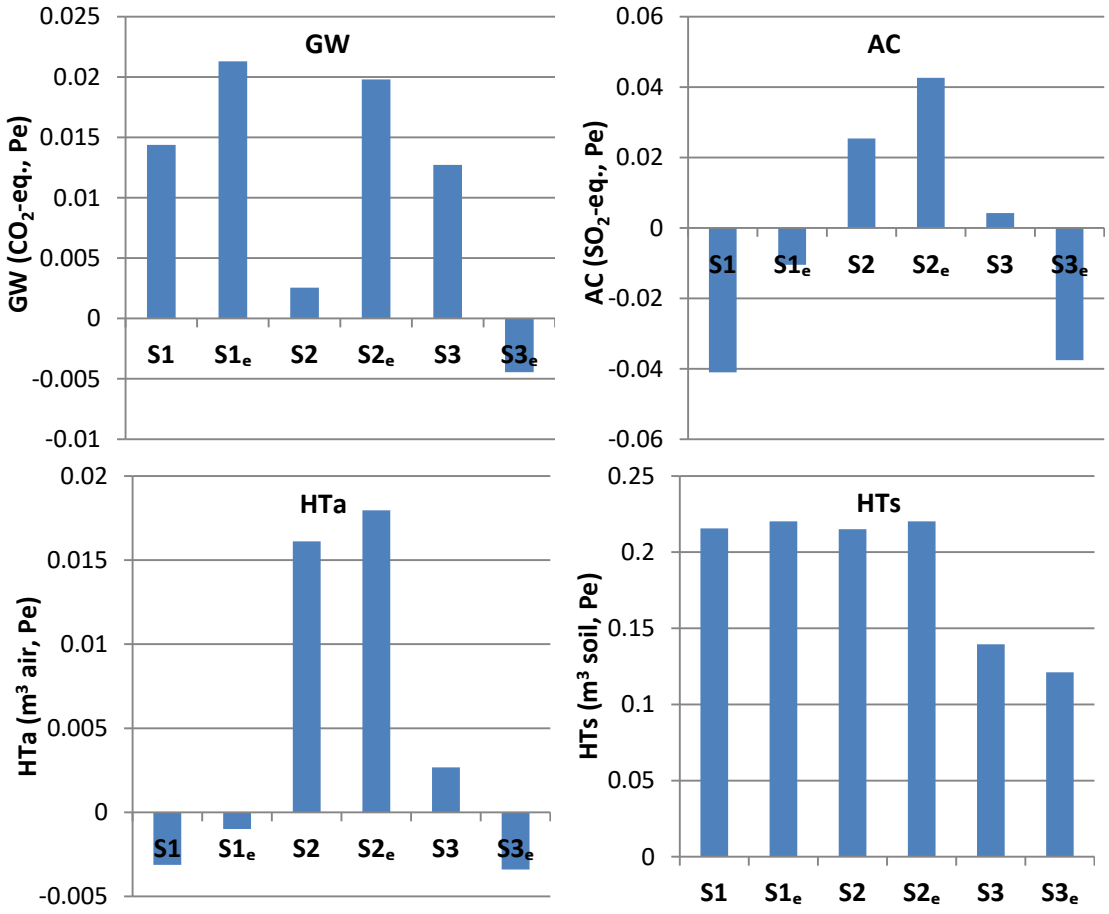

Figure 6. 15 Sensitivity analysis of different WtE technologies. Results are presented as normalized environmental impacts: S1, gasification-based plant in Finland; S2, conventional MSW incineration plant in France; S3, conventional MSW incineration plant in China; subscript letter 'b' represents the use of local electricity mix data in specified countries

In **Section 6.2**, the electricity produced at the WtE plant is delivered to the power grid thus substituting the energy produced by conventional means. In default situation, the EU energy structure is set as the calculation baseline. However, since the electricity mix profile under each local country differs significantly, its effect on the final results is thus further investigated.

Figure 6. 15 illustrates the comparison of the relevant environmental impacts, with GW, AC, HTa and HTs taken for depth analysis. The influence of the electricity mix is found to be significantly crucial to the overall result. If the local electricity grid data are adopted, conventional MSW incineration under the Chinese condition ($S3_e$) could even surpass gasification system (S1, $S1_e$) and becomes the most environmental friendly treatment option. This is because the energy structure of China is highly relied on fossil fuels, which produces significantly higher emissions compared with renewable energy-based electricity production. Conversely, $S1_e$ and $S2_e$ become less environmental friendly than their baseline systems, since the proportion of cleaner energy used in these two countries is higher than the EU average. The results reveal that the systems are highly sensitive to the changes in electricity substitution, hence, assumptions on the marginal electricity are critical for the final scores of different WtE technologies.

6.4.3 Emission factors derived from literature

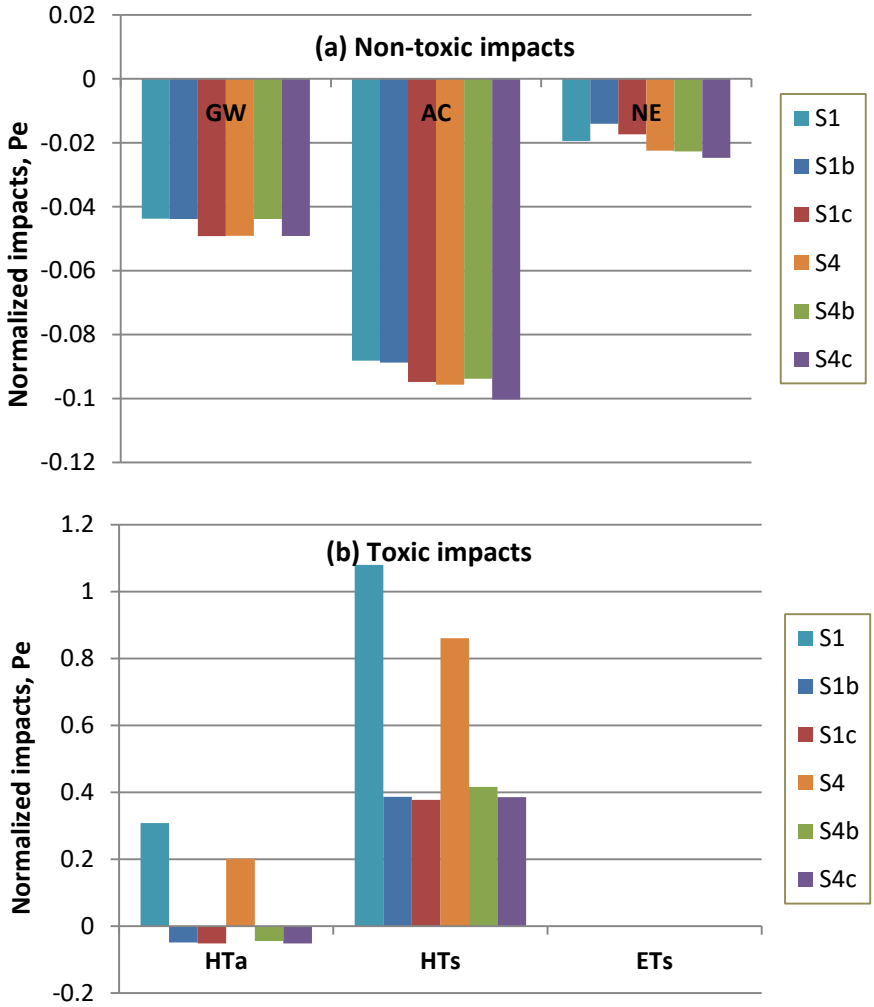

Figure 6. 16 Sensitivity analysis of different pyrolysis/gasification energy utilization cycles by using different emission factors. Results are presented as normalized environmental impacts: S1, pyrolysis + steam turbine; S4, gasification + steam turbine; b, emission factors based on UK plant; c, emission factors based on Chinese plant

Due to the data unavailability, the direct emissions from **Section 6.3** are derived from the Pollution Control Standards. However, as shown in **Figure 6. 10**, direct emissions have posed significant effect to the overall environmental impacts. As a result, sensitivity analysis is conducted regarding different emission sources. Two sets of emission factors are adopted, which are derived from literatures based on UK and China's on-site operating (defined as set 'b' and 'c', respectively) [23, 35]. S1 and S4 systems, presenting pyrolysis and gasification using steam turbine, are compared to demonstrate the changed tendency, with the relevant results shown in **Figure 6. 16**. Results show that compared with baseline systems of S1 and

S4, all the environmental impacts experience a significantly decrease when using real operating data (S1b, S1c, S4b, S4c). Especially, HTa is turned from positive to negative values, which represent the net environmental benefit instead of environmental loading. It reveals that, pyro-gasification based WtE plants are feasible to meet the pollution control standards, which are suitable to be served as potential improvement for the current MSW direct incineration technology.

6.5 Summary of Chapter

To verify the environmental and energetic performance of MSW pyro-gasification technologies, as well as to seek for potential improvement approaches, two LCA studies are conducted in this chapter. In **Section 6.2**, three commercial operated WtE plants, including one MSW gasification-based power plant in Finland and two conventional incineration plants in both France and China, are quantitatively compared. In **Section 6.3**, pyrolysis and gasification coupled with three types of energy utilization cycles, i.e., gas boiler-steam turbine, gas turbine and internal combustion engine, are modeled. The major findings based on the analysis are summarized as follows.

- Gasification-based WtE system shows a better environmental performance than the conventional MSW incineration technology. The reduced process emissions as well as the increased electricity generation, are the main reasons for the environmental benefits. By using gasification, acid gases such as HCl and SO_2 could be removed prior to combustion; so that the quality of superheated steam can be improved to a higher level. As a result, a significant increased amount of electricity can be recovered, which thus avoids more emissions generated by fossil fuel-based energy production.
- For different pyro-gasification energy utilization cycles, gasification equipped with gas turbine leads to the least environmental loadings, steam turbine systems rank after and internal combustion engine systems tread on the heels. Effective syngas purification coupled with gas turbine cycle could be an effective optimization for the current gasification technique.

Based on the results and the sensitivity analysis, some potential improvements are thus proposed:

- For both MSW gasification and conventional incineration technologies, the use of CHP as energy recovery mode is an effective approach to maximize the plant efficiency and to reduce the environmental impacts. However, more attentions should be paid to avoid heavy metals leaching during the ash disposal phase.
- To achieve a higher overall plant efficiency if gas turbine and internal combustion engine systems are adopted, the heat during syngas cooling phase needs to be effectively recovered. Especially for pyrolysis systems, the utilization of by-products as tar and char is of great importance due to the higher input process energy required.
- For conventional MSW incineration, the plants based on French condition are primarily affected by NO_x emission, thus effective control measurements would be essential. The main issue regarding incineration plants in China is the low MSW calorific value, which leads to a high quantity of required auxiliary fuel as well as a lower amount of recovered energy. Improving the level of MSW source-separated collection could be an effective approach. Besides, more strictly dioxin emission limit for dioxin emission is expected to be regulated to reduce toxic-related impacts.

6.6 Bibliography

[1] ISO. ISO 14040: Environmental management-Life cycle assessment-Principles and Framework. Geneva: ISP copyright office; 1997.

[2] Wenzel H., Hauschild M.Z., Alting L. Environmental Assessment of Products, Volume 1: Methodology, tools and case studies in product development. London, UK: Chapman and Hall; 1997.

[3] Panepinto Deborah, Tedesco Vita, Brizio Enrico, Genon Giuseppe. Environmental performances and energy efficiency for MSW gasification treatment. Waste and Biomass Valorization. 2015;6:123-135.

[4] Consonni Stefano, Viganò Federico. Waste gasification vs. conventional Waste-To-Energy: A comparative evaluation of two commercial technologies. Waste Management. 2012;32:653-666.

[5] McDougall Forbes R, White Peter R, Franke Marina, Hindle Peter. Integrated solid waste management: a life cycle inventory. 2nd ed. ed. UK: Blackwell Science Ltd.; 2008.

[6] Leckner Bo. Process aspects in combustion and gasification Waste-to-Energy (WtE) units. Waste Management. 2015;37:13-25.

[7] Chen Dezhen, Christensen Thomas H. Life-cycle assessment (EASEWASTE) of two municipal solid waste incineration technologies in China. Waste Management & Research. 2010;28(6):508-519.

[8] Hoornweg Daniel, Bhada-Tata Perinaz. What a waste: a global review of solid waste management. Washington DC: The World Bank; 2012.

[9] Ning Shu-Kuang, Chang Ni-Bin, Hung Ming-Chien. Comparative streamlined life cycle assessment for two types of municipal solid waste incinerator. Journal of Cleaner Production. 2013;53:56-66.

[10] Turconi Roberto, Butera Stefania, Boldrin Alessio, Grosso Mario, Rigamonti Lucia, Astrup Thomas. Life cycle assessment of waste incineration in Denmark and Italy using two LCA models. Waste Management & Research. 2011:0734242X11417489.

[11] Lahti Energia. http://www.lahtigasification.com/.

[12] Savelainen Janne, Isaksson Juhani. Kymijärvi II plant: High-efficiency use of SRF in power production through gasification. Report by Lahti Energy Ltd and Metso Power Oy, Finland 2015.

[13] Beylot Antoine, Villeneuve Jacques. Environmental impacts of residual Municipal Solid Waste incineration: A comparison of 110 French incinerators using a life cycle approach. Waste Management. 2013;33:2781-2788.

[14] Spliethoff Hartmut. Power generation from solid fuels: Springer Science & Business Media; 2010.

[15] Kourkoumpas Dimitrios-Sotirios, Karellas Sotirios, Kouloumoundras Spiros, Koufodimos Georgios, Grammelis Panagiotis, Kakaras Emmanouel. Comparison of waste-to-energy processes by means of life cycle analysis principles regarding the global warming potential impact: applied case studies in Greece, France and Germany. Waste and Biomass Valorization. 2015;6:605-621.

[16] Directive EC Waste Incineration. Directive 2000/76/EC of the European Parliament and of the Council on Incineration of Waste. European Commission, Brussels. 2000.

[17] Dong Jun, Chi Yong, Zou Daoan, Fu Chao, Huang Qunxing, Ni Mingjiang. Comparison of municipal solid waste treatment technologies from a life cycle perspective in China. Waste Management & Research. 2014;32:13-23.

[18] Hangzhou Environmental Protection Bureau. Hangzhou environmental state bulletin 2014. Hangzhou: Hangzhou Environmental Protection Bureau; 2015.

[19] Hangzhou Municipal Solid Waste Disposal Supervision Center. Hangzhou municipal solid waste physical property analysis and disposal method. Hangzhou: Municipal Solid Waste Disposal Supervision Center; 2011.

[20] Frankenhaeuser Martin. European standardisation of solid recovered fuels. VTT Symposium: VTT; 1999; 2002. p. 283-286.

[21] Pressley Phillip N, Aziz Tarek N, DeCarolis Joseph F, Barlaz Morton A, He Feng, Li Fanxing, et al. Municipal solid waste conversion to transportation fuels: a life-cycle estimation of global warming potential and energy consumption. Journal of Cleaner Production. 2014;70:145-153.

[22] Roberts Kelli G, Gloy Brent A, Joseph Stephen, Scott Norman R, Lehmann Johannes. Life cycle assessment of biochar systems: estimating the energetic, economic, and climate change potential. Environmental Science & Technology. 2009;44:827-833.

[23] DEFRA UK. Review of Environmental and Health Effects of Waste Management: municipal solid waste and similar wastes. London: Defra Publications; 2004.

[24] U.S. Energy Information Administration (EIA). International Energy Statistics 2012 (http://www.eia.gov/). 2012.

[25] Arena Umberto, Ardolino Filomena, Di Gregorio Fabrizio. A life cycle assessment of environmental performances of two combustion-and gasification-based waste-to-energy technologies. Waste Management. 2015;41:60-74.

[26] Bridgwater AV. Catalysis in thermal biomass conversion. Applied Catalysis A: General. 1994;116:5-47.

[27] Molino Antonio, Chianese Simeone, Musmarra Dino. Biomass gasification technology: The state of the art overview. Journal of Energy Chemistry. 2016;25:10-25.

[28] McKendry Peter. Energy production from biomass (part 3): gasification technologies. Bioresource Technology. 2002;83:55-63.

[29] Dong Jun, Chi Yong, Tang Yuanjun, Ni Mingjiang, Nzihou Ange, Weiss-Hortala Elsa, et al. Effect of Operating Parameters and Moisture Content on Municipal Solid Waste Pyrolysis and Gasification. Energy & Fuels. 2016;30:3994-4001.

[30] Belgiorno V, De Feo G, Della Rocca C, Napoli RMA. Energy from gasification of solid wastes. Waste Management. 2003;23:1-15.

[31] Morris Michael, Waldheim Lars. Energy recovery from solid waste fuels using advanced gasification technology. Waste Management. 1998;18:557-564.

[32] MEP AQSIQ. GB 13223-2011, Emission Standard of Air Pollutants for Thermal Power Plants. China Environmental Science Press, Beijing. 2011.

[33] China State Environmental Protection Administration. Pollution Control Standard for Municipal Solid Waste Incineration (GB 18485-2001). Beijing: China Environmental Science Press; 2001.

[34] Burnley Stephen, Coleman Terry, Peirce Adam. Factors influencing the life cycle burdens of the recovery of energy from residual municipal waste. Waste Management. 2015;39:295-304.

[35] Liu Yangsheng, Liu Yushan. Novel incineration technology integrated with drying, pyrolysis, gasification, and combustion of MSW and ashes vitrification. Environmental Science & Technology. 2005;39:3855-3863.

Chapter 7

General Conclusions and Prospects

7.1 Conclusions

The proper development of a well-functioned waste management system is a complex task, which requires both technological improvement and systematic evaluation. To help guide an energy-efficient and environmental-sound waste management system, this research work mainly focuses on 'MSWs gasification with emphasis on energy, environment and life cycle assessment'. MSW pyro-gasification characteristics are experimentally studied to achieve high-quality syngas production, while life cycle assessment is conducted for the optimization of the whole system. Based on this research work, the following conclusions are obtained:

- **Pyro-gasification characteristics of typical MSW components and the development of pyro-gasification prediction model**

The pyro-gasification characteristics of MSW are highly variable owing to the complexity in MSW components and reaction agent. For better pyro-gasification process design, operation and optimization, four typical MSW components (poplar wood, cardboard, food waste and PE) have been pyro-gasified under three atmosphere (N_2, steam and CO_2). Both single-component and the interactions between multi-components are experimentally investigated, aiming at promoting high-quality syngas production. Besides, a practical pyro-gasification prediction model is also developed, so that the pyro-gasification properties and potential syngas utilization of varied MSW composition could be quantified and optimized instead of a large segment of on-site test works.

Results from the pyro-gasification of MSW single-component show that, different MSW components exhibit varied syngas composition due to their difference in compositions and chemical bonds. Their reactivity is highly linked to the structure of char. The one obtained from food waste is porous and shows a larger specific surface area, which effectively improves cracking reactions to increase the syngas production. PE char exhibits limited reactivity, since the remained fixed carbon and carbohydrates are relatively low. With regard to the effect of gasifying agent, both steam and CO_2 gasification are effective to enhance the syngas yield as compared with pyrolysis under N_2 atmosphere. Steam gasification shows a higher reaction rate compared with CO_2 gasification. Meanwhile, the obtained syngas offers different potential utilization: syngas obtained from steam gasification exhibits the desired H_2/CO ratio for Fischer-Tropsch synthesis processes; while the lower H_2/CO of the syngas obtained from CO_2 gasification is suitable as chemical raw material. Pyro-gasification of MSW multi-components is then examined. Nonlinear phenomena are commonly observed for the mixtures. The interactions could be explained by complex mechanisms such as the presence of alkali metals, char structures, and reaction kinetics. Both inhibiting and synergistic effects exist, resulting in deviated syngas properties compared with theoretical calculations.

Based on the experimental data obtained, a MSW pyro-gasification prediction model based on ANN mathematical method is established. The model uses three-layer structure: one input layer, one output layer and one hidden layer. Proper training and validation processes are conducted to verify its feasibility and reliability. The established ANN model is then applied to compare MSW pyro-gasification characteristics between France and China based on waste composition. Results indicate that, syngas obtained from both France and China is suitable to be used for Fischer-Tropsch process or energy recovery; ANN is an appropriate means to predict gasification characteristics of MSW.

- **Pyro-gasification optimization: steam catalytic gasification for H_2-rich gas production and investigation CaO catalyst reactivity**

Steam catalytic gasification of MSW for H_2-rich gas production is conducted as a potential pyro-gasification optimization approach. CaO is used as an in-bed catalyst; while poplar wood, one of the most representative components in MSW, is selected as feedstock. The influence of CaO/wood mass ratio, steam flowrate and reaction temperature is studied; and results are further compared with non-catalyst high-temperature gasification situations to investigate the potential of reducing the reaction temperature by using catalyst. Results

reveal that, the addition of CaO provides an obvious catalytic effect on H_2 improvement as well as tar reduction in the syngas. Furthermore, injection of steam is beneficial for H_2 production. A maximum H_2 concentration and yield is achieved at a steam flowrate of 160 g/h; however, a further excessive steam injection will lead to an opposite effect due to decreased available heat. The optimal reaction temperature should be balanced between the gasification performance and the CaO carbonation ability, and the optimal temperature is found to be 700 ^{o}C in this study. Comparing the results with non-catalyst high-temperature gasification, 50% CaO addition at 700 ^{o}C could provide as much H_2 as that gasified at 800 ^{o}C without catalyst. Meanwhile, a much higher H_2 concentration and H_2/CO ratio could be obtained from catalytic gasification cases. It could be concluded that a 50% CaO addition as catalyst at 700 ^{o}C would be effective to reduce the steam gasification reaction temperature of approximately 100 ^{o}C. CaO used as catalyst exhibits a strong potential to produce H_2-rich gas as pyro-gasification process optimization approach. The decreased gasification reaction temperature could also be a measument showing benefits in energy saving.

However, despite the positive effect of using CaO as catalyst, its reactivity shows significant decrease over multiple CO_2 capture and release cycles. To better serve CaO as catalyst in industrial application, the reactivity of CaO is investigated especially its de-activation mechanism, influence factor, and re-generation methods. Results indicate that the degradation of CaO during cyclic carbonation/calcination reaction is mainly driven by two phenomena: (1) clogging of small pores during carbonation; and (2) sintering during calcination. The specific surface area and porosity after carbonation/calcination is increased from the original sample, due to the creation of pores upon CO_2 release during calcination. However, both specific surface area and porosity are decreased with the increasing number of carbonation/calcination cycles due to de-activation of CaO. To delay such de-activation, 650 ^{o}C is found to be the most suitable carbonation temperature; while calcination temperature should be controlled below 800 ^{o}C. Steam hydration is an effective approach for CaO re-generation, which is positive to maintain the pore structure and morphology of CaO.

- **Systematic evaluation and optimization of MSW pyro-gasification technology based on life cycle assessment**

For the development of an energy-efficient and environmental-sound WtE technology, the environmental and energetic performance of different MSW thermal processes is evaluated from the life cycle perspective.

First, a quantitative comparison between MSW gasification and conventional incineration technologies is conducted, which is based on three commercial operated WtE plants including one MSW gasification-based power plant in Finland and two conventional incineration plants in both France and China. Results indicate a better environmental performance from gasication-based WtE system. The environmental benefits are mainly from two-folds: 1) the reduced process emissions, and 2) the increased electricity generation. It has been proved that acid gases such as HCl and SO_2 could be removed prior to combustion when using gasification, so that the quality of superheated steam would be improved to a higher level. As a result, a significant increased amount of electricity could be recovered, which thus avoids more emissions generated by fossil fuel-based energy production. For the improvement of conventional MSW incineration, plants based on the French condition are primarily affected by NO_x emission; thus effective control measurements are essential. The main issue regarding incineration plants in China is the low MSW calorific value; and improving the level of MSW source-separated collection could be an effective approach. Besides, more strictly dioxin emission limit for dioxin emission is expected to be regulated to reduce toxic-related impacts.

The products utilization approaches of pyro-gasification process are then modeled for optimization. Three types of energy utilization cycles are compared: gas boiler-steam turbine, gas turbine and internal combustion engine. Results reveal that gasification equipped with gas turbine leads to the least environmental loadings, steam turbine systems rank after and internal combustion engine systems come last. Effective syngas purification coupled with gas turbine cycle could be an effective optimization for the current gasification technique.

7.2 Prospects

Developing a sustainable and integrated waste management system is a long-term and complex task. The previous section sums up the main conclusions related to this research work. Nevertheless, new challenges come up from both technological and theoretical evaluation perspectives. This section is dedicated to the prospects for future research investigations.

- **Investigation of environmental emissions (PM, Cl, etc.) from MSW pyro-gasification**

Experimental studies of this work are mainly focused on examining and optimizing the operating parameters related to MSW pyro-gasification process. However, great concerns should also be paid to the environmental emissions during MSW thermal treatment, since they may cause potential negative impacts to human health. Of great interest is particulate matter (PM) and chlorine (Cl) emissions. This is because, trace elements of heavy metals and alkali metals, such as cadmium, lead, mercury, sodium, and potassium, can be concentrated on the particles and escape as airborne aerosols existing the stack. Those contaminants are toxic that they can accumulate in the human body such as in kidneys, bones, and liver, causing serious health disorders [1, 2]. However, the Cl contained in MSW, particularly in plastic component, can not only form HCl but also hazardous chlorinated organic compounds especially dioxin and furnan. HCl is the main factor limiting the efficiency of electricity generation due to high-temperature corrosion [3]; and dioxin and furan have been consistently observed to cause negative health effects such as carcinogenicity, immunotoxicity, and disturbance of lipid metabolism in humans [4]. Realizing these facts, investigation of these environmental emissions during pyro-gasification process should arise highly attentions.

Accordingly, additional research works would be of great importance to: (i) examine both concentration and composition of PM emission from MSW pyro-gasification, in order for effective monitoring and controlling strategies; (ii) investigate and quantify the fate of Cl during pyro-gasification process, seeking for HCl removal approaches, or, the use of catalysts as suitable materials to capture HCl.

- **Improvement of catalyst properties for optimizing pyro-gasification**

Results from this study have proved that, the use of catalyst, for example in-situ CaO addition, is effective to optimize MSW pyro-gasification process. As a result, in-depth investigation in this field is essential to fulfill the research, which could include:

(i) Investigation of effective catalyst re-generation methods. Results from this study have observed that catalysts might undergo de-activation during high temperature and/or long duration usage, which may be attributed to pore structure losing and sintering. Steam hydration is proven to be effective for CaO catalyst re-generation; however, in-depth investigation for the

re-generation procedures is still essential. For example, the effects of temperature, steam flowrate need to be quantified to optimize the re-generation process. Besides, as it has been indicated by literature [5], steam hydration could be applied in different approaches: addition during carbonation, or calcination, or separate hydration after calcination (used in this study). Those approaches need further comparison with the aim to obtain an effective and cost-benefit re-generation method.

(ii) Development of effective pyro-gasification catalyst. On the other hand, the development of new and effective catalyst is also an approach for catalyst optimization [6, 7]. For example synthetic catalysts, with the main aim to enhance catalytic performance and catalyst re-activity towards pyro-gasification process.

- **Systematic evaluation and comparison of various pyro-gasification processes**

In this study, two modeling methods as ANN and LCA have been applied for the evaluation and optimization of MSW pyro-gasification processes. ANN has proven to be an appropriate means to predict gasification characteristics of MSW. Nevertheless, the model established is based on four MSW components of wood, paper, food waste and plastic. The accuracy of the model can be further improved by adding more training samples related to more MSW components, e.g. textile.

Comprehensive comparisons between MSW pyro-gasification and incineration, as well as the potential products downstream applications, have been evaluated using LCA methodology. Results highlight the potential advantages that could be brought by pyro-gasification technologies. From this context, a systematic assessment of various pyro-gasification processes is meaningful. The comparison could include systems using different gasifying agents, catalytic and non-catalytic gasification, and systems under varied operating parameters; incorporating the environmental emissions data obtained by aforementioned experiments. For example, steam catalytic gasification is worth evaluated. Results from **Chapter 4** indicated that the use of CaO is effective to improve the syngas quality; however 20%, or even 50% addition of CaO inside the gasifier is used. How about the impact of CaO production from the life-cycle perspective? And, CaO is generally produced from $CaCO_3$ through high-temperature decarboxylation that requires a lot of energy, how

about its impact especially if the energ is supplied by the combustion of fossil fuels? In addition, the issues of carbon credits market as well as a holistic life cycle cost analysis are also essential with regard to industrial application of the pyro-gasification technique. Results obtained by this systematic evaluation could be helpful to further optimize the pyro-gasification process and to enhance the competitiveness of the pyro-gasification technology.

Bibliography

[1] Singh Anita, Sharma Rajesh Kumar, Agrawal Madhoolika, Marshall Fiona M. Health risk assessment of heavy metals via dietary intake of foodstuffs from the wastewater irrigated site of a dry tropical area of India. Food And Chemical Toxicology. 2010;48:611-619.

[2] Nzihou Ange, Stanmore Brian. The fate of heavy metals during combustion and gasification of contaminated biomass—A brief review. Journal Of Hazardous Materials. 2013;256:56-66.

[3] Wang Zhiqi, Huang Haitao, Li Haibin, Wu Chuangzhi, Chen Yong, Li Baoqing. HCl formation from RDF pyrolysis and combustion in a spouting-moving bed reactor. Energy & Fuels. 2002;16:608-614.

[4] Flesch-Janys Dieter, Berger Jürgen, Gum Petra, Manz Alfred, Nagel Sibylle, Waltsgott Hiltraud, et al. Exposure to polychlorinated dioxins and furans (PCDD/F) and mortality in a cohort of workers from a herbicide-producing plant in Hamburg, Federal Republic of Germany. American Journal Of Epidemiology. 1995;142:1165-1175.

[5] Rong Nai, Wang Qinhui, Fang Mengxiang, Cheng Leming, Luo Zhongyang, Cen Kefa. Steam hydration reactivation of CaO-based sorbent in cyclic carbonation/calcination for CO_2 capture. Energy & Fuels. 2013;27:5332-5340.

[6] Shen Yafei, Yoshikawa Kunio. Recent progresses in catalytic tar elimination during biomass gasification or pyrolysis—a review. Renewable and Sustainable Energy Reviews. 2013;21:371-392.

[7] Abu El-Rub Z, Bramer EA, Brem G. Review of catalysts for tar elimination in biomass gasification processes. Industrial & Engineering Chemistry Research. 2004;43:6911-6919.

Appendix

Appendix I

List of Figures

Appendix II

List of Tables

Appendix III

Publications Related to This Work

Publications in International Journals

- Jun Dong, Ange Nzihou, Yong Chi, Elsa Weiss-Hortala, Mingjiang Ni, Nathalie Lyczko, Yuanjun Tang, Marion Ducousso. Hydrogen-rich gas production from steam gasification of bio-char in the presence of CaO. **Waste and Biomass Valorization** 2016, DOI: 10.1007/s12649-016-9784-x

- Jun Dong, Yong Chi, Yuanjun Tang, Mingjiang Ni, Ange Nzihou, Elsa Weiss-Hortala, Qunxing Huang. Effect of operating parameters and moisture content on municipal solid waste pyrolysis and gasification. **Energy & Fuels** 2016, 30, 3394-4001

- Jun Dong, Yong Chi, Yuanjun Tang, Mingjiang Ni, Ange Nzihou, Elsa Weiss-Hortala, Qunxing Huang. Partitioning of heavy metals in municipal solid waste pyrolysis, gasification, and incineration. **Energy & Fuels** 2015, 29, 7516-7525

- Jun Dong, Yong Chi, Daoan Zou, Chao Fu, Qunxing Huang, Mingjiang Ni. Comparison of municipal solid waste treatment technologies from a life cycle perspective in China. **Waste Management & Research** 2014, 32, 13-23

- Yuanjun Tang, Jun Dong, Yong Chi, Zhaozhi Zhou, Mingjiang Ni. Energy and exergy analyses of fluidized-bed municipal solid waste air gasification. **Energy & Fuels** 2016, 30, 7629-7637

- Jouni Havukainen, Mingxiu Zhan, Jun Dong, Miia Liikanen, Ivan Deviatkin, Xiaodong Li, Mika Horttanainen. Environmental impact assessment of municipal solid waste management incorporating mechanical treatment of waste and incineration in

Hangzhou, China. **Journal of Cleaner Production**, 2017, 141, 453-461

Publications in international conferences

- Jun Dong, Ange Nzihou, Yong Chi, Marion Ducousso, Yuanjun Tang, Elsa Weiss-Hortala, Mingjiang Ni. Experimental study on MSW fluidized bed gasification characteristics under N_2/CO_2/Steam atmosphere. The 8th International Conference on Combustion, Incineration-Pyrolysis, Emission and Climate Change. October 15-18, 2014, Hangzhou, China (Oral presentation)
- Jun Dong, Yong Chi, Mingjiang Ni. Municipal solid waste pyrolysis, gasification versus incineration: A life cycle assessment. 5th International Conference on Engineering for Waste and Biomass Valorisation. August 25-28, 2014, Rio de Janeiro, Brazil (Oral presentation)
- Yong Chi, Jun Dong, Mingjiang Ni, Ange Nzihou. Life cycle energy-environment-economy assessment model and its application in waste management. Franco-Chinese Workshop on Processes for Energy and Environmental Issues. June 12-13, 2014, Albi, France (Oral presentation)
- Jun Dong, Ange Nzihou, Yong Chi, Elsa Weiss-Hortala, Mingjiang, Qunxing Huang, Yuanjun Tang, Marion Ducousso. Hydrogen-rich gas production from steam catalysic gasification of bio-char. 6th International Conference on Engineering for Waste and Biomass Valorisation. May 23-26, Albi, France (Oral presentation)

Etude de la gazéification d'ordures ménagères avec un intérêt particulier pour les bilans énergétiques, environnementaux couplés à l'analyse de cycle de vie

Résumé: Récemment, la pyro-gazéification de déchets ménagers solides (DMS) a suscité une plus grande attention, en raison de ses bénéfices potentiels en matière d'émissions polluantes et d'efficacité énergique. Afin de développer un système de traitement de ces déchets, durable et intégré, ce manuscrit s'intéresse plus spécifiquement au développement de la technique de pyro-gazéification des DMS, à la fois sur l'aspect technologique (expérimentations) et sur son évaluation globale (modélisation). Pour cette étude, quatre composants principaux représentatifs des DMS (déchet alimentaire, papier, bois et plastique) ont été pyro-gazéifiés dans un lit fluidisé sous atmosphère N_2, CO_2 ou vapeur d'eau. Les expériences ont été menées avec les composés seuls ou en mélanges afin de comprendre les interactions mises en jeu et leurs impacts sur la qualité du syngas produit. La présence de plastique améliore significativement la quantité et la qualité du syngas (concentration de H_2). La qualité du syngas est améliorée plus particulièrement en présence de vapeur d'eau, ou, dans une moindre mesure, en présence de CO_2. Les résultats obtenus ont été ensuite intégrés dans un modèle prédictif de pyro-gazéification basé sur un réseau de neurones artificiels (ANN). Ce modèle prédictif s'avère efficace pour prédire les performances de pyro-gazéification des DMS, quelle que soit leur composition (provenance géographique). Pour améliorer la qualité du syngas et abaisser la température du traitement, la gazéification catalytique in-situ, en présence de CaO, a été menée. L'impact du débit de vapeur d'eau, du ratio massique d'oxyde de calcium, ainsi que de la température de réaction a été étudié en regard de la production (quantité et pourcentage molaire dans le gaz) d'hydrogène.la présence de CaO a permis d'abaisser de 100 ^{o}C la température de gazéification, à qualité de syngas équivalente. Pour envisager une application industrielle, l'activité du catalyseur a aussi été évaluée du point de vue de sa désactivation et régénération. Ainsi, les températures de carbonatation et de calcination de 650 ^{o}C et 800 ^{o}C permettent de prévenir la désactivation du catalyseur, tandis que l'hydratation sous vapeur d'eau permet la régénération. Ensuite, une étude a été dédiée à l'évaluation et à l'optimisation de la technologie de pyro-gazéification par la méthode d'analyse de cycle de vie (ACV). Le système de gazéification permet d'améliorer les indicateurs de performances environnementales comparativement à l'incinération conventionnelle. De plus, des systèmes combinant à la fois la transformation des déchets en vecteur énergétique et la mise en œuvre de ce vecteur ont été modélisés. La pyro-gazéification combinée à une turbine à gaz permettrait de maximiser l'efficacité énergétique et de diminuer l'impact environnemental du traitement. Ainsi, les résultats permettent d'optimiser les voies actuelles de valorisation énergétique, et de d'optimiser les techniques de pyro-gazéification.

Mots clés: Déchets ménagers solides; Pyro-gazéification; Syngas de haute qualité; Réseau de neurones artificiels; Catalyseur in-situ; Analyse de cycle de vie

MSWs gasification with emphasis on energy, environment and life cycle assessment

Abstract: Due to the potential benefits in achieving lower environmental emissions and higher energy efficiency, municipal solid waste (MSW) pyro-gasification has gained increasing attentions in the last years. To develop such an integrated and sustainable MSW treatment system, this dissertation mainly focuses on developing MSW pyro-gasification technique, including both experimental-based technological investigation and assessment modeling. Four of the most typical MSW components (wood, paper, food waste and plastic) are pyro-gasified in a fluidized bed reactor under N_2, steam or CO_2 atmosphere. Single-component and multi-components mixture have been investigated to characterize interactions regarding the high-quality syngas production. The presence of plastic in MSW positively impacts the volume of gas produced as well as its H_2 content. Steam clearly increased the syngas quality rather than the CO_2 atmosphere. The data acquired have been further applied to establish an artificial neural network (ANN)-based pyro-gasification prediction model. Although MSW composition varies significantly due to geographic differences, the model is robust enough to predict MSW pyro-gasification performance with different waste sources. To further enhance syngas properties and reduce gasification temperature as optimization of pyro-gasification process, MSW steam catalytic gasification is studied using calcium oxide (CaO) as an in-situ catalyst. The influence of CaO addition, steam flowrate and reaction temperature on H2-rich gas production is also investigated. The catalytic gasification using CaO allows a decrease of more than 100 ^{o}C in the reaction operating temperature in order to reach the same syngas properties, as compared with non-catalyst high-temperature gasification. Besides, the catalyst activity (de-activation and re-generation mechanisms) is also evaluated in order to facilitate an industrial application. 650 ^{o}C and 800 ^{o}C are proven to be the most suitable temperature for carbonation and calcination respectively, while steam hydration is shown to be an effective CaO re-generation method. Afterwards, a systematic and comprehensive life cycle assessment (LCA) study is conducted. Environmental benefits have been achieved by MSW gasification compared with conventional incineration technology. Besides, pyrolysis and gasification processes coupled with various energy utilization cycles are also modeled, with a gasification-gas turbine cycle system exhibits the highest energy conversion efficiency and lowest environmental burden. The results are applied to optimize the current waste-to-energy route, and to develop better pyro-gasification techniques.

Keywords: Municipal solid waste; Pyro-gasification; High-quality syngas production; Artificial neural network; In-situ catalyst; Life cycle assessment